AN ABSTRACT OF THE THESIS OF

Elinor S. Utevsky for the degree of Master of Science in Geology presented on July 16, 2015.

Title: Geochemistry of Plutonic Rocks of the Western Cascades, Washington & Oregon: Relationship to Crustal Segmentation and Ore Genesis

Abstract approved:

John H. Dilles

The volcanic (~45-10 Ma) and plutonic rocks (~37-12 Ma) comprising the Western Cascades extend from northernmost California to southern British Columbia and are ancestral to modern arc magmatism. The ancestral arc hosts a series of small plutons that are locally associated with porphyry (Cu-Mo) and epithermal (Au) ore deposits. Three crustal segments identified by Schmidt et al. (2008, 2013) in the modern arc are potentially reflected in the geochemistry of the ancestral Cascades as well: Paleozoic-Mesozoic accreted terranes, metamorphic rocks, and granites to the north; thin Paleocene Siletzia oceanic crust of the Columbia Embayment in the center; and Paleozoic-Mesozoic ultramafic sheets and marine arc-related volcanic and sedimentary rocks of the Klamath Terrane to the south. Therefore, the Western Cascades of Washington and Oregon provide a field laboratory to examine the chemical compositions and ages of granitoid intrusions associated with a variety of magmatic-hydrothermal ore deposits, and to compare the compositions with the along-arc variation of the age, composition and thickness of the underlying crust.

The majority of the 15 new zircon U-Pb ages reported in this study are 27 to 12 Ma with the exception of the ~37 Ma Snoqualmie North Fork intrusions of central WA. A total of 610 zircons were analyzed, of which 118 have ages older than the main population and are considered to be xenocrystic or inherited. The north segment contains the oldest (up to 67 Ma) and most continuous inherited population. The absence of inherited grains older than 67 Ma suggests that neither the North Fork nor White River districts overlie old crystalline crust, but instead overlie Paleocene-Eocene volcanics that are the likely source of inherited zircons. Districts of the Columbia segment have sparse inherited zircon populations (n = 38 of 350 total), ranging from 54 to 20 Ma. The dearth of inherited zircons in the center of the arc suggests limited contamination by a source no older than 55 Ma, likely the dominant Eocene sources of detrital zircon found within the Tyee Formation. Districts overlying the Klamath Terrane have slightly more substantial inherited zircon populations than districts overlying Siletzia but still decidedly few inherited grains (a total of 25 out of 85 grains analyzed, ranging from 44 to 19 Ma); these grains are likely sourced from similar contaminants to those underlying the central segment of the arc, instead of from accreted Mesozoic rocks of the Klamath Terrane.

The hypabyssal plutonic rocks represent a small area (~1%) of exposures in the Western Cascades, and range in composition from diorites to granodiorites and minor granite. Fe-Ti oxides, where preserved, include magnetite and ilmenite in proportion of ~2:1, and together with presence of hornblende and biotite are suggestive of modest oxidation states of ~ ΔNNO of 0 to 1 (Carmichael & Nicholls, 1967). Abundant hornblende is observed in 31 of 36 available petrographic sections. Ba/Nb values are not obviously correlated with SiO_2 content from any given district, but tend to increase at any given SiO_2 content from north to south. Th/Ta ratios notably increase with SiO_2, and are lowest in the mid-latitude districts (North Santiam, Detroit Dam, Quartzville, and Blue River). While increased slab fluid could increase Ba relative to Nb, the greater abundance of Ba, Th, and Th/Ta southward at given SiO_2 are more consistent with an increased role of crustal contamination. Dy/Yb ratios decrease with increasing SiO_2 contents with the exception of the North Fork District. V/Sc ratios decrease with increasing SiO_2 with the exception of samples of the Spirit Lake Pluton, and slightly increase from south to north at any given SiO_2 content.

Zircons in the Western Cascades plutonic rocks have characteristically large negative Eu anomalies (Eu/Eu* < 0.5) and small positive Ce anomalies, correlated with relatively reduced oxidation states and low water contents, even when directly associated with moderately economic porphyry Cu deposits. Although these magmas are sufficiently water-rich to abundantly crystallize and fractionate amphibole (at least 3 wt. % H_2O), it is evident that plagioclase likely crystallized early and was not suppressed by high water contents (> 3 wt. % H_2O). There is no evidence that Western Cascade magmas were strongly oxidized (> NNO +1).

Although crustal thickness is poorly constrained in the north and south segments, it is evidently variable along-arc (and may thicken slightly to the south), but is likely relatively thin. I therefore suggest that crustal thickness and lithology substantially control ore potential within the Western Cascade Arc.

Geochemistry of Plutonic Rocks of the Western Cascades, Washington & Oregon:
Relationship to Crustal Segmentation and Ore Genesis

by

Elinor S. Utevsky

A THESIS

submitted to

Oregon State University

in partial fulfillment of
the requirements for the
degree of

Master of Science

Presented July 16, 2015
Commencement June 2016

Master of Science thesis of Elinor S. Utevsky presented on July 16, 2015

APPROVED:

Major Professor, representing Geology

Dean of the College of Earth, Ocean and Atmospheric Sciences

Dean of the Graduate School

I understand that my thesis will become part of the permanent collection of Oregon State University libraries. My signature below authorizes release of my thesis to any reader upon request.

Elinor S. Utevsky, Author

ACKNOWLEDGEMENTS

What a whirlwind experience of education and growth. These past two years have been the most enlightening and productive time of my life and I have many people to thank for the experiences and challenges associated with this accomplishment. I have been extremely honored to work with Dr. John Dilles, who is an amazing mentor and a superb scholar. My gratitude for the time, energy, and knowledge that John has shared with me is unsurpassed and I am confident that I am a much better geologist and person after having studied with him.

I would like to thank my committee members, Anita Grunder and Adam Kent, for their contributions to this thesis; their unique outlook was critical to the production of the ideas that are described in these pages. A special thank you to the Sons of Dilles: Federico Cernuschi, Nansen Olson III, Curtis Johnson, Mike Sepp, Mike Hutchinson, Rocky Barker, and Chris Gibson – I can't believe I was so lucky to get to learn with you and I will treasure your friendship and support for the rest of my life. To Nansen and Fede especially – your knowledge and ideas are as much in here as my own and I don't think this thesis would have been possible without your guidance. Additional VIPER shout-outs to Jenny DiGiulio, Nikki Moore, Allan Lerner and Henri Sanville - thank you for the conversations, help, and serious contributions to the map, geochemistry, and broader impact of this work. Thank you to Gaylen Sinclair for assistance with figures and computer software. To Shiloh Sundstrom and Joseph Kemper of Wilk 217: I will miss our camaraderie and feel blessed to know you. Many thanks and love to my friends and family in Corvallis, the $2 pint-night at Bombs, and the delicious noodle shop on 14th street.

This thesis would not be possible without financial support form NSF grant 61415 and GSA Graduate Research Grant. Thank you to Ed du Bray, Dave John and Rob Fleck with USGS for sharing data with me. Thank you to Weyerhaueser Inc., Alexander Iveson at WSU, and Jim Mattinson at UBC for providing samples.

I would like to express deep appreciation to my parents, sisters, and extended family for their everlasting support and pride. Thank you for the enthusiasm you have for my research and for geology in general. Aunt Ann, thank

you for hosting me in Corvallis and for keeping my spirits bright. Finally, to my love and my rock, Samuel Schnake, I can't express how grateful I am to know you, to love you, to be supported by you every day. CHEERS.

-Nora Utevsky

TABLE OF CONTENTS

LIST OF FIGURES

LIST OF TABLES

LIST OF APPENDICES

LIST OF APPENDIX FIGURES

LIST OF APPENDIX TABLES

LIST OF DIGITAL APPENDICES

INTRODUCTION

Compositional variation within subduction-related arc magmas can be attributed to distinct mantle and crustal regimes. Hildreth and Moorbath (1988) demonstrated that trace elements, alkali, and isotopic compositions in the Andes vary along arc as crustal thickness and composition changes. They proposed a relationship between the distribution of these compositions and the underlying crustal composition and thickness. Porphyry ore deposits are the most significant source of copper, gold, silver, and molybdenum, which are important resources to human civilization. The Andes arc overlies relatively thin to very thick crust (Beck et al., 1996) and hosts some of the world's largest porphyry Cu-(Mo-Au) ores.

In general, porphyry Cu-(Mo-Au) deposits form in oceanic or continental arcs above subduction zone settings. Large porphyry and epithermal deposits may require a thick, evolved crust (Kay & Mzopodis, 2001) that hosts a magma chamber with high amounts of water, oxidized conditions and potentially anomalous concentrations of metals and sulfur (Richards 2003; Wilkinson 2013; Richards *in press*). Porphyry Cu-Au-Mo deposits are associated with small intrusions that are emplaced several kilometers beneath the surface and carry ore-forming hydrothermal fluids. There is a consensus in economic geology (Gustafson 1979; Chambefort et al., 2008; Wilkinson 2013; Dilles et al., 2015) that sulfur-rich magmas are essential for the generation of large magmatic-hydrothermal mineral deposits. Trace element concentrations in zircons can be used to discern the oxidation state of the melt (Ballard et al., 2001; Farmer 2012), which is potentially caused by sulfur degassing (Dilles et al., 2015). Oxidized, sulfur-rich magmas may saturate in anhydrite, which breaks down during cooling once a water-rich fluid phase forms, and the sulfur is reduced from sulfate ($S^{6+}O_4$) to sulfur dioxide ($S^{4+}O_2$). This reduction requires the complementary oxidation of iron in an amount inversely proportional to the ratio of Fe to S.

Loucks (2014) proposed that whole rock trace element ratios are sensitive to water contents and oxidation states and can also be used to determine the potential ore fertility of a magma. High Sr/Y (> 35 at SiO_2 > 57 wt. %) is likely a product of elevated water content at low crustal pressure (0.6-1.2 GPa) of magmas and results from partitioning and removal of early and prolific crystallization of Y-rich hornblende and delayed, minimal crystallization of Sr-rich plagioclase. High V/Sc (> 10) is potentially due to high oxidation of magmas of V from 3+ to 4+ and 5+ valence. V^{3+} is compatible in magnetite, but V^{4+} and V^{5+} are not. As the oxidation state of magma increases from ΔNNO = 0 to ΔNNO = +3, the magnetite/melt partition coefficient for vanadium drops from ~20 to ~1 (Toplis and Corgne, 2002). Therefore vanadium acts incompatibly in strongly oxidized magmas (ΔNNO> +1; Loucks, 2014). Elevated Sr/Y and V/Sc trace element ratios are typical of arc magmas parental to magmatic-hydrothermal ore deposits (Loucks 2014).

The Western Cascade Arc

The Western Cascades of Washington and Oregon (Figure 1) provide a field laboratory to examine the chemical compositions and ages of granitoid intrusions associated with a variety of magmatic-hydrothermal ore deposits, and to compare the compositions with the along-arc variation of the age, composition and thickness of the underlying crust. The volcanic (~42-10 Ma) and plutonic rocks (~37-12 Ma) comprising the Western Cascades extend from northernmost California to southern British Columbia and are ancestral to modern arc magmatism (<10 Ma).

Du Bray and John (2011) documented the temporal tectonic and geochemical evolution of the Western Cascades using major oxide, trace element, and rare earth elements (REE) geochemical data, illustrating variations in magma geochemistry that likely correspond to variations of contributions from the underlying crust as well as the subducting slab. They concluded that early (pre-40 Ma to 35 Ma), tholeiitic basaltic and basaltic andesitic volcanism was largely restricted to southern Washington corresponds to subduction of the Kula-Farallon spreading ridge and the associated slab window magmatism. Crustal thicknesses are inferred to be thin(<10 km). The next phase of magmatism was dominated by calc-alkaline compositions and began circa35 Ma after the crust evolved and thickened to~10-20 km. du Bray &

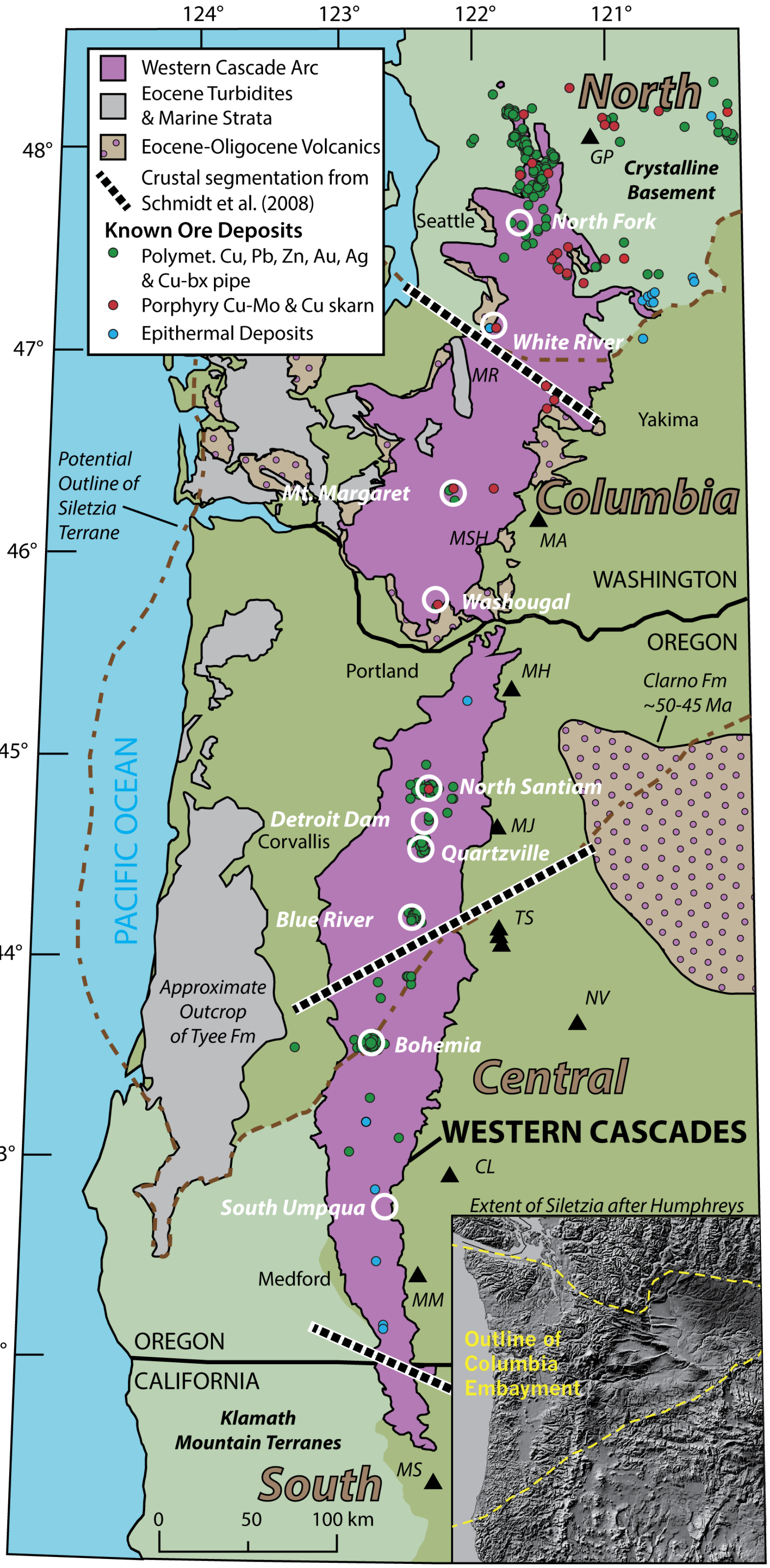
124°
123°
122°
121°
48°
47°
46°
45°
44°
43°
42°
Western Cascade Arc
Eocene Turbidites & Marine Strata
Eocene-Oligocene Volcanics
Crustal segmentation from Schmidt et al. (2008)
Known Ore Deposits
Polymet. Cu, Pb, Zn, Au, Ag & Cu-bx pipe
Porphyry Cu-Mo & Cu skarn
Epithermal Deposits
North
GP
Crystalline Basement
Seattle
North Fork
White River
MR
Yakima
Potential Outline of Siletzia Terrane
Mt. Margaret
Columbia
MSH
MA
WASHINGTON
Washougal
OREGON
Portland
MH
Clarno Fm ~50-45 Ma
PACIFIC OCEAN
North Santiam
Detroit Dam
Corvallis
MJ
Quartzville
Blue River
TS
Approximate Outcrop of Tyee Fm
NV
Bohemia
Central
WESTERN CASCADES
CL
Extent of Siletzia after Humphreys
South Umpqua
Medford
MM
Outline of Columbia Embayment
OREGON
CALIFORNIA
Klamath Mountain Terranes
South
MS
0
50
100 km

Figure 1 (Above): Map of Western Cascades region adapted from du Bray & John (2011) showing sample locations as white circles. Active Cascade Arc denoted by black triangles.

John (2011) argue these partial melts were likely generated at higher pressures beneath thicker crust in which plagioclase was unstable and garnet was stable. The last stage of Western Cascade magmatism prior to the onset of modern Cascade magmatism at ~10 Ma is characterized by more iron-rich compositions related to a decreased dip of the subducted slab (du Bray & John 2011). The concentrations of K, Rb, and Sr in Western Cascade samples suggest limited magmatic evolution. Elevated TiO_2 as well as Nb/Ta and Ba/Ta data for early volcanics (45-36 Ma) could support a slab window association (Cole & Stewart, 2009). Futhermore, Ba/Nb increase from <15 in early volcanics (45-36 Ma) to 15-140 in younger samples (25-4 Ma), and plutonic samples have significantly elevated Ba/Nb ratios compared to their 25-18 Ma extrusive equivalents. REE patterns are sub-parallel and gently negatively sloping. Higher overall REE concentrations in older Western Cascade volcanics are likely related to REE incompatibility and successive partial melting sources (du Bray & John, 2011).

Schmidt et al. (2008, 2013) noted that the modern Cascade arc volcanoes vary in chemical and isotopic composition along strike, and proposed four crustal segments (Figure 1) interpreted as the result of variations in mantle domains and melting regimes at depth along the length of the arc. The north segment, the portion of the arc north of Mount St. Helens, overlies old continental crust composed of Paleozoic-Mesozoic accreted terranes, metamorphic rocks, and granites. The Columbia segment, from southernmost Washington to central Oregon, is inferred to be built on young and thin Paleocene (<54 Ma) Siletzia oceanic crust of the Columbia Embayment (Fig. 1) possibly overlain by turbidites of the Tyee Formation (Wells et al., 2000). In this sector, the Siletzia Terrane is estimated to range in thickness from 10 to 15 km thick in southern Washington to 30 km thick in Oregon on the basis of seismic data (Stanley et al., 1990; Trehu et al., 1994; Parsons et al., 1999). In central Oregon, there is a distinct shift in $^{87}Sr/^{86}Sr$ ratios of basalts in the modern Cascade Arc, from 0.7028 in the segment underlain by the Columbia Embayment to 0.7034 in the segment to the south underlain by Klamath Terrane. This shift is interpreted as due to magma interactions with two crustal blocks produced by juxtaposition of two accreted terranes - Siletzia oceanic crust to the north and Klamath Mountain Terrane to the south (Schmidt et al., 2008). The south segment of the arc overlies the Klamath Terrane, which was accreted over several periods in the Jurassic and forms a thicker more complex crust containing ultramafic sheets and marine arc-related volcanic and sedimentary rocks (Irwin 1981; Snoke and Barnes 2006). These distinct basement rocks may be reflected in the geochemistry of the Miocene-age magmatism of the ancestral Cascades as well.

The ancestral arc hosts a series of small plutons that are locally associated with porphyry (Cu-Mo) and epithermal (Au) ore deposits (du Bray & John 2011). Although the metal production is modest, moderate-sized porphyry Cu-Mo-Au ores are present at Mount Margaret (523 MT at 0.36 % Cu and 0.25 g/t Au, Lasmanis 1995) and North Fork (80.5 MT of 0.44 % Cu and 0.102 g/t Au reserve, Smithson 2004) in Washington State. In Oregon, modest-sized epithermal gold deposits are widely distributed, and the largest production is from the Bohemia district (28,285 oz. Au produced, Power 1984). The characteristics of all ten districts included in this study are summarized in Table 1.

Temporal-Spatial Setting of The Western Cascade Arc

In the late Cretaceous-Eocene prior to the onset of Western Cascade magmatism, arc magmatism in the Idaho and Colorado Batholiths and related volcanics was far to the east as a result of flat-slab subduction (Schmandt & Humphreys 2011). This subduction zone had a large embayment along the current Washington-Oregon border known as the Columbia Embayment, partially defined by the boundaries of the older Cascade Crystalline Core to the north, the Blue Mountains accreted terranes to the east, and the Klamath Terrane to the south (Christiansen & Yeats 1992; Brown & Gehrels 2007; LaMaskin et al., 2011; Schmandt & Humphreys 2011). When flat-slab subduction terminated at about 60 Ma and slab roll-back initiated north to south, magmatism migrated southwestward,

Table 1. Name, location, and description of porphyry-epithermal mineral districts of the Western Cascades

	Name	Location	Deposit Type	Resources and/or Production	References
Washington	North Fork	47.69, 121.65	Porphyry Cu-Mo	80.5 MT of 0.44 wt.% Cu, 0.102 g/t Au	Smithson 2004
	White River	47.15, 121.83	High-sulfidation epithermal Au-Ag with underlying porphyry Cu-Mo deposit	Silica production	Thompson 1983; Blakely et al., 2007
	Mount Margaret	46.35, 122.11	Porphyry Cu-Au & surrounding Cu-breccia pipes & polymetallic veins	523 MT at 0.36 wt.% Cu, 0.25 g/t Au	Evarts et al., 1987; Evarts & Ashley 1993; Lasmanis 1995
	Washougal	45.77, 122.20	Porphyry Cu-Au with tourmaline-bearing breccia pipes	2.6 MT at 1.62 wt.% Cu, 0.058 wt.% MoS_2, 0.2 g/t Au, 8.6 g/t Ag	Schriener 1978; Shepard 1979; Power 1984; Lasmanis 1995; du Bray & John 2011
Oregon	North Santiam	44.85, 122.23	Porphyry Cu & breccia pipe	Small historical Cu-(Pb-Zn) production; Bornite breccia pipe: 2.2 MT at 2.53 wt.% Cu, 0.57 opt Ag, 0.021 opt Au	Winters 1985; Stone et al., 1994
	Detroit Dam	44.70, 122.25	Not well constrained, small epithermal-poylmetallic veins	No record of production	Power 1984
	Quartzville	44.58, 122.37	Small epithermal-poylmetallic veins; suspected hydrothermal porphyry-type system at depth in Boulder Ck area	Produced 8557 oz. Au and 2920 oz. Ag	Munts 1978; Nicholson 1988; Oregon DOGAMI 1951
	Blue River & Nimrod	44.11, 122.63	Small epithermal-polymetallic veins; suspected underlying porphyry Cu system	Produced 257 lbs. Cu and 17,162 oz. Ag	Callahan & Buddington 1928; Storch 1978; Power 1984
	Bohemia	43.58, 122.65	Intermediate-sulfidation epithermal-polymetallic vein, possibly porphyry-style mineralization at depth	28,285 oz Au produced	Schaubs 1978; Power 1984
	South Umpqua	42.75, 122.78	Not constrained, possibly porphyry-style mineralization at depth	Small silica production at Quartz Mountain	Oregon DOGAMI 1951; du Bray & John 2011

initiating the Lowland Creek Volcanics in the Butte-Anaconda area of Montana (52.9-48.6 Ma, Dudás et al., 2010) and Absaroka Volcanics near Yellowstone (53-43.5 Ma, Hiza 1999), the Challis Volcanics of central Idaho (51-40 Ma, Norman & Mertzman 1991) and the Clarno Volcanics of central Oregon (53-43 Ma, Robinson et al., 1990), and continued volcanics to the southwest into northeastern Nevada and Utah (Castor et al., 2003). These Eocene volcanic units form an east-west belt of magmatism and initiate approximately concurrently with the accretion of Siletzia at about 51 Ma (Christiansen & Yeats 1992; Wells et al., 2000). The docking of Siletzia caused the subduction zone to step to the west outboard of the accreted terrane, and was followed by significant and rapid deposition of Tyee Formation turbidite strata within a new forearc basin system between 49.4 and 46.5 Ma in Western Oregon (Dumitru et al., 2013). Turbidite sequences deposited concurrently to the north in Western Washington. Western Cascade magmatism initiated at approximately 42 Ma (du Bray & John, 2011), and temporally overlaps with other magmatic events in the Pacific Northwest, most notably silicic volcanism forming John Day Formation of eastern Oregon which is possibly a result of early Cascade volcanism (37-19 Ma, Robinson et al., 1984) and the initial eruption of the Columbia River Basalts (CRB) ca. 16.9 Ma and following main phase of CRB volcanism between 16 and 15.5 Ma (Barry et al., 2013). The exact age of transition from western to modern Cascade magmatism is debated and ranges from 10 to 2 Ma but is likely ca. 8-7 Ma (Priest 1990, du Bray & John 2011).

This study was designed to investigate the relationship of magma compositions and processes with mineral deposit formation by examining the along-arc variation in Western Cascade plutons. The U-Pb zircon method was used to obtain the age of plutons as well as the age of crustal contaminants via inherited grains. Zircon trace element geochemistry was used to assess temperature, oxidation state, and magmatic mineral fractionation processes (Dilles et al., 2015). These data are integrated with the whole rock major element geochemical data of Western Cascades igneous rocks compiled and discussed by du Bray and John (2011) as well as new trace element data on Western Cascade plutons to assess the relationships of underlying crustal composition and generation of hydrothermal mineral deposits.

METHODS

We collected 35 samples of plutonic rocks locally associated with porphyry (Cu-Mo) and epithermal (Au) in five districts: North Santiam, Quartzville, Blue River, and South Umpqua in the summers of 2013 and 2014 (Figure 1). Additional sampling is summarized in Appendix 2.1**.** Weathered or hydrothermally altered samples were systematically avoided wherever possible, but in many cases background propylitic alteration was ubiquitous and unavoidable. The 35 samples were analyzed for whole rock major and trace element compositions by X-ray Fluorescence (XRF) and inductively coupled plasma mass spectrometry (ICP-MS) at Washington State University's (WSU) Peter Hooper GeoAnalytical Lab via techniques described by Jenner et al. (1990) and Johnson et al. (1999). Sample preparation for zircon analyses is summarized in Appendix 2.2**.**

Thirteen U-Pb zircon ages were determined by laser ablation ICP-MS (LA-ICP-MS) at the W.M. Keck Collaboratory for Plasma Spectrometry at Oregon State University. Between 20 and 100 zircons were analyzed per sample using a DUV Excimer laser (192 nm), a spot diameter of 30-40 μm , and an ablation interval of 30 seconds. Temora-1 (Black et al., 2003) and Plešovice PL-1 (Slama et al., 2008) were analyzed approximately one standard per three unknowns during each analytical session and used for internal age standardization. Raw data from LA-ICP-MS analyses were processed at Oregon State University using LaserTRAM software as summarized by Kent et al. (2004) and Loewen (2013), and external standardization and common lead corrections were manually calculated via methods described in Olson (2015). Terra-Wasserburg Concordia diagrams and age probability plots were used to identify potentially inherited xenocrystic zircons (with ages older than main population) as well as zircons that have experienced post-crystallization Pb-loss (with ages younger than main population).

Three U-Pb zircon ages were determined by sensitive high-resolution ion-microprobe in reverse geometry (SHRIMP-RG) at the Stanford USGS Micro Analysis Center (SUMAC) at Stanford University in February 2014. Reduction and age standardization (to Temora-1) was performed using SQUID version 2.51 (Ludwig, 2009). All zircons analyzed by LA-ICP-MS and SHRIMP-RG were also concurrently analyzed from Hf, Rare Earth Elements (REE), and Y trace element abundance. Trace element data were reduced manually. SHRIMP-RG-analyzed samples were standardized to MADDER at Stanford University; LA-ICP-MS-analyzed samples were standardized to MADDER with NIST-612 glass used as a secondary standard. NIST-612 was used as a primary standard for trace elements at or below detection limits in the MADDER trace element standard on the OSU LA-ICP-MS (e.g., La, Ce, Pr). The concentrations obtained via LA-ICP-MS were screened for anomalously high concentrations of P, La, Pr, and Nd to eliminate analyses that were potentially contaminated by fluid, melt, apatite, or other phase inclusions.

Potential crystallization temperatures of zircon were estimated using Ti-in-zircon concentrations as described by Ferry & Watson (2007). Ti content of zircon was measured via SHRIMP-RG using the ^{48}Ti isotope ($M/\Delta M = 7760$; Mazdab & Wooden, 2006) and measured via LA-ICP-MS using the ^{49}Ti isotope. For the Ti-in-zircon geothermometry we estimated a TiO_2 activity of 0.7 following previous work on arc andesite compositions (see Walker et al., 2013). If the Ti activity is estimated incorrectly the relative temperatures between zircons from the same sample should not be affected generally (Olson 2015). Additionally, underestimating the Ti activity should lead to an overestimation of the absolute temperature of no more than 50° C (Hayden and Watson, 2007).

We calculated a lower detection limit (3 σ above background) of ^{49}Ti via LA-ICP-MS on the standard NIST-612 glass to be approximately 9 ppm. This detection limit does not permit us to distinguish Ti-in-zircon temperatures from background at or below approximately 770° C using the Ferry & Watson (2007) method. Furthermore, the uncertainty in ^{49}Ti via LA-ICP-MS is ~10%. Many of the zircons analyzed via LA-ICP-MS were below the detection limit of 9 ppm. Therefore, due to the high detection limit and poor reproducibility of the standard via LA-ICP-MS these calculations are not included in our interpretation of zircon crystallization temperatures (see Appendix 7.1 for results).

RESULTS

Zircon U-Pb Geochronology

Zircons dated by LA-ICP-MS and SHRIMP-RG from Western Cascade plutons are characteristically colorless to light pink and small (30-50 by 50-150 μm typically). Zircons are euhedral acicular to equant in shape, commonly have irregular, potentially inherited cores and often contain small inclusions of apatite and glass (melt inclusions, Figure 2). Fractures are common in most zircons. Standard-corrected isotopic data were plotted on Terra-Wasserburg diagrams $^{207}Pb/^{206}Pb$ versus $^{238}U/^{206}Pb$ (Appendix Figure 4) with two standard deviations (95% confidence) percent error ellipses to identify discordant analyses ($^{207}Pb/^{206}Pb$ above concordia). Ages older than the main population, which are potentially inherited xenocrystic zircons, and ages younger than the main population, a result of post-crystallization Pb-loss, were omitted. From the remaining data I calculated a weighted mean age, standard error of the mean (reported at 2σ or 95% confidence interval), and mean square weighted deviation (MSWD). This technique yielded ages that overlap in error with the majority of previous available U-Pb zircon analyses (Bohemia dike and stock, Nimrod Stock, Yellowbottom Stock, and Detroit Dam Stock; John and Fleck, *pers. comm.* 2013, Figure 3). Nonetheless, I obtained a mean age for the mafic latite porphyry of the North Fork that is younger than and not in agreement with the 37.1 ± 0.2 Ma U-Pb zircon TIMS age reported by Smithson (2004) from the same zircon separate of sample SMR-113. Our 33.79 ± 0.46 Ma is based on the 26 (of 45 total) youngest grains analyzed which have overlapping error ellipses on the Terra-Wasserburg Concordia, but this sample contains 19 zircons with older ages of 36 to 41 Ma. The Smithson SMR-113 data includes 5 zircon ages ranging from 37.1 ± 0.2 to 35.8 ± 0.1 Ma and these ages remain the best estimate for the emplacement of the mafic latite porphyry in the North Fork district. The majority of zircon U-Pb ages reported in this study are 27 to 12 Ma (Miocene or latest Oligocene age) with the exception of the late Eocene to early Oligocene Snoqualmie North Fork intrusions of central WA. New U-Pb ages from this study are

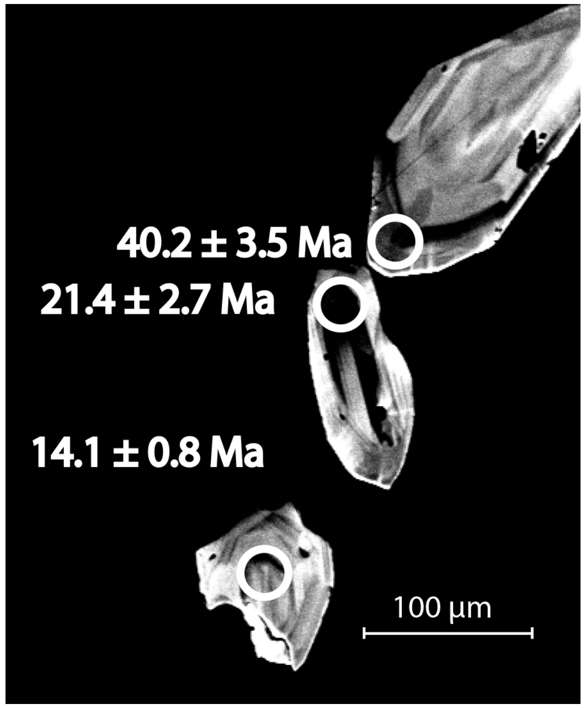

***Figure 2*:** Cathodoluminescence images of zircons from White River with three LA-ICP-MS ages (1s error) that include one 40 Ma inherited grain as compared to the mean zircon age of 18.03 ± 0.46 (2s).

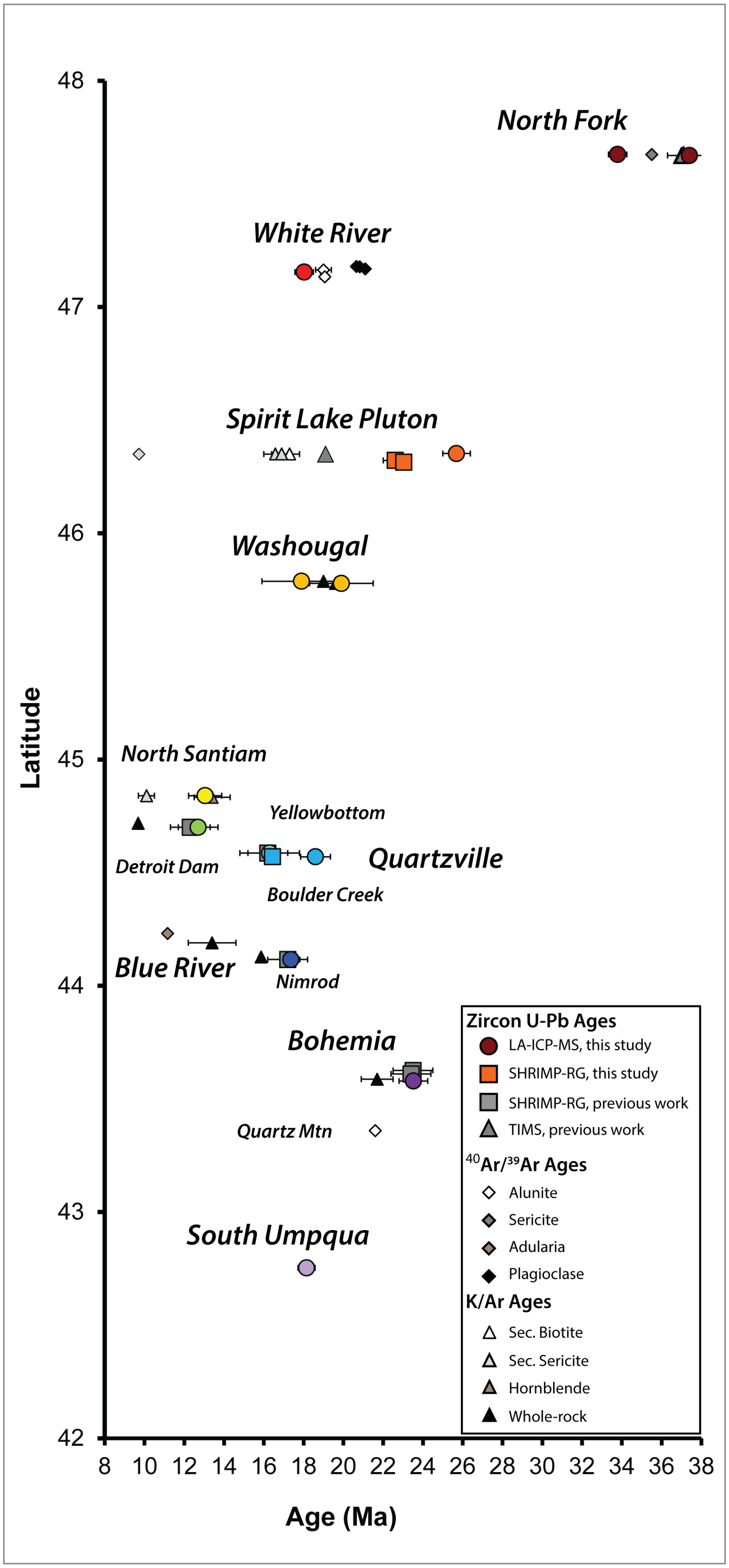

North Fork
White River
Spirit Lake Pluton
Washougal
North Santiam
Yellowbottom
Quartzville
Detroit Dam
Boulder Creek
Blue River
Nimrod
Bohemia
Quartz Mtn
South Umpqua
Latitude
48
47
46
45
44
43
42
8 10 12 14 16 18 20 22 24 26 28 30 32 34 36 38
Age (Ma)
Zircon U-Pb Ages
LA-ICP-MS, this study
SHRIMP-RG, this study
SHRIMP-RG, previous work
TIMS, previous work
40Ar/39Ar Ages
Alunite
Sericite
Adularia
Plagioclase
K/Ar Ages
Sec. Biotite
Sec. Sericite
Hornblende
Whole-rock

Figure 3 (Above): North-south variation in age of plutons and ores of the Western Cascades by Latitude including new U-Pb zircon ages (Table 2) and previously reported U-Pb zircon, $^{40}Ar/^{39}Ar$, and K-Ar ages (Appendix 4.1) for comparison.

summarized in Table 2.

In the north segment of the arc (Figure 1), mineralization at the North Fork deposit is developed in a 37.1-36.7 Ma quartz monzodiorite as well as a 37.1 to 35.8 Ma mafic latite porphyry (Smithson 2004). A new U-Pb age for the quartz monzodiorite (37.4 ± 1.1 Ma) reported here overlaps in error with these TIMS ages, but the new U-Pb age for the mafic latite porphyry (37.4 ± 1.1 Ma) is likely inaccurately young. Zircons from the monzodiorite host rock of the White River deposit crystallized 18.03 ± 0.46 Ma.

Plutonic rocks associated with deposits in the Columbia segment of the arc range from 26.49 to 12.7 Ma (Figure 2) from North to South. Three samples of the Spirit Lake Pluton, which hosts the Mt. Margaret deposit, yield ages of 25.62 ± 0.67 Ma, 22.6 ± 0.6 Ma, and 23.0 ± 0.2 Ma. Two samples from the Washougal district overlap in error at 19.9 ± 1.6 Ma and 17.9 ± 2 Ma. A porphyritic granodiorite dike from the North Santiam district yields an age of 13.05 ± 0.83 Ma, and the Detroit Dam stock immediately to the south yields 12.7 ± 1.0 Ma – the youngest age reported in this study. The Yellowbottom Granodiorite Stock and Boulder Creek granodiorite porphyry dike from the Quartzville district have ages that overlap in error at 16.3 ± 1.5 Ma and 16.4 ± 0.2 respectively. The Nimrod stock from the Blue River district is 17.36 ± 0.45 Ma.

The Central segment of the arc hosts the Bohemia mining district and South Umpqua area (Figure 1). A porphyritic quartz diorite dike from the Bohemia district has an age of 23.52 ± 0.72 Ma, and a diorite from South Umpqua is 18.2 ± 0.4 Ma.

Inherited Zircons

A total of 610 zircons were analyzed, of which 118 have ages older than the main population and are considered to be antecrystic or inherited (Table 2). Ages of inherited zircons in Western Cascade plutons range from 67.2 to 20 Ma (Figure 4). Inherited zircons are derived from the underlying crust and therefore offer a

Table 2. U-Pb Ages of Zircon

Sample	Lithology	Locality	Longitude	Latitude	Date of Analysis	Method	# of Grains	206/238 Age	2σ Error	MSWD	# Inherited†	% Inherited†
SRM01-113*	Mafic latite porphyry	Snoqualmie North Fork	-121.641	47.674	3/11/15	LA-ICP-MS	26 of 45	33.79	0.46	0.93	13	29
SRM01-108*	Qtz Monzodiorite	Snoqualmie North Fork	-121.648	47.670	3/11/15	LA-ICP-MS	25 of 45	37.40	1.1	1.40	17	38
WCOSWR-01	Ppy Monzodiorite	White River	-121.829	47.154	10/7/14	LA-ICP-MS	34 of 85	18.03	0.46	1.06	25	29
WCOS-SL-3	Ppy Granodiorite	Spirit Lake Pluton (Mt. Margaret)	-122.106	46.322	2/8/14	SHRIMP-RG	15 of 15	22.61	0.6	1.70	0	0
WCOS-SL-11	Ppy Granodiorite	Spirit Lake Pluton (Mt. Margaret)	-122.107	46.314	2/8/14	SHRIMP-RG	14 of 15	23.0	0.2	1.53	0	0
WCOS14-03	Porphyritic aplitic dike	Spirit Lake Pluton (Mt Margaret)	-122.107	46.352	3/11/15	LA-ICP-MS	26 of 45	25.69	0.69	1.30	11	24
WA-6	Granodiorite	Washougal (Silver Star)	-122.205	45.788	7/30/13	LA-ICP-MS	14 of 20	17.90	2.0	2.30	2	10
WA-11	Granodiorite	Washougal (Silver Star)	-122.040	45.779	7/30/13	LA-ICP-MS	16 of 20	19.90	1.6	0.85	1	5
WCOSJD-152	Granodiorite porphyry	North Santiam	-122.245	44.840	3/11/15	LA-ICP-MS	38 of 45	13.05	0.83	1.90	5	11
WCOS-12	Qtz diorite	Detroit Dam	-122.250	44.701	7/30/13	LA-ICP-MS	35 of 40	12.70	1.0	1.30	4	10
WCOS-2	Granodiorite porphyry	Boulder Creek (Proximal to Quartzville)	-122.383	44.570	2/8/14	SHRIMP-RG	10 of 15	16.4	0.2	1.78	4	27
WCOS-2	Granodiorite porphyry	Boulder Creek (Proximal to Quartzville)	-122.383	44.570	7/30/13	LA-ICP-MS	13 of 40	18.60	0.75	0.78	2	5
WCOS-7	Qtz diorite	Yellowbottom Stock (Proximal to Quartzville)	-122.369	44.587	7/30/13	LA-ICP-MS	18 of 38	16.30	1.5	0.39	7	18
WCOSNU-33	Granodiorite	Nimrod Stock (Blue River)	-122.439	44.116	10/7/14	LA-ICP-MS	57 of 97	17.36	0.45	2.00	4	4
WCOSNU-25	Porphyry Qz Diorite	Bohemia	-122.631	43.579	3/11/15	LA-ICP-MS	30 of 45	23.52	0.72	1.40	7	16
WCOSNU-11	Diorite	South Umpqua	-122.783	42.753	10/7/14	LA-ICP-MS	15 of 40	18.15	0.43	0.99	18	40

† error ellipse at 95% confidence of weighted mean age. Additional grains were screened as inherited on the basis of population probability plots and distinct geochemistry.

* Location Approximate

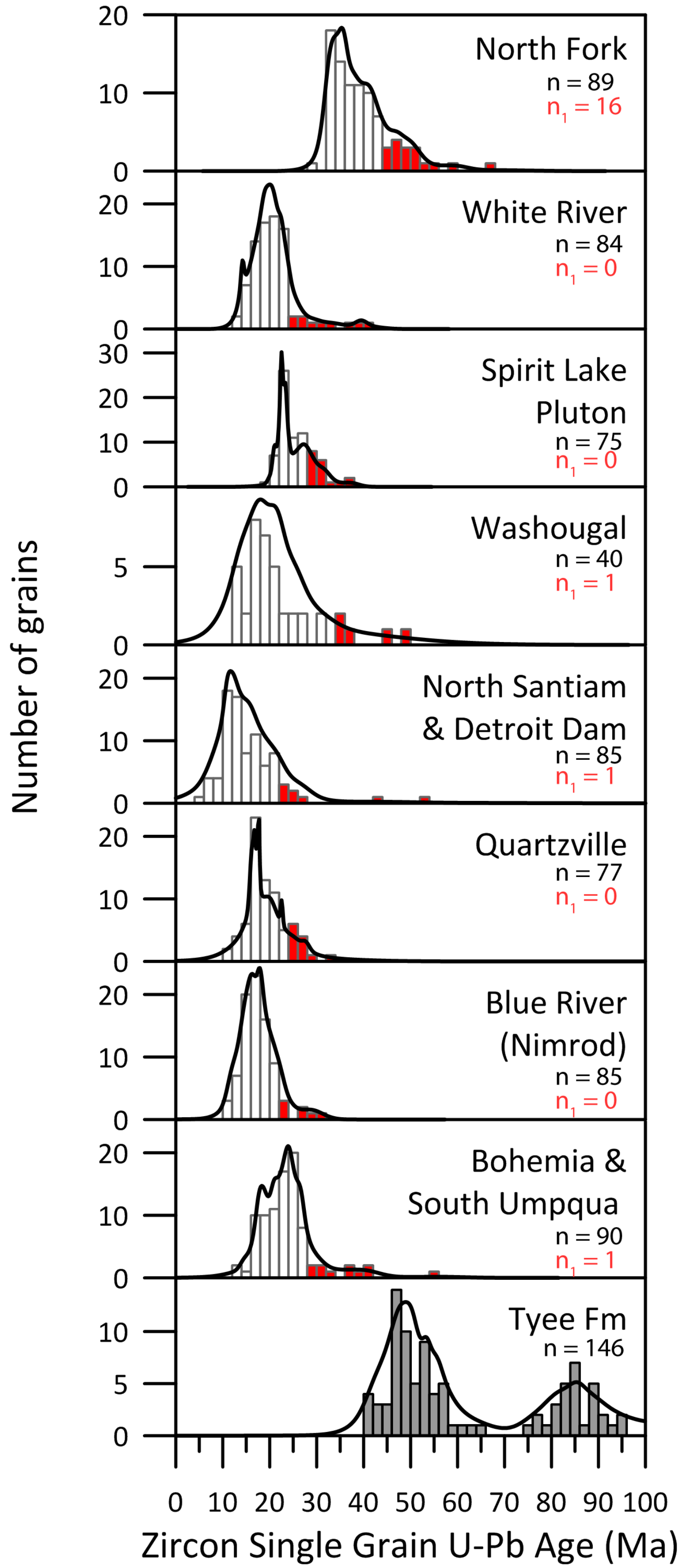

North Fork
n = 89
n_1 = 16
White River
n = 84
n_1 = 0
Spirit Lake Pluton
n = 75
n_1 = 0
Washougal
n = 40
n_1 = 1
North Santiam & Detroit Dam
n = 85
n_1 = 1
Quartzville
n = 77
n_1 = 0
Blue River (Nimrod)
n = 85
n_1 = 0
Bohemia & South Umpqua
n = 90
n_1 = 1
Tyee Fm
n = 146
Number of grains
0 10 20 30 40 50 60 70 80 90 100
Zircon Single Grain U-Pb Age (Ma)

Figure 4 (Above): Single-grain Histograms and age probability plots of Zircon U-Pb ages by Latitude, compared to <100 Ma detrital zircon ages from the Tyee Formation (Dumitru et al., 2013). Inherited ages are shown in red, defined as any grain with a calculated age including error at 95% confidence that does not overlap with the 2 standard error ellipse at 95% confidence of weighted mean age. N is the total number of grains included in each plot. N_1 is the total number of grains with ages > 45 Ma.

potential opportunity to assess the age and composition of the crust beneath the Cascades. In Western Cascade plutons, inherited zircons in most cases cannot be distinguished from the main populations via distinct textures or cores observed by cathodoluminescence imaging (Figure 2).

The north segment contains the oldest inherited zircons (up to 67 Ma). Samples from White River and North Fork districts in the north segment of the arc contain the most substantial, continuous inherited grain populations and are as young as 20.3 Ma at White River and 36.0 Ma at North Fork (Mafic Latite Porphyry) up to 67.2 Ma (n=55 of 175 grains analyzed).

In districts overlying Siletzia (the Columbia Segment), a total of 38 of the 350 grains analyzed have ages older than the main population and are considered inherited. The majority of districts within the Columbia segment (Siletzia) have no inherited grains >35 Ma with the exception of samples from Washougal, North Santiam and Detroit Dam districts, which have inherited populations between 22.0 and 53.9 Ma. These districts have sparse discontinuous inherited populations (1-2 grains) up to 54 Ma.

Districts overlying the Klamath terrane have slightly more substantial inherited zircon populations than districts overlying Siletzia but still decidedly few inherited grains (a total of 25 out of 85 grains analyzed). Samples from Bohemia and South Umpqua districts have inherited zircon populations spanning from 20.8 to 55.7 Ma with the majority of inherited ages clustered and continuous between 21 and 36 Ma.

Lithology Description & Petrography

The hypabyssal plutonic rocks represent a small area (~1%) of exposures in the Western Cascades and range in composition from diorites to granodiorites and lesser granite. In general, petrographic features include a hypidiomorphic-granular texture that ranges from equigranular to weakly or distinctly porphyritic and are consistent with shallow levels of emplacement (<5 km depth, e.g. Dilles 1987). True porphyries, characteristic of porphyry Cu-Mo-Au deposits, were sampled at North Fork, North Santiam, White River (Figure 5c) and Boulder Creek (Figure 5a), and are characterized by 50-70 vol% groundmass that ranges from aplitic to graphic texture and includes plagioclase, quartz, and alkali feldspar. The mineralogy of all granitoids includes plagioclase, alkali feldspar, quartz with accessory opaques, apatite, and trace amounts of zircon. Plagioclase is typically strongly zoned and intermediate in composition. It commonly displays sieved textures, melt inclusions zones, and overgrowths (Figure 5e) indicative of magma recharge and mixing, as is typical of intermediate composition arc magmas. In many intrusions, weak hydrothermal alteration has affected plagioclase by alteration to epidote, albite and local calcite (propylitic, Figure 5f) or alkali feldspar along fractures (potassic, Appendix Figure 3d), and in a few cases (Boulder Creek and Blue River) by sericite and pyrite (Figure 5a). Mafic silicates are also extensively replaced (Appendix Figure 3c) by actinolite, chlorite, and minor amounts of rutile or other TiO_2 polymorphs. Pseudomorphs of hornblende crystals are mainly actinolite (Appendix Figure 3b) with lesser magnetite and rutile, but hornblende is observed intact in rare instances (Figure 5d). Nonetheless, pyroxene and biotite are partially preserved. On the basis of replacement textures, the common primary mafic silicate assemblage was hornblende with local augite cores with minor biotite, which attests to relatively high water contents (>3 wt.%) of the magmas. Fe-Ti oxides, where preserved, include magnetite and ilmenite in proportion of approximately 2:1 (Figure 5b), and together with the presence of hornblende and biotite are suggestive of modest oxidation states of ~ ΔNNO of 0 to 1 (Carmichael & Nicholls, 1967).

Despite weak alteration that has certainly modified igneous alkali and alkali earth element contents, the more immobile elements (Si, Al, Ti, REE, Nb, Y, P, and transition metals) are likely modified little. Petrography from all samples is summarized in Appendix Table 2.

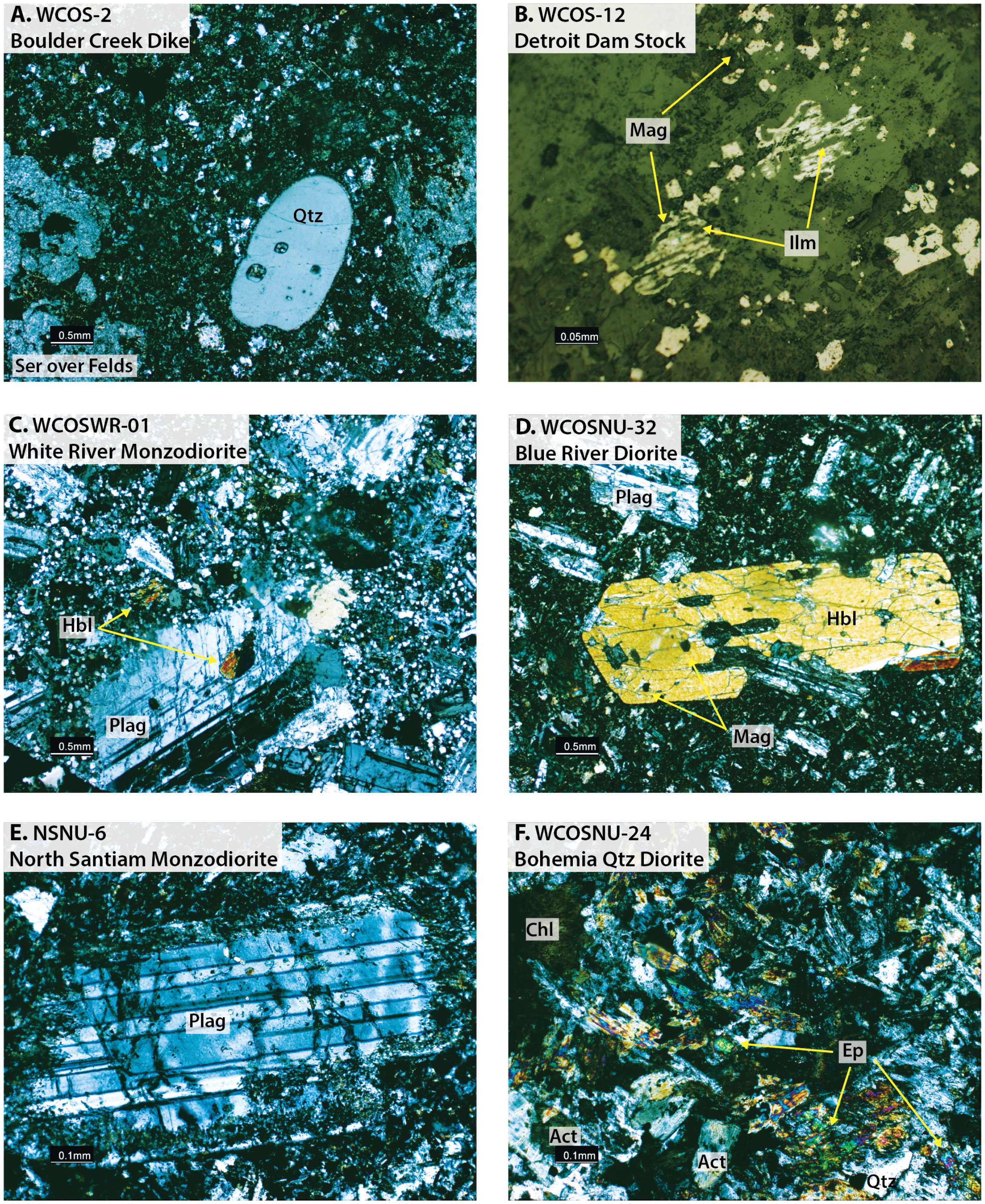

Figure 5: Photomicrographs of representative textures and mineralogy of Western Cascade plutons. Mineral phases are labeled: Actinolite - Act, Chlorite - Chl, Epidote - Ep, Feldspar - Felds, Hornblende - Hbl, Ilmenite - Ilm, Magnetite - Mag, Plagioclase - Plag, Quartz - Qtz, Sericite - Ser. Individual photomicrographs show: A) Resorbed quartz phenocrysts in porphyry dike in Boulder Creek; B) Preserved Fe-Ti-oxide pairs in Detroit Dam Stock with observed approximate magnetite: ilmenite ratio of 2:1; C) Aplitic groundmass in White River monzodiorite and a plagioclase phenocryst with small hornblende inclusion and secondary alkali-feldspar/albite veining; D) Large embayed hornblende phenocryst with magnetite inclusion in Blue River diorite porphyry; E) Heavily sieved plagioclase phenocryst in North Santiam monzodiorite porphyry; F) Representative of propylitic alteration in Western Cascades: Pervasive alteration of mafics and feldspars to actinolite + chlorite +

epidote assemblage with intact quartz. All photomicrographs are in cross-polarized light with the exception of B) which is in reflected light.

The Boulder Creek dike near Quartzville is a true granite porphyry; the texture is dominated by ~65% aplitic fine-grained groundmass that is comprised of 45% alkali feldspar, 30% quartz, 15% plagiolcase and 5% biotite. The phenocryst assemblage includes 30% plagioclase replaced by sericite (0.2-0.5 mm), 25% untwinned alkali feldspar ~75% replaced by sericite (0.1-0.5 mm), 30% anhedral biotite (0.2 mm) replaced by chlorite (80%) and sericite (20%), and 15% fresh rounded quartz with thin reaction rims (0.3-0.75 mm).

North Santiam dikes are porphyritic with 30-55% phenocrysts and range in composition from diorite to granodiorite and rare tonalite. The groundmass (45-70%) in these dikes is typically graphic and plagioclase dominated (30-65%) with alkali feldspar, quartz, mafics (typically hornblende with uncommon biotite and pyroxene) and minor opaques. The mineralogy of all granitoids in North Santiam includes plagioclase, hornblende, and alkali feldspar, and typically pyroxene and quartz with rare biotite although these phases are not ubiquitous. Mafic silicate minerals are often partially to completely replaced by actinolite + chlorite + epidote assemblages with minor local Fe-Ti oxide replacement. Plagioclase are typically intact with localized secondary epidote, albite, and alkali feldspar replacement with rare calcite – although, sieved textures, melt inclusion zones and growth rims are observed in all samples. Secondary replacement of the groundmass is typically less pervasive than that of the phenocrysts and is limited to the mafic phases. Disseminated pyrite is common.

Whole Rock Geochemistry

As noted by du Bray & John (2011), plutonic samples from the Western Cascades have a more limited geochemical compositional range and lack mafic compositions compared to the associated volcanic rocks. They are generally calc-alkaline in nature (Figure 6). Most Western Cascade volcanics are calc-alkaline but tholeiitic rocks are well represented, particularly in southwestern Washington (45-36 Ma) and the southern Cascades (7-4 Ma, du Bray & John 2011). Essentially all

Western Cascade volcanic rocks and plutons are subalkaline (Irvine & Baragar 1971; du Bray & John 2011, Figure 4). With the exception of the North Fork district, all the plutons in this study are Miocene, whereas Western Cascade volcanics range from Eocene to Miocene. SiO_2 concentrations in volcanic rocks range from 47-77 wt. %, whereas most plutonic rocks have elevated SiO_2 contents (>~60 wt. %).

There is a temporal trend in Western Cascade volcanics, from mafic to diverse to mafic. Late Eocene and early Miocene volcanics (45-25 Ma) range from basalts to andesites (47-60 wt. % SiO_2). The earliest magmatism in the arc (45-36 Ma) is dominantly focused in southwestern Washington; the subsequent phase of magmatism, from 35 to 26 Ma, covered nearly the length of the arc, but remained primarily basaltic and andesitic with some dacitic and rhyolitic compositions in southern Oregon. Volcanics between 25-18 Ma range from 50-77 wt. % SiO_2 and cover the largest area of the arc. This phase of magmatism is considered the most compositionally diverse and spans the full length of the arc. 17-8 Ma volcanics are dominantly basaltic andesite and andesite. Finally, the youngest age group (7-4 Ma) is dominantly basalt or basaltic andesite and is mostly found in the southern Oregon and northern California portion of the arc. The majority of older samples (45-26 Ma) included in du Bray & John (2011) are relatively primitive, iron-enriched, and tholeiitic. In contrast, with the exception of the youngest age group (7-4 Ma), which is mafic, tholeiitic, the majority of younger samples (25-8 Ma) are more evolved, magnesium enriched, and calc-alkaline in nature.

Although hydrothermal alteration is widespread in all districts there is little geochemical evidence that alkali earth element concentrations were modified substantially by weathering and alteration processes. In Western Cascade magmas Ba generally acts very incompatibly and increases steadily with increasing SiO_2 content (Figure 7a). Similarly, Sr acts compatibly by decreasing with increasing SiO_2 content and is likely incorporated into plagioclase (Figure 9e). There are no apparent extreme additions or removals of Ba or Sr geochemically by hydrothermal alteration in samples from any district. Despite the presence of substantial hydrothermal alteration (Figure 5f) and weathering within the Western Cascades, these data are likely robust enough to include in geochemical interpretations. I focus

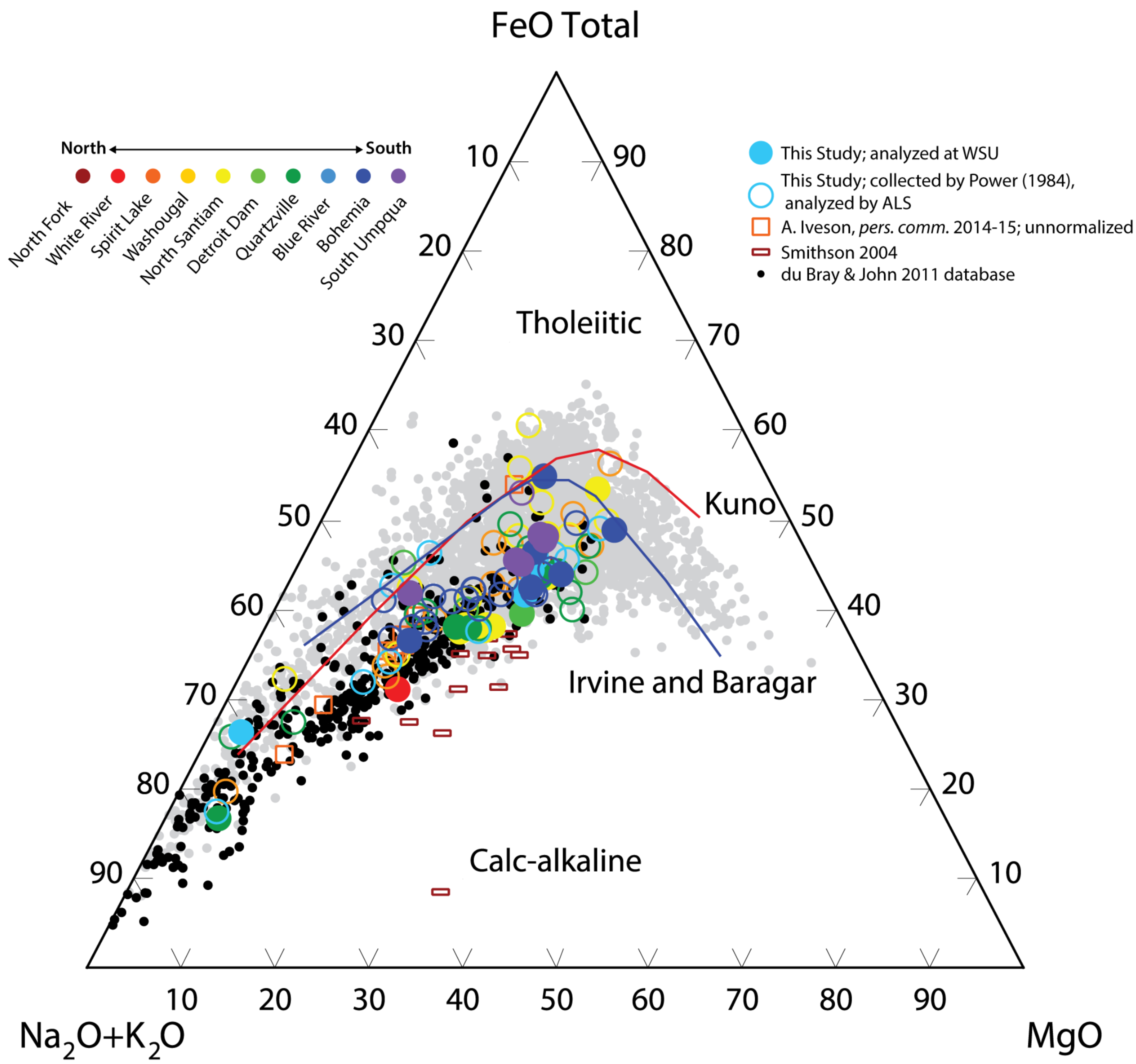

Figure 6: AFM Diagram. Samples collected by the author were analyzed via ICP-MS and XRF at WSU (Appendix 6.1), samples collected by S. Powers (1984) were analyzed in 2014 by Four-Acid ICP-MS by ALS (Appendix 6.2). Gray symbols are all volcanic samples from the du Bray & John (2011), whereas black samples are all plutonic samples.

here on relationships of Ba and Nb as mantle and slab fluid tracers, of Th and Ta as crust and mantle tracers, of Sc and V as fractionation of mafic silicates and relative oxidation states tracers, of Sr and Y as tracers of magmatic water contents, and of REEs as tracers of fractionation of various phases.

Ba and Nb both generally increase with SiO_2 in each suite. Some low values of Ba (< 200 ppm) at elevated SiO_2 are lower than expected of alkali feldspar fractionation and may potentially be affected by alteration. Ba in the south is generally slightly higher, at given SiO_2, than in the north. In contrast, Nb contents are generally lower in the south than in the north, at given SiO_2 and overall (ie., 3.4-7.05 ppm in South Umpqua samples, 8-19.74 ppm in Spirit Lake Pluton samples) (Figure 7b). Ba/Nb values are not obviously influenced by SiO_2 content from any given district (Fig. 7c) and remain stable as magmas evolve, but tend to increase at any given SiO_2 content from north to south (Figure 8).

Both Th and Ta contents increase with SiO_2 content (Figure 7d,e), with the highest Ta (up to 1.2 ppm) found in the northern districts at any given SiO_2 content. Th increases moderately with SiO_2 at more mafic compositions but shifts to a greater rate of increase around SiO_2 contents of 64 wt.%. Th/Ta ratios range from 1 to 24 and are lowest in the mid-latitude districts (North Santiam, Detroit Dam, Quartzville, and Blue River, Figure 7f). Th/Ta ratios notably increase with SiO_2 (Figure 7f). It should be noted that some Spirit Lake Pluton samples (Iveson, *pers. comm.*, 2014-15) have anomalously elevated concentrations of Nb, Th, and Sc and will not be included in petrogenetic interpretations.

Sc contents of Western Cascade plutons decrease with increasing SiO_2 content in any given district (Figure 9a) and tend to increase from north to south along the arc (Figure 9b). V also acts incompatibly and decreases from ~250 ppm to ~20 ppm with increasing SiO_2 content (Figure 9d). However, V is less variable from north to south and only increases slightly and irregularly to the north. V/Sc ratios decrease with increasing SiO_2, from between 7 and 11 at SiO_2 of 52-60 wt. % to

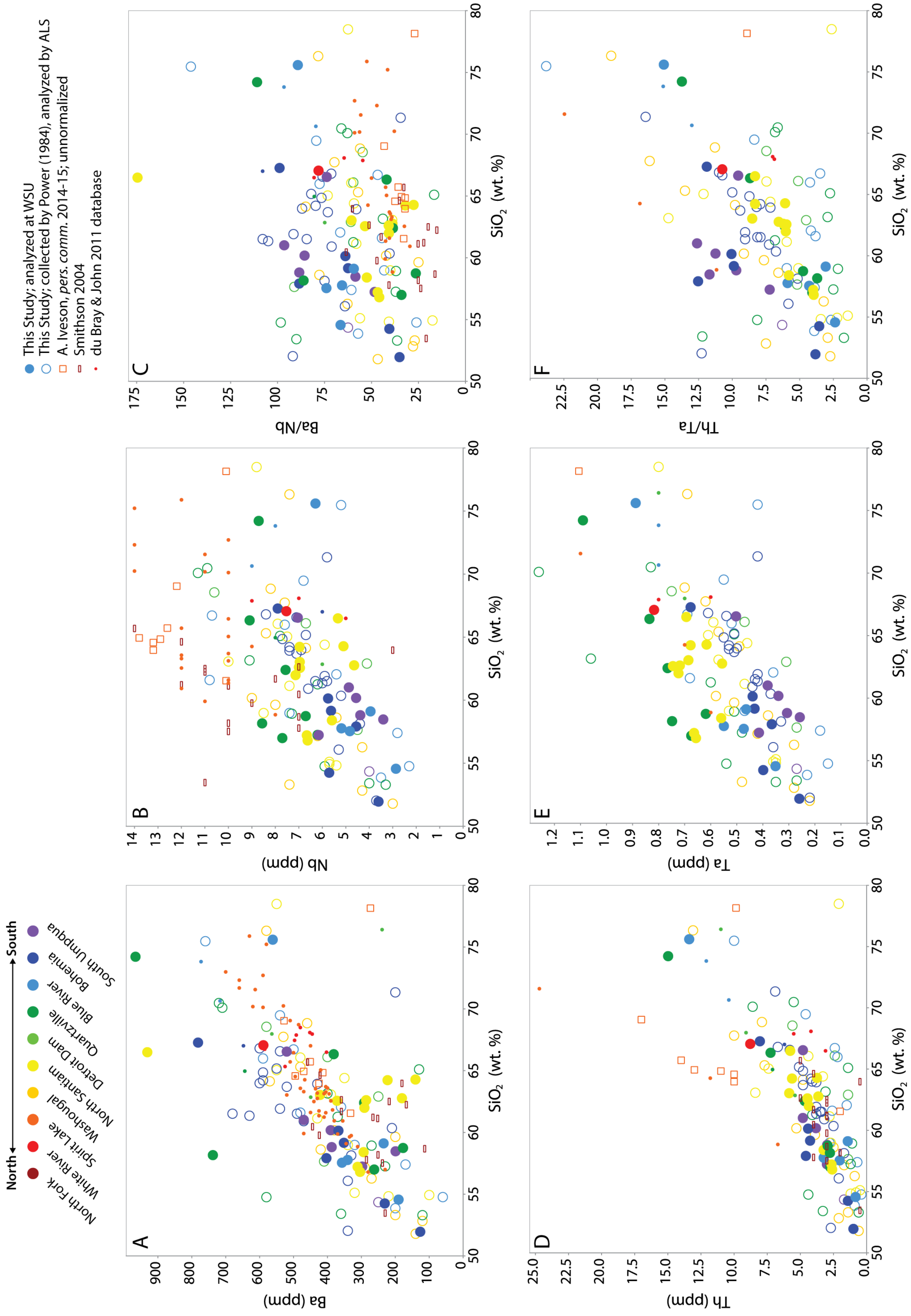
North
South
North Fork
White River
Spirit Lake
Washougal
North Santiam
Detroit Dam
Quartzville
Blue River
Bohemia
South Umpqua
This Study; analyzed at WSU
This Study; collected by Power (1984), analyzed by ALS
A. Iveson, pers. comm. 2014-15; unnormalized
Smithson 2004
du Bray & John 2011 database
A
B
C
D
E
F
Ba (ppm)
Nb (ppm)
Ba/Nb
Th (ppm)
Ta (ppm)
Th/Ta
SiO2 (wt. %)

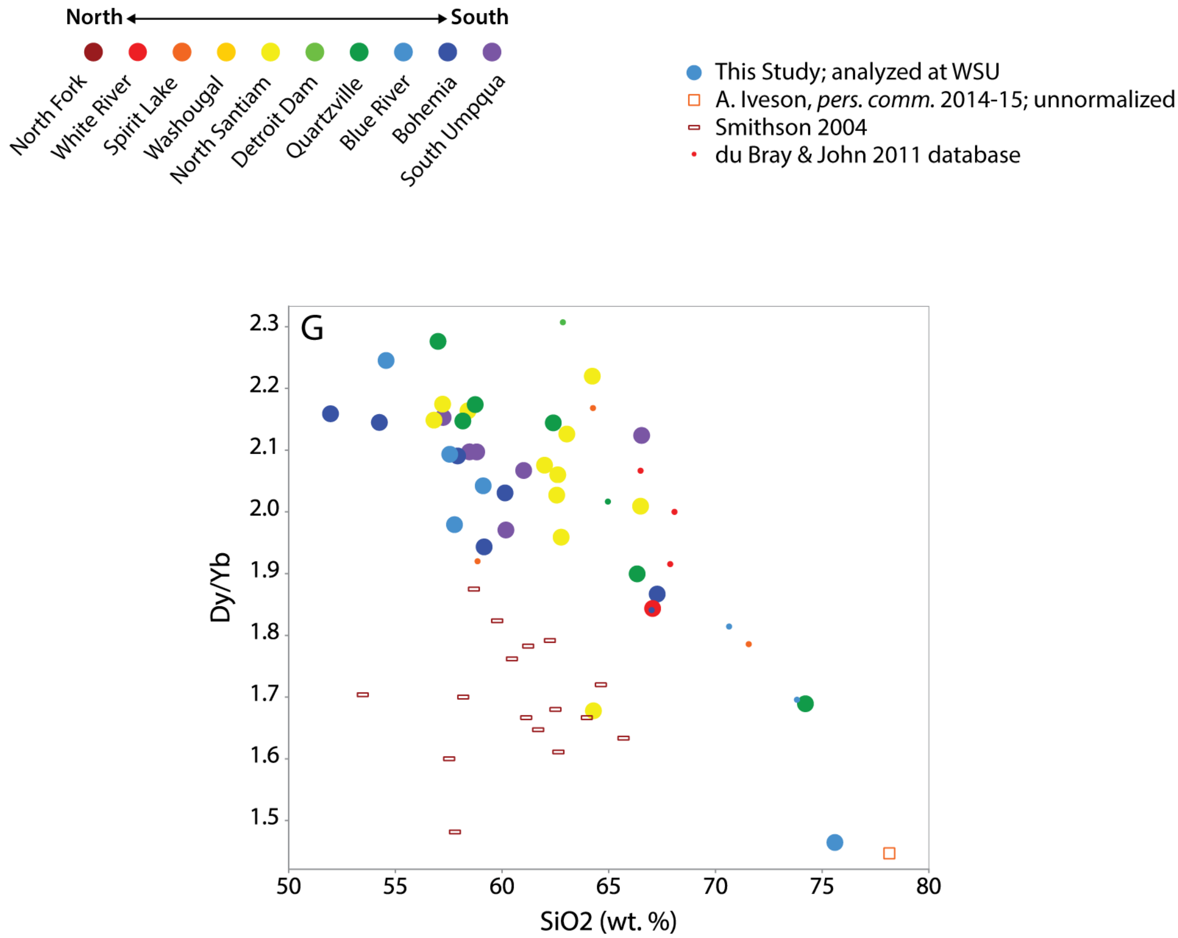

Figure 7 (Above): Trace Element Diagrams. A) SiO_2 vs. Ba; B) SiO_2 vs. Nb; C) SiO_2 vs. Ba/Nb; D) SiO_2 vs. Th; E) SiO_2 vs. Ta; F) SiO_2 vs. Th/Ta; G) SiO_2 vs. Dy/Yb. Data from the du Bray & John database (2011) include: White River samples from Thompson (1983) and du Bray, *unpublished* data, 2005; Spirit Lake Pluton samples from Evarts, *unpublished data*, 2005; Washougal samples from Schriener (1978), Felts (1939), USGS National Geochemical Database, 2005, Shepard (1979), Power (1984), and Evarts, *unpublished data*, 2005; North Santiam samples from Olson (1978); Detroit Dam samples from Power (1984), Curless (1991), du Bray, *unpublished data*, 2005, Lexa, *unpublished data,* 2005, and USGS National Geochemical Database, 2005; Quartzville samples from Munts (1978) and du Bray, *unpublished data*, 2005; Blue River samples from Storch (1978); Bohemia samples from Buddington & Callahan (1936), Schaubs (1978), and du Bray, *unpublished data*, 2005.

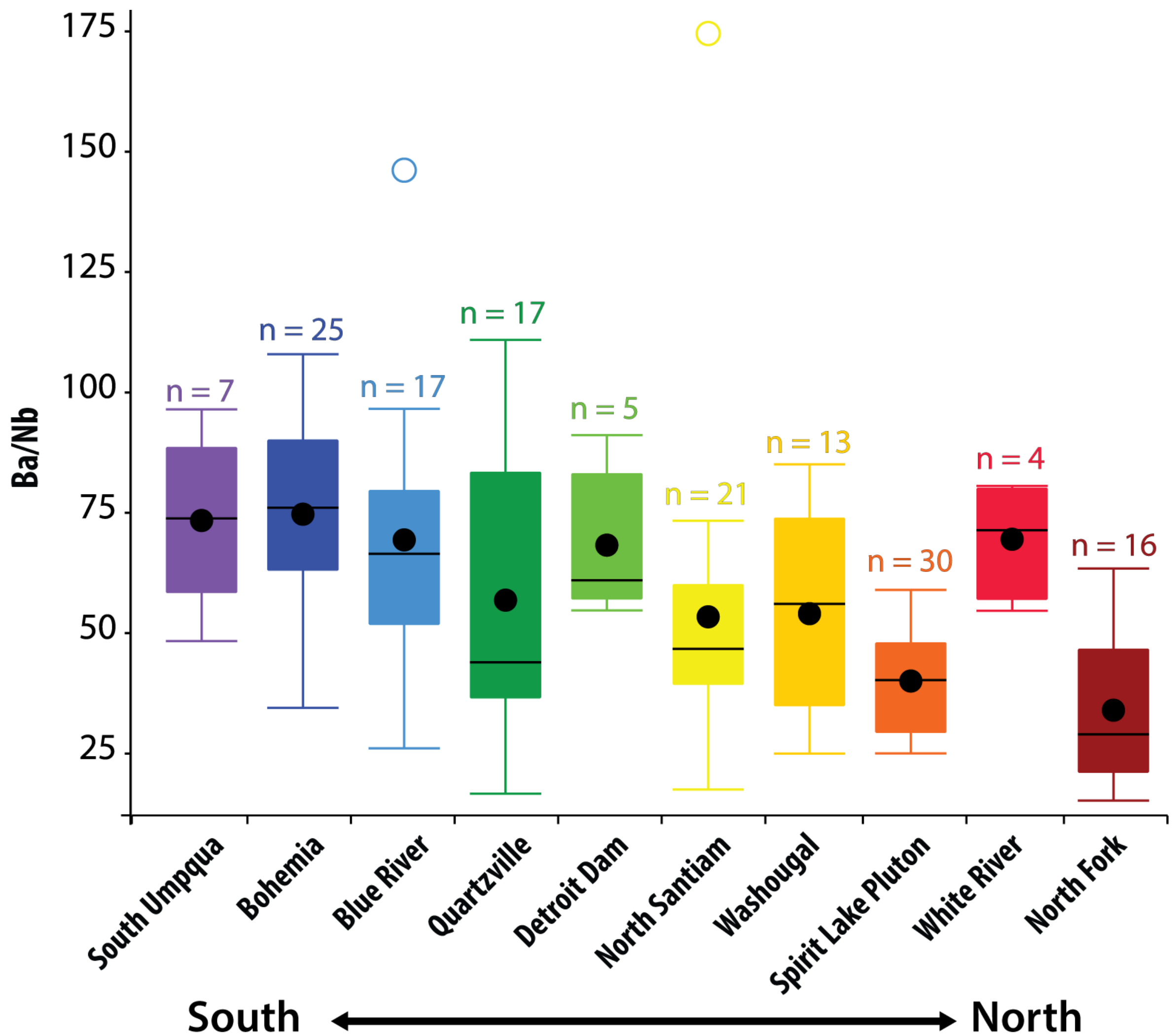

Figure 8: Ba/Nb Boxplots by Latitude. 25%, 50%, and 75% values define box units, medians shown as black dots. Whiskers are minimum and maximum with outliers >1.5 of the Quartile value are shown separately. n here is the number of combined analyses incorporated into the boxplot.

between 0 and 6 at SiO_2 of ~75 wt. %, with the exception of samples of the Spirit Lake Pluton (Figure 9c). In general, V/Sc values slightly increase from south to north at any given SiO_2 content.

Sr concentrations decrease smoothly with increasing SiO_2 within any given district, suggesting compatible behavior. Despite the fluid-mobile nature of Sr, these data are likely robust enough to be included in this study. We consider that extremely elevated (> ~550 ppm) and reduced (<100 ppm) Sr concentrations can be disregarded as potentially a result of alteration. Western Cascades samples display large ranges in Sr/Y values in more mafic compositions (~15-80). The Sr/Y range decreases and narrows to 1-15 in more evolved compositions (ie. 74 wt. % SiO_2, Figure 9f).

As SiO_2 contents increase in Western Cascade plutons, chondrite-normalized REE patterns steepen and transition from elevated Eu anomalies (chondrite-normalized Eu/Eu* values) corresponding to small negative Eu anomalies (between 1 and 1.15 at SiO_2 between 52 and 56 wt. %) and lower light REE (LREE) contents (2.5-20 ppm in the same SiO_2 range) to larger negative Eu anomalies and higher LREE contents, with Eu/Eu* between 0.7 and 1.0 and La contents between 10 and 35 ppm at SiO_2 >73 wt. % (Figure 10, Appendix Figure 5a). Dy contents experience more variability than Yb in Western Cascade plutons and range from 1 to 5.4 ppm. In Western Cascade plutons, Dy/Yb values range from 1.44 to 2.31 and decrease with increasing SiO_2 contents with the exception of the North Fork District (Figure 7g).

Trace Elements in Zircon

Zircons from all 16 samples analyzed for U-Pb ages were also analyzed for Hf, Y, and REE compositions. The Eu_N/Eu_N^* chondrite-normalized ratio is a measure of the magnitude of the negative Eu anomaly in zircon REE trends calculated by the ratio of the measured Eu content to the predicted Eu content based on the adjacent REE, e.g. $Eu_N^* = (Sm_N*Gd_N)^{0.5}$. The chondrite-normalized Ce/Nd ratio is a measure of the magnitude of the positive Ce anomaly in zircon REE trends as calculated by the ratio

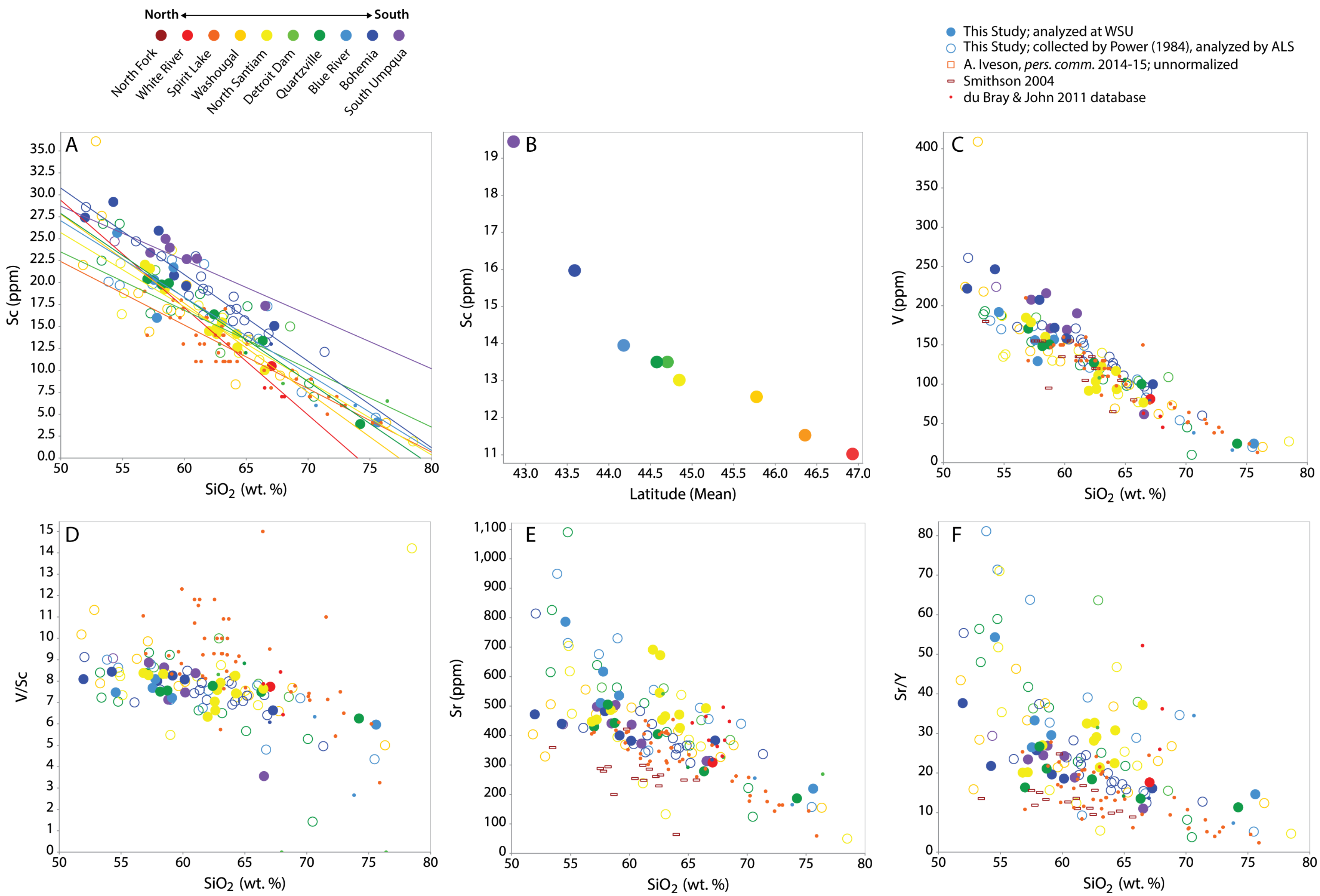

North
South
North Fork
White River
Spirit Lake
Washougal
North Santiam
Detroit Dam
Quartzville
Blue River
Bohemia
South Umpqua
This Study; analyzed at WSU
This Study; collected by Power (1984), analyzed by ALS
A. Iveson, pers. comm. 2014-15; unnormalized
Smithson 2004
du Bray & John 2011 database
A
B
C
D
E
F
Sc (ppm)
V (ppm)
V/Sc
Sr (ppm)
Sr/Y
SiO2 (wt. %)
Latitude (Mean)

Figure 9 (Above): Sc A) vs. SiO_2 (with best-fit lines for each district), and B) by Latitude (Sc at SiO_2 = 65). C) V/Sc vs. SiO_2; D) V vs. SiO_2; E) Sr vs. SiO_2, and F) Sr/Y vs. SiO_2. Data from the du Bray & John database (2011) include: White River samples from Thompson (1983) and du Bray, *unpublished* data, 2005; Spirit Lake Pluton samples from Evarts, *unpublished data*, 2005; Washougal samples from Schriener (1978), Felts (1939), USGS National Geochemical Database, 2005, Shepard (1979), Power (1984), and Evarts, *unpublished data*, 2005; North Santiam samples from Olson (1978); Detroit Dam samples from Power (1984), Curless (1991), du Bray, *unpublished data*, 2005, Lexa, *unpublished data,* 2005, and USGS National Geochemical Database, 2005; Quartzville samples from Munts (1978) and du Bray, *unpublished data*, 2005; Blue River samples from Storch (1978); Bohemia samples from Buddington & Callahan (1936), Schaubs (1978), and du Bray, *unpublished data*, 2005.

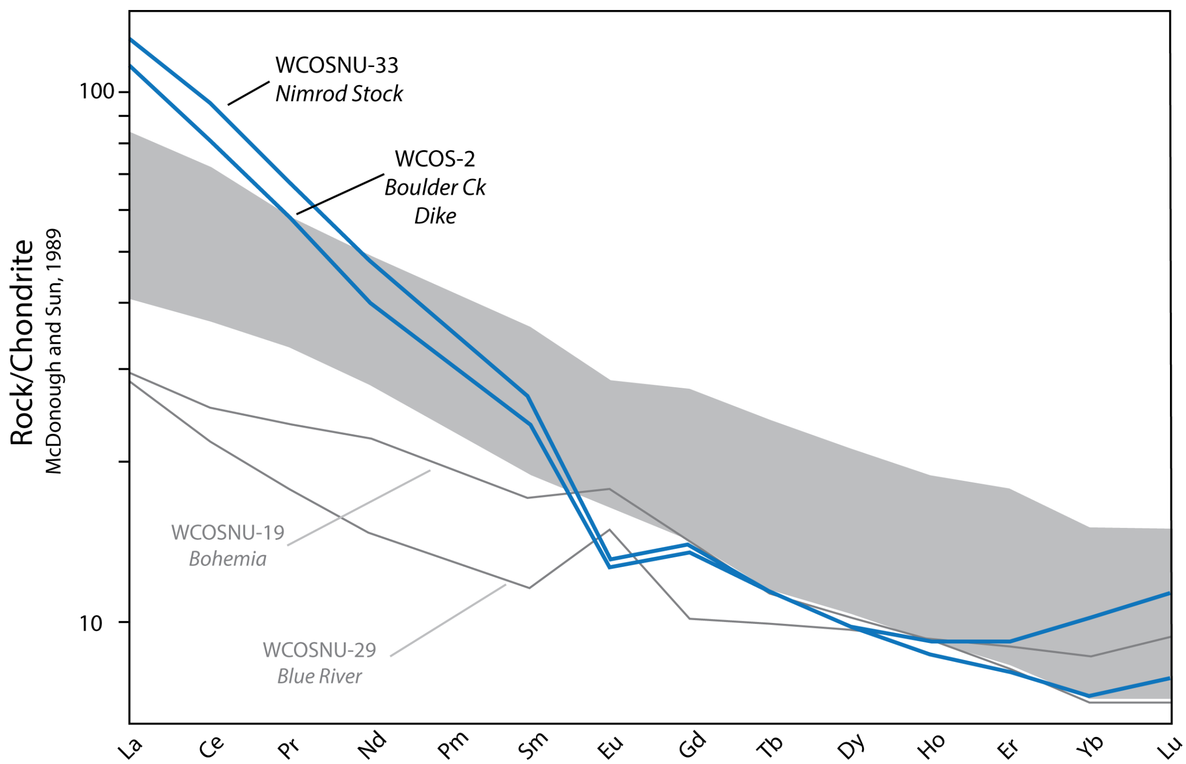

Figure 10: Rare Earth Element Diagram. Samples shown are only those from this study. Grey field represents all samples with SiO_2 < 68 wt. %. Blue trends are data from only two samples with SiO_2 > 74 wt. %: the Boulder Creek Dike near Quartzville and the Nimrod Stock near Blue River.

of measured Ce content to the measured Nd content. Zircons crystallized from oxidized magmas (>NNO +1) display small negative Eu anomalies (Eu_N/Eu_N* values of 0.4-1.0) and large positive Ce anomalies (Ce/Nd > 30) (Ballard et al., 2002; Dilles et al., 2015; Olson 2015).

Zircons in Western Cascades plutonic rocks have characteristically large negative Eu anomalies ($Eu_N/Eu_N* < 0.5$; Figure 11a) and small positive Ce anomalies (Ce/Nd < 30 typically; Figure 11b), even when directly associated with moderate economic porphyry Cu deposits (ie. mafic latite porphyry in North Fork district). All zircon grains analyzed from all deposits have Eu_N/Eu_N* values between 0 and 0.5. With the exception of five grains from the Boulder Creek dike near Quartzville and two grains from the White River monzodiorite with Ce/Nd > 30, the majority of grains have Ce/Nd values between 0.1 and 30. In general, Eu_N/Eu_N* ratios from each sample decrease systematically with increasing Hf content. In general, Ce/Nd ratios increase to higher values with increase of Hf content, which is a proxy for progressive crystallization of melt and zircon (Clairborne et al., 2010) .

Th/U of zircon typically decreases with increasing Hf content in zircon and can trace differentiation or crystallization of magmas. High Th/U ratios (up to 4.5) in zircon are related to more mafic, less evolved, higher temperature melts, and low Th/U ratios (<1.5) are associated with evolved, fractionated, cooler melts (Claiborne et al., 2010). Yb/Gd ratios in zircon tend to increase with increasing Hf content (Lee 2008) likely due to fractionation of phases with high affinity for MREEs such as amphibole, pyroxene, or apatite. Yb/Gd can also be initially low due to fractionation of Yb-enriched garnet from the magma. Th/U ratios vs. Yb/Gd ratios in zircon can therefore be used to distinguish between fractionation and potential mixing trends. Low Th/U and high Yb/Gd ratios are characteristic of fractionated melts. Western Cascades plutonic zircons exhibit a typically limited range in zircon compositions with a range of Th/U ratios from 0.25 to ~2. Yb/Gd ratios in zircons from Western Cascade plutons typically range from 10 to 35 (Figure 11c).

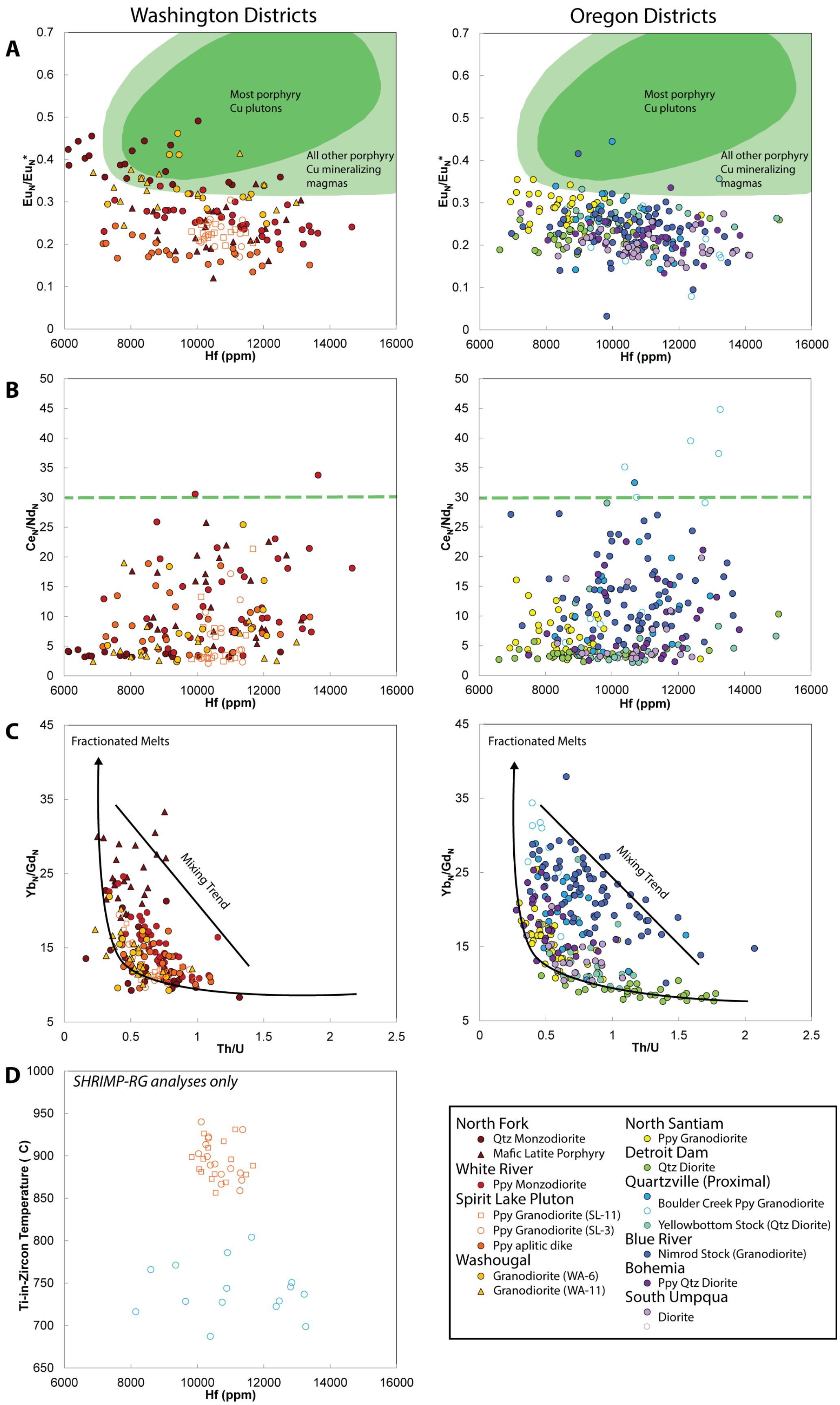

Washington Districts
Oregon Districts
A
B
C
D
Most porphyry Cu plutons
All other porphyry Cu mineralizing magmas
Eu_N/Eu_N^*
Ce_N/Nd_N
Yb_N/Gd_N
Hf (ppm)
Th/U
Fractionated Melts
Mixing Trend
SHRIMP-RG analyses only
Ti-in-Zircon Temperature (°C)
North Fork
Qtz Monzodiorite
Mafic Latite Porphyry
White River
Ppy Monzodiorite
Spirit Lake Pluton
Ppy Granodiorite (SL-11)
Ppy Granodiorite (SL-3)
Ppy aplitic dike
Washougal
Granodiorite (WA-6)
Granodiorite (WA-11)
North Santiam
Ppy Granodiorite
Detroit Dam
Qtz Diorite
Quartzville (Proximal)
Boulder Creek Ppy Granodiorite
Yellowbottom Stock (Qtz Diorite)
Blue River
Nimrod Stock (Granodiorite)
Bohemia
Ppy Qtz Diorite
South Umpqua
Diorite

Figure 11: Zircon Trace Element versus Hf content: A) Eu/Eu* and B) Ce/Nd. C) Th/U vs. Yb/Gd; and D) Hf vs. Ti-in-zircon in ° Celsius for SHRIMP-RG analyses only. Open symbols are zircons analyzed via SHRIMP-RG, closed symbols are analyzed via LA-ICP-MS. Eu, Eu*, Ce, Nd, Yb, and Yb values are chondrite-normalized (Anders & Grevesse, 1989). Green fields in A) & B) are interpreted from Dilles et al., 2015. Mixing and fractionation trends (black) on C) are interpreted from Lee (2008) and Claiborne et al., 2010. Ti-in-zircon temperatures calculated using Ferry & Watson method (2007) and an estimated Ti activity of 0.7.

Ti-in-Zircon and Thermometry

Ti^{48} concentrations in zircons analyzed by SHRIMP-RG range from 20.2 to 39.7 in Spirit Lake Pluton samples and from 3.6 to 12.6 in the Boulder Creek dike sample. Crystallization temperatures estimated by Ti-in-zircon thermometry for Western Cascade zircon analyzed by SHRIMP-RG are between 675 and 950°C (Figure 11d). The Boulder Creek porphyry near Quartzville is a porphyry intrusion (Figure 5a, Appendix Figure 3a) and has lower estimated temperatures between 675-800 °C than the Spirit Lake Pluton hypabyssal granodiorite, which have a limited range of temperatures between 850 and 950 °C. Ti-in-zircon thermometry for LA-ICP-MS analyses are summarized in Appendix 7.1.

DISCUSSION

I compare new U-Pb zircon ages with previously reported ages of plutonism and hydrothermal mineralization in the Western Cascades (Appendix 3). I then consider the implications for the underlying crust based on inherited zircon populations before considering Western Cascades' magma genesis and ore fertility.

U-Pb Ages & Along-Arc Magmatic History of the Western Cascades Plutons

Du Bray & John (2011) concluded that the majority of intrusions in the Western Cascade arc were emplaced between 25 and 8 Ma, but here we have further temporally constrained the emplacement of plutons along arc. With the exception of the North Fork deposit, all plutonic rocks we sampled were emplaced between 26 and 12.7 Ma (Figure 3). The majority of plutons presented here were emplaced in a 10 m.y. span between ~26 and ~16 Ma. The youngest ages are clustered in the center of the arc, with older and more diverse ages found in the north and south segments.

In the north segment of the arc, the emplacement ages of the quartz monzodiorite and late mafic latite porphyry from the North Fork deposit support a duration of magmatism of at least one m.y. in the district. Smithson's (2004) ages for the quartz monzodiorite (37.0 ± 0.2 Ma and 37.2 ± 0.1 Ma) and the mafic latite porphyry (36.8 ± 0.2 Ma and 37.1 ± 0.2 Ma) also suggest some plutonic rocks were present in the northern portion of the arc during the earliest (44-26 Ma) phase of ancestral arc magmatism (du Bray & John 2011).

A monzodiorite from the White River deposit is approximately 15 m.y. younger and within the phase of ancestral arc magmatism when plutonic rocks were most dominant (25-18 Ma; du Bray & John, 2011). Our monzodiorite age of 18.03 ± 0.46 Ma substantially postdates $^{40}Ar/^{39}Ar$ ages on plagioclase from the Fifes Peak Formation, the older volcanic rocks of the area (21.1-20.65 Ma, Blakely et al., 2007). However, the zircon crystallization age we report only slightly postdates and nearly overlaps in error previously reported $^{40}Ar/^{39}Ar$ ages from alunite resulting from hydrothermal alteration of the Fifes Peak Formation (19.06-19.0 Ma, Blakely et al., 2007). This hydrothermal alteration could be related to emplacement of the monzodiorite. The age data also suggest 2-3 m.y. of magmatic emplacement in the White River district.

In the Columbia segment of the arc, the zircon U-Pb ages from three samples of the Spirit Lake Pluton reported here are 25.69 ± 0.69 Ma, 23.04 ± 0.2 Ma, and 22.61 ± 0.6 Ma. These ages substantially predate previously reported alteration ages, which include K-Ar analyses of secondary biotite and secondary sericite and range from 17.3 ± 0.5 Ma to 16.6 ± 0.5 Ma (Evarts et al., 1987; Evarts & Ashley 1993). The discordance between these age groups cannot be attributed solely to long-lived (approximately 9 m.y.) magmatism or analytical error. Therefore it is likely we report ages from plutonic rocks that are older and likely unrelated to porphyry Cu mineralization in the Mt. Margaret district.

Two U-Pb zircon ages of samples from the Washougal district overlap in error at ~19 Ma. Two previously reported K-Ar ages of fresh granodiorite (19.6 ± 0.7 Ma) and granodiorite completely replaced by secondary minerals (quartz + sericite + tourmaline + pyrite; K-Ar of sericite of 19.0 ± 0.7 Ma) from the Washougal district are consistent with the ages we report here, suggesting pluton emplacement and hydrothermal alteration both occurred ca. 19 Ma (Power et al., 1981).

Both the Spirit Lake and Washougal plutons predate the onset of Columbia River Basalt (CRB) volcanism, however, the North Santiam and Detroit Dam districts in the center of the arc (Figure 3) are the youngest intrusions at 13.05 ± 0.83 Ma and 12.70 ± 1.00 Ma, respectively, and the only plutons to postdate the most voluminous phase of CRB magmatism (Barry et al., 2013). A hornblende K-Ar age of 13.4 ± 0.9 Ma on fresh granodiorite from the North Santiam district is consistent with the 13.05 ± 0.83 Ma zircon U-Pb age we report here (Power et al., 1981). A previously reported K-Ar age of 10.1 ± 0.4 Ma on hydrothermal sericite from the Bornite Breccia Pipe in the North Santiam district (Winters 1985) could suggest approximately three m.y. of hydrothermal alteration associated with magmatism, or may be spuriously too young. In the Detroit Dam district, a previously reported whole-rock K-Ar age of 9.68 ± 0.18 Ma (Sutter 1978) from the same diorite for which we obtained a 12.70 ± 1 Ma age is likely too young, as whole-rock K-Ar ages would be impacted by the amount of hydrothermal alteration present.

The Yellowbottom stock and Boulder Creek porphyry of the Quartzville district were both emplaced nearly simultaneously at 16.30 ± 1.5 Ma (16.2 ± 0.3 Ma, John and Fleck, *pers. comm.* 2013) and 16.44 ± 0.20 Ma, respectively, with the onset of CRB magmatism. The Boulder Creek porphyry is associated with sericitic alteration, breccia pipes, and polymetallic Zn-Pb-Cu-bearing veins (Nicholson 1988), and therefore our new age provides evidence for porphyry style mineralization locally. No other known ages exist on hydrothermal alteration from the Quartzville district.

The Nimrod stock of the Blue River district (U-Pb zircon = 17.36 ± 0.45 Ma) overlaps in error with Quartzville samples, which suggests there was concurrent magmatism 50 km to the south. The discrepancy between our U-Pb zircon age and a previously reported whole-rock K-Ar age of 15.86 ± 0.18 Ma (Sutter 1978) on the Nimrod stock is likely due to analytical error in both dating methods. A whole-rock K-Ar on quartz diorite of the Blue River district of 13.4 ± 1.2 Ma (Power et al., 1981) and a nearly-overlapping $^{40}Ar/^{39}Ar$ adularia age of 11.16 ± 0.14 Ma from Quartz + Adularia veins (R. Fleck, *pers comm.* 2006) suggest a younger stage of magmatism and related hydrothermal alteration similar to age of magmatism in Detroit Dam and North Santiam districts discussed above.

In the southern segment, samples of a stock and two dikes from the Bohemia district yield overlapping ages of approximately 23.5 Ma, consistent with short-lived magmatism in this district (Figure 3, Fleck & du Bray, *pers. comm*., 2013). These ages are comparable to the age of plutonism at Spirit Lake described above (25.69 Ma to 22.6 Ma), as well as the 21.6 Ma $^{40}Ar/^{39}Ar$ alunite age from Quartz Mountain ~25 km to the south (du Bray & John 2011). A whole-rock K-Ar age of 21.7 ± 0.8 Ma on porphyrtic quartz diorite from the Bohemia district (Power et al., 1981) nearly overlaps in error with the zircon U-Pb age, further extending this 26-~22 Ma interval of plutonism.

The diorite pluton we analyzed from the South Umpqua district crystallized zircon at 18.15 ± 0.43 Ma, approximately 5 m.y. after the Bohemia plutonism. No known hydrothermal ages exist for the South Umpqua area.

Plutons from White River, Washougal, Quartzville, Blue River, and South Umpqua districts were emplaced at very similar ages circa 18-16 Ma, suggesting that plutonism was very active along the entire arc at this time.

Inherited Zircons & Evidence for Age of Underlying Crust

Zircons predating the age of crystallization of a given pluton are interpreted as xenocrysts from the crust or as antecrysts derived from an earlier phase of magmatism or crystal-melt mush (Miller et al., 2007). These older zircons provide a window into the crust underlying the Western Cascade arc, and into the nature of crustal contamination required to produce evolved magma compositions in the Miocene Western Cascade arc magmas.

Inherited zircons could be sourced from older Western Cascade volcanics (~42-25 Ma) such as the Naches and Ohanapecosh Formations described below. Another potential contaminant is the Tyee Formation (~48-45 Ma), a sequence of turbiditic sandstone containing Eocene and older detrital zircons derived from sources to the east including the Challis volcanics and the Idaho Batholith (Dumitru et al., 2013). A final possibility is these inherited zircons are directly sourced from older crustal material that may underlie the arc, such as the Clarno Formation (53-43, Robinson et al., 1990). Zircon is an accessory mineral that only forms in substantial amounts when Zr occur in relatively evolved magmas of dioritic-andesitic or more silicic composition. Therefore, it is unlikely that basaltic rocks of the early Western Cascades such as the Kalama Formation of southern Washington (Evarts & Ashley, 1991) would be the source of significant zircon contamination.

In the North Segment, 55 (of 175 total, or 31%) xenocrystic zircons have inherited ages up to 67 Ma (> 20.3 Ma for White River and > 36 Ma for North Fork samples). The absence of grains older than the Cretaceous-Paleocene boundary (i.e., ~67 Ma) in samples from the North Segment suggests that neither the North Fork nor White River districts overlie old (95 Ma) crystalline crust that lies east of the

Straight Creek Fault, but instead overlie Paleocene-Eocene volcanics, such as the Naches, Ohanapecosh and possibly Barlow Ridge (46-35, Tabor et al., 1988) Formations, that are likely sources of inherited zircons (Fig. 1). The Naches Formation (~43-29 Ma, Tabor et al., 1984) is exposed west of the Straight Creek Fault in central Washington and is composed of interbedded volcanic rocks, ranging from rhyolite flows to basalts, and feldspathic sandstones, and is at least 1,500 meters thick (Tabor et al., 1984). The Eocene Ohanapecosh Formation (middle to upper Eocene in age, Fiske et al., 1963) is the oldest unit exposed in Mt. Rainier National Park and its composition is dominated by volcanic debris flows but also contains mudflows, basaltic to rhyolitic lavas, and coarse tuff-breccias (Fiske et al., 1963). The North Fork and White River districts overlie the Helena-Haystack mélange and Western and Eastern Mélange Belts (Tabor 1994), which lie to the west of the Straight Creek fault and are comprised of Jurassic to Early Cretaceous metamorphic units, but we see no substantial xenocrystic zircons with these ages.

The minimal numbers of inherited zircons (n=38 of 350 total, or 11%, ranging from 54-20 Ma) in samples from the Columbia Segment of the arc are consistent with limited contamination by a source no older than 55 Ma, likely the dominant Eocene sources of detrital zircons found within the Tyee Formation (Dumitru et al., 2013). The absence of inherited grains > 54 Ma suggests this population is distinct from the detrital zircons within the Tyee Formation, which contains grains as old as Triassic. The Siletzia terrane in this segment is inferred to be thin (< 30 km) and mafic, and is therefore unlikely to contribute xenocrystic zircon to the overlying younger arc magmas. Some of these inherited zircons may be sourced directly from older volcanics such as the Clarno Formation, which could potentially underlie the arc in central Oregon.

The ages of inherited grains (n = 25 of 85 total, or 29%) from samples overlying the Klamath Terrane (i.e. Bohemia and South Umpqua) overlap with the Tyee Formation detrital zircon peak between 65 and 40 Ma (Fig 2). The lack of older inherited populations in this segment and the similarity to the Tyee Formation detrital peak suggests that no grains were inherited directly from accreted Mesozoic rocks of Klamath Terrane source, and instead these grains are sourced from similar contaminants to those underlying the central segment of the arc. These contaminants are likely older Western Cascade volcanics and older volcanics to the east (ie. Clarno Formation).

Petrogenesis of Western Cascade Magmas

This portion of the discussion is separated into three sections: A) evidence supporting magma mixing within plutons of the Western Cascades, B) an evaluation of the potential variation in crustal thickness beneath the Western Cascades, C) an examination of evidence for water-rich, oxidized magmas along the arc that would be capable of generating porphyry Cu deposits.

A. Evidence for Magma Mixing

Th/U versus Yb/Gd in zircon can be used to track fractionation and mixing trends in zircon. With pure fractionation, a melt would initially crystallize zircon with high Th/U and low Yb/Gd ratios. As the magma evolved, the Th/U ratios decreased due to the relative incompatibly of U versus Th. Fractionation of amphibole, pyroxene, or apatite would yield an increase in Yb/Gd ratios in zircon as MREE are incorporated into these phases (Claiborne et al., 2010, Lee 2008, Olson 2015). Western Cascade magmas do not have zircons with high (> 2) Th/U ratios, which are typically associated with hot, primitive magmas (Claiborne et al., 2010). Furthermore, Western Cascade zircons do not display high Yb/Gd ratios (> 35) comparative to more evolved arcs (Lee 2008, Olson 2015). The lack of evidence for more fractionated melts in zircon compositions may be a result of thin crust. Thinner crust would allow for limited fractionation of amphibole.

Variations in the least evolved Th/U and Yb/Gd ratios in zircon between different districts are likely a result of variation in initial melt composition at the time of crystallization. The discrepancy in Th/U versus Yb/Gd trends between the quartz monzonite and the mafic latite porphyry from the North Fork district could suggest a mixing trend between the initial quartz monzonite magma and a more evolved magma that is not represented in zircon compositions. Alternately, it could suggest the mafic latite porphyry zircons crystallized in a different magma with initially higher Yb/Gd and lower Th/U.

Plagioclase was an important phase in magma differentiation as indicated by the decrease in Sr with increasing SiO_2 in all suites. The plagioclase phenocrysts are complex, sieved, and have disequilibrium textures such as resorbed rims and complex zoning patterns. Sieved plagioclase and other disequilibrium textures are typically considered to be the product of magma mixing (Dungan & Rhodes, 1978). Examples of sieved, melt inclusion-rich plagioclase are common in thin sections from the sample intrusions and support magma mixing at some stage of magma gensis (Figure 5e). In the samples that show the strongest evidence for magma mixing in their zircon geochemistry - the Nimrod stock, Boulder Creek dike, and Yellowbottom Stock - sieved texture is ubiquitous in plagioclase and affect ~10-50% volume of plagioclase crystal. Large melt inclusions are also common. Hence, magma mixing was a significant process in pluton emplacement and it mainly predates zircon crystallization as indicated by large Eu anomalies in zircon.

B. Assessment of Crustal Assimilation and Thickness

To assess the variation in crustal thickness beneath the Western Cascades as well as the potential for crustal assimilation in Western Cascade magmas we use Ba/Nb, Th/Ta, REE patterns, Sc contents, and Yb/Gd in zircon.

Ba/Nb ratios have been used to distinguish between mantle-derived magma components and potential fluid fluxes derived from the subducting slab (Pearce & Peate, 1995). Ba contents will decrease only if alkali feldspar fractionates. Nb contents also increase with SiO_2 suggesting incompatible behavior but are more variable.

Ba/Nb may increase with differentiation (ie. increase in SiO_2 content), correlating with more substantial input of fluid from the subducting plate (Pearce 1983). In the Western Cascade magmas, Ba/Nb does not vary greatly with SiO_2 and therefore does not appear to be sensitive to differentiation (Figure 7c). However, Ba/Nb values are correlated with latitude and increase broadly from north to south (Figure 8). In addition to tracking fluid fluxes, Ba/Nb could rather track crustal contamination and potentially crustal thickness. Hildreth and Moorbath (1988) were able to show that K_2O contents at a given SiO_2 increase with crustal thickness. K and Ba are both very fluid mobile elements that should behave similarly. The observed increase in Ba/Nb southward in the Western Cascades is correlated with an increase in crustal thickness from ~10 km in southern Washington to ~30 km at the north edge of the Klamath Mountain Terrane (Trehu, *pers comm.* 2015; Trehu 2010).

Both Th and Ta are high field strength elements and relatively immobile. Th and Ta both act incompatibly and increase with increasing SiO_2. While Ta is considered an athsenospheric mantle signature due to its fluid immobility and extremely incompatible nature, Th is likely stored in the crust due to its release via metamictization of Th-rich minerals by radioactive decay (Woodhead et al., 1991). By this process Th is likely concentrated in sediments. Th/Ta increase with increasing SiO_2 for any given Western Cascade district, which suggests these magmas are assimilating Th-rich crustal material. Variation in Th/Ta ratios geographically can be attributed to the degree of crustal assimilation – lower Th/Ta ratios at any given SiO_2 in districts in the center of the arc (ie., Detroit Dam, Quartzville, and Blue River) suggests that the crust is likely thinner in this region. An alternative interpretation of low Th/Ta ratios in districts in the center of the arc might be that these magmas are assimilating crustal material that lacks Th-rich sediments.

We interpret the southward increase in Ba/Nb, Th, and Th/Ta in Western Cascade plutons to reflect an increased role of crustal contamination. While increased slab fluid flux could increase Ba relative to Nb, the greater abundance in Ba at given SiO_2 southward (Figure 7a) and of Th and Th/Ta (Figure 7d,f) are more consistent with a crustal input. We cannot exclude some increased slab fluid source of Ba to the south.

There is little evidence for garnet fractionation in Western Cascade plutons, which supports relatively thin underlying crust. Dy/Yb ratios are generally influenced by fractionation of phases with either an affinity for middle REEs (MREE) such as amphibole, apatite and titanite, or affinity for Y and heavy REEs (HREE) such as garnet. Garnet is stable in basaltic and andesitic magma compositions at > ~30 km depth. Dy/Yb is not largely affected by fractionation of pyroxene, which contains lower REE contents than amphibole and is a minor primary phase in the Western Cascade plutons. Dy/Yb ratios decrease with increasing SiO_2 within any given district. Similarly, HREE concentrations increase with increasing SiO_2. HREE appear to act incompatibly and are not incorporated into garnet or other phases. Kay and Mpodozis (2001) applied Sm/Yb ratios to track the increasing thickness of the Andean crust over time. Sm/Yb ratios are significantly limited in Western Cascade samples (1.25-3.25) compared to Andean samples and suggest the dominant mafic phases are pyroxene and lesser amphibole, but not garnet (Appendix Figure 5b).

Th/U versus Yb/Gd in zircon illustrate that magma mixing plays a significant role in some Western Cascade plutons (ie. North Fork and the Nimrod Stock near Blue River). Additionally, the absence of elevated Yb/Gd ratios in the majority of samples suggests that substantial fractionation of amphibole or pyroxene did not occur in these plutons concurrently with zircon crystallization. Yb/Gd highlights the degree of fractionation, which may be limited by a thin crust.

The strongly pyroxene-compatible element Sc is consistently elevated to the south at any given SiO_2 content (Figure 9a,b). Sc acts perfectly compatibly in Western Cascade magmas and is incorporated into pyroxene and amphibole. One possible inference is that there is more Sc to the south because less pyroxene fractionated. Kay & Mpodozis (2001) estimated clinopyroxene is the dominant mafic phase below depths of 35 km. Minimal pyroxene fractionation to the south compared to the north could, therefore, potentially be a product of thicker crust.

C. Estimation of Ore Fertility

Studies of large porphyry Cu-(Au-Mo) deposits worldwide (Dilles 1987; Richards 2003; Loucks 2014; Richards *in press*) have found that many ore-forming arc magmas are strongly oxidized (NNO+2) and water-rich (> 3-4 wt. %, Dilles 1987). The formation of large porphyry Cu-(Au-Mo) deposits may require elevated water contents and oxidation states of parental magmas. We can therefore assess the potential ore fertility of Western Cascade magmas by examining geochemical and petrographic tracers for high water contents and elevated oxidation states. Here we apply zircon REE geochemistry, whole-rock trace element geochemistry, and petrographic observations.

Rare Earth Element (REE) compositions of zircons record variations in the water content and oxidation state of the magma which are linked to ore-forming conditions (Ballard et al., 2002). The majority of REE (with the exception of Ce and Eu) are trivalent. Under reducing conditions, zircon REE compositions have a large negative anomaly in Eu_N/Eu_N* because Eu partitions into plagioclase most readily. Rare earth elements are primarily trivalent (III) cations excluding Eu, which is a 2^+ cation in most magmas, but under oxidizing conditions Eu^{2+} becomes Eu^{3+} (Hoskin & Schaltegger, 2003). The oxidized Eu^{3+} is more readily incorporated into zircon crystals rather than plagioclase or other major phases, and if plagioclase crystallization is suppressed by high water content of the melt, oxidation results in small negative Eu/Eu* anomalies in zircon REE (Ballard et al., 2002). As a result, most porphyry-Cu mineralizing magmas have characteristically small negative Eu anomalies (Dilles et al., 2015).

Conversely, under oxidizing magmatic conditions a small fraction of Ce^{3+} is oxidized to Ce^{4+}, which is strongly partitioned into zircon preferentially over Ce^{3+} because its identical charge and similar atomic radius to Zr (Ballard et al., 2002). As a result, zircons forming in porphyry-Cu mineralizing magmas have characteristically large positive Ce anomalies. These anomalies are typically quanitified by Ce(III)/Ce(IV) ratios and Ce_N/Ce_N* ratios. Due to characteristically low concentrations of LREE in zircons (Ballard et al., 2002), La and Pr are often at or below the detection limit of LA-ICP-MS analyses. Here, we use Ce_N/Nd_N ratios as a proxy for quantifying the positive Ce anomaly in zircons. Ce_N/Nd_N values ≥ 30 are typical of zircons crystallized in porphyry-Cu mineralizing magmas (Olson 2015).

Low Eu_N/Eu_N* in zircon (<0.5) indicate that Western Cascade magmas are relatively water-poor and crystallized abundant early plagioclase. These large negative Eu anomalies in zircon are supported by the presence of plagioclase in all samples, which together suggest that early crystallization of plagioclase occurred in all magmas studied. Early plagioclase crystallization would only be suppressed in relatively water-rich magmas (>~3 wt. %, Dilles et al., 2015). Small Ce_N/Nd_N values corresponding to small positive Ce anomalies in zircon suggest that very little Ce in Western Cascade magmas was in the trivalent state and therefore did not preferentially partition into zircon. Small positive Ce anomalies characterize the Western Cascade magmas as not strongly oxidized. These data together suggest the oxidation state of Western Cascade magmas was initially too low, or the amount of SO_2 degassed was insufficient, to oxidize Ce and Eu (cf. Dilles et al., 2015).

In addition to Ce and Eu anomalies in zircon, we can assess the oxidation state of a magma by examining whole-rock V/Sc ratios (Loucks 2014). The transition metals scandium and vanadium are both sensitive to fractionation of mafic silicates and oxides. Sc contents are generally controlled by fractionation of pyroxene or amphibole as magma differentiates. In oxidized magmas, V will be in the 4+ or 5+ state and act incompatible instead of partitioning into magnetite. V/Sc ratios are a good tool to assess the fractionation of magnetite (which incorporates V^{3+}) relative to pyroxene (pyroxene incorporates Sc, which behaves compatibly in Western Cascade plutons as we have shown). With the exception of samples from the Spirit Lake Pluton (Evarts, *in* du Bray & John, 2011), all Western Cascade districts included in this study have V/Sc contents that decrease with increasing SiO_2 content (Figure 9d). This observation suggests that V acted compatibly by incorporation into magnetite and mafic silicates and fractionation. Additionally, relative oxidation state can be estimated using the relative presence of Fe-oxides. In Western Cascade plutons we observe an approximate 2:1 ratio of magnetite:ilmenite where present, suggesting magmas are not strongly oxidized.

Large negative Eu anomalies support early plagioclase crystallization and therefore that Western Cascade magmas had relatively low water contents insufficient to suppress plagioclase. Early plagioclase crystallization is also supported by whole-rock REE trends because small Eu anomalies are present in all districts and increase in magnitude in more evolved plutons (Appendix Figure 5a). Additionally, Sr/Y values can be used to estimate relative magmatic water contents in unaltered samples. Sr/Y ratios decrease with increasing SiO_2 (Figure 9e), which suggests that Sr was incorporated into plagioclase early and was not concentrated in the melt.

In contrast, evidence for hornblende stability suggests relatively moderate water contents of at least 3 wt. % (Burnham 1979). In the Western Cascades abundant hornblende is observed in 31 of 36 available petrographic sections; therefore water contents must be sufficient to stabilize the phase. Additionally, hornblende partitions MREEs with respect to LREE and HREEs. Therefore, hornblende fractionation can be interpreted from both Dy/Yb ratios, which decrease in any given district with differentiation (Figure 7g), and overall REE trends, which increase in concavity with increasing SiO_2 (Figure 10), correlated with depletion of MREE with respect to LREE and HREE. We can therefore infer that water must be sufficient to stabilize hornblende, >3 wt. % H_2O.

CONCLUSIONS

As recognized by Schmidt and others in the modern arc (2008, 2013), the Western Cascade arc overlies three distinct crustal blocks. Although crustal thickness is poorly constrained in the north and south segments, it is evidently variable along-arc (and may thicken slightly to the south on the basis of Ba/Nb ratios and elevated Sc content), but likely relatively thin. There is no geochemical or physical evidence for garnet fractionation in any district, so the crust is < ~30 km thick. The paucity of inherited zircon populations in samples from the Columbia segment that is underlain by Siletzia crust also is correlated with generally low Th/Ta ratios, both of which suggest that assimilation of evolved crust was limited in the center of the arc. The central Western Cascade Arc overlies the relatively thin (10-30 km, Parsons et al., 1999) Siletzia terrane, which is likely dominated by basaltic material overlain by minor Tyee turbiditic sandstone and is subsequently unlikely to be enriched in Th, nor can it serve as a source of contaminant zircon. In the north and south segments, the absence of inherited zircons older than 67 Ma suggests these areas do not overly older, evolved crust as might be expected. Where pre-Cenozoic crust is present it either was not assimilated into Western Cascade magmas, or was mafic and contained little zircon. Instead, these inherited zircons are likely derived from underlying older volcanics of the earlier part of the Western Cascade arc or detrital zircons incorporated into Tyee Formation turbidites to the west (Dumitru et al., 2013).

Although our data and observations suggest that these magmas are sufficiently water-rich to abundantly crystallize and fractionate amphibole (at least 3 wt. % H_2O), it is evident that plagioclase crystallized early and was not suppressed by high water contents (> 3 wt. % H_2O). There is no evidence from zircon and whole-rock geochemistry to suggest that Western Cascade magmas were substantially oxidized (> NNO or NNO +1), despite the presence of moderate- and small-sized porphyry Cu and epithermal Au deposits.

These data altogether suggest that crustal thickness and lithology substantially control ore potential within the Western Cascade Arc. The plutons sampled in this study are on the cusp of ore fertility. These conclusions need to be tested with sampling of plutons associated with mineralization in both the Mount Margaret and Glacier Peak districts. More trace element data (specifically REEs) from plutonic samples, as well as more robust age constraints, could yield spatial and temporal comparisons to resolve the magmatic evolution within a given district or segment of the arc. Analysis of plagioclase anorthite content may help distinguish crystallization of early, Ca-rich plagioclase versus a later, Na-rich relative.

REFERENCES

Anders, E., and Grevesse, N, 1989, Abundances of the elements: Meteoritic and solar: Geochimica et Cosmochimica act, v. 53, no. 1, p. 197-214.

Ballard, J., Palin, J., Williams, I., Campbell, I., Faunes, A., 2001, Two ages of porphyry intrusion resolved for the super-giant Chuquicamata copper deposit of northern Chile by ELA-ICP-MS and SHRIMP: Geology, v. 29 no. 5 p. 383-386.

Ballard, J., Palin, J., and Campbell, I., 2002, Relative oxidation states of magmas inferred from Ce(IV)/Ce(III) in zircon: application to porphyry copper deposits of northern Chile: Contributions to Mineralogy and Petrology, v. 144, p. 347-364.

Barry, T.L., Kelley, S.P., Reidel, S.P., Camp, V.E., Self, S., Jarboe, N.A., Duncan, R.A., Renne, P.R., 2013, Eruption chronology of the Columbia River Basalt Group: The Geological Society of America Special Paper 497, p. 45-66.

Beck, S., Zandt, G., Myers, S., Wallace, T., Silver, P., and Drake, L., 1996, Crustal-thickness variations in the central Andes: Geology, v. 24, no. 5, p. 407-410.

Black, L.P., Kamo, S.J., Allen, C.M., Aleinikoff, J.N., Davis, D.W., Korsch, R.J., and Foudoulis, C., 2003, Temora 1: A new zircon standard for Phanerozoic U-Pb geochronology: Chemical Geology, v. 200, no. 1-2, p. 155-170.

Blakely, R.J., John, D.A., Box, S.E., Berger, B.R., Flekc, R.J., Ashley, R.P., Newport, G.R., Heinmeyer, G.R., 2007, Crustal controls on magmatic-hydrothermal systems: A geophysical comparison of White River, Washington, with Goldfield, Nevada: Geosphere, v. 3, no.2, p. 91-107.

Brown, E., and Gehrels, G., 2007, Detrital zircon constraints on terrane ages and affinities and timing of orogenic events in the San Juan Islands and North Cascades, Washington: Canada Journal of Earth Science, v. 44, p. 1375-1396.

Burnham, C., 1979, The importance of volatile constituents, in The Evolution of the Igneous Rocks (Yoder, H.S., Ed), p. 439-482: Princeton University Press, Princeton, N.J.

Callahan, E., and Buddington, A.F., 1938, Metalliferous mineral deposits of the Cascade Range in Oregon: U.S. Geological Society Bulletin 893, 114 p.

Carmichael, I., and Nicholls, J., 1967, Iron-Titanium Oxides and Oxygen Fugacities in Volcanic Rocks: Journal of Geophysical Research, v. 72, no. 18, p. 4665-4687

Castor, S., Boden, D., Henry, C., Cline, J., Hofstra, A., McIntosh, W., Tosdal, R., and Wooden, J., 2003, The Tuscarora Au-Ag Distict: Eocene Volcanic-Hosted Epitehrmal Deposits in the Carlin Gold Region, Nevada: Economic Geology, v. 98, p. 339-366.

Chambefort, I., Dilles, J.H., and Kent, A.J.R., 2008, Anhydrite-bearing andesite and dacite as a source for sulfur in magmatic-hydrothermal mineral deposits: Geology, v. 36, no. 9., p. 719-722.

Christiansen, R., Yeats, R., Graham, S., Niem, W, Riem, A., and Snavely, P. Jr., 1992, Post-Laramid geology of the U.S. Cordilleran region, in The Geology of North America, v. 3, p. 261-406.

Claiborne, L., Miller, C., Wooden, J., 2010, Trace element composition of igneous zircon: a thermal and compositional record of accumulation and evolution of a large silicic batholith, Spirit Mountain, Nevada: Contributions to Mineralogy & Petrology, v., 160: p. 511-531.

Cole, R., and Stewart, B., 2009, Continental margin volcanism at sites of spreading ridge subduction: Examples from southern Alaska and western California: Tectonophysics, v. 464, no. 1-4, p. 118-136.

Curless, J., 1991, Geology and hydrothermal mineralization in the vicinity of Rocky Top, Marion County, Oregon [M.S. Thesis]: Oregon State University.

Dilles, J., 1987, Petrology of the Yerington Batholith, Nevada: Evidence for Evolution of Porphyry Copper Ore Fluids: Economic Geology, v. 82, p. 1750-1789.

Dilles, J., Kent, A., Wooden, J., Tosdal, R., Koleszar, A., Lee, R., and Farmer, L., 2015, Zircon compositional evidence for sulfur-degassing from ore-forming arc magmas: Economic Geology, v. 110, p. 241-251.

du Bray, E., and John, D., 2011, Petrologic, tectonic, and metallogenic evolution of the Ancestral Cascades magmatic arc, Washington, Oregon, and northern California: Geosphere, v. 7 p. 1102-1133.

Dudás, F., Isploatov, V., Harlan, S., and Snee, L., 2010, 40Ar/39Ar Geochronology and Geochemical Reconnaissance of the Eocene Lowland Creek Volcanic Field, West-Central Montana: The Journal of Geology, v. 118, p. 295-304.

Dumitru, T., Ernst, W., Wright, J., Wooden, J., Wells, R., Farmer, L., Kent, A., Graham, S., 2013, Eocene extension in Idaho generated massive sediment floods into the Franciscan trench and into the Tyee, Great Valley, and Green River basins: Geology, v. 41, p. 187-190.

Evarts, R., Ashley, R., and Smith, J., 1987, Geology of the Mount St. Helens Area: Record of Discontinuous Volcanic and Plutonic Activity in the Cascade Arc of Southern Washington: Journal of Geophysical Research, v. 92, no. B10, p. 10,155-10,169.

Evarts, R., and Ashley, R., 1991, Preliminary geologic map of the Lakeview Peak quadrangle, Cowlitz County, Washington: U.S. Geological Survey Open-File Report 91-289, scale 1:24,000, 35 p.

Farmer, L., 2012, Trace Element Characteristics of Zircon: A Means of Assessing Mineralization Potential of Intrusions in Northern Nevada [M.S. Thesis]: Oregon State University

Felts, W., 1939, A granodiorite stock in the Cascade Mountains of south-western Washington: Ohio Journal of Science, v. 39, no. 6, p. 297-316.

Ferry, J.M., and Watson, E.B., 2007, New thermodynamic models and revised calibrations for the Ti-in-zircon and Zr-in-rutile thermometers: Contributions to Mineralogy & Petrology, v. 154, p. 429-437.

Fiske, R., Hopson, C., and Waters, A., 1963, Geology of Mount Rainier National Park, Washington: U.S. Geological Suvery Professional Paper 444, 93 p.

Gustafson, L.B., 1979, Porphyry copper deposits and calc-alkaline volcanism, in Mc Elhinny, MW, The Earth: Its origin, structure, and evolution, p. 579.

Hayden, L., and Watson, E., 2007, Rutile saturation in hydrous siliceous melts and its bearing on Ti-thermometry of quartz and zircon: Earth and Planetary Science Letters, v. 258, p. 561-568.

Hildreth, W., and Moorbath, S., 1988, Crustal contributions to arc magmatism in the Andes of Central Chile: Contributions to Mineralogy and Petrology, v. 98, p. 455-489.

Hoskin, P., and Schaltegger, U., 2003, The composition of zircon and igneous and metamorphic petrogenesis: Reviews in Mineralogy and Geochemistry, v. 53, no. 1, p. 27-62.

Hiza, M.M., 1999, The Geochemistry and Geochronology of the Eocene Absaroka Volcanic Province, Northern Wyoming and Southwest Montana, USA [Doctorate Thesis]: Oregon State University

Irvine, T., and Baragar, W., 1971, A guide to the chemical classification of the common volcanic rocks: Canadian Journal of Earth Sciences, v. 8, p. 455-489.

Irwin, W., 1981, Tectonic accretion of the Klamath Mountains, in The Geotectonic Development of California (Ernst, W., Ed), p. 29-49: Rubey I. Prentice Hall, New York.

Jenner G.A., Longerich H.P., Jackson S.E., and Fryer B.J., 1990, ICP-MS - A powerful tool for high-precision trace-element analysis in Earth sciences: Evidence from analysis of selected U.S.G.S. reference samples: Chemical Geology, v. 83, p. 133-148.

Johnson, D.M., Hooper P.R., and Conrey, R.M., 1999, XRF Analysis of rocks and minerals for major and trace elements on a single low dilution Li-tetraborate fused bead: Advances in X-ray Analysis, v. 41, p. 843-867.

Kent, A.J.R., Jacobsen, B., Peate, D.W., Waight, T.E., and Baker, J.A., 2004, Isotope dilution MC-ICP-MS rare earth element analysis of geochemical reference materials NIST SRM 610, NIST SRM 612, NIST SRM 614, BHVO-2G, BHVO-2, BRC-2G, JB-2, WS-E, W-2, AGV-1 and AGV-2: Geostandards Newsletter, v. 28, no. 3, p. 417–429.

LaMaskin, T., Vervoort, J., Dorsey, R., and Wright, J., 2011, Early Mesozoic paleogeography and tectonic evolution of the western United States: Insights from detrital zircon U-Pb geochronology, Blue Mountains Province, northeastern Oregon: Geology Society of America Bulletin, v. 123, no. 9-1, p. 1939-1965.

Lasmanis, R., 1995, Regional geological and tectonic setting of porphyry deposits in Washington State in Porphyry Deposits of the Northwestern Cordillera of North America [Schroeter, T., Ed.]: Geological Society of CIM Special Volume 46, p. 77-102.

Lee, R., 2008, Genesis of the El Salvador Porphyry Copper Deposit, Chile and Distribution of Epithermal Alteration at Lassen Peak, California [Ph.D. Dissertation]: Oregon State University.

Loewen, M., 2013, Volatile Mobility of Trace Metals in Volcanic Systems [Ph.D. Dissertation]: Oregon State University.

Loucks, R., 2014, Distinctive composition of copper-ore-forming arc magmas: Australian Journal of Earth Sciences, v. 61, p. 5-16.

Ludwig, K.R., 2009, SQUID 2: A User's Manual, rev. 12 Apr, 2009: Berkley Geochronology Center Special Publication No. 5, p. 1-110.

Mazdab, F., and Wooden, J., 2006, Trace element analysis in zircon by ion microprobe (SHRIMP-RG): technique and applications: Geochimica et Cosmochimica Acta, v. 70, no. 18.

Miller, J., Mtazel, J., Miller, C., Burgess, S., and Miller, R., 2007, Zircon growth and recycling during the assembly of large, composite arc plutons: Journal of Volcanology and Geothermal Research, v. 167, p. 282-299.

Munts, S., 1978, Geology and mineral deposits of the Quartzville mining district, Linn County, Oregon [M.S. Thesis] University of Oregon.

Nicholson, D., 1988, Geology, Geochemistry, and Mineralization of the Yellowbottom-Boulder Creek Area, Linn County, Oregon [M.S. Thesis]: Oregon State University.

Normal, M., and Mertzman, S., 1991, Petrogenesis of Challis Volcanics from Central to Southwestern Idaho: trace element and Pb isotopic evidence: Journal of Geophysical Research, v. 96, no. B8, p. 13279-13293.

Olson, J.P., 1978, Geology and Mineralization of the North Santiam Mining District, Marion County, Oregon [M.S. Thesis]: Oregon State University.

Olson, N.H., 2015, The Geology, Geochronology, and Geochemistry of the Kaskanak Batholith, and other Late Cretaceous to Eocene magmatism at the Pebble Porphyry Cu-Au-Mo deposit, SW Alaska [M.S. Thesis]: Oregon State University.

Oregon DOGAMI, 1951, Oregon Metal Mines Handbook: State of Oregon Department of Geology and Mineral Industries.

Parsons, T., Wells, R., Fisher, M., Flueh, E., Brink, U., 1999, Three-dimensions velocity structure of Siletzia and other accreted terranes in the Cascadia forearc of Washington: Journal of Geophysical Research, v. 104, p. 18015-18039.

Pearce, J., 1983, Role of the Sub-continental Lithosphere in Magma Genesis at Active Continental Margins, in Continental Basalts and Mantle Xenoliths (Hawkesworth, C., and Norry, M., Eds), p. 230-249: Birkhauser Boston, Inc., Cambridge, MA.

Pearce, J., and Peate, D., 1995, Tectonic implications of the composition of volcanic arc magmas: Annual Review of Earth and Planetary Sciences, v. 23, p. 956-983.

Power, S., Field, C.W., Armstrong, R., Harakal, J.E., 1981, K-Ar Ages of plutonism and mineralization, western Cascades, Oregon and Southern Washington: Isochron/West no. 31, p. 27-29.

Power, S., 1984, The "Tops" of Porphyry Copper Deposits – Mineralization and Plutonism in the Western Cascades, Oregon [Ph.D. Thesis]: Oregon State University.

Priest, G., 1990, Volcanic and Tectonic Evolution of the Cascade Volcanic Arc, Central Oregon: Journal of Geophysical Reach, v. 95, no. B12, p. 19582-19599.

Richards, J., 2003, Tectono-magmatic precursors for porphyry Cu-(Mo-Au) formation: Economic Geology and the Bulletin of the Society of Economic Geologists, v. 98, p. 1515-1533.

Richards, J., *in press*, The oxidation stae, and sulfur and Cu contents of arc magmas: Implications for metallogeny: Lithos.

Robinson, P., Brem, G., and McKee, E., 1984, John Day Formation of Oregon: A distal record of early Cascade volcanism, Geology: v. 12, p. 229-232.

Schmandt, B., and Humphreys, E., 2011, Seismically imaged relict slab from the 55 Ma Siletzia accretion to the northwest United States: Geology, v. 39, no. 9, p. 175-178.

Schmidt, M., Grunder, A., and Rowe, M., 2008, Segmentation of the Cascade Arc as indicated by Sr and Nd isotopic variation among diverse primitive basalts: Earth and Planetary Science Letters, v. 266, p. 166-181.

Schmidt, M., Grunder, A., Rowe, M., and Chesley, J., 2013, Re and Os isotopes of the central Oregon Cascades and along the arc indicate variable homogenization and mafic growth in the deep crust: Geochimica et Cosmochimica Acta, v. 109, p. 345-364.

Schriener, A., Jr., 1978, Geology and mineralization of the north part of the Washougal mining district, Skamania County, Washingtion [M.S. Thesis]: Oregon State University.

Shepard, R., 1979, Geology and mineralization of the southern Silver Star stock, Washougal Mining District, Skamania County, Washington [M.S. Thesis]: Oregon State University.

Sláma, J., Košler, J., Condon, D.J., Crowley, J.L., Gerdes, Z., Hanchar, J.M., Horstwood, M.S.A., and Morris, G.A., 2008, Plešovice zircon — A new natural reference material for U-Pb and Hf isotopic microanalysis: Chemical Geology, v. 249, no. 1-2, p. 1-35.

Smithson, D.M., 2004, Late Eocene tectono-magmatic evolution and genesis of reduced porphyry copper-gold mineralization at the North Fork deposit, West Central Cascade Range, Washington, U.S.A. [M.S. Thesis]: University of British Columbia.

Snoke, A. and Barnes, C. (Eds.), 2006, Geological Studies in the Klamath Mountains Province, California and Oregon: A Volume in Honor of William P. Irwin: Spec. Pap. – Geol. Soc. Am., v. 410.

Stanley, W., Mooney, W., Fuis, G., 1990, Deep crustal structure of the Cascade Range and surrounding regions from seismic refractions and magentotelluric data: Journal of Geophysical Research, v. 95, p. 19,419-19,438.

Stone, B.G., 1994, The Bornite breccia pipe, Marion County, Oregon: Oregon Geology, v. 56, no. 5, p. 99-108.

Storch, S., 1978, Geology of the Blue River mining distict, Linn and Lane Counties, Oregon [M.S. Thesis]: Oregon State University.

Sutter, J.F., 1978, K-Ar Ages of Cenozoic Volcanic Rocks from the Oregon Cascades West of 121°30', Isochron/West, no.21, p. 15-21.

Tabor, R., Frizzell, V. Jr., Vance, J., Naeser, C., 1984, Ages and stratigraphy of lower and middle Tertiary sedimentary and volcanic rocks of the central Cascades, Washington: Application to the tectonic history of the Straight Creek fault: Geological Society of America Bulletin, v. 95, p. 26-44.

Tabor, R., Booth, D., Vance, J., and Ort, M., 1988, Preliminary geologic map of the Sauk River 30 x 60 minute quadrangle, Washington: U.S. Geological Survey Open-File Report 88-692.

Tabor, R., 1994, Late Mesozoic and possible early Tertiary accretion in western Washington State: The Helena-Haystack mélange and the Darrington-Devils Mountain fault zone: Geological Society of America Bulletin, v. 106, p. 217-232.

Thompson, M., 1983, Solidification in magmas – Part 1, the magmatic history of the Tatoosh volcanic-plutonic complex, Mount Rainier National Park, part 2, numerical simulation of heat and mass transfer in solidifying magmas [M.S. Thesis]: University of Oregon.

Toplis, M., and Corgne, A., 2002, An experimental study of element partitioning between magnetite, clinopyroxene, and iron-bearing silicate liquids with particular emphasis on vanadium: Contributions to Mineralogy & Petrology, v. 144, p. 22-37.

Trehu, A., Asudeh, I., Brocher, T., Luetgert, J., Mooney, W., Nabelek, J., and Nakamura, Y., 1994, Crustal Architecture of the Cascadia Forearc: Science, v. 266, p. 237-243.

Trehu, A., 2010, Plate boundary segmentation and upper/lower plate structure in Cascadia, Abstract T14B-03 presented at 2010 Fall Meeting, AGU, San Francisco, CA., 13-17 Dec.

Walker, B., Jr., Klemetti, E., Grunder, A., Dilles, J., Tepley, F., and Giles, D., 2013, Crystal reaming during the assembly, maturation, and waning of an eleven-million-year crustal magma cycle: thermobarometry of the Aucanquilcha Volcanic Cluster: Contributions to Mineralogy & Petrology, v. 165, p. 663-682.

Walker, G., and Robinson, P., 1990, Paleocene(?), Eocene, and Oligocene(?) rocks of the Blue Moutains region *in* Walker, G., ed., Geology of the Blue Mountains region of Oregon, Idaho, and Washington, Censozoic geology of the Blue Mountains region: U.S. Geologic Survey Professional Paper 1437, p. 13-28.

Wells, R., Jayko, A., Niem, A., Black, G., Wiley, T., Baldwin, E., Molenaar, K., Wheeler, K, Givler, R., and DuRoss, C., 2000, Geologic map and database of the Roseburg, Oregon 30' x 60' Quadrangle, Douglas and Coos Counties, Oregon: U.S. Geological Survey Open-File Report OF00-376, p. 55, scale 1:100,000.

Wells, R., Bukry, D., Friedman, R., Pyle, D., Duncan, R., Haeussler, P, and Wooden, J., 2014, Geologic history of Siletzia, a large igneous province in the Oregon and Washington Coast Range: Correlation to the geomagnetic polarity time scale and implications for a long-lived Yellowstone hotspot: Geosphere, v. 10, no. 4, p. 1-28.

Wilkinson, J., 2013, Triggers for the formation of porphyry ore deposits in magmatic arcs: Nature Geoscience, v. 6, p. 917-925.

Winters, M., 1985, An Investigation of Fluid Inclusions and Geochemistry of Ore Formation in the Cedar Creek Breccia Pipe, North Santiam Mining District, Oregon [Ph.D. Dissertation]: Western Washington University.

APPENDICES

Appendix 1. Field Mapping in the North Santiam District, Marion County, OR

In addition to sample collection during the summers of 2013 and 2014, a geologic map of the North Santiam district was completed at the 1:10,000 scale, covering an area of approximately 4.5 km by 3 km during the summer of 2014. Mapping was completed on a 3 ft LiDAR map by DOGAMI, with reference to U.S. Geological Survey Topographic 7.5-minute Quadrangles of the Battle Ax Quadrangle, Detroit Quadrangle, the Elkhorn Quadrangle, and Lawhead Creek Quadrangle. Sample locations were recorded on the LiDAR map as well as by hand-held GPS.

Geologic mapping was directed towards identifying field relationships of plutonic rocks and hydrothermal mineralization. The aim was to identify the location, orientation and distribution of plutonic dikes and mineralized veins. These dikes intrude earlier Western Cascades volcanics, here identified as the Sardine Formation. The Sardine Formation is typically less resistant to weathering. This area is densely forested and outcrops along hill slopes are rare; therefore outcrop mapping focused on cliffs to the south of the map area and exposures along the Little North Santiam River, Cedar Creek, Opal Creek, and Battle Ax Creek.

Field data concludes that dikes in the North Santiam district are between 10 and 40 m wide and strike NW-SE. These dikes are porphyritic with typically graphic and rare aplitic groundmass, ranging in composition from diorite to granodiorite. Disseminated pyrite (< 2 volume %) is common. Hydrothermal alteration is somewhat widespread but concentrated near the Bornite Breccia Pipe exposure to the south and to tourmaline-bearing breccia exposure just south of the Little North Santiam River. These brecciated zones contain the dominant Cu-sulfide and oxide mineralization of the district. Chalcopyrite, pyrite, tourmaline, and minor chalcocite and glassy limonite are observed. These brecciated zones tend to be somewhat lineated in the NW-SE direction, same as the dikes. Thin (< 2 cm) quartz veins were identified near brecciated zones as well as adjacent to dike contacts with host rock. These veins are typically oriented NW-SE and are near vertical. A small subset of veins (~20% of all veins observed) dip NE-SW and are near vertical. Small, discontinuous faults were observed along the Little North Santiam River that are oriented NE-SW.

This field data is compiled on the map below. The compilation map also includes previous work by Olson (1978) and Stone (1994).

Appendix Figure 1 (Below): Geologic Interpretation of North Santiam District, Marion County. Miocene dikes and brecciated zones mapped by the author; other geologic data compiled from previous work by Olson (1978) and Stone (1994).

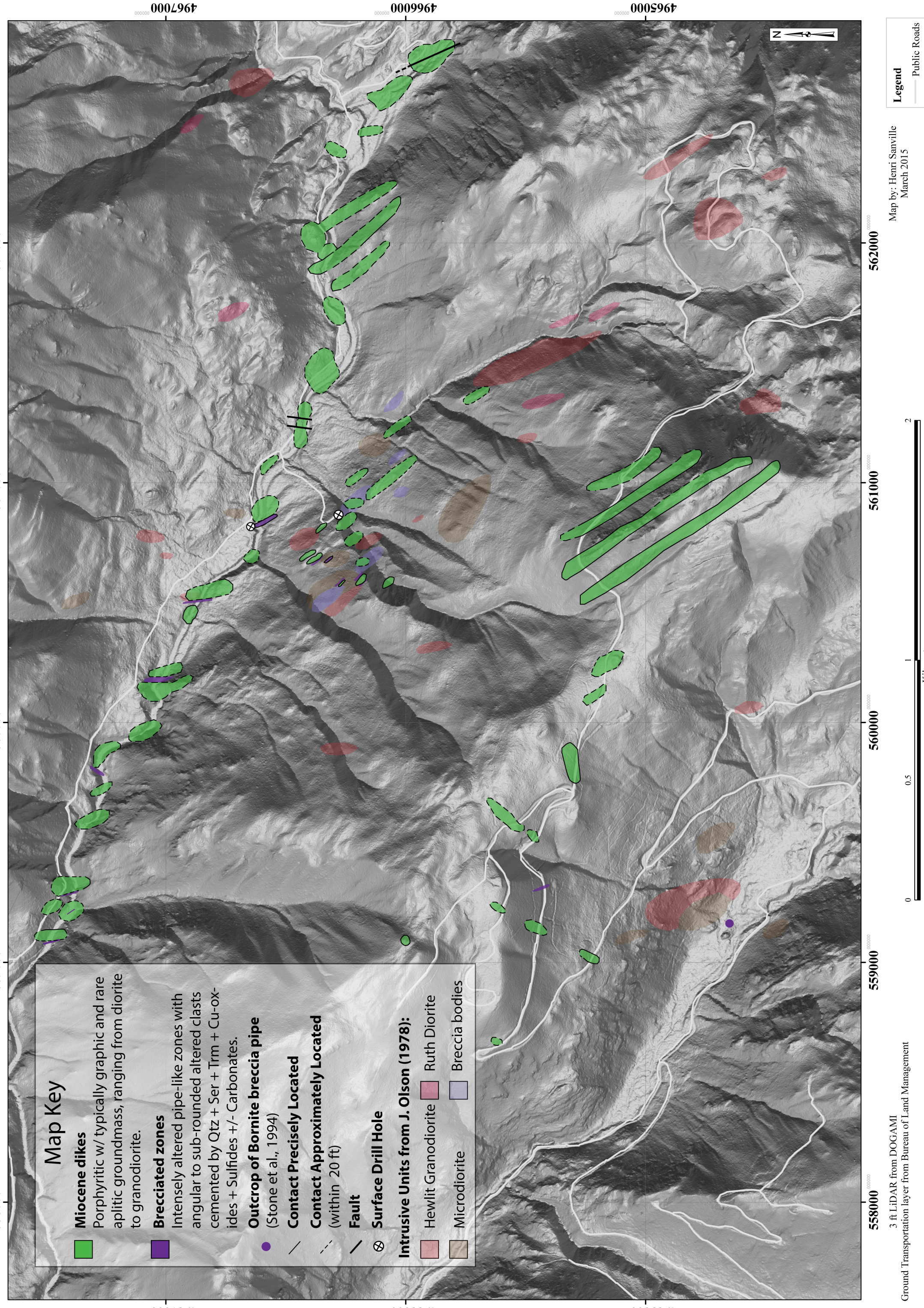
Map Key
Miocene dikes
Porphyritic w/ typically graphic and rare aplitic groundmass, ranging from diorite to granodiorite.
Brecciated zones
Intensely altered pipe-like zones with angular to sub-rounded altered clasts cemented by Qtz + Ser + Trm + Cu-oxides + Sulfides +/- Carbonates.
Outcrop of Bornite breccia pipe
(Stone et al., 1994)
Contact Precisely Located
Contact Approximately Located
(within 20 ft)
Fault
Surface Drill Hole
Intrusive Units from J. Olson (1978):
Hewlit Granodiorite
Ruth Diorite
Microdiorite
Breccia bodies
4967000
4966000
4965000
558000
559000
560000
561000
562000
N
3 ft LiDAR from DOGAMI
Ground Transportation layer from Bureau of Land Management
Datum: NAD 1983 (2011) UTM Zone 10N
Projection:Transverse_Mercator
0
0.5
1
2
Kilometers
Map by: Henri Sanville
March 2015
Legend
Public Roads

Appendix 2. Methods

2.1 Additional Sample Collection

Alexander Iveson provided three samples of the Spirit Lake Pluton associated with the Mt. Margaret deposit. Two additional samples collected by Sarah Power from the Washougal district were acquired (Power, 1984). A sample of monzodiorite was taken from representative skeleton drill core from the White River deposit.

2.2 Sample Preparation for Zircon Analyses

Samples were crushed, powdered, and zircon separated using pan concentration, ultrasonic bath, Frantz magnetic separation, and handpicking by binocular microscope in mineral processing facilities at Oregon State University. Selected zircon grains were placed in rows on double-sided Kapton® tape and mounted in 2.5 cm epoxy plugs, polished to expose zircon cores, imaged by polarizing light microscope to identify apatite and melt inclusion-free zones. Cathodoluminescence (CL) imaging was used to target uranium-rich zones.

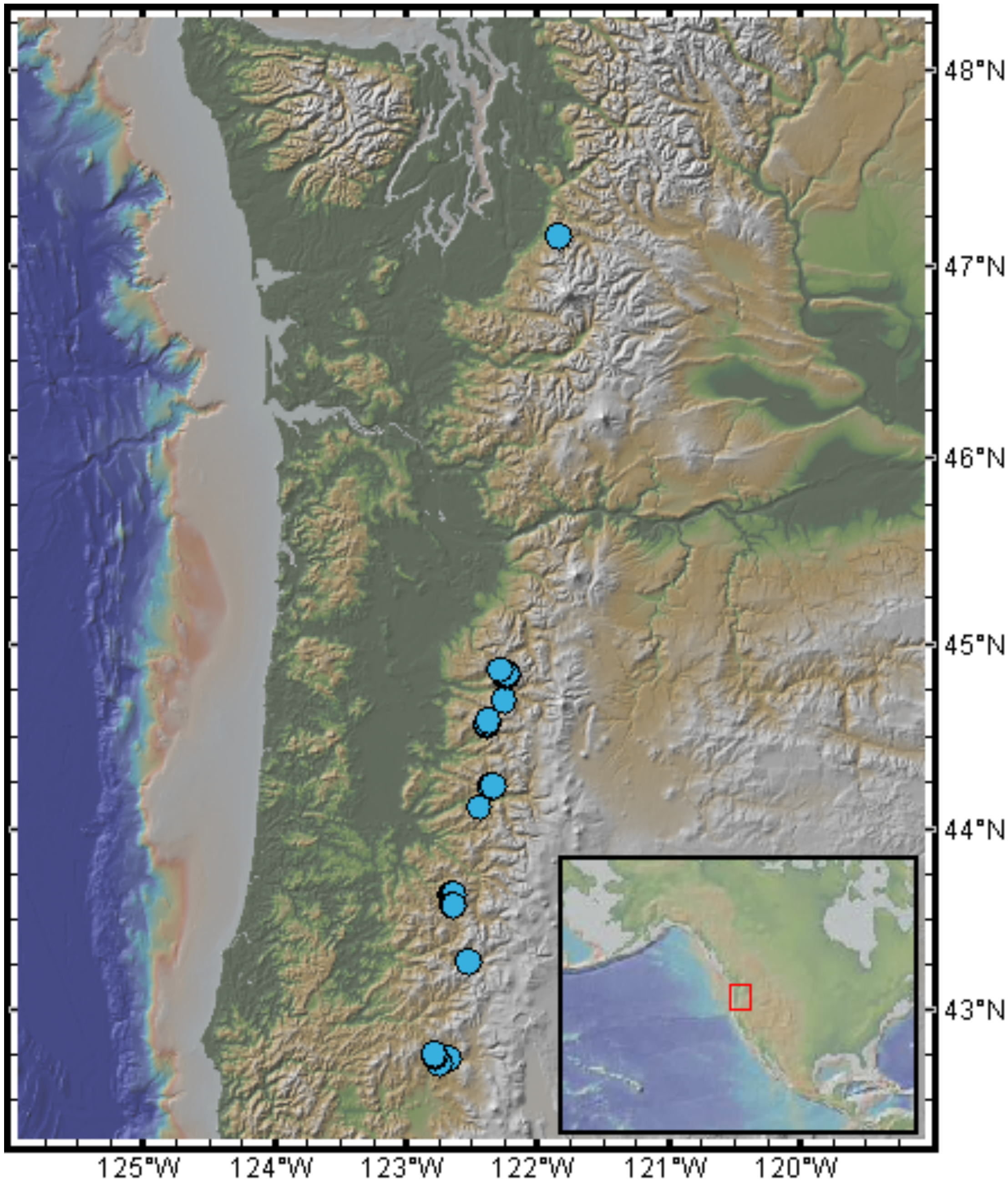

<u>Appendix Figure 2:</u> Location map for samples collected and analyzed by XRF and ICP-MS at Washington State University. Made with *GeoMapApp*.

Appendix 3. Previously Reported Ages

Appendix Table 1. Previously Reported Ages of Plutonism & Hydrothermal Mineralization in the Western Cascades

Location	Sample	Rock Description	Longitude	Latitude	Method	Mineral	Age	Error	MSWD	References
North Fork	SMR-108*	Qz monzodiorite	-121.648	47.670	U/Pb TIMS	Zircon	37.00	0.2		Smithson 2004
	SMR-113*	Mafic latite porphyry	-121.641	47.674	U/Pb TIMS	Zircon	37.10	0.2		Smithson 2004
	SMR-111	Qz monzodiorite			U/Pb TIMS	Zircon	37.20	0.1		Smithson 2004
	SMR-106	Mafic latite porphyry			U/Pb TIMS	Zircon	36.80	0.2		Smithson 2004
	SRM-110	Porphyritic andesite			U/Pb TIMS	Zircon	38.90	0.3		Smithson 2004
	OC-42-1	Pervasively sericitized andesite			$^{40}Ar/^{39}Ar$	Sericite	35.50	0.2		Smithson 2004
White River	03-C-94	Porphyritic Plg-Px dacite flow	-121.811	47.179	$^{40}Ar/^{39}Ar$	Plagioclase	20.65	0.08	0.08	Blakely et al., 2007
	05-C-30	Coarsely porphyritic Plg-Px-Hbl dacite flow	-121.862	47.178	$^{40}Ar/^{39}Ar$	Plagioclase	20.82	0.08	0.08	Blakely et al., 2007
	03-C-92	Porphyritic Plg-Px dacite flow	-121.803	47.169	$^{40}Ar/^{39}Ar$	Plagioclase	21.10	0.06	0.06	Blakely et al., 2007
	02-C-7	Pink alunite in Qz-Alu cemented HT breccia	-121.841	47.164	$^{40}Ar/^{39}Ar$	Alunite	19.00	0.4	0.4	Blakely et al., 2007
	05-C-49	Coarse-grained sprays of Al in Qz-Alu alt'n	-121.805	47.134	$^{40}Ar/^{39}Ar$	Alunite	19.06	0.21	0.21	Blakely et al., 2007
Mount Margaret	*	Diss sulfides in a matrix of Qz+Plg+Ser+Bt	-122.067	46.350	K/Ar	Sericite	16.60	0.6		Evarts & Ashley 1993, Lasmanis 1995
	MDH6-408/410*	Ser-Bt from Potassic Zone	-122.067	46.350	K/Ar	Biotite	17.30	0.5		Evarts et al., 1987
	MDH& 684/687*	Ser-Bt from Phyllic Zone	-122.067	46.350	K/Ar	Sericite	16.90	0.5		Evarts et al., 1987
Washougal	WA-058A*	Granodiorite completely replaced by Qz+Ser+Trm+Py	-122.205	45.788	K/Ar	Whole-rock	19.00	0.7		Power et al., 1981
	WA-11	Fresh Granodiorite	-122.040	45.779	K/Ar	Whole-rock	19.60	0.7		Power et al., 1981
North Santiam		Bornite Breccia Pipe	-122.245	44.840	K/Ar	Sericite	10.10	0.4		Winters 1985
	NS-11*	Fresh Granodiorite	-122.249	44.833	K/Ar	Hornblende	13.40	1.2		Power et al., 1981
Detroit Dam	DMS-53	Detroit pluton (diorite)	-122.250	44.718	K/Ar	Whole-rock	9.68	0.18		Sutter 1978
	DJ04-C46	Diorite	-122.250	44.701	U/Pb SHRIMP-RG	Zircon	12.3	0.8†	3.03	John & Fleck, *pers. comm*., 2013
Quartzville (Proximal)	DJ04-C36	Granodiorite	-122.369	44.587	U/Pb SHRIMP-RG	Zircon	16.2	0.3†	1.21	John & Fleck, *pers. comm*., 2013
Blue River	04-C-4	Qz+Adularia Veins from Tate Mine	-122.344	44.231	$^{40}Ar/^{39}Ar$	Adularia	11.16	0.14	27.14	Fleck, *pers. comm.*, 2006
	BR-6*	Qz diorite	-122.233	44.190	K/Ar	Whole-rock	13.40	1.2		Power et al., 1981
	DMS-77	Nimrod Stock (Leucogranite)	-122.401	44.128	K/Ar	Whole-rock	15.86	0.18		Sutter 1978
Bohemia	046-10B	Qz diorite dike	-122.631	43.626	U/Pb SHRIMP-RG	Zircon	23.5	0.6†	0.6	John & Fleck, *pers. comm*., 2013
	046-11A	Qz diorite stock	-122.635	43.610	U/Pb SHRIMP-RG	Zircon	23.4	0.5†	1.02	John & Fleck, *pers. comm*., 2013
	BO-7*	Qz diorite ppy	-122.633	43.587	K/Ar	Whole-rock	21.7	0.8		Power et al., 1981
Quartz Mountain			-122.670	43.360	$^{40}Ar/^{39}Ar$	Alunite	21.6			du Bray & John 2011

* location approximate
† Reported at 2σ confidence; others unknown
MSWD - Mean Standard Weighted Deviation

Appendix 4. Petrography

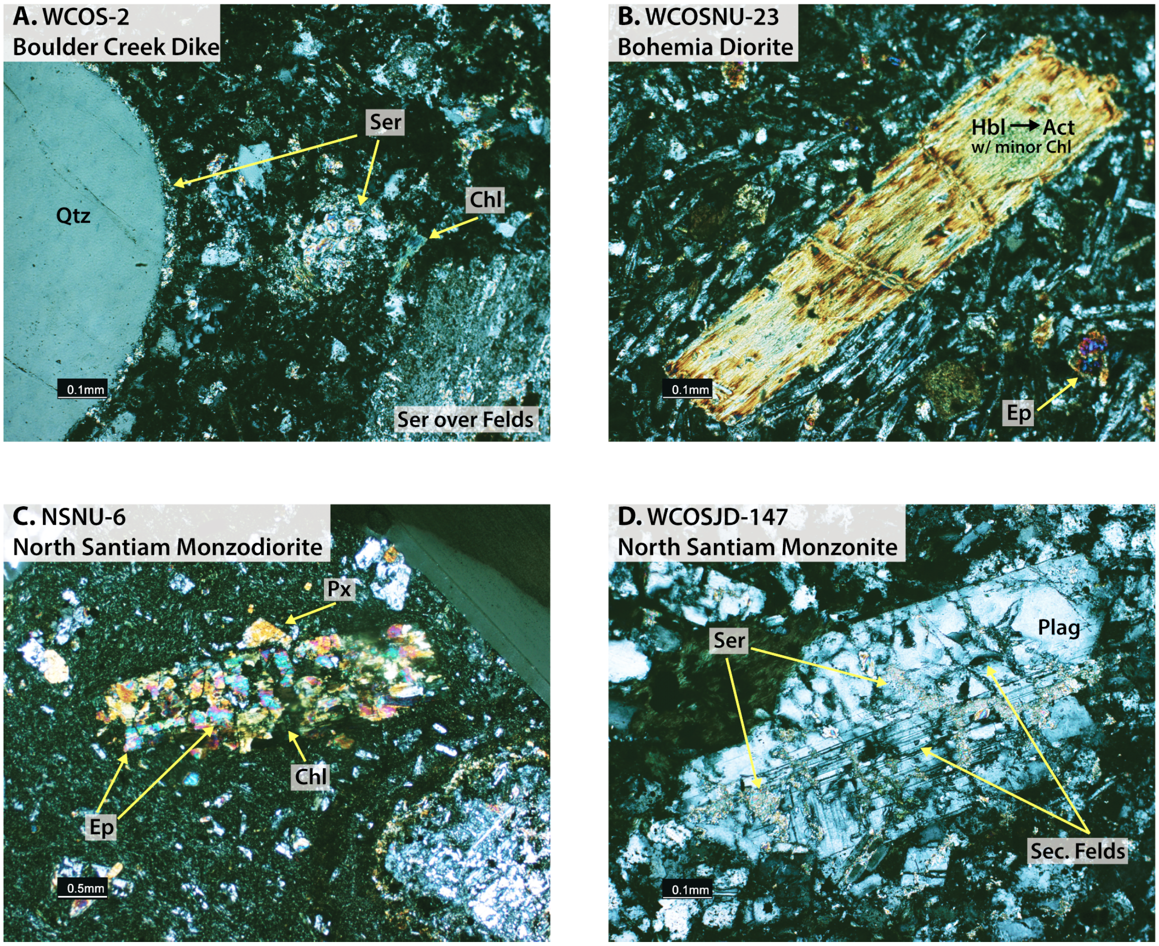

Appendix Figure 3: Additional photomicrographs. Mineral phases are labeled: Actinolite – Act, Chlorite - Chl, Epidote - Ep, Feldspar - Felds, Hornblende - Hbl, Plagioclase - Plag, Pyroxene - Px, Quartz - Qtz, Sericite - Ser. Individual photomicrographs show: A) Resorbed quartz phenocryst and sericitized feldspar phenocryst in porphyry dike from Boulder Creek; B) Typical alteration of Hbl completely replaced by Act with minor Chl; C) Intense Ep alteration of mafics with minor Chl and remnant Px; D) Intense replacement of Felds by Alkali Felds and Albite with remnant Plag.

Appendix Table 2. Western Cascades Petrography & Mineralogy Summary

Sample	District	Rock Type/ Texture	Alteration Summary	Phenocrysts	Matrix
WCOS-2: Boulder Creek	Quartzville	Strongly porphyritic granodiorite with aplitic gm	Feldspars: Plag is 100% replaced by Ser, K-spar is 75% replaced by Ser. Px: 45% by Chlor, 55% by Ser. Bt: 80% to Chlor, 20% to Ser. Quartz is fresh. Mafics in GM to Chlor.	35% phenos of: Plag (30%, 0.2-0.5 mm), Quartz (15%, 0.3-0.75 mm), K-Spar (25%, 0.1-0.5 mm), Px (20%, 1-3 mm), Bt (10%, 0.2 mm)	Fine-grained; 55%; K-spar (45%) + Qtz (30%) + Plag (15%) + Biotite (5%)
WCOS-3	Quartzville	Dacite porphyry	Plag: Fluid fractures common, <5% small secondary Ep or Chlor common. Bt: Altered to microcrystals of Act (50%) + Chlor (35%). Hbl: completely replaced by Act (90%) + Chlor (10%). Matrix: Mafics to Chlor + Act (80-100%)	35% phenos of: Feldspar (40%, 1-3 mm), Bt (30%, 0.2-0.75 mm), Hbl (20%, 0.1-0.3 mm), Qtz (10%, 0.4 mm)	60%, 0.01-0.15 mm; Feldspar (40%), Bt (15%, 65% to Chlor + Act), Hbl (30%, completely replaced by Act + Chlor), Opaques (15%)
WCOS-4	Quartzville	Coarse equigranular Quartz Monzodiorite	Plag: Rims commonly altered to seriicite (5-10%). K-Spar: Fluid fractures ubiquitous. Hbl: 70-95% replaced by Actinolite.	95% grains of: Plag (50%, 0.5-4 mm), Hbl (25%, 0.35-1.5 mm), Quartz (10%, 0.1-0.4 mm), K-spar (10%, 0.5-1 mm), Opaques (5%, 0.1-0.3 mm)	No matrix, equigranular intrusion
WCOS-7	Quartzville	Altered weakly porphyritic monzodiorite stock	Plag: 50-60% to Alb, Small Ep inclusions (5-10%). K-spar: Rims to Ep (5-10%), Opaque inclusions. Hbl: Completely replaced by Chlor (90-95%) with Ep rims (5-10%)	70% phenos of: Feldspar (65%, up to 6 mm), K-spar (15%, 0.2-0.75 mm) Hbl (15%, up to 2 mm), Qtz (5%, 0.1-0.2 mm)	25%, 0.01-0.1 mm: Feldspar (70%), Qtz (15%), Hbl (10%), Ep (10%), Opaques (5%)
WCOS-8	Quartzville	Weakly porphyritic andesitic dike	Plag: Ser (80%) + Ep (10-20%) + Sec Felds (0-10%). Px: Pseudomorphed by Chlor (90-100%) + minor Clays. Qtz: Rimmed in Ser. Hbl: Ep (80-100%) + Chlor (10-20%) + Ser (0-10%) + Trace Fe-Oxides	Phenocrysts (20%): Plag (60%, 0.05 mm), Px (25%), Skeletal Hbl (15%), Qtz (5%, 0.2 mm)	75%, 0.01-0.1 mm: Feldspar (55%), Hbl (25%), Px (10%), Qtz (10%)
WCOS-12	Detroit Dam	Very weakly porphyritic Qtz Monzodiorite stock	Plag: Fresh. K-spar: ~50% to Alb. Px: 70% Chlor + <5% Ep. Hbl: pseudomorphed by HT Bt (> 80%). Mafics in matrix also altered, feldpsars intact.	85% phenos of: Feldspar (65%, 0.25-1.25 mm), K-Spar (10%, 1-2 mm), Qtz (5-10%, 0.1-0.5 mm), Hbl (15%, 0.05-0.1 mm), CPX (10%, 0.05-0.15 mm),	Characterized by interstitial Qtz + Kspar; (10%): Feldspars (70%) + Qtz (20%) + Opaques + Px, grains rounded and ~0.1 mm

Appendix Table 2 (continued). Western Cascades Petrography & Mineralogy Summary

Sample	Plagioclase	K-Feldspar	Pyroxene	Biotite	Quartz	Hornblende	Oxides/Sulfides
WCOS-2: Boulder Creek	Euhedral; No twinning present, completely replaced by sericite (100%).	Sub; Gray, twinless, blotchy. 75% altered to Sericite	Rounded; 100% reaplced by Chlor(45%) + Sericite (55%)	Anhedral; Replaced by Chlor (80%) + Ser (20%). Some may be hydrothermal but now completely altered	Rounded; thin reaction rims, fresh.	Not observed	Pyrite (5%, 0.05-0.2 mm), Hematite (4.5%, 0.03-0.04 mm)
WCOS-3	Euh; Twinning faint. Often resorbed. Commonly sieved with (<5%) inclusions of either Ser (20% of grains) or Ep (20% of grains). Fluid fractures common	Not observed	Not observed	Sub; bird's-eye extinction visible. Often in clumps. Altered tomicrocrystals of Act (50%) + Chlor (35%)	Rounded; thin reaction rims, fresh.	Skeletal; completely replaced by Act (90%) + Chlor (10%)	Opaques likely disseminated pyrite (5%, 0.01-0.5 mm)
WCOS-4	Euh; Twinning strong. Rims are resorbed and altered to Ser (5-10%).	Sub; Fluid fractures common, twinning faint.	Not observed	Not observed	Anh; thin reaction rims. Filling in cracks.	Sub; Px cores common, rims or whole xtal altered to Act (70-95%), somewhat skeletal. Small (~0.01 mm) opaque inclusions common.	Opaques typically within hornblende, small.
WCOS-7	Euh; Altered to albite (50-60%), very large complete laths, small Ep replacements (5-10%), perfect twinning	Euh; rims resorbed typically to Ep (5-10%), inclusions of opaques	Not observed	Not observed	Anh; fillin in cracks.	Euh/Sub; completely replaced by Chlor (90-95%) and rimmed by Ep (5-10%)	Opaques as inclusion in phenos and overprinting matrix
WCOS-8	Skeletal; Typically replaced by Ser (80%) with minor Ep (10-20%) and some secondary Feldspar (0-10%)	Not observed	Sub; Pseudomorphed by Chlor (90-100%) with minor clays	Not observed	Rounded; Rimmed in Sericite	Sub; Typically replaced by Ep (80-100%) with minor Chlor (10-20%) and Sericite (0-10%)	Opaques (likely pyrite) 5%, 0.01-0.5 mm
WCOS-12	Euh; Twinning strong, thin reaction rims common but not ubiquitous	Euh; Full of melt inclusions (too large to call sieves), possibly ~50% replaced by Albite	Sub; Replaced by Chlor (30%) + Minor Ep + Ser (<5%)	Not observed	Sub/Rounded ; strong concoidal fracture	Sub-anh; Weak Hydrothermal Bt (>80%) throughout, some remaining CPX cores. Opaque inclusions ubiquitous.	Opaques likely pyrite (%%, 0.05 mm) and Magnetite and Ilmenite pairs (1-3%, 2:1 ratio) disseminated thorughout, typically euhedral

Appendix Table 2 (continued). Western Cascades Petrography & Mineralogy Summary

Sample	District	Rock Type/ Texture	Alteration Summary	Phenocrysts	Matrix
WCOSNU-01	South Umpqua	Finegrained andesite	Plagioclase 20-80% replaced by fg Chlor. Px: Intact, minor Opaque replacement.	20% phenos of: Feldspar (85%, 0.2-1 mm), Quartz (10%, 0.2-0.5 mm), Px (15%, 0.1-0.7 mm)	70%, 0.01-0.15 mm, Less altered than phenos with exception of reheated devitrified glass(?) now Hbl + Px + Chlor (20-30% matrix); Feldspar (IEu Laths, 80%), Px (Somewhat rounded; 20%)
WCOSNU-07	South Umpqua	Flow-banded Andesite	Plag: Fresh. Px: Fractured and repl. by minor Calc (5-10%) + Opaques (5%). Matrix: Overprinting clays.	20-30% phenos of: Feldspar (75%, 0.2-1.5 mm), Px (25%, 0.2-1 mm)	65%, 0.01-0.175 mm, less altered than phenos but pervasively replaced by clays; Feldspar (80%, acicular), Qtz (10%), Px (10%)
WCOSNU-09	South Umpqua	Porphyritic diorite	Plag: Fresh. K-spar: Sec fluid fractures + Sec Felds (10-20%). Px: Fresh. Hbl: ~50% repl. by Chlor + Minor Ep. Matrix: Mafics + Feldspars intact.	45% phenos of: Feldspar (45%, 0.5-2 mm), K-spar (15%, 0.3 mm), Px (20%, 0.2-0.6 mm), Hbl (10%, up to 0.75 mm), Minor Quartz (< 10%, 0.05-0.15 mm)	55%, 0.01-0.5 mm, Feldspar (70%), Hbl (5%), Px (10%); Qtz (15%). Mafics relatively intact.
WCOSNU-10	South Umpqua	Porphyritic tonalite	Plag: Ep (typically in veints, 5-15%) + Sec fluid fractures (5-15%). Px: Fresh. Bt: Act (50-80%) + Ep (10-20%) + Chlor (5-10%). Hbl: Chlor (typically in core, 80-90%) + Act (5-20%) +/- Minor Ep. Matrix: Mafics to Act (80-100%)	45% phenos of: Feldspar (50%, 1-2 up to 5 mm), Qtz (15%, 0.2-0.6 mm), Hbl (15%, 0.5 mm), Bt (15%, 0.1-1mm), Px (5%, 0.1 mm)	55%, 0.05-0.1 mm; Feldspar (50%), Bt (5%), Hbl (5%), Qtz (25%), Opaques (15%)
WCOSNU-11	South Umpqua	Strongly porphyritic diorite	Plag: Sec Phases along fractures (Act + Sec Felds + Opaques - not occuring together, up to 30%). K-spar: 30% Sec Felds + 10% HT Bt + Fluid fractures. Bt: Ep (10-15%) + Sec Felds (10%) + Opaque (10%). Px: Fresh	45% phenos of:Plagioclase (40%, 0.5-1 up to 3 mm), K-spar (20%,1-2 mm), Bt (25%, 0.5-3 mm), Px (15%, 0.5-1 mm)	55%, 0.01-0.15 mm; Felds (50%), Bt (20%), Qtz (25%), Opaques (15%)

Appendix Table 2 (continued). Western Cascades Petrography & Mineralogy Summary

Sample	Plagioclase	K-Feldspar	Pyroxene	Biotite	Quartz	Hornblende	Oxides/Sulfides
WCOSNU-01	Euh/Sub;Twinning faint or absent; 20-80% replaced by fg Chlor, appear to be infilling sieved texture in places.	Not observed	Euh commonly; Well intact with strong cleavage, some inc. of opaques.	Not observed	Not observed	Not observed	Small (0.05 m)Mag & Ilm (2:1) (1-3%?)
WCOSNU-07	Euh with irregular rims; strong twinning, fractured and thin reaction rims.	Not observed	Euh; Strong cleavage, fractured and replaced by minor Calcite (5-10%) + opaques (5%)	Not observed	Not observed	Not observed	Opaques (5%, 0.01-0.1 mm) rounded, in band along section with flow-banding
WCOSNU-09	Euh; strong twinning, often sieved and fractured with reaction rims	Sub; typically heavily eroded by secondary fluid fractures and/or Sec Feld xtals (10-20%) thick irregular reaction rims.	Rounded; Strong cleave, reaction rims. Fresh	Not observed	Rounded/Anh; Oscillatory extinction clear. Thin reaction rims.	Sub; Heavily embayed, lots of opaque inclusions. Irregularly replaced by Chlor (~50% phenos). Minor Ep (<5%),	Opaques (5%, 0.01-0.1 mm), rounded
WCOSNU-10	Euh; strong twinning if a bit irregular, heavily fractured. Rims resorbed to lighter, irregular rims. Large glomerocryst of feldspar. Replaced by Ep (typically in veins, 5-15%).	Not observed	Sub; Fractured, rims typically resorbed	Euh/sub; Completely replaced by Act (50-80%) + Ep (10-20%) + Chlor (5-10%)	Rounded; Concoidal fracture, typically clumped	Sub; Opaque inclusion (5%) intact. Replaced by Chlor (typically in cor, 80-90%) + Act (5-20%) +/- Ep	Opaques in GM
WCOSNU-11	Euh; nicely twinned with rxn rims and secondary phases along fractures (Act + Sec Felds + Opaques - not occuring together). Some (~50%) are sieved.	Euh; All phenos 30% replaced by Sec Felds + 10% to HT Bt; Fluid fractures common.	Sub; Fractured, resorbed rims, inclusion of opaques	Sub but skeletal; Bird's-eye extinction intact but fragmented; Replaced by Ep (10-15%) + Sec Felds (10%) + Opaque (10%)	Not observed	Not observed	~1-2% disseminated Pyrite (<0.01 mm) Magnetite + Ilmenite - estimate ratio?

Appendix Table 2 (continued). Western Cascades Petrography & Mineralogy Summary

Sample	District	Rock Type/ Texture	Alteration Summary	Phenocrysts	Matrix
WCOSNU-12	South Umpqua	Coarse-grained equigranular diorite	Plag: Fractures/wormy fluid paths (<20%), K-spar: 20% of phenos replaced by Sec Felds (100%), Qtz: Fresh, Hbl: Typically completely replaced by Act (90-95%) with minor Chlor (5-10%)	85% grains of: Feldspar (50%, 0.5-4 mm), Hbl (25%, 0.4-1.2 mm), K-spar (15%, 0.5-2 mm), Qtz (15%, 0.2-1.2 mm)	15%, no true groundmass but secondary phases seem to suround major phenocrysts: Acicular (0.05 mm) Chlor ± Act dominate (80%) + Opaq (15%) + Ep (5%)
WCOSNU-19	Bohemia	Weakly porphyritic monzodiorite dike	Plag: Sec Chlor + Ep + Felds in fractures (5-10%), K-spar: 10-15% of phenos full of Chlor +/- Calc (50-70%) in cyrstal core, Px: Faintly replaced by Calc (<5%) + Chlor (5-10%), Hbl: 20% Fresh, majority replaced by Chlor (70-90%) +/- Ep (10-20%).	30% phenos of: Plag (55%, 0.1-0.5 mm), K-spar (15%, 0.5-1.2 mm), Hbl (10%, 0.5mm), Px (20%, 0.2-0.8 mm)	70%; Plag (50%, up to 0.075 mm), K-spar (20%), Qtz (5%, 0.025 mm) Mafics (10%, 0.01-0.05 mm), Opaques (15%, 0.01-0.05mm)
WCOSNU-20	Bohemia	Andesite dike	Plag: Ep (<3%) + Calc (<5%) + Opaques (5-10%, K-spar: minor Ep (<3%) + Sec Felds (10-15%) replacement, Hbl: Act (50-70%) + Chlor (20%) + Calc (0-15%) + Ep (5-20%	45% phenos of: Plag (55%, 0.2-0.6 mm) K-spar (20%, 0.3 mm), Hbl (25%, up to 1 mm)	55%: Feldspar (50%, 0.05 mm), Mafics (30%, 0.01-0.05 mm), Opaques (0.01-0.05)
WCOSNU-21	Bohemia	Weakly porphyritic granodiorite	Plag: small (<0.1 mm) replacement of Hbl → HT Bt → Chlor & Quartz (15%). K-spar: ~ 20% replaced by Albite. Hbl: Act (5-60%) + Chlor (20-95%) + Ep (<5%). GM: Hbl replaced to same degree as phenocrysts	70% phenos of: Plag (35%, 1-4 mm), Quartz (15%, 0.2-1 mm), K-spar (25%, 1 mm), Hbl (25%, 0.5 mm)	30%, rounded, 0.05-0.1 mm; mostly Qtz (45%) + K-spar (40%)+ Minor Hbl (5%) + Opaques (10%)

Appendix Table 2 (continued). Western Cascades Petrography & Mineralogy Summary

Sample	Plagioclase	K-Feldspar	Pyroxene	Biotite	Quartz	Hornblende	Oxides/Sulfides
WCOSNU-12	Euh; nice twinning, often surrounded by broken up Qtz. Larger laths have twinning interrupted by fractures w/ wormy fluid paths and melt inclusions. Somewhat sieved.	Anh; often intergrown with Qtz. Sometimes (20%) replaced by Sec Felds (100%).	Not observed	Not observed	Sub/anh; Very bright/high relifed, fluid inclusions; thin rxn rims	Sub/skeletal; Typically completely replaced by Act (90-95%) with minor Chlor (5-10%); Opaques often accumulated around rims	Opaques within Hbl
WCOSNU-19	Euh; Lots of fractures filled with secondary chlorite and others (5-10%), resorbed rims typical. Not sieved but definitely lots of melt inclusions.	Sub; Typically thorougly sieved and full of melt inclusion. Some of the more alt'd feldspars I have seen – some(10-15%) full of chlorite +/- calcite(50-70%) in center of xtal.	Euh; Rimmed entirely in thick (~0.01 mm) reaction rim and possibly calcite (,<5%) ; faintly replaced by chlorite (5-10%).	Not observed	Not observed	Sub; Nearly completely replaced by chlorite (70-90%) s +/- epidote (10-20%). Typically rims are most intact portion. Interestingly, some phenos are globbed together and nearly completely fresh (20%). Opaque inclusions intact.	Opaques in GM and as inlcusions with hbl
WCOSNU-20	Euh; Very fractured and eroded, interrupting twinning. Secondary phases include Ep (<3%) + Calc (<5%) + Opaques (5-10%). Fluid inclusions present in some, some (10%) heavily sieved.	Euh; More intact than Plag; melt inclusions common and some minor Ep (<3%) + Sec Felds (10-15%) replacement	Not observed	Not observed	Not observed	Sub/Skeletal; Completely replaced by Act (50-70%) + Chlor (20%) + Calc (0-15%) + Ep (5-20%), dispersing into matrix. Zoning outwards: chlorite → opaques	Opaques in matrix and preserved within Hbl
WCOSNU-21	Euh; Very fresh comparatively, small (<0.1 mm) replacement of Hbl → HT Bt → Chlor & Quartz (15%)	Sub; Heavily resorbed rims, maybe altered to albite? (20%) Very nice twinning with some fractures	Not observed	Not observed	Sub; Irregular rims but otherwise intact. Lots of fluid inclusions	Sub; Typically replaced by Act (5-60%) + Chlor (20-95%) + Ep (<5%), Opaques intact	Opaques within Hbl, and groundmass

Appendix Table 2 (continued). Western Cascades Petrography & Mineralogy Summary

Sample	District	Rock Type/ Texture	Alteration Summary	Phenocrysts	Matrix
WCOSNU-23	Bohemia	Porphyritic diorite	Plag: Repl. by Ep in fractures (1-3%). Some grains (~20%) more substantially replaced by Ep (5-10%) +/- Chlor (5%). Hbl: typically Act (30-100%) + Chlor (0-30%) + Minor Ep (0-10%). Px and Qtz are fresh.	30% phenos of: Plag (55%, 0.2-0.5, up to 1 mm), Qtz (10%, 0.2 mm), CPX (10%, 0.1-0.3 mm), Hbl (25%, 0.05-1 mm)	70%; Feldspar (55%, 0.015 mm), Hbl (15%, 0.001 mm, replaced by Act + Chlor), CPX (10%, 0.001-0.005 mm), Qtz (10%, 0.005 mm), Opaques (5-10%, 0.001-0.005 mm)
WCOSNU-24	Bohemia	Porphyritic Qtz Diorite	Plag intact. K-spar: Partially replaced by Chlor(10-20%) + Ep (up to 30%). Px: Pseudomorphed by Ep (95%). Hbl: at least 75% replaced by Act + Minor Chlor (10-20%) + Ep (up to 20%)	50% phenos of: Plag (45%, 1.5-3 mm), Hbl (25%, 0.05-1 mm), Px (10%, 0.05 mm), K-spar (15%, 1-3 mm), Qtz (15%, 0.05 mm)	50%; Feldspars (55%, 0.01-0.2 mm), Hbl (to Act + Chlor + Ep, 15%, 0.005 mm), Qtz (10%, 0.005-0.01 mm), Opaques (10%, 0.1 mm).
WCOSNU-25	Bohemia	Porphyritic diorite	Plag; Intact. K-spar: partially replaced by Ep (5-10%) +/- Opaques (up to 5%). Px: Large replacements of Sec K-spar (5%) + Act (5-10%). Hbl: 20% completely replaced by Chlor, 50% completely replaced by Act, 30% a mixture of the two (typically Chlor in cores	55% phenos of: Plag (45%, up to 3 mm), Hbl (20%, 0.5 mm), Px (0.5-2.5 mm), K-spar (20%, 0.5-1.5 mm), Qtz (10%, 0.5 mm)	
WCOSNU-28	Blue River	Porphyry diorite	Plag: Intact. K-spar: ~45% have varying replacement phases: Ser (0-15%) + Calc (0-65%) + Ep (0-10%) + Minor Iron Oxide staining. Px: Intact. Hbl: Chlor (cores, 40-90%) + Act (rims, 10-40%) + minor Ep (5-10%), often (30%) rimmed by Calcite.	40% phenos of: Plag (40%, 0.25-0.5 mm), K-spar (25%, 0.5-1.25 mm), Hbl (20%, up to 1.5 mm), Px (15%, 0.1-0.2 mm)	~20% thin section is covered in calcing bands ranging from 0.2-1mm thick! GM is 40%: Feldspar (70%, 0.1 mm), Mafics (10%, 0.05 mm), Opaques (20%, 0.02-0.05 mm)

Appendix Table 2 (continued). Western Cascades Petrography & Mineralogy Summary

Sample	Plagioclase	K-Feldspar	Pyroxene	Biotite	Quartz	Hornblende	Oxides/Sulfides
WCOSNU-23	Euh; Heavily resorbed rims, very fractured. Or, nice twinning in place suggestive of replacement by albite. Secondary phases in fractures typically Ep (1-3%). Some grains (~20%) more substantially replaced by Ep (5-10%) +/- Chlor (5%)	Not observed	Sub; Lots of inclusions opaques, slightly resorbed rims, otherwise intactt.	Not observed	Sub; Irregular rims, lots of fluid inclusions	Sub; Varying degrees of alteration, typically Act (30-100%) + Chlor (0-30%) + Minor Ep (0-10%), opaque inclusions common, structure and cleavage intact with eroded rims	Opaques in GM and as inlcusions with hbl
WCOSNU-24	Euh; Fractured with thin reaction rims but relatively intact. Strong twinning	Sub; Weak/soft zoning or not present, full of melt inclusions and fractures. Partially replaced by Chlor(10-20%) + Ep (up to 30%).	Euh; completely replaced by Ep with cleavage and rims remaining (95%)	Not observed	Anh; Concoidal fracture, filling in around other phases, thin reaction rims.	Sub; Typically at least 75% replaced by Act + Minor Chlor (10-20%) + Ep (up to 20%)	Opaques in GM
WCOSNU-25	Euh; Fractured with thin reaction rims but relatively intact. Often has "sieved" texture	Euh/Sub; Albitized, commonly fractured, thin reaction rims, sometimes partially replaced by Ep (5-10%) +/- Opaques (up to 5%)	Sub; Cleavage still present, large repl. by Sec K-spar (5%) + Act (5-10%),reaction rims typical	Not observed	Anh; Conchoidal fracture, fluid inclusions.	Sub; 20% completely replaced by Chlor, 50% completely replaced by Act, 30% a mixture of the two (typically Chlor in cores), opaque inclusions intact.	
WCOSNU-28	Euh; Lots of fracturing, reaction rims common.	~30% heavily sieved, ~45% have varying replacement phases: Ser (0-15%) + Calc (0-65%) + Ep (0-10%) + Minor Iron Oxide staining.	Sub; Typically rimmed with secondary Chlor	Not observed	Not observed	Sub; Typically fractured and replaced by Chlor (cores, 40-90%) + Act (rims, 10-40%) + minor Ep (5-10%), often (30%) rimmed by Calcite.	

Appendix Table 2 (continued). Western Cascades Petrography & Mineralogy Summary

Sample	District	Rock Type/ Texture	Alteration Summary	Phenocrysts	Matrix
WCOSNU-29	Blue River	Porphyritic diorite intrusion with finegrained groundmass	Feldspars are most altered (20% Sec Felds, 30% Ser, 5% Chlor, <5% Ep), Mafics relatively intact (10% Serc, 5% Chlor), GM alt'n unclear	55% phenos of: Plag (60%, 0.2-0.5 mm), Hbl (30%, 0.3-1.5 mm), Px (10%, 0.1-0.4 mm)	40%, <0.005 mm grains, too fg to identify specific phases. Grains appear somewhat rounded, with likely assemblage 30% Feldspar, 40% Sericite, 30% Mafics + Opaques w/ overprinting clays
WCOSNU-31	Blue River	Porphyritic Qtz Diorite	Feldspars heavily altered (30-40% Sec. Felds, 30% Ser, 5% Chlr, 3-5% Ep), Hbl completely replaced (70% Act, 20% Chlor, 10% Ksp, Minor Ser + Ep), Qtz fresh; GM alt'n similar	40% phenos of: Plag (60%, 0.2-0.6 mm), Hbl (30%, 0.1-0.25 mm), Quartz (10%, 0.75 mm)	40%, Fine-grained (typically 0.02-0.05 mm), ~70% replaced. ~50 Felds repl. By Ser + Ksp (85%), ~20% Fresh Qtz, ~30% Mafics repl. By Act + Chlor (100%)
WCOSNU-32	Blue River	Porphyritic diorite or Qtz Diorite	Hbl: some fresh but typically replaced by Chlor (5-10%) and Ep (5%) and sometimes completely pseudomorphed. Px: fresh but similar to Hbl. Felds: Ser veins/fluids (0-20%), localized Chlor replacement (10%), minor Ep (<5%), thin reaction rims common, or completely replaced by all. GM: less altered than phenos w/ Mafics to Chlor + Ep (20%) and Felds to Ser (15%).	40% phenos of: Plag (60%, 0.4-4.5 mm), Hbl (30%, 0.5-1.5 mm, up to 4 mm), Px (10%, 0.4-0.5 mm)	60%, Plag laths dominate (60%, up to 0.1 mm long, 15% replaced by Ser), Mafics (20%, 0.05 mm, replaced by Chlor + Ep), at leat 15% Opaques (Blocky, 0.1 mm), some anhedral Qtz (10%, 0.1-0.3 mm, fluid inclusions & reaction rims)
WCOSNU-33	Blue River	Porphyritic granodiorite	Bt in GM: 95% repl. By radial Act (dom) +/- Chlor +/- Ep, bird's eye extinction intact - may be replacing Primary Hbl. Some K-spar may be secondary.	40% phenos of: Plag (65%, 0.3-1.5 mm), Kspar (15%, up to 0.5 mm), Qtz (20%, 0.1-0.25 mm)	60%, aplitic texture, grains typically 0.1 mm, rounded. Qtz (40%), Ksp (35%), Pyrite (10%), Bt (10%, up to 0.3 mm, subh), Plag (5%)

Appendix Table 2 (continued). Western Cascades Petrography & Mineralogy Summary

Sample	Plagioclase	K-Feldspar	Pyroxene	Biotite	Quartz	Hornblende	Oxides/Sulfides
WCOSNU-29	Euh; twinning destroyed by Sericite (30%) + less abundanct Chlor (5%) +Ep (<5%), some replaced by albite (15-20%) and secondary fluid pathways	Not observed	Sub/blocky; replaced by Ser (10%) + Chlor (5%) but cores intact	Not observed	Not observed	Sub; Moderately fractured with opaque inclusions, commonly rimmed in Ser. Partially replaced by Chlor (10%) but otherwise intact.	
WCOSNU-31	Euh; Twinning moderately defined but mostly replaced by secondary K-spar (30-40%) and Ser (20-30%), some Chlor (10%), minor Ep (3-5%). Sometimes nearly completely replaced by microcrystals of K-spar	Not observed	Not observed	Not observed	Sub/anh; Thin reaction rims	Sub; Blocky shape with pronounced singular cleavage. Typically replaced by Act + Chlor + Minor K-spar +/- Ep, Sometimes completely replaced by Chlor or Act	
WCOSNU-32	Euh; Twinning and cleavage intact although commonly sieved. Most common alteration is crossing fractures/fluid pathways of Ser (0-20%), localized Chlor replacement (10%), small Ep replacement (<5%), Some completely replaced by sericite (95%)	Not observed	Sub; Rounded, reaction rims, relatively intact but sometimes replaced by Chlor + Ep (20%)	Not observed	Not observed	Euh; the majoritey of phenos are nearly completely intact with minor/localized replacement by Chlor (5-10%) or Ep (5%). Osme completely pseudomorphed by Chlor +/- Ep	
WCOSNU-33	Euh; Weak twinning and heavily sieved texture, typically centered in core of xtal but can dominate entire xtal. Typically slightly rounded with thin reaction rims. Fluid fractures are rare.	Not observed	Not observed	Only in GM	Sub/Anh; Fresh, somewhat rounded, fluid inc. common.	Not observed	Pyrite in matrix

Appendix Table 2 (continued). Western Cascades Petrography & Mineralogy Summary

Sample	District	Rock Type/ Texture	Alteration Summary	Phenocrysts	Matrix
WCOSNU-091	North Santiam	Porphyritic andesite or fine-grained monzodiorite	Feldspars mostly intact (K-spar to secondary Ksp fluids + Minor Chlor = 20%), Hbl completely replaced (~50% Chlor, ~30% Ser, ~20% Ep)	30% phenos of: Plag (65%, 0.4-1.6 up to 5 mm), Kspar, (15%, up to 0.5 mm), Hbl (20%, 0.3-0.6 mm)	65%, dominated by Plag laths (up to 0.1 mm but typ. Smaller, 60%), minor K-spar (10%, 0.025 mm, rounded), Mafics (20%, aphanitic), Opaques (~5 µm, 10%)
WCOSNU-119	North Santiam	Porphyritic monzodiorite	Feldspars: Mostly intact, Kspar alt'n dominated by fluid fractures (20%) and minor local Ep (5%). Hbl: mostly replaced by Chlor (45%, cores) + Act (35%, outer core/rim) + Ep (10%). GM: contains lots of chlor (difficult to ID primary phases) but likely less altered than phenos	55% phenos of: Plag (60%, 0.5-1.5, up to 3 mm), K-spar (10%, up to 0.5 mm), Px (10%, 0.25-0.5 mm), Hbl (20%, 0.1-0.5 mm)	Matrix very fg (<0.01 mm), mineral ID difficult. Estimates: 55% Plag, 15% Opaques, 20% Mafics, 20% K-spar
WCOSNU-162	North Santiam	Porphyritic tonalite?	Feldspars: replaced by Ep (15%) + Calc (20%) + Sec. Felds (30%) + Act/Chlor (15%), thick reaction rims. Mafics: Nearly complete replacement by Ep (15%) + Act (25%) + Chlor (25%) + Sec. Felds (5-10%) + Opaques (10%) + Clays (5%). Quartz + Opaques relatively fresh.	35% phenos of: Plag (40%, 0.75 mm), Hbl (30%, up to 1.5 mm), Qtz (20%, 0.1 mm), Opaques (10%, 0.1 mm)	65%, 0.01-0.02 mm rounded grains. Dominated by Felds + Quartz, 20-30% altered mafics, 5% opaques

Appendix Table 2 (continued). Western Cascades Petrography & Mineralogy Summary

Sample	Plagioclase	K-Feldspar	Pyroxene	Biotite	Quartz	Hornblende	Oxides/Sulfides
WCOSNU-091	Euh; Strong twinning, somewhat rounded corners, fluid pathways common although not ubiquitous.	Sub; Weak irregular twinning (tartan twinning rare), distinct fluid fractures common. Reaction rims and sieved textures common.	Not observed	Not observed	Not observed	Sub/Rounded; ID'd as Hbl due to opaque inclusions and some faint twinning. Commonly replaced by Chlor (50%) rimmed by Ser (30%), sometimes more substantially replaced by Ser + Ep + minor Chlor in bands.	Opaques in matrix
WCOSNU-119	Euh; Strong twinning, small reaction rims and fluid pathways common, sieved zone near rim somwhat common	Sub; Twinning irregular and typically faint. Irregular sieved zones, lots of fluid alt'n (pathways/fractures), rare secondary Ep	Sub; Intact, minor Chlor+Act+Ep (10%) rims and some fracturing, but cleavage and shape primary	Not observed	Not observed	Sub/Rounded; Cores are replaced by anomalous blue Chlor (45%), rims are commonly repl. By Act (35%), Minor Ep in cores (10%). Primary Hbl uncommonly remnant in cores. Opaque inclusions common.	Opaques in matrix
WCOSNU-162	Sub; Twinning faintly intact in places, otherwise replaced to: Ep (15%) + Cac (20%) + Sec. Felds (30%) + Act/Chlor (15%), thick reaction rims to the point that cannot distinguish original crystal edge.	Not observed	Not observed	Not observed	Sub; Typically rounded with thin reaction rims.	Sub; Opaque inclusions, hard to ID cleavage or phase boundaries due to alteration: Ep (15%) + Act (25%) + Sec. Felds (5-10%) + Opaques (10%) + Clays (5%)	Euh/blocky; Thin band of Fe-oxides surrounding Opaques

Appendix Table 2 (continued). Western Cascades Petrography & Mineralogy Summary

Sample	District	Rock Type/ Texture	Alteration Summary	Phenocrysts	Matrix
WCOSWR-01	White River	Porphyritic monzonite	Feldspars: Kspar +/- Qtz in fluid fractures (10-20%) + Minor local Ep replacement (5%). Bt: pseudomorphed by Ep (100%) or repl. By Chlor + Act +/- Clays (50%). Hbl: commonly pseudomorphed by Ep and Chlor+Act (up to 50%) with ligher reaction rims, sometimes (10%) replaced by Sec Bt.	60% phenos of: Plag (40%, up to 2 mm), Hbl (20%, up to 0.5 mm), K-spar (20%, 0.75 mm), Bt (10%, 0.2-0.3 mm), Qtz (10%, 0.1-0.2 mm)	40%, 0.02-0.03 mm rounded grains. K-spar (40%) + Qtz (50%), 10% mafics, Disseminated tarnished Pyrite (<5%)
WCOSJD-147	North Santiam	Quartz monzodiorite	Plag: Repl. By Ser (10-15%) + Act (5%) + K-spar (10-20%). K-spar: Twinning not intact, heavily replaced by Ser (20-30%) + Ep (10%). Px: Repl. By Ep (45%) + Chlor (35%). Hbl: near complete replacement by Act (80-100%) + minor Ep + Chlor (10-20%). Matrix: Abundant alteration to Ser (20% Plag + 20% K-spar), Act (100% Hbl + ~60% Px), Rare Chlor + Ep replacing mafics.	30% phenos of: Plag (50%, 1-5 mm), Hbl (30%, 0.3-1 mm), Qtz (0.4-1 mm), Cpx (10%, up to 0.5 mm), K-spar (5%, 0.2-0.5 mm), Pyrite (5%, up to 0.5 mm typically 0.2 mm)	70%, 0.04-0.1 mm grains. Rounded K-spar (20%) + Qtz (30%) + Euh Plag (40%) + Minor Mafics + Opaques. Abundant alteration to Ser (20% Plag + 20% K-spar), Act (100% Hbl + ~60% Px), Rare Chlor + Ep replacing mafics.
WCOSJD-152	North Santiam	Porphyritic Quartz Monzodiorite	Plag: replaced by Sec K-spar via fluid pathways (20-30%) + minor Ep + Chlor (5-10%). K-spar: replaced by secondary K-spar (40-50%, breaking up the grain) + minor Ep + Chlor (5-10%). Hbl: Some very intact with thin reaction rims, others pseudormoprhed by Act (20%), others repl. by Act (20%) + Ep (5-10%) + K-spar (5-10%) + Chlor (10%).	30% phenos of: Plag (50%, 1-5 mm), Hbl (30%, 0.3-1 mm), Qtz (10%, 0.1-0.3 mm), K-spar (5%, up to 3 mm), Pyrite (5%, up to 0.4 or 0.5 mm)	70%, graphic and intergrown: Plag (50-60%, up to 0.08 mm) + Qtz (5-10%, round, 0.05 mm), Hbl (Repl. by Act+Opaques, 5%), K-spar (trace, 10%?), Opaques (10-15%, blocky, 0.05 mm). Plag laths are somewhat banded.

Appendix Table 2 (continued). Western Cascades Petrography & Mineralogy Summary

Sample	Plagioclase	K-Feldspar	Pyroxene	Biotite	Quartz	Hornblende	Oxides/Sulfides
WCOSWR-01	Sub; Strong twinning, partially disturbed by fluid fracture pathways (10-20%) carrying Sec. Felds +/- Qtz. Secondary Ep somewhat common (5%, <0.01 mm)	Sub; Twinning not always visible, and typically interrupted by Sec. Felds (some albitic twinning observed in ~20% of phenos) replacement (10-20%), minor (up to 0.1 mm long) Ep also common (5-10%)	Not observed	Sub; Cleavage intact but commonly pseudomorphed by Ep (100%) or replaced by Chlor + Act (50%), some clays present. Thin reaction rims common.	Rounded/Anh; Fresh with thin reaction rims, lots of fluid inclusions	Sub; Texturally intact with big (up to 0.1 mm) opaque inclusions, but strangely banded across cleavage planes that is probably a product of alteration. Commonly pseudomorphed by Ep and Chlor+Act (up to 50%). Ligher reaction rims ubuiquitous. Sometimes repaced by Sec Bt (shreddy)	Magnetite + Ilmenite - estimate ratio?
WCOSJD-147	Euh; Strong twinning, eroded edges. Repl. By Ser (10-15%) + Act (5%) + K-spar (10-20%), Sec. Felds gives it slighlty "fuzzy" texture. Ser dominantly in fluid pathways/fractures.	Sub; Cleavage not intact, more heavily replaced by Ser (20-30%) + Ep (10%).	Sub; Cleavage intact but repl. By Ep (45%) + Chlor (35%)	Not observed	Anh/rounded; Typically anh with prominent reaction rims (0.025 mm thick)	Sub; near complete replacement by Act (80-100%) + minor Ep + Chlor (10-20%). Opaque (Mag) inclusions remain.	Pyrite: Rounded, often surrounded by Chlor alteration but intact
WCOSJD-152	Euh; Twinning strong but replaced by Sec K-spar via fluid pathways (20-30%) + minor Ep + Chlor (5-10%).	Sub; Twinning intact but otherwise replaced by secondary K-spar (40-50%, breaking up the grain) + minor Ep + Chlor (5-10%). One is cut by an Ep vein.	Not observed	Not observed	Anh; thin reaction rims that are not uniform in thickness	Sub; Some very intact with thin reaction rims, others pseudormoprhed by Act (20%), others repl. by Act (20%) + Ep (5-10%) + K-spar (5-10%) + Chlor (10%). Magnetite inlcusions abundant throughout.	Pyrite: Blocky, thin iron oxide rings, fresh.

Appendix Table 2 (continued). Western Cascades Petrography & Mineralogy Summary

Sample	District	Rock Type/ Texture	Alteration Summary	Phenocrysts	Matrix
NSNU-2	North Santiam	Porphyritic Qtz monzodiorite	Plag: Secondary phases are uncommon and limited to Qtz + Minor Ep + Rare Sericite (10%). Hbl: Characteristically altered to anomalously dark purple and blue Chlor + Ep restricted to cores (100%), or Ep pseuodmorphs Sec Bt/Act, or intact cores with chloritized rims and minor Ep (50%).	35% phenos of: Plag (50%, 0.3-1.2 mm), K-spar (20%, 0.1-0.5 mm), Hbl (20%, 0.3-0.7 mm), Qtz (10%, 0.1-0.3 mm)	65%, Qtz (25%) + K-spar (35%) + 20% Plag (laths up to 0.1 mm) + Hbl (15%, heavily alter'd and does not retain its shape) + Opaques (10%).
NSNU-3	North Santiam	Ignimbrite	Plag: secondary Ep (20-30%). K-spar: Heavily replaced by Quartz + Chlor + Epidote + Biotite → Actinolite (70%). Px: Fresh. Hbl: Some intact (50%), some replaced by either or a combination of both Act + Ep (80%).	20% phenos of: Plag (55%, 0.5-2 mm), Hbl (25%, 0.3-0.7 mm), CPX (15%, 0.5-1 mm), K-spar (5%, 1.5 mm)	80%, very fg (<0.02 mm) and clay-rich. Plag-dominated with substantial proportions of mafics (20-30%), very tiny opaques disseminted (~10 microns)
NSNU-4	North Santiam	Porphyritic Granodiorite	Quartz + Plag intact, Hbl completely replaced by Chlor (cores - 50-70%) + Ep (outer cores to rims - 30-40%) + Clays (10%), K-spar heavily sieved and fractured with minor sec. Ep (5-10%). GM: Mafics completely replaced but K-spar intact.	45% phenos of: Plag (60%, 0.5-2 mm), Hbl (20%, 0.5-1 mm), K-spar (15%, 0.3 mm), Qtz (5%, 0.1 mm)	55%; Rounded K-spar (35%) and quartz (30%) (grains ~0.05 mm), plag laths (20%, 0.1-2 mm), minor opaques (10%, 0.05 mm), mafics <5%
NSNU-6	North Santiam	Porphyritic monzodiorite	Plag + CPX fresh. Hbl: 90% completely replaced by Act (70%) + Ep (15%) + Chlor (15%). K-spar: Minor epidote replacement (5%). Matrix: ~70% mafics replaced by Ep + Chlor + Act (dominant), clays common.	55% phenos of: Plag (60%, 0.5-2 mm), Hbl (20%, 0.15 mm), K-spar (15%, 0.3-0.6 mm), Px (5%, 1.5 mm)	50%; Grains typically 0.02 mm. 35% Mafics + 25% K-spar + Plag (20%) +20% opaques. Lots of clay and chlorite alteration, difficult to quantify.

Appendix Table 2 (continued). Western Cascades Petrography & Mineralogy Summary

Sample	Plagioclase	K-Feldspar	Pyroxene	Biotite	Quartz	Hornblende	Oxides/Sulfides
NSNU-2	Euh; strong twinning, reaction rims common but not ubiquitous. Some grains have defined sieved zone near rim or closer to core, several are cut by thick (0.01-0.02 mm) Sec. Felds bands, others sieved throughout. Secondary phases are uncommon and limited to Qtz + Minor Ep + Rare Sericite (10%)	Sub; defined reaction rims ubiquitous and fractures common.	Not observed	Not observed	Sub; thin reaction rims, irregular shape.	Sub; Characteristically altered to anomalously dark purple and blue Chlor + Ep restricted to cores (100%). In some cases Ep pseuodmorphs Sec Bt/Act, some have intact cores with chloritized rims and minor Ep (50%).	Opaques in GM
NSNU-3	Euh; Twinning is weak and absolutely full of sieved texture and secondary epidote (20-30%)	Skeletal; Heavily replaced by Quartz + Chlor + Epidote + Biotite → Actinolite (70%)	Sub; Very fresh, with very thin reaction rims and some fracturing.	Not observed	Not observed	Sub; Either relatively intact with thin reaction rims and opaque inclusions OR remarkably destroyed and replaced by either or a combo of both: Actinolite and epidote (80%).	Opaques in matrix
NSNU-4	Euh; Rims are somewhat irregular, secondary fluid fracturing is common, but otherwise fresh, (+/- some clays), Twinning common and often albite.	Skeletal; Heavily sieved and fractured, twinning in place but weak, secondary epidote common (5-10%) and some iron oxides	Not observed	Not observed	Sub; Very fresh with eroded grain boundaries	Sub; Completely replaced by chlorite (cores – 50-70%), epidote (outer cores to rims – 30-40%), and clays (10%), no grain boundaries left.	Minor opaques in matrix
NSNU-6	Euh; Albite twinning, Sieved zones, reaction rims, and fluid fractures common. Sieved zones may have clays +/- secondary Feldspar (10%). ~20% have oscillatory zoned with thin reaction rims.	Sub; Embayed, lots of fractures, rare (5%) epidote inclusions. Heavily sieved.	Euh; Embayed rims but otherwise fresh	Not observed	Not observed	Sub; The majority of phenos (90%) completely replaced by Act (70%) + Ep (15%) + Chlor (15%). Some (10%) are completely fresh with thin lighter reaction rims.	Opaques in matrix

Appendix Table 2 (continued). Western Cascades Petrography & Mineralogy Summary

Sample	District	Rock Type/ Texture	Alteration Summary	Phenocrysts	Matrix
NSNU-7	North Santiam	Porphyritic diorite	Plag + CPX fresh + Opaques. K-spar: Lots of fluid fractures, 5% epidote inlcusions. Hbl: Replaced by Act (70%) + Ep (5-10%) + Chlor (20%), Lots of opaque inclusions (up to 15-20%), Secondary feldspar near rim (<5%) common.	55% phenos of: Plag (55%, 0.3-1.5 mm), Px (20%, 1.5 mm), Hbl (15%, 0.2 mm), K-spar (5%, 0.3-0.6 mm), Opaques (<5%, 0.2 mm)	45%; Grains typically 0.01-0.02 mm. 35% Mafics +15% K-spar + Plag (25%) + 25% Opaques; Lots of clay and chlorite alteration, difficult to quantify. Mafics → Act + Chlor
NSNU-8	North Santiam	Porphyritic diorite	Plag: Rare secondary Ep (5-15%), sometimes within fractures. K-spar: Epidote inclusions common (5-10%), ~10% completely replaced by Sec. Felds microcrystals. Px: Typically ~30% replaced by Act + Chlor + minor Ep. Hbl: Typically pseudomorphed by Act (90%) with minor Chlor near rims (10%), uncommon Ep in core. Mafics: Mafics green, alt'n unclear	30% phenos of: Plag (65%, 0.2-1.5 mm), Hbl (15%, 0.1-0.4 mm), Px (10%, 0.1-0.4 mm), K-spar (5%, 0.2-0.5 mm), Opaques (5%, 0.05-0.2 mm)	70%; Plag laths (70%, 0.02 mm), Opaques (10%, <0.01 mm), Green mafics (20%, <0.01 mm)
NSNU-9	North Santiam	Porphyritic diorite	Plag: Secondary epidote (0.05 mm, 15%). K-spar: Ep + Sec Felds veins (10-20%), OR completely replaced by Sec Felds microcrystals with secondary Ep (10%). Px: Fresh. Hbl: Typically pseudomorphed by Act (100%). Some (15%) have cores filled with Sec Felds (45%) with minor Ep + Fe-oxides (10%)+ Act in thick (0.05 mm) rims (45%). Matix: Alteration unclear but at leat 20% mafics replaced by Chlor + Act.	35% phenos of:Plag (65%, up to 2 mm), Px (15%, 0.05-0.6 mm), Hbl (10%, 0.05-0.4 mm), K-spar (10%, 0.2-0.5 mm), Opaques (<5%, 0.05-0.1 mm)	65%; Feldspars (50%), Mafics (35%), Opaques (15%), grains typically 0.01-0.03 mm. Alteration unclear but at leat 20% mafics replaced by Chlor + Act.

Appendix Table 2 (continued). Western Cascades Petrography & Mineralogy Summary

Sample	Plagioclase	K-Feldspar	Pyroxene	Biotite	Quartz	Hornblende	Oxides/Sulfides
NSNU-7	Euh; Moderately sieved with secondary fluid fractures, reaction rims. Rare secondary Ep (5%)	Sub; Embayed, lots of fractures, rare (5%) epidote inclusions. Heavily sieved. Thick reaction rims (0.01 mm)	Euh; Embayed rims, feldspar inclusion. Otherwise intact.	Not observed	Not observed	Skeletal; Replaced by Act (70%) + Ep (5-10%) + Chlor (20%). Lots of opaque inclusions (up to 15-20%). Secondary feldspar near rim (<5%) common.	Opaques: Sub; Typically near altered Hbl; Rounded.
NSNU-8	Euh; Moderately sieved with secondary fluid fractures, reaction rims. Rare secondary Ep (5-15%), sometimes within fractures.	Sub; Embayed, lots of fractures, common epidote inclusions (5-10%). Heavily sieved. Thick reaction rims (0.01 mm). Sometimes completely replaced by microcrystals of secondary feldspar (10%).	Euh; Embayed, Thin reaction rims, typically ~30% replaced by Act + Chlor + minor Ep. Often associated with opaques	Not observed	Not observed	Skeletal; Typically pseudomorphed by Act (90%) with minor Chlor near rims (10%), uncommon Ep in core.	Fresh, Typically near Px and/or altered Hbl. Rounded, or anhedral. If anhedral surrounded by feldspar microcrystals.
NSNU-9	Euh; Typically heavily sieved with large melt inclusions and secondary epidote (0.05 mm, 15%). Thin reaction rims common.	Sub; Either rounded with thick (0.05 mm) reaction rims and Ep + Sec Felds veins (10-20%), OR completely replaced by Sec Felds microcrystals with secondary Ep (10%)	Euh; Embayed, Thin reaction rims, otherwise intact.	Not observed	Not observed	Skeletal; Typically pseudomorphed by Act (100%). Some (15%) have cores filled with Sec Felds (45%) with minor Ep + Fe-oxides (10%)+ Act in thick (0.05 mm) rims (45%).	Rounded/Sub; Appear to have thin reaction rims.

Appendix 5. Zircon U-Pb Geochronology

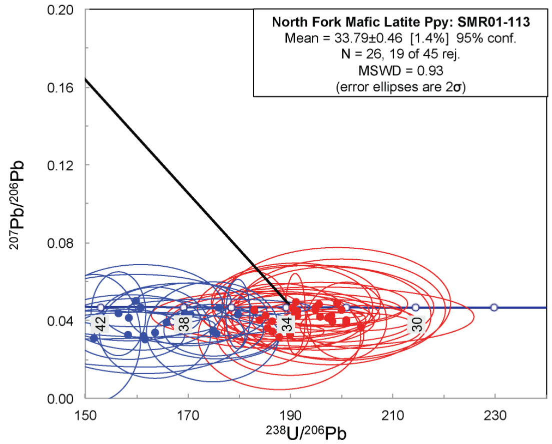

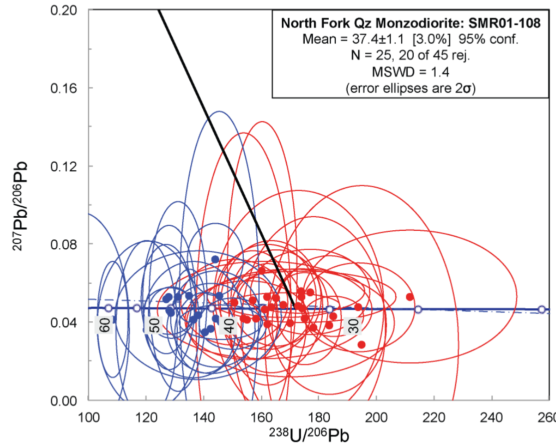

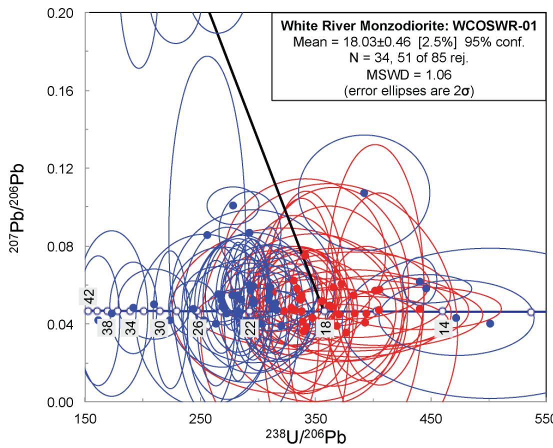

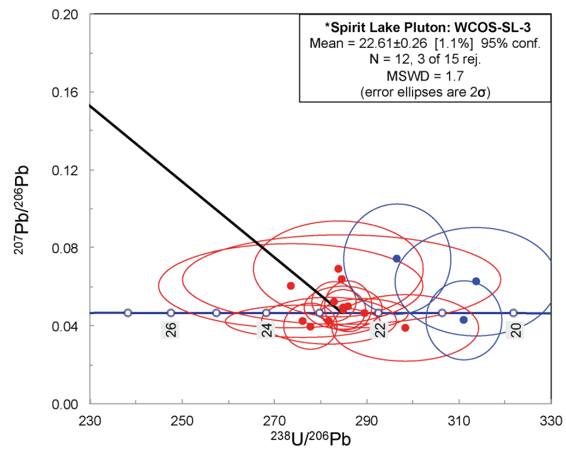

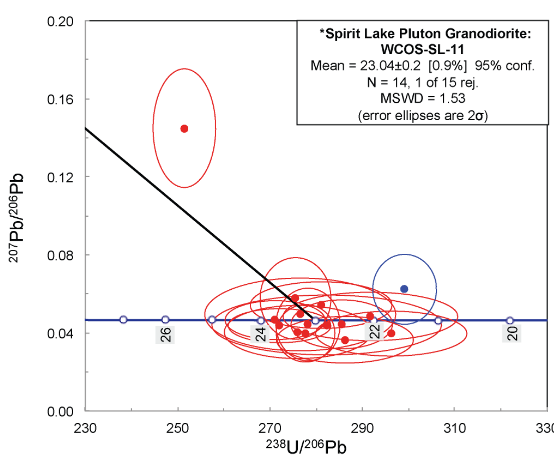

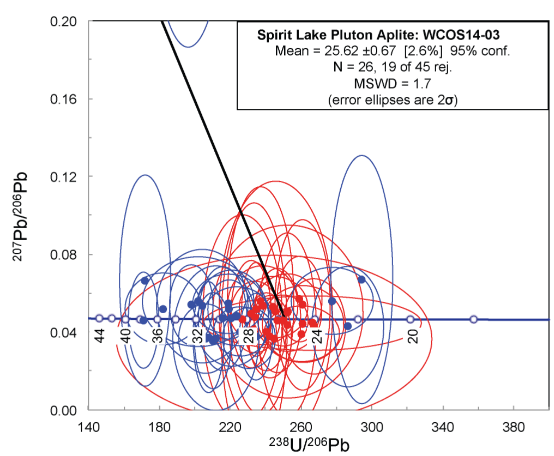

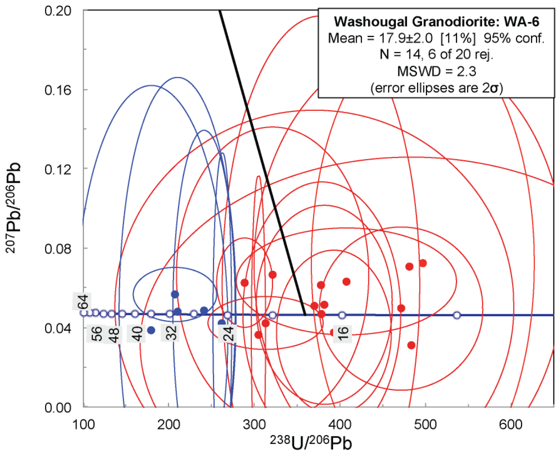
Washougal Granodiorite: WA-6
Mean = 17.9±2.0 [11%] 95% conf.
N = 14, 6 of 20 rej.
MSWD = 2.3
(error ellipses are 2σ)
207Pb/206Pb
238U/206Pb

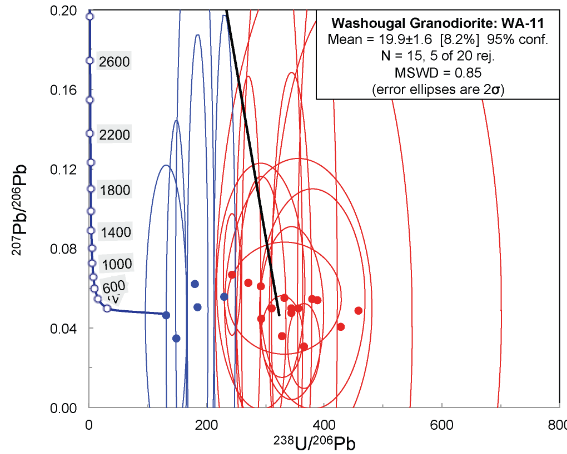
Washougal Granodiorite: WA-11
Mean = 19.9±1.6 [8.2%] 95% conf.
N = 15, 5 of 20 rej.
MSWD = 0.85
(error ellipses are 2σ)
207Pb/206Pb
238U/206Pb

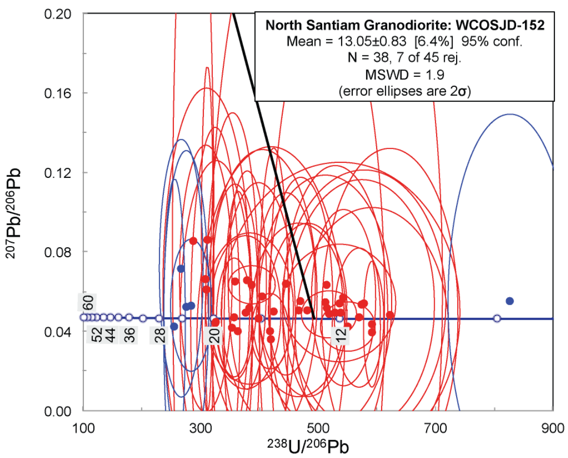
North Santiam Granodiorite: WCOSJD-152
Mean = 13.05±0.83 [6.4%] 95% conf.
N = 38, 7 of 45 rej.
MSWD = 1.9
(error ellipses are 2σ)
207Pb/206Pb
238U/206Pb

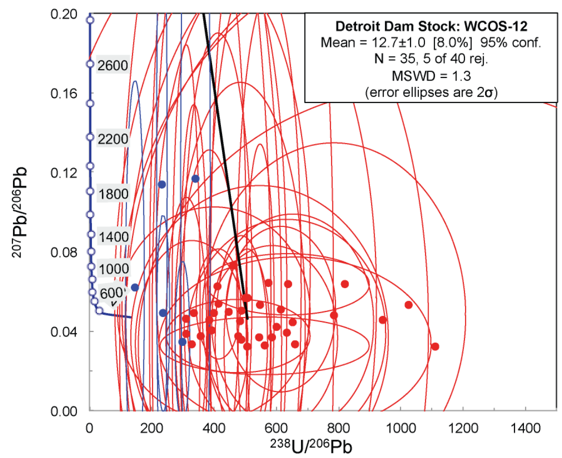
Detroit Dam Stock: WCOS-12
Mean = 12.7±1.0 [8.0%] 95% conf.
N = 35, 5 of 40 rej.
MSWD = 1.3
(error ellipses are 2σ)
207Pb/206Pb
238U/206Pb

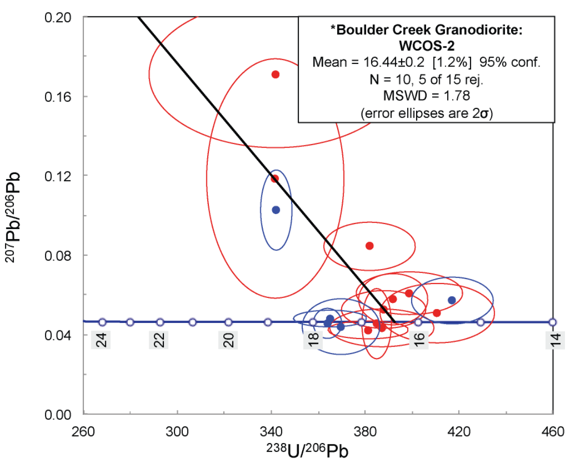
*Boulder Creek Granodiorite: WCOS-2
Mean = 16.44±0.2 [1.2%] 95% conf.
N = 10, 5 of 15 rej.
MSWD = 1.78
(error ellipses are 2σ)
207Pb/206Pb
238U/206Pb

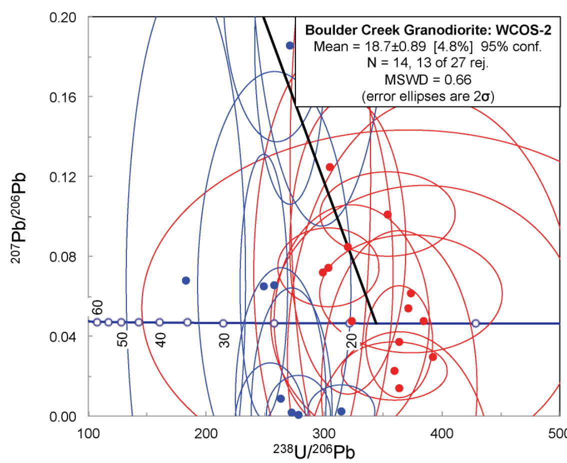
Boulder Creek Granodiorite: WCOS-2
Mean = 18.7±0.89 [4.8%] 95% conf.
N = 14, 13 of 27 rej.
MSWD = 0.66
(error ellipses are 2σ)
207Pb/206Pb
238U/206Pb

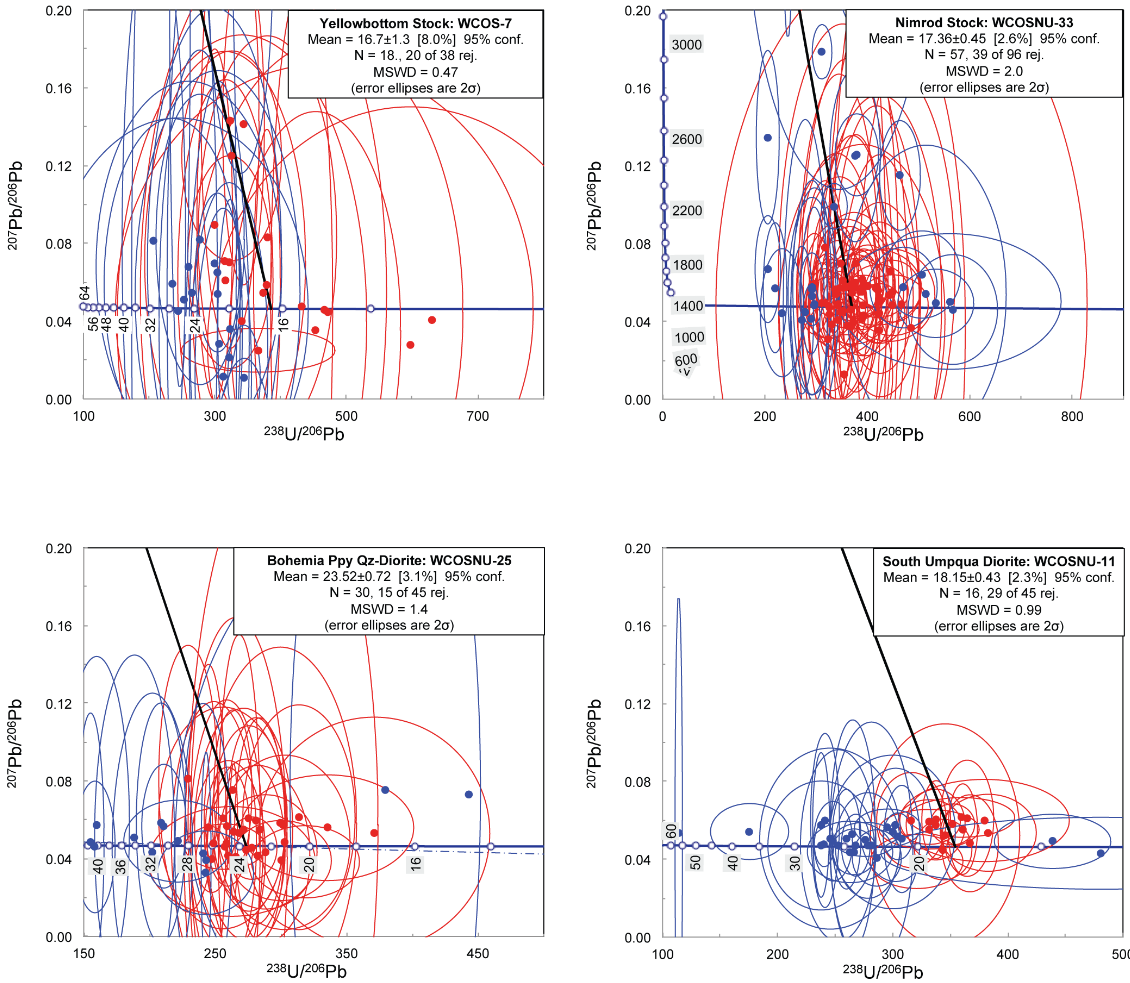

Appendix Figure 4: Inverse concordia plots with 2σ error ellipses for all. Samples analyzed by SHRIMP-RG (n = 3) denoted with *; all other sampes analyzed by LA-ICP-MS at OSU. All error ellipses are uncorrected for common lead. Red ellipses were included in the age calculation. Blue ellipses were excluded on the basis of inheritance, discordance, or Pb-loss. Chords are common Pb corrections to the concordia after Stacey and Kramer (1975).

Appendix Table 3. U-Pb Spot Analyses by LA-ICP-MS

Sample Spot	Note	Total $^{238}U/^{206}Pb$	±%	Total $^{207}Pb/^{206}Pb$	±%	7-corr $^{206}Pb/^{238}U$	±%	$^{206}Pb/^{238}U$ Age	1σ	% Discor-dant
SRM01-108-01	Inherited	127.0	2.8	0.05176	22.1	0.00781	5.0	50.2	2.5	0.9
SRM01-108-02	Inherited	144.0	2.8	0.07207	10.4	0.00663	4.3	42.6	1.8	4.5
SRM01-108-03	Inherited	135.1	1.5	0.05351	10.3	0.00732	2.6	47.0	1.2	1.2
SRM01-108-04		167.7	4.8	0.04869	5.3	0.00594	5.5	38.2	2.1	0.3
SRM01-108-05		153.9	4.4	0.04179	92.9	0.00656	11.8	42.2	5.0	-0.9
SRM01-108-06		155.1	5.7	0.04099	20.0	0.00652	7.6	41.9	3.2	-1.1
SRM01-108-07		177.0	4.8	0.05544	16.1	0.00556	6.7	35.8	2.4	1.6
SRM01-108-08		185.1	2.3	0.04292	9.8	0.00544	3.1	35.0	1.1	-0.7
SRM01-108-09		183.6	4.4	0.03848	37.7	0.00553	7.3	35.5	2.6	-1.5
SRM01-108-10		158.2	2.0	0.04183	20.6	0.00638	3.6	41.0	1.5	-0.9
SRM01-108-11	Inherited	145.9	4.1	0.03994	9.0	0.00694	4.9	44.6	2.2	-1.3
SRM01-108-12	Inherited	128.0	2.9	0.05257	28.7	0.00774	5.8	49.7	2.9	1.0
SRM01-108-13		194.9	7.0	0.02813	118.7	0.00530	13.8	34.1	4.7	-3.4
SRM01-108-14		157.1	3.4	0.05137	20.0	0.00631	5.5	40.6	2.2	0.8
SRM01-108-15	Inherited	120.1	3.6	0.03589	52.2	0.00849	7.1	54.5	3.9	-2.0
SRM01-108-16	Inherited	136.4	5.2	0.04124	29.5	0.00741	7.7	47.6	3.7	-1.0
SRM01-108-17	Inherited	144.2	4.4	0.04155	24.2	0.00700	6.5	45.0	2.9	-1.0
SRM01-108-18		162.0	4.3	0.05286	20.8	0.00611	6.6	39.2	2.6	1.1
SRM01-108-19	Inherited	128.1	2.9	0.04563	10.7	0.00783	3.8	50.3	1.9	-0.3
SRM01-108-20	Inherited	140.4	3.0	0.03455	24.4	0.00728	4.7	46.8	2.2	-2.3
SRM01-108-21	Inherited	97.3	7.1	0.03690	65.5	0.01047	12.1	67.2	8.1	-1.9
SRM01-108-22	Inherited	145.4	3.9	0.05319	72.7	0.00680	11.3	43.7	4.9	1.1
SRM01-108-23		172.9	7.0	0.04797	50.6	0.00577	12.2	37.1	4.5	0.2
SRM01-108-24		175.0	3.0	0.04175	23.1	0.00576	4.8	37.1	1.8	-0.9
SRM01-108-25		161.2	9.5	0.04617	22.0	0.00621	12.4	39.9	5.0	-0.1
SRM01-108-26		163.5	4.4	0.04787	28.8	0.00610	7.2	39.2	2.8	0.2
SRM01-108-27	Inclusion	204.7	42.0	0.07326	166.6	0.00465	111.7	29.9	33.4	4.8
SRM01-108-28	Inherited	150.1	3.2	0.03918	13.7	0.00675	4.3	43.4	1.9	-1.4
SRM01-108-29		162.1	3.4	0.03881	32.7	0.00626	5.8	40.2	2.3	-1.5
SRM01-108-30		170.2	8.7	0.03952	28.5	0.00595	11.7	38.3	4.5	-1.3
SRM01-108-31	Inherited	108.4	2.0	0.04134	29.4	0.00933	4.2	59.8	2.5	-1.1
SRM01-108-32		165.1	3.9	0.05231	19.3	0.00600	5.9	38.5	2.3	1.0
SRM01-108-33		173.8	5.2	0.05587	8.3	0.00566	6.4	36.4	2.3	1.6
SRM01-108-34		178.1	5.7	0.03687	63.2	0.00572	10.4	36.7	3.8	-1.8
SRM01-108-35		211.6	7.2	0.05306	26.2	0.00467	10.4	30.0	3.1	1.2
SRM01-108-36	Inherited	120.8	6.0	0.03799	46.7	0.00842	9.7	54.0	5.2	-1.6
SRM01-108-37	Inherited	138.1	8.6	0.04353	30.9	0.00729	11.9	46.8	5.6	-0.6
SRM01-108-38		160.3	3.1	0.06649	46.7	0.00602	9.1	38.7	3.5	3.6
SRM01-108-39		174.2	2.1	0.04718	17.4	0.00574	3.7	36.9	1.4	0.1
SRM01-108-40	Inherited	131.1	3.1	0.05310	37.3	0.00755	6.9	48.5	3.4	1.1
SRM01-108-41		174.0	7.7	0.05294	10.1	0.00568	9.4	36.5	3.4	1.1
SRM01-108-42	Inherited	142.5	4.4	0.03673	25.6	0.00714	6.3	45.9	2.9	-1.9
SRM01-108-43		150.6	5.0	0.05010	17.9	0.00660	7.0	42.4	3.0	0.6
SRM01-108-44	Inherited	128.8	2.5	0.04484	12.0	0.00780	3.6	50.1	1.8	-0.4
SRM01-108-45		193.7	4.2	0.04752	19.6	0.00516	6.1	33.2	2.0	0.1
SRM01-113-01	Inherited	175.6	2.8	0.03313	15.9	0.00584	3.9	37.5	1.5	-2.5
SRM01-113-02		185.2	4.9	0.04265	11.8	0.00544	6.1	35.0	2.1	-0.7
SRM01-113-03	Inherited	169.5	3.9	0.04360	14.6	0.00593	5.2	38.1	2.0	-0.6
SRM01-113-04		201.0	2.5	0.03924	5.0	0.00504	2.9	32.4	0.9	-1.3
SRM01-113-05		199.2	4.5	0.04888	23.9	0.00500	7.0	32.2	2.2	0.4
SRM01-113-06		195.8	6.3	0.04190	14.9	0.00515	7.9	33.1	2.6	-0.9

Appendix Table 3 (continued). U-Pb Spot Analyses by LA-ICP-MS

Sample Spot	Note	Total $^{238}U/^{206}Pb$	±%	Total $^{207}Pb/^{206}Pb$	±%	7-corr $^{206}Pb/^{238}U$	±%	$^{206}Pb/^{238}U$ Age	1σ	% Discor-dant
SRM01-113-07		186.4	4.4	0.03978	14.5	0.00543	5.6	34.9	2.0	-1.3
SRM01-113-08	Inherited	151.7	6.4	0.03764	7.8	0.00670	7.3	43.1	3.2	-1.7
SRM01-113-09	Inherited	156.5	1.4	0.04346	20.3	0.00643	3.0	41.3	1.2	-0.6
SRM01-113-10		190.4	3.4	0.04678	18.9	0.00525	5.1	33.8	1.7	0.0
SRM01-113-11	Inherited	170.6	2.9	0.04316	15.3	0.00590	4.2	37.9	1.6	-0.7
SRM01-113-12		191.5	2.7	0.04269	2.0	0.00526	2.9	33.8	1.0	-0.7
SRM01-113-13		197.4	1.8	0.04123	4.5	0.00512	2.2	32.9	0.7	-1.0
SRM01-113-14		191.4	3.0	0.04486	10.1	0.00524	3.9	33.7	1.3	-0.3
SRM01-113-15		185.5	1.9	0.03587	21.8	0.00549	3.3	35.3	1.2	-2.0
SRM01-113-16	Inherited	159.9	4.7	0.05022	10.9	0.00622	6.0	39.9	2.4	0.6
SRM01-113-17		198.2	3.2	0.03976	11.2	0.00511	4.2	32.9	1.4	-1.3
SRM01-113-18		183.0	1.4	0.04546	17.7	0.00548	2.9	35.2	1.0	-0.2
SRM01-113-19	Inherited	158.5	3.6	0.04137	11.7	0.00637	4.6	41.0	1.9	-1.0
SRM01-113-20		200.0	4.1	0.04552	23.4	0.00501	6.3	32.2	2.0	-0.2
SRM01-113-21	Inherited	158.4	2.8	0.03284	16.0	0.00647	3.9	41.6	1.6	-2.5
SRM01-113-22	Inherited	179.8	0.5	0.04329	16.8	0.00560	1.8	36.0	0.7	-0.6
SRM01-113-23		186.5	2.2	0.03422	5.8	0.00548	2.6	35.3	0.9	-2.3
SRM01-113-24	Inherited	161.4	5.0	0.03206	24.7	0.00636	6.7	40.9	2.8	-2.7
SRM01-113-25	Inherited	175.0	2.3	0.03501	15.5	0.00583	3.3	37.5	1.2	-2.1
SRM01-113-26	Inherited	176.1	4.2	0.04667	3.8	0.00568	4.7	36.5	1.7	0.0
SRM01-113-27	Inherited	161.7	6.6	0.03014	19.1	0.00637	8.1	40.9	3.3	-3.0
SRM01-113-28	Inherited	174.9	3.0	0.03414	30.8	0.00585	5.0	37.6	1.9	-2.3
SRM01-113-29	Inherited	163.6	2.7	0.03369	28.4	0.00626	4.5	40.2	1.8	-2.4
SRM01-113-30		191.1	3.5	0.04940	16.6	0.00521	5.2	33.5	1.7	0.5
SRM01-113-31	Inherited	134.3	2.8	0.03473	17.7	0.00761	4.0	48.9	2.0	-2.2
SRM01-113-32	Inherited	151.8	2.4	0.03087	43.4	0.00678	4.9	43.6	2.1	-2.9
SRM01-113-33		190.0	3.1	0.03282	26.2	0.00540	4.7	34.7	1.6	-2.5
SRM01-113-34	Inherited	165.8	6.1	0.03912	8.2	0.00611	7.1	39.3	2.8	-1.4
SRM01-113-35		203.9	2.4	0.03659	12.3	0.00499	3.3	32.1	1.1	-1.8
SRM01-113-36		201.0	1.6	0.03989	20.3	0.00504	3.1	32.4	1.0	-1.2
SRM01-113-37		194.9	4.8	0.04657	19.1	0.00513	6.8	33.0	2.2	0.0
SRM01-113-38		191.0	0.4	0.04339	19.5	0.00527	1.9	33.9	0.7	-0.6
SRM01-113-39		194.9	3.6	0.04534	7.5	0.00514	4.3	33.1	1.4	-0.2
SRM01-113-40		187.9	3.5	0.03170	35.1	0.00547	5.6	35.2	2.0	-2.7
SRM01-113-41		184.0	1.5	0.04014	7.4	0.00550	2.1	35.4	0.7	-1.2
SRM01-113-42		189.0	3.4	0.04050	8.9	0.00535	4.2	34.4	1.4	-1.1
SRM01-113-43	Inherited	160.8	4.1	0.04674	19.2	0.00622	5.9	40.0	2.4	0.0
SRM01-113-44		195.6	3.6	0.04861	9.2	0.00509	4.6	32.8	1.5	0.3
SRM01-113-45		198.0	4.0	0.04236	24.3	0.00509	6.1	32.7	2.0	-0.8
WCOSWR-01-01	Inherited	173.0	7.4	0.04534	38.3	0.00580	11.3	37.3	4.2	-0.3
WCOSWR-01-02	Inherited	309.1	3.9	0.05268	21.4	0.00320	6.2	20.6	1.3	1.1
WCOSWR-01-03	Discordant	142.2	7.8	0.32038	5.2	0.00356	14.9	22.9	3.4	49.5
WCOSWR-01-04		368.3	8.3	0.03917	19.3	0.00275	10.5	17.7	1.9	-1.3
WCOSWR-01-05		347.2	9.3	0.04322	40.7	0.00290	13.7	18.7	2.6	-0.6
WCOSWR-01-06	Inherited	161.3	4.7	0.04165	32.7	0.00626	7.5	40.2	3.0	-0.9
WCOSWR-01-07	Pb Loss	445.9	3.6	0.05806	5.1	0.00220	4.3	14.1	0.6	2.1
WCOSWR-01-08		355.8	4.7	0.05212	16.0	0.00278	6.5	17.9	1.2	1.0
WCOSWR-01-09	Inherited	273.1	5.9	0.04544	39.7	0.00367	9.7	23.6	2.3	-0.2
WCOSWR-01-10		336.2	3.9	0.05292	19.0	0.00294	6.0	18.9	1.1	1.2
WCOSWR-01-11	Discordant	264.8	6.5	0.21297	7.3	0.00264	11.2	17.0	1.9	30.1
WCOSWR-01-12	Inherited	289.9	7.7	0.04153	31.0	0.00348	10.9	22.4	2.4	-0.9

Appendix Table 3 (continued). U-Pb Spot Analyses by LA-ICP-MS

Sample Spot	Note	Total $^{238}U/^{206}Pb$	±%	Total $^{207}Pb/^{206}Pb$	±%	7-corr $^{206}Pb/^{238}U$	±%	$^{206}Pb/^{238}U$ Age	1σ	% Discor-dant
WCOSWR-01-13	Inherited	292.4	2.3	0.05980	16.5	0.00334	4.2	21.5	0.9	2.4
WCOSWR-01-14	Inherited	263.5	2.5	0.04043	32.6	0.00384	5.0	24.7	1.2	-1.1
WCOSWR-01-15	Discordant	134.7	6.8	0.64266	7.0	-0.00059	-103.5	-3.8	3.9	107.9
WCOSWR-01-16		328.9	4.7	0.04825	16.1	0.00303	6.4	19.5	1.2	0.3
WCOSWR-01-17		405.3	3.9	0.05795	34.8	0.00242	7.9	15.6	1.2	2.1
WCOSWR-01-18		337.7	3.6	0.05503	36.8	0.00292	7.5	18.8	1.4	1.5
WCOSWR-01-19		333.7	4.7	0.05818	15.2	0.00293	6.6	18.9	1.3	2.1
WCOSWR-01-20	Inherited	312.3	2.9	0.04901	14.4	0.00319	4.3	20.5	0.9	0.5
WCOSWR-01-21	Inherited	271.3	1.8	0.04778	7.2	0.00368	2.4	23.7	0.6	0.2
WCOSWR-01-22		383.8	8.9	0.04543	20.1	0.00261	11.6	16.8	1.9	-0.2
WCOSWR-01-23		339.4	1.6	0.03612	45.0	0.00300	4.5	19.3	0.9	-1.9
WCOSWR-01-24	Inherited	244.0	3.4	0.04801	12.0	0.00409	4.6	26.3	1.2	0.3
WCOSWR-01-25	Inherited	295.4	2.1	0.05244	24.1	0.00335	4.5	21.6	1.0	1.1
WCOSWR-01-26	Inherited	286.7	6.8	0.03603	56.1	0.00355	11.1	22.9	2.5	-1.9
WCOSWR-01-27	Inherited	191.7	4.4	0.04827	19.9	0.00520	6.4	33.5	2.1	0.3
WCOSWR-01-28		337.8	5.9	0.04675	28.0	0.00296	8.7	19.0	1.7	0.0
WCOSWR-01-29		331.1	5.0	0.06229	21.9	0.00293	7.9	18.9	1.5	2.9
WCOSWR-01-30	Inherited	309.8	5.5	0.05478	11.2	0.00318	7.0	20.5	1.4	1.5
WCOSWR-01-31	Inherited	268.2	2.4	0.05217	21.3	0.00369	4.6	23.8	1.1	1.0
WCOSWR-01-32	Inherited	282.4	4.1	0.05464	21.8	0.00349	6.5	22.5	1.5	1.5
WCOSWR-01-33		363.4	4.9	0.04880	8.2	0.00274	5.9	17.6	1.0	0.4
WCOSWR-01-34	Discordant	161.9	2.7	0.27111	6.3	0.00368	8.1	23.7	1.9	40.6
WCOSWR-01-35	Inherited	295.5	5.3	0.05091	6.1	0.00336	6.2	21.6	1.3	0.8
WCOSWR-01-36	Discordant	230.8	10.0	-0.18707	31.0	0.00615	2.9	39.5	1.2	-42.2
WCOSWR-01-37	Discordant	278.3	5.4	0.10075	6.3	0.00324	7.0	20.9	1.5	9.8
WCOSWR-01-38	Discordant	223.4	9.7	0.09789	56.4	0.00406	22.9	26.1	6.0	9.3
WCOSWR-01-39	Inherited	277.8	1.5	0.05460	13.4	0.00355	2.9	22.8	0.7	1.5
WCOSWR-01-40		392.8	7.5	0.04094	13.1	0.00257	9.2	16.6	1.5	-1.0
WCOSWR-01-41	Inherited	310.7	5.4	0.05869	15.4	0.00315	7.5	20.3	1.5	2.2
WCOSWR-01-42	Discordant	228.6	6.5	0.20663	7.2	0.00311	11.0	20.0	2.2	28.9
WCOSWR-01-43		370.8	13.7	0.04462	17.1	0.00271	17.4	17.4	3.0	-0.3
WCOSWR-01-44	Inherited	320.2	3.8	0.03917	18.2	0.00316	5.3	20.4	1.1	-1.3
WCOSWR-01-45	Inherited	309.9	1.9	0.05820	22.2	0.00316	4.3	20.3	0.9	2.1
WCOSWR-01-46	Pb Loss	472.2	5.8	0.04315	18.3	0.00213	7.7	13.7	1.1	-0.6
WCOSWR-01-47		393.9	3.7	0.04529	31.2	0.00254	6.5	16.4	1.1	-0.2
WCOSWR-01-48	Inherited	268.9	7.1	0.04865	25.9	0.00370	10.0	23.8	2.4	0.4
WCOSWR-01-49		382.9	9.0	0.05500	16.3	0.00257	11.6	16.6	1.9	1.5
WCOSWR-01-50		401.6	4.3	0.05724	53.5	0.00244	10.4	15.7	1.6	2.0
WCOSWR-01-51		405.0	7.9	0.04688	15.6	0.00247	9.9	15.9	1.6	0.1
WCOSWR-01-52	Pb Loss	440.2	1.4	0.06193	8.1	0.00221	2.4	14.2	0.3	2.8
WCOSWR-01-53		341.8	4.5	0.03786	75.9	0.00297	10.0	19.1	1.9	-1.6
WCOSWR-01-54		440.4	6.6	0.04800	9.3	0.00226	7.9	14.6	1.1	0.3
WCOSWR-01-55	Inherited	295.9	9.7	0.05938	27.0	0.00330	14.0	21.2	3.0	2.3
WCOSWR-01-56		361.6	12.6	0.03573	87.3	0.00282	20.7	18.1	3.8	-1.9
WCOSWR-01-57	Inherited	282.6	1.8	0.04634	31.4	0.00354	4.4	22.8	1.0	0.0
WCOSWR-01-58	Inherited	315.4	1.8	0.05072	21.2	0.00315	3.8	20.3	0.8	0.8
WCOSWR-01-59		365.3	7.3	0.05912	35.3	0.00268	12.0	17.2	2.1	2.3
WCOSWR-01-60	Inherited	209.7	6.1	0.05019	14.7	0.00474	7.9	30.5	2.4	0.6
WCOSWR-01-61	Inherited	253.2	9.6	0.04176	43.3	0.00398	14.1	25.6	3.6	-0.9
WCOSWR-01-62	Discordant	196.6	5.7	0.21675	13.8	0.00353	14.3	22.7	3.3	30.8
WCOSWR-01-63	Inherited	223.9	2.8	0.04214	34.3	0.00450	5.5	29.0	1.6	-0.8
WCOSWR-01-64	Inherited	296.4	7.1	0.05083	29.0	0.00335	10.5	21.5	2.3	0.8

Appendix Table 3 (continued). U-Pb Spot Analyses by LA-ICP-MS

Sample Spot	Note	Total $^{238}U/^{206}Pb$	±%	Total $^{207}Pb/^{206}Pb$	±%	7-corr $^{206}Pb/^{238}U$	±%	$^{206}Pb/^{238}U$ Age	1σ	% Discor-dant
WCOSWR-01-65		337.1	4.3	0.05234	10.1	0.00294	5.5	18.9	1.0	1.1
WCOSWR-01-66	Inherited	265.4	4.5	0.05522	10.5	0.00371	5.9	23.9	1.4	1.6
WCOSWR-01-67		338.2	2.3	0.05284	10.3	0.00292	3.4	18.8	0.6	1.2
WCOSWR-01-68		340.8	8.4	0.07533	21.3	0.00278	12.4	17.9	2.2	5.2
WCOSWR-01-69		312.2	5.7	0.05679	14.9	0.00314	7.6	20.2	1.5	1.9
WCOSWR-01-70	Discordant	292.9	6.1	0.08705	15.9	0.00316	9.3	20.4	1.9	7.3
WCOSWR-01-71		331.6	6.3	0.04743	20.2	0.00301	8.6	19.4	1.7	0.2
WCOSWR-01-72	Inherited	289.2	1.7	0.04116	9.1	0.00349	2.4	22.5	0.5	-1.0
WCOSWR-01-73		372.5	8.3	0.06063	12.3	0.00262	10.6	16.8	1.8	2.6
WCOSWR-01-74	Inherited	302.2	3.1	0.04034	24.7	0.00335	5.0	21.5	1.1	-1.1
WCOSWR-01-75	Discordant	392.1	9.6	0.10737	18.2	0.00227	15.0	14.6	2.2	11.0
WCOSWR-01-76	Inherited	255.9	5.3	0.08565	43.8	0.00363	13.3	23.4	3.1	7.1
WCOSWR-01-77	Inherited	316.3	4.2	0.04713	23.0	0.00316	6.4	20.3	1.3	0.1
WCOSWR-01-78	Pb Loss	501.4	10.5	0.04032	39.1	0.00202	14.8	13.0	1.9	-1.1
WCOSWR-01-79		362.1	7.2	0.04979	41.7	0.00275	11.7	17.7	2.1	0.6
WCOSWR-01-80		330.5	5.8	0.04716	28.4	0.00302	8.7	19.5	1.7	0.1
WCOSWR-01-81		376.6	4.5	0.03564	16.5	0.00271	5.8	17.4	1.0	-2.0
WCOSWR-01-82	Inherited	285.4	3.2	0.05227	22.3	0.00347	5.5	22.3	1.2	1.0
WCOSWR-01-83	Inherited	293.5	3.5	0.05708	10.1	0.00334	4.7	21.5	1.0	1.9
WCOSWR-01-84		322.5	12.3	0.04685	37.0	0.00310	17.6	19.9	3.5	0.1
WCOSWR-01-85		339.1	5.2	0.04108	36.7	0.00298	8.3	19.2	1.6	-1.0
WCOS14-03-01		286.4	2.9	0.04278	29.5	0.00352	5.3	22.6	1.2	-0.7
WCOS14-03-02	Inherited	215.8	2.6	0.04689	23.2	0.00463	4.7	29.8	1.4	0.1
WCOS14-03-03		246.7	2.2	0.04593	23.8	0.00406	4.2	26.1	1.1	-0.1
WCOS14-03-04	Inherited	211.9	4.7	0.03684	41.2	0.00480	7.7	30.9	2.4	-1.8
WCOS14-03-05		267.3	2.7	0.04292	23.3	0.00377	4.6	24.2	1.1	-0.7
WCOS14-03-06		244.5	3.2	0.05279	12.2	0.00404	4.5	26.0	1.2	1.1
WCOS14-03-07		277.6	3.4	0.05604	12.5	0.00354	4.9	22.8	1.1	1.7
WCOS14-03-08	Inherited	204.3	5.2	0.05333	22.3	0.00484	7.7	31.1	2.4	1.2
WCOS14-03-09	Discordant	196.3	4.4	0.27263	12.9	0.00302	15.8	19.4	3.1	40.9
WCOS14-03-10		249.8	2.3	0.04592	11.6	0.00401	3.4	25.8	0.9	-0.1
WCOS14-03-11	Inherited	201.9	6.4	0.05562	16.9	0.00487	8.6	31.3	2.7	1.6
WCOS14-03-12		234.1	2.5	0.04778	15.7	0.00426	3.9	27.4	1.1	0.2
WCOS14-03-13	Inherited	182.2	4.8	0.05195	14.5	0.00544	6.5	35.0	2.3	0.9
WCOS14-03-14		252.6	6.9	0.05054	35.9	0.00393	10.9	25.3	2.8	0.7
WCOS14-03-15		240.5	1.9	0.04015	20.3	0.00421	3.4	27.1	0.9	-1.2
WCOS14-03-16	Inherited	171.0	2.0	0.04612	21.9	0.00585	3.9	37.6	1.5	-0.1
WCOS14-03-17	Inherited	210.3	2.0	0.03560	28.3	0.00485	3.9	31.2	1.2	-2.0
WCOS14-03-18		294.3	2.4	0.06699	38.9	0.00327	7.5	21.1	1.6	3.7
WCOS14-03-19		226.9	4.0	0.04681	46.7	0.00441	8.3	28.3	2.4	0.0
WCOS14-03-20		233.5	3.3	0.04113	64.8	0.00433	8.3	27.8	2.3	-1.0
WCOS14-03-21		252.3	3.1	0.05002	16.3	0.00394	4.7	25.3	1.2	0.6
WCOS14-03-22	Inherited	172.0	3.4	0.06645	33.3	0.00561	7.8	36.1	2.8	3.6
WCOS14-03-23		260.9	2.4	0.05395	33.2	0.00378	5.8	24.3	1.4	1.3
WCOS14-03-24		245.8	5.3	0.05063	54.0	0.00404	10.8	26.0	2.8	0.7
WCOS14-03-25		238.4	3.4	0.05377	15.4	0.00414	5.1	26.6	1.4	1.3
WCOS14-03-26		260.4	3.3	0.03914	14.9	0.00389	4.5	25.0	1.1	-1.3
WCOS14-03-27		252.2	2.6	0.04375	44.0	0.00398	6.2	25.6	1.6	-0.5
WCOS14-03-28	Inherited	225.8	2.8	0.04035	12.8	0.00448	3.8	28.8	1.1	-1.1
WCOS14-03-29		266.5	9.4	0.04460	12.8	0.00377	11.5	24.2	2.8	-0.3
WCOS14-03-30		231.9	2.0	0.04919	22.9	0.00429	4.1	27.6	1.1	0.5

Appendix Table 3 (continued). U-Pb Spot Analyses by LA-ICP-MS

Sample Spot	Note	Total $^{238}U/^{206}Pb$	±%	Total $^{207}Pb/^{206}Pb$	±%	7-corr $^{206}Pb/^{238}U$	±%	$^{206}Pb/^{238}U$ Age	1σ	% Discor-dant
WCOS14-03-31	Inherited	234.6	1.6	0.03763	24.1	0.00433	3.3	27.9	0.9	-1.6
WCOS14-03-32	Inherited	219.0	3.8	0.05452	11.4	0.00450	5.1	29.0	1.5	1.4
WCOS14-03-33	Inherited	220.7	3.9	0.04713	21.4	0.00453	5.9	29.1	1.7	0.1
WCOS14-03-34		259.2	2.0	0.05695	15.8	0.00379	3.7	24.4	0.9	1.9
WCOS14-03-35	Inherited	206.2	3.0	0.03663	19.9	0.00494	4.4	31.8	1.4	-1.8
WCOS14-03-36		244.8	14.9	0.03641	48.3	0.00416	21.1	26.8	5.6	-1.8
WCOS14-03-37		242.5	2.0	0.03761	23.0	0.00419	3.6	27.0	1.0	-1.6
WCOS14-03-38	Inherited	219.5	2.2	0.05159	12.1	0.00451	3.4	29.0	1.0	0.9
WCOS14-03-39		261.1	3.6	0.04413	18.3	0.00385	5.2	24.7	1.3	-0.4
WCOS14-03-40		237.2	3.2	0.05613	42.6	0.00414	7.8	26.7	2.1	1.7
WCOS14-03-41	Inherited	207.8	1.7	0.03739	31.1	0.00489	3.8	31.5	1.2	-1.7
WCOS14-03-42	Inherited	198.1	2.5	0.05401	15.5	0.00498	4.2	32.0	1.3	1.3
WCOS14-03-43	Inherited	224.0	3.5	0.04815	12.8	0.00445	4.8	28.6	1.4	0.3
WCOS14-03-44	Inherited	230.6	2.6	0.03691	17.3	0.00441	3.9	28.4	1.1	-1.7
WCOS14-03-45		234.7	1.4	0.05166	19.1	0.00422	3.3	27.2	0.9	0.9
WA-6-01	Inherited	207.1	9.6	0.05665	9.9	0.00474	11.8	30.5	3.6	1.8
WA-6-02		481.3	15.4	0.07085	63.8	0.00199	28.3	12.8	3.6	4.4
WA-6-03	Inherited	262.5	1.7	0.04226	83.2	0.00384	8.1	24.7	2.0	-0.8
WA-6-04		393.0	7.0	0.03763	44.9	0.00259	10.7	16.6	1.8	-1.6
WA-6-05		321.3	14.3	0.06666	45.6	0.00300	23.3	19.3	4.5	3.6
WA-6-06		304.7	1.1	0.03630	91.0	0.00334	7.0	21.5	1.5	-1.8
WA-6-07	Inherited	179.5	20.4	0.03859	130.6	0.00565	36.7	36.3	13.3	-1.5
WA-6-08		381.7	8.5	0.05145	39.8	0.00260	13.4	16.7	2.2	0.9
WA-6-09		407.6	12.9	0.06323	17.4	0.00238	17.1	15.3	2.6	3.0
WA-6-10		378.8	10.0	0.04678	58.1	0.00264	16.5	17.0	2.8	0.1
WA-6-11		471.6	8.3	0.04955	33.9	0.00211	12.3	13.6	1.7	0.6
WA-6-12	Inherited	241.1	6.2	0.04848	76.6	0.00413	13.7	26.6	3.6	0.3
WA-6-13		288.5	4.6	0.06261	14.7	0.00337	6.6	21.7	1.4	2.9
WA-6-14	Inherited	210.2	13.3	0.04811	100.1	0.00474	25.3	30.5	7.7	0.3
WA-6-15		496.9	10.7	0.07241	66.8	0.00192	22.2	12.4	2.7	4.7
WA-6-16		377.8	12.5	0.06134	90.3	0.00258	26.0	16.6	4.3	2.7
WA-6-17		483.5	26.8	0.03136	123.1	0.00212	45.8	13.7	6.3	-2.7
WA-6-18		313.1	8.8	0.04232	12.9	0.00322	10.7	20.7	2.2	-0.8
WA-6-19	Apatite	333.1	19.2	0.05071	148.6	0.00298	40.6	19.2	7.8	0.8
WA-6-20		370.1	25.7	0.05079	79.4	0.00268	44.5	17.3	7.7	0.8
WA-11-21		328.2	7.2	0.03565	38.0	0.00311	10.3	20.0	2.1	-2.0
WA-11-22		355.9	23.2	0.04998	99.4	0.00279	41.9	18.0	7.5	0.6
WA-11-23		344.5	6.6	0.04971	157.7	0.00289	22.2	18.6	4.1	0.6
WA-11-24	Inherited	131.2	17.7	0.04609	108.5	0.00763	32.3	49.0	15.8	-0.2
WA-11-25		332.4	19.2	0.05497	33.8	0.00296	28.0	19.1	5.3	1.5
WA-11-26	Inherited	148.5	7.7	0.03458	210.2	0.00688	22.1	44.2	9.8	-2.2
WA-11-27		428.1	18.8	0.04077	264.8	0.00236	46.7	15.2	7.1	-1.0
WA-11-28		458.1	35.0	0.04892	285.0	0.00217	92.6	14.0	13.0	0.5
WA-11-29		293.1	9.5	0.04487	105.0	0.00342	19.8	22.0	4.4	-0.3
WA-11-30		388.4	5.8	0.05400	210.3	0.00254	28.1	16.4	4.6	1.4
WA-11-31		311.4	11.0	0.04995	277.7	0.00319	40.5	20.5	8.3	0.6
WA-11-32		292.1	17.0	0.06089	67.1	0.00333	29.5	21.5	6.3	2.6
WA-11-33		243.3	4.0	0.06688	30.2	0.00396	8.1	25.5	2.1	3.7
WA-11-34		270.8	5.2	0.06249	110.0	0.00359	18.9	23.1	4.4	2.9
WA-11-35		380.2	15.5	0.05458	66.9	0.00259	26.2	16.7	4.4	1.5

Appendix Table 3 (continued). U-Pb Spot Analyses by LA-ICP-MS

Sample Spot	Note	Total $^{238}U/^{206}Pb$	±%	Total $^{207}Pb/^{206}Pb$	±%	7-corr $^{206}Pb/^{238}U$	±%	$^{206}Pb/^{238}U$ Age	1σ	% Discor-dant
WA-11-36		365.5	5.0	0.03090	45.6	0.00281	7.8	18.1	1.4	-2.8
WA-11-37	Inherited	230.7	5.2	0.05594	167.3	0.00426	23.4	27.4	6.4	1.7
WA-11-38	Inherited	184.8	6.3	0.05036	180.6	0.00538	24.2	34.6	8.4	0.7
WA-11-39	Inherited	180.0	12.0	0.06216	229.3	0.00540	43.4	34.7	15.1	2.8
WA-11-40		344.4	10.5	0.04745	60.5	0.00290	17.4	18.7	3.3	0.2
WCOSJD-152-01		387.3	6.8	0.06338	10.0	0.00250	8.5	16.1	1.4	3.1
WCOSJD-152-02	Inherited	255.5	4.8	0.04251	115.3	0.00394	14.2	25.4	3.6	-0.7
WCOSJD-152-03		358.4	7.1	0.06484	50.1	0.00270	14.1	17.4	2.5	3.3
WCOSJD-152-04		311.4	2.1	0.08625	66.7	0.00298	13.6	19.2	2.6	7.2
WCOSJD-152-05		574.3	14.2	0.05367	77.0	0.00172	25.4	11.1	2.8	1.3
WCOSJD-152-06		405.2	15.2	0.05751	84.8	0.00242	28.4	15.6	4.4	2.0
WCOSJD-152-07	Inherited	275.5	9.1	0.05201	100.1	0.00359	20.4	23.1	4.7	1.0
WCOSJD-152-08		383.2	12.9	0.05143	48.8	0.00259	20.0	16.7	3.3	0.9
WCOSJD-152-09		515.8	12.4	0.05150	204.5	0.00192	36.1	12.4	4.5	0.9
WCOSJD-152-10		591.7	1.6	0.04356	47.9	0.00170	5.5	10.9	0.6	-0.5
WCOSJD-152-11		470.5	7.6	0.05509	74.7	0.00209	16.4	13.5	2.2	1.6
WCOSJD-152-12		550.4	5.6	0.04236	19.3	0.00183	7.5	11.8	0.9	-0.7
WCOSJD-152-13		356.9	5.5	0.04695	42.0	0.00280	9.6	18.0	1.7	0.1
WCOSJD-152-14		364.1	4.4	0.04029	114.7	0.00278	13.2	17.9	2.4	-1.1
WCOSJD-152-15		482.3	9.2	0.05074	56.7	0.00206	15.8	13.2	2.1	0.8
WCOSJD-152-16		445.3	7.4	0.06385	47.4	0.00217	14.1	14.0	2.0	3.2
WCOSJD-152-17		591.7	14.6	0.03934	105.6	0.00171	25.7	11.0	2.8	-1.3
WCOSJD-152-18		418.0	5.0	0.04005	31.3	0.00242	7.6	15.6	1.2	-1.1
WCOSJD-152-19	Inherited	283.7	8.1	0.05309	41.3	0.00348	13.2	22.4	3.0	1.2
WCOSJD-152-20		376.7	10.5	0.04952	51.4	0.00264	16.9	17.0	2.9	0.6
WCOSJD-152-21		466.8	11.3	0.05075	56.8	0.00213	18.6	13.7	2.5	0.8
WCOSJD-152-22		287.4	8.1	0.08532	163.2	0.00324	38.1	20.8	7.9	7.0
WCOSJD-152-23		578.3	15.9	0.05395	82.2	0.00171	28.5	11.0	3.1	1.4
WCOSJD-152-24		518.6	6.0	0.04851	16.1	0.00192	7.9	12.4	1.0	0.4
WCOSJD-152-25	Inherited	266.9	9.2	0.07170	59.7	0.00358	19.0	23.0	4.4	4.5
WCOSJD-152-26		354.2	8.7	0.04150	172.4	0.00285	23.4	18.3	4.3	-0.9
WCOSJD-152-27		536.4	11.8	0.05422	36.0	0.00184	17.4	11.8	2.1	1.4
WCOSJD-152-28		529.1	11.2	0.04912	99.7	0.00188	22.5	12.1	2.7	0.5
WCOSJD-152-29		538.2	24.9	0.04946	100.9	0.00185	45.2	11.9	5.4	0.6
WCOSJD-152-30		512.2	14.6	0.05437	77.9	0.00192	26.1	12.4	3.2	1.5
WCOSJD-152-31		424.4	3.9	0.04973	109.4	0.00234	14.3	15.1	2.2	0.6
WCOSJD-152-32		308.8	9.6	0.06645	66.7	0.00312	19.7	20.1	4.0	3.6
WCOSJD-152-33		315.1	6.3	0.04705	9.3	0.00317	7.6	20.4	1.6	0.1
WCOSJD-152-34	Inherited	91.3	4.0	0.17707	66.6	0.00840	32.8	53.9	17.7	23.5
WCOSJD-152-35		514.3	25.3	0.06305	252.4	0.00189	73.5	12.1	8.9	3.0
WCOSJD-152-36		309.8	15.8	0.06088	110.0	0.00314	33.4	20.2	6.8	2.6
WCOSJD-152-37	Pb Loss	826.8	8.4	0.05495	113.2	0.00119	21.7	7.7	1.7	1.6
WCOSJD-152-38		324.8	8.5	0.04439	146.0	0.00309	22.0	19.9	4.4	-0.4
WCOSJD-152-39		398.5	10.4	0.04659	96.6	0.00251	20.6	16.2	3.3	0.0
WCOSJD-152-40		543.4	6.6	0.05691	51.4	0.00180	12.9	11.6	1.5	1.9

Appendix Table 3 (continued). U-Pb Spot Analyses by LA-ICP-MS

Sample Spot	Note	Total $^{238}U/^{206}Pb$	±%	Total $^{207}Pb/^{206}Pb$	±%	7-corr $^{206}Pb/^{238}U$	±%	$^{206}Pb/^{238}U$ Age	1σ	% Discor-dant
WCOSJD-152-41		569.8	4.9	0.04687	49.3	0.00175	9.5	11.3	1.1	0.1
WCOSJD-152-42		419.5	19.8	0.03604	177.3	0.00243	38.7	15.6	6.1	-1.9
WCOSJD-152-43		622.4	12.3	0.04818	114.9	0.00160	25.4	10.3	2.6	0.4
WCOSJD-152-44		379.4	5.7	0.06571	55.2	0.00254	13.2	16.4	2.2	3.5
WCOSJD-152-45		326.6	12.4	0.04474	119.7	0.00307	25.1	19.8	5.0	-0.3
WCOS-12-01	Inherited	236.8	3.6	0.04885	41.4	0.00421	7.5	27.1	2.0	0.4
WCOS-12-02		461.2	22.0	0.07295	79.2	0.00206	42.1	13.3	5.6	4.8
WCOS-12-03		1025.5	36.7	0.05323	135.9	0.00096	78.9	6.2	4.9	1.3
WCOS-12-04		576.5	7.3	0.06419	93.1	0.00168	19.9	10.8	2.2	3.2
WCOS-12-05	Discordant	340.4	5.7	0.11656	91.1	0.00257	29.2	16.5	4.8	12.7
WCOS-12-06	Discordant	232.4	3.0	0.11362	66.0	0.00378	18.9	24.3	4.6	12.1
WCOS-12-07		546.2	30.9	0.03675	85.1	0.00186	52.8	12.0	6.3	-1.7
WCOS-12-08		501.3	34.3	0.05680	124.7	0.00196	71.8	12.6	9.1	1.9
WCOS-12-09		1110.8	35.1	0.03240	166.0	0.00092	68.7	5.9	4.1	-2.4
WCOS-12-10		335.0	5.5	0.04930	86.8	0.00297	14.0	19.1	2.7	0.5
WCOS-12-11		614.4	11.7	0.05108	33.3	0.00161	16.8	10.4	1.7	0.9
WCOS-12-12		414.1	7.1	0.05368	21.1	0.00238	9.8	15.3	1.5	1.3
WCOS-12-13		310.8	8.6	0.03876	72.3	0.00326	14.8	21.0	3.1	-1.4
WCOS-12-14		586.6	14.7	0.03664	51.8	0.00173	21.1	11.2	2.4	-1.7
WCOS-12-15		412.5	10.9	0.06262	83.1	0.00235	23.0	15.2	3.5	2.9
WCOS-12-16		652.4	16.3	0.04435	50.3	0.00154	24.3	9.9	2.4	-0.3
WCOS-12-17		483.7	17.7	0.04489	109.5	0.00207	32.2	13.4	4.3	-0.3
WCOS-12-18		637.8	16.7	0.06359	9.9	0.00152	21.5	9.8	2.1	3.1
WCOS-12-19		399.5	31.6	0.04903	44.6	0.00249	52.0	16.0	8.3	0.5
WCOS-12-20		310.1	5.9	0.04600	122.8	0.00323	17.1	20.8	3.6	-0.1
WCOS-12-21		820.1	48.0	0.06363	139.7	0.00118	123.9	7.6	9.4	3.2
WCOS-12-22		785.3	22.0	0.04786	74.2	0.00127	36.5	8.2	3.0	0.3
WCOS-12-23		392.3	19.9	0.04037	258.1	0.00258	47.9	16.6	8.0	-1.1
WCOS-12-24		488.2	24.8	0.05031	290.1	0.00203	68.0	13.1	8.9	0.7
WCOS-12-25		941.8	35.8	0.04560	166.0	0.00106	77.0	6.8	5.3	-0.1
WCOS-12-26		562.8	24.4	0.03264	18.2	0.00182	33.6	11.7	3.9	-2.5
WCOS-12-27		601.6	33.1	0.04186	181.6	0.00168	69.7	10.8	7.5	-0.8
WCOS-12-28		506.6	6.0	0.03197	63.1	0.00203	10.2	13.0	1.3	-2.6
WCOS-12-29		547.6	3.4	0.05322	62.1	0.00180	9.7	11.6	1.1	1.2
WCOS-12-30		328.4	22.5	0.03364	63.1	0.00312	33.8	20.1	6.8	-2.3
WCOS-12-31		447.0	5.4	0.04953	137.3	0.00222	18.7	14.3	2.7	0.6
WCOS-12-32		507.8	10.2	0.05667	114.3	0.00193	24.5	12.4	3.1	1.9
WCOS-12-33		384.7	10.0	0.04556	76.8	0.00260	18.1	16.8	3.0	-0.2
WCOS-12-34		660.2	27.0	0.03349	53.5	0.00155	41.4	10.0	4.1	-2.3
WCOS-12-35		487.8	7.0	0.03556	60.3	0.00209	11.7	13.5	1.6	-2.0
WCOS-12-36		633.7	20.5	0.03909	59.8	0.00160	31.0	10.3	3.2	-1.3
WCOS-12-37		357.1	29.8	0.03738	286.9	0.00285	69.3	18.3	12.7	-1.6
WCOS-12-38		477.8	19.7	0.03755	20.1	0.00213	26.2	13.7	3.6	-1.6
WCOS-12-39	Inherited	146.0	8.4	0.06206	68.7	0.00666	17.8	42.8	7.6	2.7
WCOS-12-40	Inherited	298.4	3.2	0.03476	47.8	0.00342	6.4	22.0	1.4	-2.1
WCOS-2-3	Inherited	248.9	3.3	0.06494	41.6	0.00388	8.6	25.0	2.2	3.3
WCOS-2-4	Inherited	182.8	11.3	0.06777	91.9	0.00526	25.9	33.8	8.7	3.8
WCOS-2-6		371.5	24.9	0.05421	67.1	0.00265	41.9	17.1	7.2	1.4
WCOS-2-7		323.5	8.3	0.04776	49.7	0.00308	13.7	19.9	2.7	0.2
WCOS-2-8	Inherited	254.5	4.9	-0.00635	212.3	0.00430	2.8	27.7	0.8	-9.6

Appendix Table 3 (continued). U-Pb Spot Analyses by LA-ICP-MS

Sample Spot	Note	Total $^{238}U/^{206}Pb$	±%	Total $^{207}Pb/^{206}Pb$	±%	7-corr $^{206}Pb/^{238}U$	±%	$^{206}Pb/^{238}U$ Age	1σ	% Discor-dant
WCOS-2-9		384.8	13.8	0.04768	58.1	0.00259	21.8	16.7	3.6	0.2
WCOS-2-12		363.8	3.2	0.03725	30.7	0.00279	5.4	18.0	1.0	-1.7
WCOS-2-14	Inherited	278.3	4.0	0.00050	1631.8	0.00389	5.6	25.0	1.4	-8.3
WCOS-2-15		359.8	5.1	0.02256	26.4	0.00290	6.4	18.7	1.2	-4.3
WCOS-2-16	Inherited	257.9	10.3	0.06560	66.6	0.00374	20.6	24.1	5.0	3.4
WCOS-2-17		363.8	7.4	0.01400	230.2	0.00291	13.9	18.7	2.6	-5.9
WCOS-2-18	Inherited	272.6	5.1	0.00180	1420.2	0.00396	9.9	25.5	2.5	-8.1
WCOS-2-19		373.8	8.5	0.06124	19.7	0.00260	11.7	16.8	2.0	2.7
WCOS-2-20	Discordant	259.8	7.1	0.21097	14.2	0.00271	15.9	17.4	2.8	29.7
WCOS-2-21	Inherited	263.3	6.0	0.00872	307.3	0.00406	11.1	26.1	2.9	-6.8
WCOS-2-23		354.0	6.6	0.10122	8.5	0.00255	8.9	16.4	1.5	9.9
WCOS-2-24		305.4	4.6	0.12472	47.3	0.00281	17.7	18.1	3.2	14.1
WCOS-2-25	Discordant	32.7	6.7	0.80166	11.6	-0.01185	-42.2	-76.8	32.4	137.1
WCOS-2-28		303.7	5.8	0.07451	10.8	0.00313	7.8	20.1	1.6	5.1
WCOS-2-29		320.2	6.3	0.08498	35.6	0.00291	12.9	18.7	2.4	7.0
WCOS-2-30		363.8	9.0	-0.03285	93.4	0.00314	4.5	20.2	0.9	-14.3
WCOS-2-33	Discordant	297.8	8.4	0.26458	26.2	0.00204	31.6	13.1	4.1	39.4
WCOS-2-37		299.5	8.1	0.07167	62.3	0.00319	17.9	20.5	3.7	4.5
WCOS-2-38		392.9	12.9	0.02946	180.0	0.00262	25.4	16.9	4.3	-3.1
WCOS-2-39	Discordant	271.0	4.5	0.18537	17.5	0.00277	12.9	17.8	2.3	25.1
WCOS-2-40	Inherited	314.7	3.7	0.00226	240.8	0.00343	4.8	22.1	1.1	-8.0
WCOS-7-01	Inherited	207.1	9.5	0.08119	81.4	0.00453	24.5	29.1	7.1	6.3
WCOS-7-02		453.3	11.7	0.03507	131.2	0.00225	22.4	14.5	3.2	-2.0
WCOS-7-03		315.5	15.8	0.07075	62.3	0.00303	28.7	19.5	5.6	4.4
WCOS-7-04	Inherited	299.4	13.9	0.06950	77.4	0.00320	27.9	20.6	5.7	4.2
WCOS-7-05	Inherited	304.1	16.9	0.05411	86.6	0.00324	30.5	20.9	6.4	1.4
WCOS-7-06	Inherited	303.6	4.5	0.06498	25.7	0.00318	7.9	20.5	1.6	3.3
WCOS-7-07		379.8	11.3	0.08324	50.8	0.00246	22.0	15.8	3.5	6.7
WCOS-7-08		466.5	27.8	0.04572	113.0	0.00215	51.4	13.8	7.1	-0.1
WCOS-7-09		365.9	13.0	0.02504	18.4	0.00284	15.9	18.3	2.9	-3.9
WCOS-7-10	Inherited	243.9	33.2	0.04513	89.9	0.00411	60.3	26.5	16.0	-0.3
WCOS-7-11	Inherited	235.1	18.0	0.05905	58.9	0.00416	29.7	26.7	8.0	2.3
WCOS-7-12	Inherited	265.4	5.9	0.05476	140.3	0.00371	21.1	23.9	5.0	1.5
WCOS-7-13		341.1	22.7	0.03992	150.7	0.00297	43.2	19.1	8.2	-1.2
WCOS-7-14	Inherited	260.4	22.2	0.06797	57.3	0.00369	37.8	23.8	9.0	3.9
WCOS-7-15		630.9	58.6	0.04051	862.0	0.00160	290.8	10.3	30.0	-1.0
WCOS-7-16		597.4	21.1	0.02753	182.0	0.00173	37.8	11.1	4.2	-3.4
WCOS-7-17		432.0	4.5	0.04774	141.7	0.00231	17.4	14.9	2.6	0.2
WCOS-7-18		315.8	9.4	0.06083	69.4	0.00308	18.9	19.9	3.8	2.6
WCOS-7-19	Discordant	366.3	10.2	-0.19977	40.3	0.00394	0.1	25.4	0.0	-44.5
WCOS-7-20	Inherited	253.1	12.9	0.05093	341.5	0.00392	50.8	25.2	12.8	0.8
WCOS-7-21		373.8	20.5	0.05483	133.2	0.00263	42.5	17.0	7.2	1.5
WCOS-7-22	Discordant	246.7	2.6	0.20887	39.8	0.00287	24.4	18.5	4.5	29.3
WCOS-7-23	Inherited	306.4	6.1	0.02841	193.9	0.00337	16.7	21.7	3.6	-3.3
WCOS-7-24	Inherited	276.6	9.1	0.04077	138.9	0.00365	21.1	23.5	5.0	-1.0
WCOS-7-25		323.1	5.6	0.14288	33.4	0.00256	16.9	16.5	2.8	17.4
WCOS-7-26	Inherited	277.5	9.9	0.08202	37.2	0.00337	17.5	21.7	3.8	6.4
WCOS-7-27		472.0	17.8	0.04450	127.9	0.00213	34.0	13.7	4.7	-0.3
WCOS-7-28		343.5	3.8	0.14150	23.9	0.00241	11.6	15.5	1.8	17.2
WCOS-7-29		322.4	8.1	0.07032	31.8	0.00297	13.4	19.1	2.6	4.3
WCOS-7-30	Inherited	323.0	2.4	0.03592	75.8	0.00316	7.3	20.3	1.5	-1.9

Appendix Table 3 (continued). U-Pb Spot Analyses by LA-ICP-MS

Sample Spot	Note	Total $^{238}U/^{206}Pb$	±%	Total $^{207}Pb/^{206}Pb$	±%	7-corr $^{206}Pb/^{238}U$	±%	$^{206}Pb/^{238}U$ Age	1σ	% Discor-dant
WCOS-7-31	Inherited	321.6	7.5	0.02157	169.7	0.00325	14.9	20.9	3.1	-4.5
WCOS-7-32	Discordant	344.7	6.4	-0.06867	53.3	0.00350	1.0	22.5	0.2	-20.8
WCOS-7-34	Inherited	344.2	2.9	0.01105	99.2	0.00309	4.9	19.9	1.0	-6.4
WCOS-7-35	Discordant	339.0	5.9	0.22407	19.7	0.00201	18.7	12.9	2.4	32.1
WCOS-7-37		379.1	2.2	0.05866	55.7	0.00258	8.4	16.6	1.4	2.2
WCOS-7-38	Inherited	312.6	5.6	0.01170	301.6	0.00340	12.3	21.9	2.7	-6.3
WCOS-7-39		325.3	9.5	0.12497	17.6	0.00264	15.6	17.0	2.7	14.2
WCOS-7-40		299.7	3.7	0.08963	41.2	0.00308	11.3	19.8	2.2	7.8
WCOSNU-33-01		370.2	7.8	0.05457	60.6	0.00266	15.0	17.1	2.6	1.5
WCOSNU-33-02		352.4	3.5	0.04556	7.8	0.00284	4.3	18.3	0.8	-0.2
WCOSNU-33-03		326.6	6.0	0.04719	13.6	0.00306	7.6	19.7	1.5	0.1
WCOSNU-33-04		361.1	2.2	0.03796	5.5	0.00281	2.6	18.1	0.5	-1.5
WCOSNU-33-05		340.0	9.4	0.05421	54.4	0.00290	16.3	18.7	3.0	1.4
WCOSNU-33-06	Discordant	169.7	3.8	0.31866	6.6	0.00300	11.7	19.3	2.3	49.2
WCOSNU-33-07	Discordant	217.8	5.1	0.57367	3.7	0.00022	90.8	1.4	1.3	95.3
WCOSNU-33-08		365.6	6.4	0.05837	21.2	0.00268	9.2	17.2	1.6	2.2
WCOSNU-33-09	Discordant	254.1	3.0	0.27902	3.3	0.00229	6.0	14.7	0.9	42.0
WCOSNU-33-10	Discordant	100.2	9.7	0.81434	6.9	-0.00396	-18.1	-25.6	4.6	139.1
WCOSNU-33-11	Discordant	209.3	7.8	0.44299	5.2	0.00135	24.6	8.7	2.1	71.8
WCOSNU-33-12	Inherited	290.1	2.4	0.04115	17.7	0.00348	3.8	22.4	0.9	-1.0
WCOSNU-33-13		317.3	4.5	0.07803	17.9	0.00297	7.5	19.1	1.4	5.7
WCOSNU-33-14	Discordant	463.6	5.7	0.11499	16.2	0.00189	10.1	12.2	1.2	12.4
WCOSNU-33-15		330.3	5.4	0.03813	36.1	0.00307	8.3	19.8	1.6	-1.5
WCOSNU-33-16		385.5	5.4	0.05546	116.9	0.00255	18.3	16.4	3.0	1.6
WCOSNU-33-17		401.3	5.4	0.05812	14.9	0.00244	7.4	15.7	1.2	2.1
WCOSNU-33-18	Inherited	296.0	3.6	0.04854	42.2	0.00337	7.6	21.7	1.6	0.4
WCOSNU-33-19	Discordant	193.9	4.8	0.43578	5.2	0.00153	19.5	9.9	1.9	70.5
WCOSNU-33-20	Discordant	81.8	8.0	0.93840	4.0	-0.00770	-3.3	-49.9	1.6	161.8
WCOSNU-33-21		322.8	6.2	0.03091	58.2	0.00319	9.9	20.5	2.0	-2.8
WCOSNU-33-22		341.6	2.2	0.04811	13.9	0.00292	3.5	18.8	0.7	0.3
WCOSNU-33-23		368.1	3.1	0.04599	16.8	0.00272	4.7	17.5	0.8	-0.1
WCOSNU-33-24		392.3	4.2	0.05977	11.9	0.00249	5.8	16.0	0.9	2.4
WCOSNU-33-25		311.2	3.2	0.04968	16.8	0.00320	4.9	20.6	1.0	0.6
WCOSNU-33-26		342.6	7.0	0.04083	40.7	0.00295	10.7	19.0	2.0	-1.0
WCOSNU-33-27	Inherited	219.7	4.3	0.05729	23.8	0.00446	7.1	28.7	2.0	1.9
WCOSNU-33-28		357.6	9.5	0.05793	24.4	0.00274	13.4	17.6	2.4	2.1
WCOSNU-33-29		325.0	2.9	0.04768	22.0	0.00307	4.9	19.8	1.0	0.2
WCOSNU-33-30		373.7	8.7	0.05767	27.1	0.00262	12.6	16.9	2.1	2.0
WCOSNU-33-31	Discordant	192.1	4.5	0.35814	10.5	0.00228	21.0	14.7	3.1	56.4
WCOSNU-33-32		376.4	6.9	0.05736	10.6	0.00260	8.7	16.8	1.5	2.0
WCOSNU-33-33	Discordant	244.6	2.4	0.24933	16.8	0.00259	14.7	16.7	2.4	36.7
WCOSNU-33-34	Inherited	291.7	3.3	0.05647	13.5	0.00337	4.9	21.7	1.1	1.8
WCOSNU-33-35	Discordant	311.4	4.1	0.17840	5.2	0.00245	6.5	15.8	1.0	23.8
WCOSNU-33-36		296.6	4.5	0.05933	17.8	0.00329	6.7	21.2	1.4	2.3
WCOSNU-33-37	Inherited	272.0	3.4	0.04072	38.1	0.00371	6.4	23.9	1.5	-1.0
WCOSNU-33-38	Discordant	124.3	6.1	0.62931	3.9	-0.00044	-81.2	-2.8	2.3	105.4
WCOSNU-33-39		347.8	4.4	0.04472	19.2	0.00288	6.2	18.6	1.1	-0.3
WCOSNU-33-40	Discordant	67.3	5.4	0.65586	5.7	-0.00157	-63.5	-10.1	6.4	110.4
WCOSNU-33-42		393.1	6.7	0.04303	19.6	0.00256	8.8	16.5	1.5	-0.6
WCOSNU-33-43		345.1	9.1	0.05704	41.0	0.00284	14.7	18.3	2.7	1.9
WCOSNU-33-44	Discordant	78.5	7.9	0.96250	4.7	-0.00860	-4.7	-55.7	2.6	166.1

Appendix Table 3 (continued). U-Pb Spot Analyses by LA-ICP-MS

Sample Spot	Note	Total $^{238}U/^{206}Pb$	±%	Total $^{207}Pb/^{206}Pb$	±%	7-corr $^{206}Pb/^{238}U$	±%	$^{206}Pb/^{238}U$ Age	1σ	% Discor-dant
WCOSNU-33-45		391.2	2.7	0.04807	21.5	0.00255	4.7	16.4	0.8	0.3
WCOSNU-33-46		354.5	10.9	0.01260	135.0	0.00299	15.5	19.3	3.0	-6.1
WCOSNU-33-47	Pb Loss	514.3	12.4	0.05424	57.5	0.00192	20.7	12.3	2.6	1.4
WCOSNU-33-48	Inherited	233.5	7.4	0.04446	30.3	0.00430	10.6	27.7	2.9	-0.4
WCOSNU-33-49		336.9	5.5	0.05666	22.7	0.00291	8.3	18.8	1.6	1.8
WCOSNU-33-50		325.9	5.2	0.04373	51.7	0.00308	9.8	19.8	1.9	-0.5
WCOSNU-33-52	Inherited	292.0	5.3	0.05744	39.1	0.00336	9.9	21.6	2.1	2.0
WCOSNU-33-53	Inherited	278.6	6.3	0.04452	91.0	0.00360	14.5	23.2	3.4	-0.4
WCOSNU-33-54	Inherited	296.6	6.3	0.04897	49.8	0.00336	11.5	21.6	2.5	0.4
WCOSNU-33-55		466.6	31.7	0.04858	151.3	0.00213	65.9	13.7	9.1	0.4
WCOSNU-33-56		417.5	8.2	0.05694	67.3	0.00235	16.6	15.1	2.5	1.9
WCOSNU-33-57		373.4	7.0	0.05732	12.2	0.00263	8.8	16.9	1.5	2.0
WCOSNU-33-58		425.2	7.6	0.05122	39.9	0.00233	12.2	15.0	1.8	0.9
WCOSNU-33-59	Pb Loss	566.8	6.3	0.04611	25.0	0.00176	8.9	11.4	1.0	0.0
WCOSNU-33-60		443.2	8.2	0.05357	18.2	0.00223	10.8	14.3	1.6	1.3
WCOSNU-33-61	Inherited	205.6	5.0	0.06689	16.8	0.00469	7.4	30.1	2.2	3.7
WCOSNU-33-62		449.4	4.9	0.05554	11.7	0.00219	6.4	14.1	0.9	1.7
WCOSNU-33-63		389.2	17.0	0.04128	88.7	0.00259	28.4	16.7	4.7	-0.9
WCOSNU-33-64		424.1	7.6	0.03548	103.8	0.00240	15.3	15.5	2.4	-2.0
WCOSNU-33-65	Pb Loss	470.6	5.7	0.05738	14.8	0.00208	7.7	13.4	1.0	2.0
WCOSNU-33-66	Pb Loss	506.5	6.1	0.06408	14.3	0.00191	8.3	12.3	1.0	3.2
WCOSNU-33-67		391.4	7.3	0.05831	95.8	0.00250	18.9	16.1	3.0	2.1
WCOSNU-33-68		371.8	6.4	0.03932	11.4	0.00272	7.7	17.5	1.3	-1.3
WCOSNU-33-69		448.8	6.4	0.04836	13.2	0.00222	8.0	14.3	1.1	0.4
WCOSNU-33-71	Inherited	291.9	6.6	0.05300	39.1	0.00339	11.1	21.8	2.4	1.2
WCOSNU-33-72	Discordant	376.0	8.6	0.12529	23.3	0.00228	16.2	14.7	2.4	14.3
WCOSNU-33-73	Discordant	171.4	8.9	0.71649	9.1	-0.00125	-51.2	-8.1	4.1	121.3
WCOSNU-33-74	Discordant	506.5	26.1	0.26885	26.5	0.00118	64.5	7.6	4.9	40.2
WCOSNU-33-75	Discordant	205.4	7.2	0.13463	21.9	0.00410	14.5	26.4	3.8	15.9
WCOSNU-33-76		390.4	6.3	0.06147	17.0	0.00249	8.7	16.0	1.4	2.7
WCOSNU-33-77	Discordant	345.0	34.8	0.26329	39.0	0.00176	100.0	11.4	11.4	39.2
WCOSNU-33-78		421.4	5.6	0.05556	10.0	0.00233	7.1	15.0	1.1	1.7
WCOSNU-33-79	Pb Loss	561.4	15.8	0.05025	28.3	0.00177	21.8	11.4	2.5	0.7
WCOSNU-33-80		445.7	11.5	0.06562	65.1	0.00217	22.0	13.9	3.1	3.5
WCOSNU-33-81		376.5	5.1	0.05979	11.9	0.00259	6.8	16.7	1.1	2.4
WCOSNU-33-82		417.3	8.6	0.05746	13.8	0.00235	11.0	15.1	1.7	2.0
WCOSNU-33-83	Discordant	335.5	4.9	0.09913	7.8	0.00270	6.8	17.4	1.2	9.5
WCOSNU-33-84		377.5	5.8	0.06984	38.7	0.00254	11.5	16.3	1.9	4.2
WCOSNU-33-86		419.2	5.1	0.05784	20.3	0.00234	7.6	15.0	1.1	2.1
WCOSNU-33-87	Discordant	197.1	7.3	0.31561	10.0	0.00261	19.9	16.8	3.3	48.7
WCOSNU-33-88		424.1	6.3	0.05217	30.4	0.00233	9.8	15.0	1.5	1.0
WCOSNU-33-89		352.0	14.6	0.06117	87.9	0.00277	28.7	17.8	5.1	2.7
WCOSNU-33-90		360.1	10.2	0.05746	83.6	0.00272	21.1	17.5	3.7	2.0
WCOSNU-33-91		485.9	8.8	0.03648	167.5	0.00209	21.6	13.5	2.9	-1.8
WCOSNU-33-92		423.2	11.7	0.04994	87.2	0.00235	22.2	15.1	3.4	0.6
WCOSNU-33-93	Pb Loss	533.6	5.7	0.04927	14.6	0.00186	7.4	12.0	0.9	0.5
WCOSNU-33-94		344.5	9.5	0.04914	98.0	0.00289	20.1	18.6	3.7	0.5
WCOSNU-33-95		389.4	2.8	0.05506	15.9	0.00253	4.5	16.3	0.7	1.6
WCOSNU-33-96		348.3	3.1	0.07001	11.0	0.00275	4.7	17.7	0.8	4.3
WCOSNU-33-97		423.1	4.8	0.04404	14.2	0.00237	6.2	15.3	1.0	-0.4
WCOSNU-33-98		317.4	4.7	0.04929	14.7	0.00313	6.3	20.2	1.3	0.5
WCOSNU-33-99	Discordant	379.2	7.4	0.12556	11.1	0.00226	11.1	14.6	1.6	14.3

Appendix Table 3 (continued). U-Pb Spot Analyses by LA-ICP-MS

Sample Spot	Note	Total $^{238}U/^{206}Pb$	±%	Total $^{207}Pb/^{206}Pb$	±%	7-corr $^{206}Pb/^{238}U$	±%	$^{206}Pb/^{238}U$ Age	1σ	% Discor-dant
WCOSNU-33-100		367.3	1.6	0.03735	16.1	0.00277	2.7	17.8	0.5	-1.6
WCOSNU-25-01		247.5	2.0	0.03958	17.5	0.00409	3.3	26.3	0.9	-1.3
WCOSNU-25-02		249.1	5.3	0.04820	61.6	0.00400	11.2	25.8	2.9	0.3
WCOSNU-25-03		371.2	9.7	0.05306	46.0	0.00266	15.6	17.1	2.7	1.2
WCOSNU-25-04		257.4	4.8	0.04617	10.3	0.00389	6.0	25.0	1.5	-0.1
WCOSNU-25-05	Inherited	242.9	6.1	0.03277	26.8	0.00422	8.1	27.1	2.2	-2.5
WCOSNU-25-06	Inherited	158.5	4.0	0.04604	30.0	0.00632	6.7	40.6	2.7	-0.2
WCOSNU-25-07		259.9	4.5	0.04155	48.1	0.00388	8.4	25.0	2.1	-0.9
WCOSNU-25-08		262.7	9.9	0.03860	29.9	0.00386	13.2	24.8	3.3	-1.4
WCOSNU-25-09		263.5	2.2	0.07510	22.6	0.00360	5.6	23.2	1.3	5.2
WCOSNU-25-10	Inherited	159.8	6.4	0.05737	61.7	0.00614	13.7	39.5	5.4	1.9
WCOSNU-25-11		259.4	2.6	0.05648	22.2	0.00379	5.0	24.4	1.2	1.8
WCOSNU-25-12		302.8	6.7	0.04842	37.9	0.00329	10.7	21.2	2.3	0.3
WCOSNU-25-13	Inherited	155.2	2.7	0.04850	56.0	0.00643	7.8	41.3	3.2	0.3
WCOSNU-25-14	Inherited	234.5	10.4	0.14313	15.8	0.00352	17.1	22.7	3.9	17.5
WCOSNU-25-15		277.9	2.8	0.04541	14.4	0.00361	4.1	23.2	0.9	-0.2
WCOSNU-25-16	Inherited	240.9	3.6	0.04247	74.5	0.00418	9.6	26.9	2.6	-0.7
WCOSNU-25-17		273.6	4.4	0.04465	42.7	0.00367	8.2	23.6	1.9	-0.3
WCOSNU-25-18	Inherited	188.6	6.6	0.05093	75.3	0.00526	14.5	33.8	4.9	0.8
WCOSNU-25-19	Inherited	211.0	3.3	0.05674	22.9	0.00465	5.8	29.9	1.7	1.8
WCOSNU-25-20		244.8	2.2	0.05633	60.6	0.00401	8.7	25.8	2.2	1.8
WCOSNU-25-21	Inherited	221.6	7.6	0.04903	17.5	0.00449	9.9	28.9	2.9	0.4
WCOSNU-25-22		299.6	7.9	0.05834	63.4	0.00327	16.0	21.0	3.4	2.1
WCOSNU-25-23		300.4	5.2	0.03905	21.6	0.00337	7.0	21.7	1.5	-1.3
WCOSNU-25-24		256.0	7.8	0.06095	38.2	0.00380	13.1	24.5	3.2	2.6
WCOSNU-25-25	Pb Loss	443.0	19.9	0.07318	90.1	0.00215	40.4	13.8	5.6	4.8
WCOSNU-25-26		288.3	5.6	0.04350	27.6	0.00349	8.2	22.4	1.8	-0.5
WCOSNU-25-27		264.1	0.5	0.05383	26.7	0.00374	3.1	24.1	0.7	1.3
WCOSNU-25-28	Pb Loss	390.6	27.2	0.04722	125.8	0.00256	52.0	16.5	8.6	0.1
WCOSNU-25-29		335.5	8.0	0.05594	19.9	0.00293	10.9	18.9	2.1	1.7
WCOSNU-25-30		271.6	5.6	0.05511	46.2	0.00362	10.9	23.3	2.5	1.6
WCOSNU-25-31	Inherited	202.3	6.2	0.04353	76.6	0.00497	12.9	32.0	4.1	-0.6
WCOSNU-25-32		275.7	4.1	0.06070	32.1	0.00353	8.1	22.7	1.8	2.6
WCOSNU-25-33		282.4	5.8	0.04157	45.6	0.00357	9.7	23.0	2.2	-0.9
WCOSNU-25-34	Inherited	243.1	0.6	0.03922	58.1	0.00417	4.7	26.8	1.3	-1.3
WCOSNU-25-35		265.7	6.0	0.04090	123.1	0.00380	15.9	24.5	3.9	-1.0
WCOSNU-25-36		283.9	2.8	0.05507	42.6	0.00347	7.2	22.3	1.6	1.5
WCOSNU-25-37		281.1	3.3	0.05941	36.6	0.00348	7.5	22.4	1.7	2.3
WCOSNU-25-38		268.3	2.4	0.05315	78.5	0.00368	10.3	23.7	2.4	1.2
WCOSNU-25-39		313.8	5.6	0.06133	38.5	0.00310	10.5	20.0	2.1	2.7
WCOSNU-25-40		258.7	4.4	0.04801	62.7	0.00386	10.3	24.8	2.5	0.3
WCOSNU-25-41		301.7	9.8	0.05750	139.4	0.00325	27.1	20.9	5.7	2.0
WCOSNU-25-42		318.7	5.3	0.03842	19.8	0.00318	7.0	20.5	1.4	-1.5
WCOSNU-25-43	Pb Loss	379.4	7.8	0.07514	125.9	0.00250	27.9	16.1	4.5	5.2
WCOSNU-25-44		229.4	4.0	0.08118	34.5	0.00409	9.7	26.3	2.6	6.3
WCOSNU-25-45	Inherited	208.8	3.7	0.05822	43.5	0.00469	8.6	30.2	2.6	2.1
WCOSNU-11-01	Inherited	302.5	4.3	0.05768	20.6	0.00324	6.7	20.9	1.4	2.0
WCOSNU-11-02		337.7	1.5	0.06036	13.6	0.00289	3.1	18.6	0.6	2.5
WCOSNU-11-03	Inherited	240.4	1.4	0.04780	9.9	0.00415	2.3	26.7	0.6	0.2
WCOSNU-11-04		316.2	3.9	0.06014	16.6	0.00308	6.0	19.9	1.2	2.5

Appendix Table 3 (continued). U-Pb Spot Analyses by LA-ICP-MS

Sample Spot	Note	Total $^{238}U/^{206}Pb$	±%	Total $^{207}Pb/^{206}Pb$	±%	7-corr $^{206}Pb/^{238}U$	±%	$^{206}Pb/^{238}U$ Age	1σ	% Discor-dant
WCOSNU-11-05	Inherited	304.5	1.7	0.05184	9.5	0.00325	2.7	20.9	0.6	1.0
WCOSNU-11-06	Inherited	276.0	4.0	0.05023	7.1	0.00360	4.9	23.2	1.1	0.7
WCOSNU-11-07	Inherited	265.1	3.0	0.05280	45.5	0.00373	7.6	24.0	1.8	1.1
WCOSNU-11-08	Inherited	278.4	4.1	0.04709	23.5	0.00359	6.4	23.1	1.5	0.1
WCOSNU-11-09	Inherited	281.5	5.2	0.04709	55.0	0.00355	10.4	22.8	2.4	0.1
WCOSNU-11-10	Inherited	295.5	4.0	0.05616	7.0	0.00332	4.9	21.4	1.1	1.7
WCOSNU-11-11		383.0	4.4	0.05363	15.1	0.00258	6.2	16.6	1.0	1.3
WCOSNU-11-12	Inherited	237.7	7.9	0.04708	28.7	0.00420	11.3	27.0	3.0	0.1
WCOSNU-11-13		320.7	5.1	0.03888	14.6	0.00316	6.5	20.3	1.3	-1.4
WCOSNU-11-14	Inherited	241.1	2.1	0.05994	30.5	0.00405	5.6	26.0	1.5	2.4
WCOSNU-11-15	Inherited	300.0	7.4	0.05405	29.8	0.00329	11.2	21.2	2.4	1.4
WCOSNU-11-16		360.8	1.4	0.05551	17.1	0.00273	3.2	17.6	0.6	1.6
WCOSNU-11-17	Pb Loss	438.9	4.7	0.04921	11.6	0.00227	6.0	14.6	0.9	0.5
WCOSNU-11-18	Pb Loss	480.7	16.2	0.04310	17.5	0.00209	21.0	13.5	2.8	-0.6
WCOSNU-11-19	Inherited	266.3	3.0	0.04385	10.9	0.00377	4.0	24.3	1.0	-0.5
WCOSNU-11-20		331.6	3.3	0.05914	7.9	0.00295	4.3	19.0	0.8	2.3
WCOSNU-11-21	Inherited	259.8	2.0	0.05034	20.8	0.00382	3.9	24.6	1.0	0.7
WCOSNU-11-22	Inherited	307.8	2.1	0.05045	22.3	0.00323	4.2	20.8	0.9	0.7
WCOSNU-11-23		379.8	7.9	0.05994	14.4	0.00257	10.3	16.5	1.7	2.4
WCOSNU-11-24	Inherited	286.2	3.0	0.04070	14.5	0.00353	4.2	22.7	1.0	-1.1
WCOSNU-11-25	Inherited	237.7	1.3	0.05764	26.3	0.00412	4.1	26.5	1.1	2.0
WCOSNU-11-26	Inherited	248.2	2.8	0.04929	16.9	0.00401	4.4	25.8	1.1	0.5
WCOSNU-11-27		364.6	2.6	0.06109	20.0	0.00267	5.0	17.2	0.9	2.6
WCOSNU-11-28	Inherited	267.8	1.9	0.04725	13.7	0.00373	3.1	24.0	0.7	0.1
WCOSNU-11-29		331.7	5.4	0.05544	7.5	0.00297	6.5	19.1	1.2	1.6
WCOSNU-11-30	Inherited	114.0	1.2	0.05327	93.4	0.00867	10.3	55.7	5.7	1.1
WCOSNU-11-31		359.7	5.2	0.06153	6.8	0.00270	6.3	17.4	1.1	2.7
WCOSNU-11-32		343.8	3.0	0.04502	14.1	0.00292	4.2	18.8	0.8	-0.3
WCOSNU-11-33		367.1	2.7	0.04822	21.1	0.00272	4.7	17.5	0.8	0.3
WCOSNU-11-34		351.9	2.2	0.05795	7.4	0.00278	3.1	17.9	0.6	2.1
WCOSNU-11-35		337.3	3.1	0.05783	12.8	0.00290	4.6	18.7	0.9	2.1
WCOSNU-11-36	Inherited	175.6	7.9	0.05427	10.8	0.00562	9.7	36.1	3.5	1.4
WCOSNU-11-37		345.5	7.7	0.05246	44.5	0.00286	12.9	18.4	2.4	1.1
WCOSNU-11-38	Inherited	262.9	5.8	0.04380	14.7	0.00382	7.3	24.6	1.8	-0.5
WCOSNU-11-39	Inherited	252.6	5.3	0.04707	42.7	0.00395	9.4	25.4	2.4	0.1
WCOSNU-11-40	Inherited	245.7	10.2	0.05062	37.5	0.00404	15.2	26.0	3.9	0.7

Appendix Table 4. U-Pb Spot Analyses by SHRIMP-RG

Sample Spot ID	Note	U (ppm)	Th (ppm)	Total $^{238}U/^{206}Pb$	±%	Total $^{207}Pb/^{206}Pb$	±%	7-corr $^{206}Pb/^{238}U$	±%	$^{206}Pb/^{238}U$ Age	1σ
WCOS-2-1.1		1706.87	1009.92	381.2	1.8	0.04240	4.3	0.00264	0.6	17.0	0.3
WCOS-2-10.1		129.82	47.27	341.7	3.5	0.11859	20.7	0.00266	1.6	17.1	0.8
WCOS-2-11.1		707.91	654.42	398.8	2.3	0.06085	7.2	0.00246	0.8	15.8	0.4
WCOS-2-12.1	Inherited	258.14	113.95	369.7	1.8	0.04403	13.0	0.00271	0.6	17.5	0.3
WCOS-2-13.1		531.15	210.08	381.9	2.1	0.08443	5.9	0.00249	0.7	16.0	0.4
WCOS-2-14.1	Inherited	2448.16	1674.92	365.0	1.7	0.04808	3.6	0.00273	0.6	17.6	0.3
WCOS-2-15.1		105.02	41.71	341.8	6.4	0.17097	8.8	0.00246	2.2	15.9	1.1
WCOS-2-2.1	Pb Loss	416.68	364.30	417.1	1.7	0.05714	8.4	0.00236	0.6	15.2	0.3
WCOS-2-3.1		322.57	197.44	391.9	1.5	0.05780	9.1	0.00251	0.5	16.2	0.3
WCOS-2-4.1		487.89	254.88	387.1	2.3	0.04339	8.9	0.00259	0.8	16.7	0.4
WCOS-2-5.1		587.54	268.16	387.9	1.9	0.05266	7.4	0.00256	0.6	16.5	0.3
WCOS-2-6.1		546.10	255.65	384.9	0.7	0.04551	15.8	0.00260	0.4	16.7	0.2
WCOS-2-7.1	Inherited	2002.82	1877.30	364.0	0.7	0.04567	6.8	0.00275	0.2	17.7	0.1
WCOS-2-8.1	Inherited	247.72	105.56	342.2	0.8	0.10268	8.0	0.00271	0.4	17.5	0.2
WCOS-2-9.1		333.21	132.48	410.7	2.4	0.05081	12.0	0.00242	0.8	15.6	0.4
WCOS-SL3-1.1		86.79	42.51	296.6	1.6	0.07414	15.6	0.00325	0.7	20.9	0.5
WCOS-SL3-10.1		306.20	237.30	284.9	1.2	0.04925	9.1	0.00350	0.4	22.5	0.3
WCOS-SL3-11.1		320.08	228.51	284.9	0.7	0.04806	8.9	0.00350	0.3	22.5	0.2
WCOS-SL3-12.1		84.80	41.33	283.9	2.6	0.06913	14.5	0.00342	0.9	22.0	0.6
WCOS-SL3-13.1		101.27	61.71	284.6	5.0	0.06366	14.7	0.00344	1.6	22.1	1.1
WCOS-SL3-14.1		373.60	290.38	282.9	0.7	0.05236	8.0	0.00351	0.3	22.6	0.2
WCOS-SL3-15.1		207.07	140.81	277.8	0.9	0.03976	12.1	0.00363	0.3	23.4	0.2
WCOS-SL3-2.1		256.15	179.41	286.0	0.7	0.04995	10.6	0.00348	0.3	22.4	0.2
WCOS-SL3-3.1		72.52	29.90	313.7	2.3	0.06256	18.1	0.00312	0.9	20.1	0.5
WCOS-SL3-4.1		103.04	59.54	311.1	1.1	0.04276	19.4	0.00323	0.5	20.8	0.3
WCOS-SL3-5.1		95.02	48.63	298.4	2.2	0.03889	17.9	0.00338	0.7	21.8	0.5
WCOS-SL3-6.1		458.73	432.23	276.2	2.5	0.04227	8.0	0.00364	0.8	23.4	0.6
WCOS-SL3-7.1		232.43	180.02	281.8	2.1	0.04257	11.5	0.00357	0.7	22.9	0.5
WCOS-SL3-8.1		97.43	49.85	273.6	4.3	0.06049	14.6	0.00359	1.4	23.1	1.0
WCOS-SL3-9.1		637.96	627.29	289.5	1.3	0.04640	6.6	0.00345	0.4	22.2	0.3
WCOS-SL11-1.1		198.11	148.71	296.2	2.3	0.03967	11.8	0.00340	0.7	21.9	0.5
WCOS-SL11-10.1		188.31	122.39	286.2	2.1	0.03652	13.4	0.00354	0.7	22.8	0.5
WCOS-SL11-11.1		141.05	95.93	282.3	3.6	0.04410	14.2	0.00355	1.2	22.9	0.8
WCOS-SL11-12.1		98.44	46.07	275.5	1.1	0.05768	14.8	0.00358	0.5	23.0	0.4
WCOS-SL11-13.1		364.92	284.75	271.1	1.6	0.04657	8.7	0.00369	0.5	23.7	0.4
WCOS-SL11-14.1		103.82	46.50	276.5	3.1	0.04950	15.4	0.00360	1.0	23.2	0.7
WCOS-SL11-15.1		139.00	80.41	277.7	0.9	0.03985	15.1	0.00363	0.4	23.4	0.3
WCOS-SL11-2.1		97.10	56.89	251.4	1.1	0.14497	8.6	0.00348	0.7	22.4	0.5
WCOS-SL11-3.1		220.08	157.67	291.7	2.6	0.04845	10.5	0.00342	0.9	22.0	0.6
WCOS-SL11-4.1		283.18	207.21	281.1	2.2	0.05427	9.0	0.00352	0.7	22.7	0.5
WCOS-SL11-4.2		213.43	153.24	285.5	1.6	0.04442	11.5	0.00351	0.5	22.6	0.4
WCOS-SL11-6.1	Pb Loss	163.64	121.69	299.1	0.9	0.06236	11.7	0.00328	0.4	21.1	0.3
WCOS-SL11-7.1		432.39	382.93	272.1	1.7	0.04373	8.1	0.00369	0.6	23.7	0.4
WCOS-SL11-8.1		94.62	48.99	278.2	1.0	0.04434	17.2	0.00360	0.4	23.2	0.3
WCOS-SL11-9.1		177.21	124.07	276.0	2.4	0.04049	13.7	0.00365	0.8	23.5	0.6
WCOSNU-11-1		529.98	382.04	268.2	1.8	0.04719	7.0	0.00373	0.6	24.0	0.4

Appendix 6. Whole Rock Geochemistry

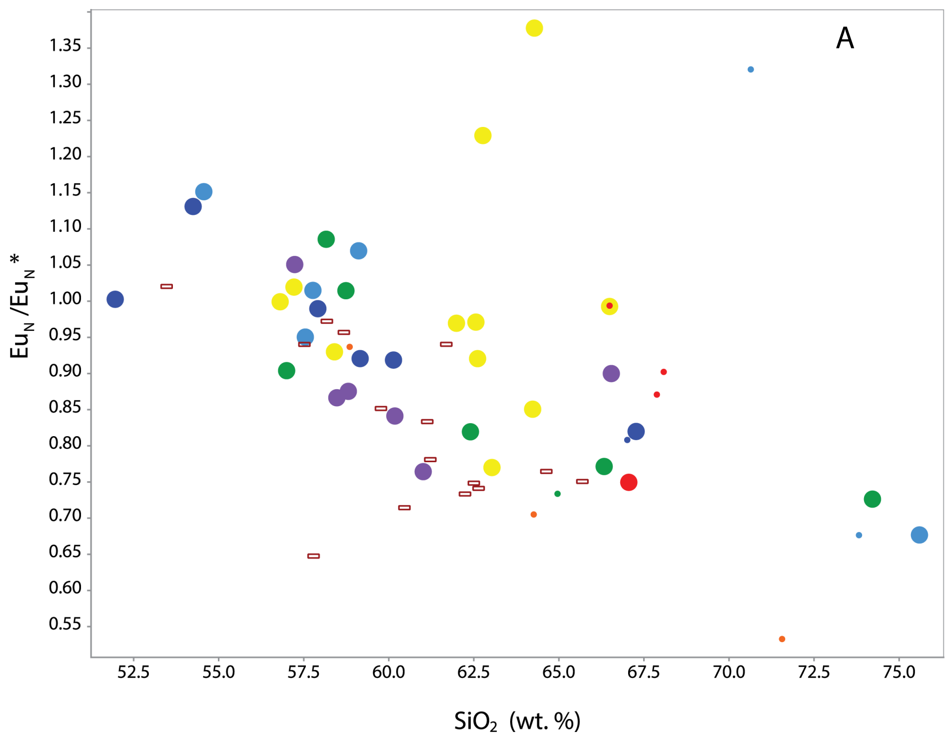

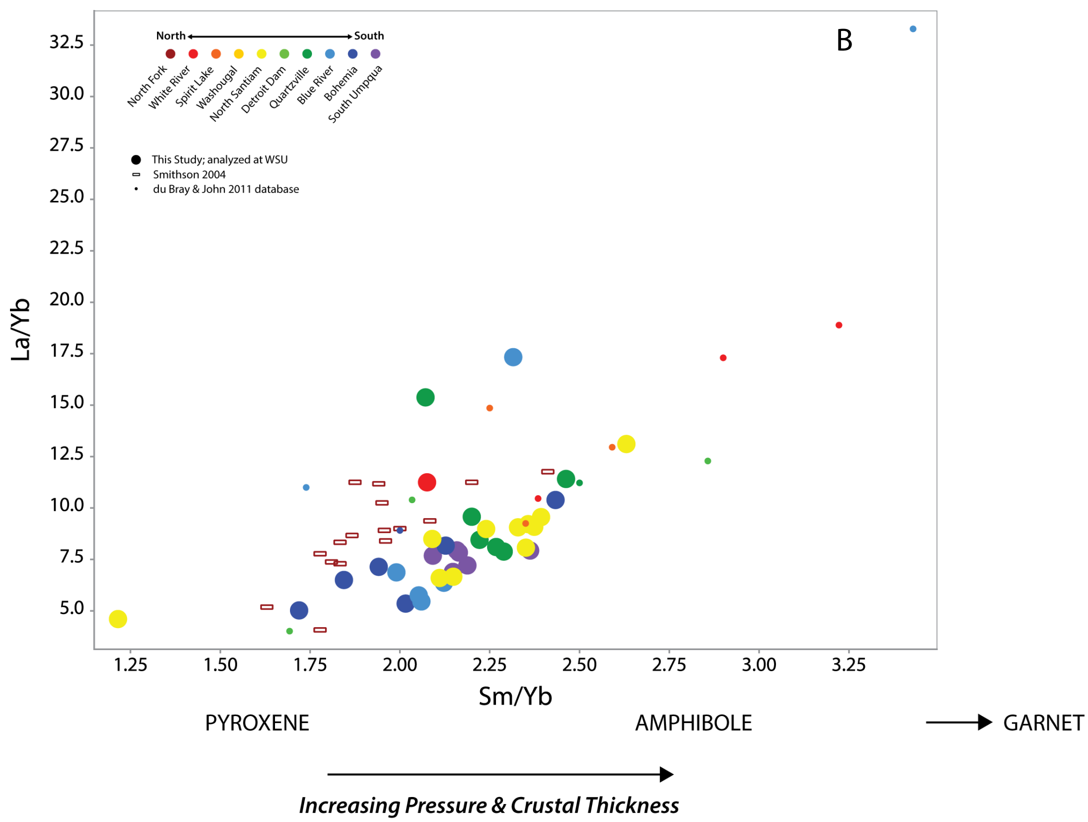

Appendix Figure 5: A) SiO_2 vs. Eu_N/Eu_N*; B) Sm/Yb vs. La/Yb after Kay & Mpodozis (2001).

Appendix Table 5. Whole Rock XRF & ICP-MS Results from WSU

Sample ID:	WCOSN U-01	WCOSN U-07	WCOSN U-09	WCOSN U-10	WCOSN U-11	WCOSN U-12	WCOSN U-19	WCOSN U-20	WCOSN U-21	WCOSN U-23	WCOSN U-24	WCOSN U-25	WCOSN U-28	WCOSN U-29
Location[1]:	SU	SU	SU	SU	SU	SU	BOH	BOH	BOH	BOH	BOH	BOH	BR	BR
Rock Type[*]	And	And	Diorite	Ton	Diorite	Diorite	Mnzd	And	Grnd	Diorite	Qz Dior	Diorite	Diorite	Diorite
Latitude	43.27	42.73	42.70	42.74	42.75	42.75	43.63	43.64	43.64	43.58	43.58	43.58	44.22	44.23
Longitude	-122.52	-122.67	-122.74	-122.78	-122.78	-122.78	-122.66	-122.64	-122.63	-122.64	-122.63	-122.63	-122.34	-122.34
(wt.% oxides)														
SiO_2	54.17	64.44	57.52	56.77	60.15	57.43	53.24	49.92	66.42	56.03	58.50	58.15	56.60	51.53
TiO_2	1.30	0.96	0.77	0.90	0.87	0.89	1.43	1.13	0.75	0.91	0.86	0.91	0.91	1.06
Al_2O_3	16.23	14.46	15.93	16.69	15.77	16.35	17.66	18.39	14.64	16.42	16.18	16.56	16.67	18.52
FeO*	7.77	5.31	6.57	7.12	6.73	7.43	9.17	7.98	4.50	7.07	6.59	7.21	6.38	6.99
MnO	0.15	0.13	0.10	0.12	0.11	0.13	0.17	0.11	0.06	0.13	0.12	0.12	0.13	0.12
MgO	3.98	1.69	3.43	3.53	3.37	3.85	3.53	5.15	1.96	4.57	4.02	3.78	3.88	3.94
CaO	6.42	3.93	6.61	7.18	6.78	7.71	8.71	10.10	4.46	7.04	5.99	6.92	6.10	7.32
Na_2O	3.28	3.96	2.99	2.81	3.03	3.19	3.27	2.36	3.35	2.92	3.37	3.19	4.01	3.81
K_2O	1.05	1.70	1.53	1.22	1.62	1.05	0.69	0.78	2.47	1.49	1.48	1.30	0.89	0.96
P_2O5	0.30	0.27	0.14	0.19	0.16	0.19	0.27	0.16	0.14	0.17	0.16	0.16	0.18	0.19
Sum	94.64	96.84	95.59	96.54	98.59	98.22	98.15	96.08	98.74	96.75	97.28	98.30	95.75	94.44
LOI %	4.26	2.48	3.73	2.86	0.62	0.91	1.26	3.14	0.86	2.19	2.17	1.63	3.21	4.91
(ppm)														
Cs[2]	0.29	0.77	0.33	1.09	4.21	0.78	0.68	0.73	0.33	1.62	4.46	0.90	0.31	2.14
Ba[2]	297.51	520.10	390.57	387.61	469.79	199.30	231.16	126.52	781.58	403.18	367.70	351.61	234.48	190.41
Rb[2]	19.61	40.52	31.21	28.81	48.32	24.09	11.89	19.15	31.69	36.35	41.35	31.37	13.69	19.80
Sr[2]	497.84	313.37	437.06	503.50	372.73	441.15	439.85	471.87	383.08	482.62	382.27	400.34	535.63	786.23
Ni	9.60	1.41	12.54	6.43	19.70	16.68	9.55	23.52	16.27	14.27	27.94	24.72	21.41	20.10
Cr	11.82	3.62	34.03	34.57	50.45	45.02	30.75	64.82	25.43	81.61	33.47	27.84	52.26	52.26
V	207.66	61.71	169.35	171.05	190.25	215.87	246.43	221.80	99.90	207.43	158.39	171.86	156.78	191.85
Sc[2]	23.41	17.35	22.68	23.98	22.73	24.98	29.19	27.41	15.07	25.91	19.61	20.80	21.72	25.67
Cu	36.87	7.34	44.87	43.11	84.62	68.94	57.08	5.53	3.92	33.67	55.98	38.39	65.93	55.78
Zn	90.80	102.71	67.16	120.50	80.00	80.30	96.08	28.44	14.27	73.26	413.96	76.78	68.74	64.82
Ga	19.39	16.78	16.42	18.49	17.39	17.29	20.50	16.88	15.98	17.39	17.19	17.69	18.89	17.39
Pb[2]	5.45	10.95	6.63	28.40	10.17	8.09	4.22	2.60	3.12	6.98	11.84	6.42	5.40	2.34
Zr[2]	129.13	159.83	127.62	104.43	141.28	99.86	92.70	59.40	235.91	111.72	134.90	133.71	112.59	68.77
Hf[2]	3.43	4.48	3.51	2.99	4.02	2.83	2.50	1.59	6.46	3.18	3.67	3.68	2.98	1.88
Nb[2]	6.15	7.05	4.56	4.38	4.87	3.40	5.71	3.61	7.90	4.56	5.75	5.63	3.95	2.86
Ta[2]	0.41	0.50	0.34	0.31	0.38	0.26	0.40	0.26	0.68	0.37	0.44	0.43	0.46	0.35
Th[2]	3.00	4.81	3.83	2.98	4.81	3.01	1.41	0.99	8.05	4.58	4.42	4.26	1.42	0.83
U[2]	0.96	1.62	1.37	1.03	1.71	1.10	0.52	0.36	1.56	1.62	1.56	1.49	0.53	0.31
Y[2]	21.25	28.47	17.99	18.71	19.76	18.02	20.19	12.53	23.74	18.74	20.57	20.38	18.11	14.48
La[2]	15.74	20.18	13.44	12.39	13.94	11.30	10.04	12.48	11.92	14.28	13.77	12.99	9.81	7.02
Ce[2]	35.03	40.16	28.54	26.09	29.85	24.91	22.88	26.40	25.04	30.01	29.01	28.06	22.79	15.60
Pr[2]	4.76	5.49	3.74	3.66	4.03	3.34	3.24	3.39	3.49	3.93	3.80	3.68	3.11	2.24
Nd[2]	20.30	22.89	15.49	15.34	16.62	14.48	14.61	13.65	15.08	16.35	15.87	15.24	13.72	10.34
Sm[2]	4.69	5.48	3.66	3.76	3.85	3.52	3.78	2.92	4.08	3.72	3.74	3.68	3.50	2.65
Eu[2]	1.58	1.64	0.98	1.06	0.96	1.00	1.45	0.95	1.10	1.19	1.12	1.10	1.23	1.04
Gd[2]	4.52	5.64	3.48	3.67	3.85	3.55	4.07	2.89	4.12	3.63	3.71	3.64	3.56	2.87
Tb[2]	0.71	0.90	0.55	0.60	0.62	0.56	0.65	0.43	0.70	0.56	0.61	0.62	0.58	0.47
Dy[2]	4.27	5.40	3.45	3.60	3.68	3.44	4.02	2.59	4.43	3.65	3.92	3.88	3.48	2.89
Ho[2]	0.84	1.07	0.68	0.73	0.74	0.70	0.80	0.52	0.89	0.70	0.77	0.77	0.72	0.59
Er[2]	2.23	2.94	1.94	1.97	2.04	1.86	2.18	1.38	2.59	1.96	2.07	2.18	1.91	1.49
Tm[2]	0.32	0.42	0.28	0.28	0.29	0.26	0.30	0.19	0.37	0.28	0.30	0.31	0.28	0.21
Yb[2]	1.98	2.54	1.75	1.72	1.78	1.64	1.87	1.20	2.37	1.75	1.93	2.00	1.71	1.29
Lu[2]	0.30	0.38	0.28	0.27	0.28	0.25	0.29	0.18	0.38	0.28	0.30	0.30	0.26	0.21

[1] - Location Codes: SU - South Umpqua, BOH - Bohemia, BR - Blue River, NS - North Santiam, WR - White River, QTZ - Quartzville, DD - Detroit Dam

[2] - Determined by ICP-MS at Washington State University (WSU). All other oxides and trace elements determines by XRF at WSU.

* - Rock Type Code: And - Andesite, Grnd - Granodiorite, Ign - Ignimbrite, Mnzn - Monzonite, Mnzd - Monzodiorite, Qz Dior - Quartz Diorite, Qz Mzd - Quartz Monzodiorite, Ton - Tonalite

Appendix Table 5 (continued). Whole Rock XRF & ICP-MS Results from WSU

Sample ID:	WCOSNU-31	WCOSNU-32	WCOSNU-33	WCOSNU-91	WCOSNU-119	WCOSWR-01	WCOSJD-147	WCOSJD-152	WCOS-2	WCOS-3	WCOS-4	WCOS-7	WCOS-8	WCOS-12
Location[1]:	BR	BR	BR	NS	NS	WR	NS	NS	QTZ	QTZ	QTZ	QTZ	QTZ	DD
Rock Type[*]	Qz Dior	Qz Dior	Grnd	Mnzd	Mnzd	Mnzn	Mnzd	Qz Mzd	Grnd	Dacite	Qz Mzd	Mnzd	And	Qz Mzd
Latitude	44.23	44.23	44.12	44.83	44.84	47.15	44.85	44.84	44.56	44.56	44.57	44.59	44.59	44.70
Longitude	-122.35	-122.33	-122.44	-122.23	-122.23	-121.83	-122.23	-122.25	-122.38	-122.38	-122.38	-122.37	-122.37	-122.25
(wt.% oxides)														
SiO_2	53.36	54.58	73.98	61.04	56.74	65.86	60.15	61.72	72.63	56.90	55.94	64.36	55.40	61.63
TiO_2	0.92	0.95	0.31	0.82	0.95	0.56	0.70	0.79	0.29	0.93	1.15	0.77	0.92	0.84
Al_2O_3	16.60	16.90	12.75	16.05	17.14	15.33	17.01	16.30	13.43	17.68	17.08	15.13	16.72	15.95
FeO*	5.82	6.63	2.42	5.10	6.41	3.69	6.56	4.58	1.85	6.45	7.33	4.77	6.50	5.71
MnO	0.08	0.12	0.01	0.09	0.14	0.07	0.09	0.12	0.20	0.12	0.14	0.08	0.12	0.10
MgO	3.12	4.09	0.28	2.80	3.98	2.06	3.38	2.88	0.60	4.06	4.42	2.51	3.70	3.81
CaO	8.38	6.26	1.60	5.40	7.38	4.49	5.52	5.06	0.21	6.52	6.87	4.07	4.81	5.69
Na_2O	2.80	3.53	4.41	2.96	3.28	3.76	1.91	3.59	1.09	3.29	3.92	3.85	4.51	3.83
K_2O	1.13	1.61	2.05	2.43	0.98	2.31	0.39	0.92	7.49	0.72	1.06	1.35	2.36	1.04
P_2O5	0.16	0.17	0.04	0.15	0.17	0.10	0.12	0.14	0.07	0.18	0.23	0.14	0.21	0.16
Sum	92.37	94.85	97.85	96.84	97.15	98.22	95.84	96.10	97.86	96.86	98.14	97.03	95.25	98.77
LOI %	7.43	4.40	1.68	2.70	2.32	1.20	3.22	3.15	2.15	2.30	1.73	2.50	4.60	1.03
(ppm)														
Cs[2]	4.97	4.62	0.89	0.79	0.27	3.10	1.12	0.23	3.76	1.22	0.59	0.82	0.90	2.23
Ba[2]	340.60	357.23	561.37	422.06	293.52	588.95	180.47	222.85	965.97	177.23	262.30	381.62	737.79	292.05
Rb[2]	22.36	37.46	39.59	43.41	16.35	55.34	9.00	16.58	224.01	17.81	26.99	27.00	56.67	26.22
Sr[2]	617.05	510.65	219.73	465.41	486.86	308.45	453.54	471.17	186.85	442.64	430.01	278.60	505.04	404.37
Ni	48.94	24.38	3.02	24.92	33.53	18.79	25.93	29.45	4.12	30.35	51.96	29.75	16.88	55.48
Cr	69.55	46.07	3.42	40.30	55.52	30.15	28.74	33.77	5.23	70.15	78.89	48.54	27.24	94.87
V	129.34	156.02	24.22	122.61	160.39	81.10	111.25	116.78	24.22	150.65	170.75	100.20	148.54	127.43
Sc[2]	15.98	20.31	4.06	15.47	19.23	10.48	14.66	14.15	3.87	19.92	20.39	13.37	19.78	16.38
Cu	31.96	61.79	4.82	19.40	166.36	39.09	191.75	148.04	23.72	55.07	47.54	24.42	58.89	7.64
Zn	58.79	66.86	15.28	67.54	96.12	28.54	60.90	98.49	787.32	151.65	169.44	67.44	78.09	36.08
Ga	18.89	18.11	13.37	17.59	17.71	18.09	19.20	18.29	14.97	20.00	19.50	17.39	18.19	17.59
Pb[2]	5.69	4.11	6.97	7.99	4.73	8.70	3.03	31.53	319.37	7.44	5.66	10.50	5.59	3.22
Zr[2]	146.06	137.33	221.54	205.66	137.90	181.86	108.47	196.82	149.83	133.78	145.92	239.75	158.48	193.86
Hf[2]	3.97	3.70	6.39	5.45	3.72	5.08	3.06	5.40	4.26	3.38	3.75	6.29	3.84	5.14
Nb[2]	5.19	4.83	6.29	6.96	5.59	7.53	4.65	6.97	8.71	6.71	7.70	9.10	8.56	7.56
Ta[2]	0.55	0.47	0.89	0.69	0.56	0.82	0.56	0.68	1.09	0.62	0.67	0.84	0.75	0.77
Th[2]	3.24	2.03	13.39	5.84	3.24	8.78	3.65	5.63	14.98	2.94	2.74	7.25	2.77	4.67
U[2]	1.11	0.78	3.00	1.94	1.02	2.98	1.14	1.91	4.74	1.00	0.95	2.47	0.88	1.33
Y[2]	18.53	19.27	15.01	21.72	18.03	17.49	15.60	20.97	16.49	20.95	26.28	20.58	18.92	21.97
La[2]	12.58	11.64	29.94	17.83	13.41	19.34	12.74	17.38	26.67	14.54	15.55	20.11	19.79	16.16
Ce[2]	27.25	26.36	58.25	37.81	29.41	39.30	25.79	37.50	49.85	30.30	31.20	44.25	40.03	35.76
Pr[2]	3.60	3.63	6.39	4.94	3.86	4.60	3.23	4.79	5.45	3.95	4.40	5.29	4.92	4.65
Nd[2]	15.09	15.46	22.41	20.32	16.34	17.20	13.14	19.38	18.69	16.46	18.81	20.77	19.35	19.37
Sm[2]	3.64	3.88	4.00	4.66	3.90	3.57	3.13	4.47	3.59	3.82	4.52	4.62	4.27	4.52
Eu[2]	1.20	1.20	0.74	1.14	1.17	0.84	1.23	1.22	0.76	1.27	1.37	1.10	1.47	1.18
Gd[2]	3.60	3.82	2.80	4.37	3.77	3.27	3.00	4.28	2.88	3.84	4.76	4.13	3.99	4.30
Tb[2]	0.60	0.62	0.42	0.71	0.60	0.52	0.50	0.68	0.49	0.62	0.74	0.67	0.63	0.72
Dy[2]	3.62	3.83	2.53	4.17	3.59	3.17	2.94	4.26	2.93	3.74	4.49	3.99	3.72	4.28
Ho[2]	0.74	0.75	0.52	0.85	0.73	0.66	0.59	0.81	0.61	0.75	0.89	0.82	0.74	0.83
Er[2]	1.96	2.01	1.54	2.21	1.90	1.72	1.60	2.15	1.69	1.99	2.36	2.18	1.89	2.17
Tm[2]	0.27	0.29	0.25	0.32	0.27	0.26	0.23	0.32	0.27	0.28	0.32	0.33	0.28	0.33
Yb[2]	1.83	1.83	1.73	1.96	1.66	1.72	1.50	1.92	1.73	1.72	1.97	2.10	1.73	1.99
Lu[2]	0.28	0.28	0.29	0.32	0.26	0.26	0.22	0.30	0.29	0.28	0.31	0.31	0.26	0.30

[1] - Location Codes: SU - South Umpqua, BOH - Bohemia, BR - Blue River, NS - North Santiam, WR - White River, QTZ - Quartzville, DD - Detroit Dam

[2] - Determined by ICP-MS at Washington State University (WSU). All other oxides and trace elements determines by XRF at WSU

* - Rock Type Code: And - Andesite, Grnd - Granodiorite, Ign - Ignimbrite, Mnzn - Monzonite, Mnzd - Monzodiorite, Qz Dior - Quartz Diorite, Qz Mzd - Quartz Monzodiorite, Ton - Tonalite

Appendix Table 5 (continued). Whole Rock XRF & ICP-MS Results from WSU

Sample ID:	NSNU-02	NSNU-03	NSNU-04	NSNU-06	NSNU-07	NSNU-08	NSNU-09
Location[1]:	NS	NS	NS	NS	NS	NS	NS
Rock Type[*]	Qz Mzd	Ign	Grnd	Mnzd	Diorite	Diorite	Diorite
Latitude	44.83	44.84	44.84	44.84	44.84	44.86	44.86
Longitude	-122.25	-122.25	-122.25	-122.22	-122.22	-122.28	-122.28
(wt.% oxides)							
SiO_2	62.70	60.90	64.84	55.56	55.92	61.56	59.80
TiO_2	0.61	0.79	0.56	1.15	1.17	0.79	0.81
Al_2O_3	16.08	16.51	16.02	17.54	17.64	16.60	16.69
FeO*	7.27	4.94	4.39	7.25	7.61	5.23	4.90
MnO	0.04	0.10	0.05	0.13	0.13	0.10	0.10
MgO	2.76	3.06	2.43	3.68	3.88	2.91	2.98
CaO	4.71	5.73	4.29	7.50	7.70	5.48	6.11
Na_2O	3.05	4.03	2.64	3.31	3.36	3.37	4.09
K_2O	0.19	1.03	2.19	0.79	0.82	2.17	0.80
P_2O5	0.13	0.18	0.11	0.21	0.21	0.18	0.19
Sum	97.55	97.26	97.52	97.11	98.43	98.40	96.46
LOI %	2.01	2.44	2.67	1.47	1.49	1.46	2.66
(ppm)							
Cs[2]	0.81	0.79	1.80	0.20	0.17	0.54	1.02
Ba[2]	140.64	285.92	931.06	311.28	303.90	371.86	291.11
Rb[2]	3.82	18.42	38.31	13.59	13.64	36.01	13.82
Sr[2]	425.87	672.60	492.73	454.16	447.24	545.09	691.45
Ni	19.80	34.97	23.01	24.28	23.22	36.88	34.37
Cr	37.69	46.63	35.48	30.75	31.05	44.02	46.93
V	93.67	93.87	76.58	178.90	184.72	103.82	91.66
Sc[2]	12.61	14.15	10.02	21.60	22.04	14.74	14.47
Cu	487.12	58.59	56.88	29.45	15.58	47.64	127.64
Zn	54.27	66.03	118.19	76.52	76.98	71.36	61.41
Ga	17.09	18.39	17.89	19.40	20.10	19.50	18.09
Pb[2]	6.54	8.88	12.59	6.18	6.36	18.88	7.12
Zr[2]	124.56	171.75	137.11	142.56	142.10	170.87	174.66
Hf[2]	3.24	4.58	3.87	3.74	3.82	4.56	4.61
Nb[2]	5.10	7.00	5.33	6.66	6.62	6.95	7.14
Ta[2]	0.62	0.72	0.69	0.66	0.66	0.75	0.72
Th[2]	3.74	4.46	5.76	2.65	2.60	4.46	4.36
U[2]	1.18	1.50	1.96	0.99	0.97	1.50	1.46
Y[2]	13.83	20.57	13.24	22.51	22.24	19.35	21.27
La[2]	6.72	17.56	16.07	13.54	13.58	16.54	18.09
Ce[2]	13.34	37.70	33.30	30.34	30.30	36.79	38.20
Pr[2]	1.69	4.94	4.01	4.10	4.15	4.60	5.10
Nd[2]	6.87	19.98	15.32	18.08	17.79	18.82	20.80
Sm[2]	1.77	4.49	3.23	4.37	4.34	4.13	4.53
Eu[2]	0.86	1.31	0.99	1.45	1.43	1.29	1.41
Gd[2]	2.05	4.22	2.90	4.35	4.39	4.01	4.37
Tb[2]	0.37	0.66	0.43	0.70	0.73	0.65	0.67
Dy[2]	2.45	3.92	2.46	4.42	4.42	3.73	3.93
Ho[2]	0.53	0.80	0.49	0.89	0.87	0.76	0.79
Er[2]	1.49	2.13	1.34	2.35	2.31	2.01	2.07
Tm[2]	0.22	0.31	0.20	0.34	0.34	0.30	0.30
Yb[2]	1.46	1.91	1.23	2.03	2.06	1.84	1.89
Lu[2]	0.24	0.29	0.20	0.31	0.34	0.28	0.30

[1] - Location Codes: SU - South Umpqua, BOH - Bohemia, BR - Blue River, NS - North Santiam, WR - White River, QTZ - Quartzville, DD - Detroit Dam

[2] - Determined by ICP-MS at Washington State University (WSU). All other oxides and trace elements determines by XRF at WSU

* - Rock Type Code: And - Andesite, Grnd - Granodiorite, Ign - Ignimbrite, Mnzn - Monzonite, Mnzd - Monzodiorite, Qz Dior - Quartz Diorite, Qz Mzd - Quartz Monzodiorite, Ton - Tonalite

Appendix Table 6. Whole Rock Four-Acid ICP-MS from ALS

Sample ID:	DD-116	DD-75	DD-53	DD-48	WA-2	WA-3	WA-8	WA-9	NR-1	BR -3	BR-5	SU-18	SS-3-A
Rock Name	Basaltic andesite	Andesite	Dacite dike	Dacite	Quartz diorite	Diorite	Granodiorite	Quartz diorite	Granite	Silicic dike	Diorite	Quartz diorite	Andesite
Longitude	-122.24	-122.25	-122.25	-122.25	-122.24	-122.20	-122.19	-122.17	-122.44	-122.32	-122.35	-122.79	-122.28
Latitude	44.72	44.69	44.70	44.71	45.83	45.80	45.79	45.79	44.42	44.23	44.24	43.04	44.86
(wt.% oxides)													
SiO_2	57.65	62.90	66.10	68.55	51.80	52.83	64.14	57.16	75.47	66.71	58.98	54.35	58.98
TiO_2	1.04	0.75	0.71	1.00	0.88	1.57	0.49	0.89	0.21	1.07	1.07	0.84	1.14
Al_2O_3	14.85	13.08	14.25	14.62	17.21	16.15	13.85	17.06	12.28	13.28	15.89	17.80	16.12
FeO*	7.26	5.67	5.45	6.10	7.35	10.37	3.87	7.20	1.67	5.67	7.01	7.20	6.65
MnO	0.12	0.10	0.09	0.09	0.13	0.23	0.08	0.14	0.02	0.10	0.11	0.13	0.14
MgO	5.07	2.89	2.75	1.48	3.81	5.06	1.66	3.63	0.46	1.46	3.80	2.67	2.16
CaO	7.95	6.34	4.27	4.04	10.62	8.55	4.17	6.62	1.36	3.85	5.74	9.11	4.49
Na_2O	3.38	3.25	3.64	3.83	2.78	2.64	3.61	4.64	4.08	3.86	3.90	2.95	2.16
K_2O	0.66	0.53	1.73	2.04	0.52	0.30	1.86	1.28	3.30	2.26	0.57	0.72	0.93
P_2O5	0.20	0.12	0.16	0.25	0.07	0.09	0.10	0.15	0.05	0.31	0.24	0.12	0.21
total_I	98.18	95.62	99.16	101.99	95.16	97.79	93.83	98.77	98.91	98.58	97.30	95.91	92.96
(ppm)													
Ba	410	250	400	580	140	120	570	290	760	500	320	250	340
La	9.00	6.70	11.20	21.20	3.60	7.00	19.10	9.10	33.80	21.70	18.10	8.10	22.40
Ce	20.20	16.10	25.70	45.20	8.57	17.30	35.80	22.20	69.20	49.70	40.00	19.60	50.90
Rb	2.20	2.40	25.70	44.50	4.00	5.60	19.20	23.10	69.40	38.80	9.90	11.10	26.80
Sr	563	560	452	385	404	329	416	473	158	456	730	438	395
Y	15.50	8.80	11.90	24.80	9.30	20.70	11.30	14.20	30.30	30.70	22.30	14.90	25.20
Zr	112.00	14.70	43.70	190.50	40.10	6.70	2.50	4.30	3.40	186.50	148.50	7.80	70.40
Nb	4.50	4.10	6.70	10.60	3.00	4.30	6.70	6.20	5.20	10.70	7.40	4.00	8.50
Co	28.30	18.90	17.10	12.30	36.60	16.20	8.00	20.30	1.90	10.70	22.00	18.00	17.40
Cr	83.00	41.00	54.00	20.00	53.00	74.00	35.00	61.00	100.00	19.00	70.00	29.00	47.00
Ni	46.80	27.60	30.50	12.10	24.80	30.60	19.30	19.10	4.40	3.00	30.90	10.80	27.90
Sc	21.40	12.00	13.20	15.00	22.00	36.10	8.40	14.40	4.60	17.30	22.60	24.70	23.70
V	185	120	104	109	224	409	69	142	20	83	161	224	130
Ag	0.04	0.08	0.09	0.09	0.05	0.07	0.03	0.19	0.04	0.11	0.03	0.03	0.43
Cu	76.50	37.00	42.10	36.40	112.00	27.10	7.50	131.00	12.50	79.50	41.50	27.30	46.70
Mo	0.78	2.43	1.32	3.92	3.04	0.77	1.03	4.23	2.75	0.82	0.33	4.54	0.59
Pb	5.10	20.30	6.90	13.90	4.40	11.80	7.10	20.70	7.70	16.30	5.70	4.00	23.70
Zn	74.00	80.00	68.00	76.00	62.00	128.00	35.00	117.00	17.00	89.00	73.00	59.00	117.00
As	0.80	3.50	6.90	5.00	7.80	45.30	7.90	3.40	3.50	4.60	4.00	26.10	11.20
Be	0.75	0.76	0.89	1.26	1.08	0.71	1.13	1.02	1.72	1.54	1.16	0.70	1.37
Bi	0.03	0.08	0.05	0.09	0.03	0.61	0.10	0.31	0.57	0.09	0.07	0.25	0.13
Cd	0.07	0.17	0.09	0.13	0.14	0.23	0.07	0.24	0.04	0.07	0.07	0.04	0.35
Cs	<0.05	0.62	0.47	0.61	0.76	0.42	0.46	7.36	1.22	0.54	4.32	3.30	4.09
Ga	18.20	18.55	18.20	19.35	19.55	19.75	17.15	20.70	15.90	18.85	19.40	21.80	21.10
Ge	0.13	0.09	0.11	0.14	0.08	0.12	0.13	0.10	0.15	0.17	0.17	0.12	0.16
Hf	2.70	0.60	1.50	5.20	1.30	0.60	0.10	0.20	0.20	5.90	4.10	0.40	2.20
In	0.05	0.05	0.05	0.05	0.06	0.27	0.04	0.08	0.03	0.07	0.09	0.08	0.08
Li	11.60	19.50	17.80	16.40	11.10	2.70	6.50	13.50	9.50	16.60	46.20	8.60	27.00
Mn	904	798	723	686	972	1780	633	1120	117	796	879	1020	1060
Re	<0.002	<0.002	<0.002	0.00	<0.002	<0.002	<0.002	0.01	<0.002	<0.002	<0.002	0.00	<0.002
S	<0.01	0.01	0.03	0.01	0.01	0.05	<0.01	0.02	0.27	0.01	<0.01	0.23	0.03
Sb	0.16	0.89	1.11	0.80	1.00	1.90	0.86	0.37	0.60	1.67	0.58	3.13	1.46
Se	1.00	<1	1.00	2.00	1.00	1.00	1.00	1.00	1.00	1.00	1.00	1.00	2.00
Sn	1.00	1.30	1.10	1.80	1.40	2.60	1.00	2.90	1.90	5.20	1.60	1.40	1.40
Ta	0.27	0.31	0.47	0.75	0.22	0.28	0.49	0.42	0.42	0.69	0.47	0.27	0.53
Te	<0.05	<0.05	<0.05	<0.05	<0.05	0.11	<0.05	<0.05	<0.05	<0.05	<0.05	0.12	<0.05
Th	1.40	1.40	2.40	5.60	0.60	2.10	4.80	1.70	10.00	2.40	2.80	1.70	2.70
Tl	0.07	0.13	0.39	0.33	0.10	0.14	0.21	0.27	0.47	0.27	0.10	0.11	0.29
U	0.60	0.30	0.70	1.90	3.20	0.60	1.00	0.50	1.60	1.00	1.40	0.40	0.90
W	0.10	0.40	0.40	0.70	0.80	0.40	0.30	1.30	0.90	0.40	0.30	0.70	0.40

Appendix Table 6 (continued). Whole Rock Four-Acid ICP-MS from ALS

Sample ID:	SS-7	TB-1	RD-1	S78-30	S78-73b	32.24	28.29	21.7	5.2	X7	X2	X3	1328
Rock Name	Andesite	Andesite	Rhyolite	Basaltic andesite	Basaltic andesite	Basaltic andesite	Basaltic andesite	Basaltic andesite	Dacite	Basalt	Dacite	Andesite	Andesite
Longitude	-122.29	-122.23	-122.19	-122.18	-122.24	-122.35	-122.33	-122.34	-122.36	-122.36	-122.28	-122.28	-122.30
Latitude	44.85	44.85	44.85	45.72	45.75	44.21	44.24	44.25	44.21	44.58	44.61	44.61	44.58
(wt.% oxides)													
SiO_2	61.14	63.07	78.49	56.81	55.14	53.86	54.77	57.40	61.60	53.41	70.47	58.93	54.76
TiO_2	1.09	0.93	0.14	1.23	1.11	1.04	1.04	0.84	1.31	1.02	0.34	1.08	0.98
Al_2O_3	15.81	15.63	10.09	15.25	17.02	16.06	16.72	15.68	13.85	16.02	13.42	15.87	15.81
FeO*	7.91	5.74	1.70	7.59	9.06	6.93	6.84	6.14	6.83	6.86	2.83	6.32	7.14
MnO	0.17	0.13	0.13	0.12	0.14	0.14	0.10	0.11	0.12	0.10	0.06	0.10	0.12
MgO	2.17	3.48	0.25	3.76	5.16	4.29	4.18	3.52	1.94	4.33	0.25	2.57	5.16
CaO	2.20	1.47	2.21	7.81	10.05	8.86	8.70	7.93	4.27	9.85	1.08	6.65	8.90
Na_2O	1.43	0.40	0.20	2.84	2.66	3.55	2.74	3.21	3.92	2.70	4.87	3.37	3.05
K_2O	1.52	1.84	3.10	0.54	0.40	0.40	0.16	0.37	2.01	0.64	2.98	0.46	1.63
P_2O5	0.25	0.13	0.02	0.23	0.16	0.20	0.17	0.17	0.36	0.26	0.06	0.22	0.34
total_I	93.70	92.82	96.33	96.19	100.89	95.33	95.42	95.37	96.21	95.19	96.35	95.57	97.88
(ppm)													
Ba	430	390	550	210	160	200	60	170	480	360	720	270	580
La	19.20	44.70	12.80	19.70	7.20	8.80	3.90	5.30	24.70	21.10	23.20	11.30	35.30
Ce	43.50	86.40	33.60	43.20	17.55	22.80	10.15	12.30	52.00	46.40	49.20	29.20	81.20
Rb	43.90	45.00	78.40	6.20	3.20	1.50	0.50	1.30	41.50	4.70	57.20	3.30	24.40
Sr	238	133	50	645	422	949	714	676	349	826	125	563	1090
Y	19.20	24.40	10.70	20.60	14.80	11.70	10.00	10.60	37.60	17.20	32.80	15.40	18.50
Zr	64.40	11.40	9.10	134.00	80.20	69.20	60.10	68.50	169.00	88.60	307.00	84.50	140.00
Nb	7.40	10.00	8.80	10.00	5.00	3.50	2.30	2.80	10.80	4.00	10.90	7.30	5.90
Co	22.30	16.40	2.00	27.10	30.40	25.80	24.10	19.40	15.40	26.00	28.10	24.10	32.10
Cr	65.00	34.00	9.00	57.00	75.00	69.00	69.00	70.00	37.00	60.00	2.00	23.00	106.00
Ni	30.30	45.60	4.20	46.60	38.10	45.50	32.10	21.30	9.80	34.70	1.60	30.80	45.00
Sc	17.40	16.00	1.90	21.30	27.90	20.10	19.70	19.80	22.10	26.70	7.00	16.80	26.70
V	143	140	27	179	209	181	170	174	149	193	10	155	188
Ag	0.78	0.04	1.15	0.05	0.07	0.11	0.05	0.04	0.11	0.05	0.11	0.06	0.10
Cu	73.30	59.50	79.80	115.50	128.50	50.70	41.50	42.70	76.90	73.10	27.80	17.20	73.50
Mo	2.00	1.96	7.29	1.93	1.54	0.56	0.33	0.62	1.23	0.83	1.42	0.73	0.81
Pb	78.80	3.00	273.00	9.20	8.60	6.00	2.20	3.30	14.40	5.50	8.60	5.40	7.90
Zn	185.00	105.00	795.00	90.00	88.00	89.00	70.00	71.00	113.00	72.00	65.00	81.00	85.00
As	21.70	222.00	2.20	9.70	4.30	9.10	2.90	1.20	3.90	2.80	1.70	2.90	2.70
Be	1.29	1.03	1.15	1.20	0.69	0.77	0.46	0.64	1.41	0.83	1.79	0.97	1.21
Bi	0.85	0.25	0.91	0.05	0.03	0.06	0.02	0.03	0.05	0.16	0.10	0.04	0.05
Cd	0.72	0.28	3.22	0.13	0.09	0.11	0.07	0.06	0.13	0.11	0.08	0.07	0.14
Cs	5.35	2.80	1.91	0.24	2.22	0.24	1.58	0.15	0.95	0.45	0.75	3.14	1.21
Ga	18.85	21.40	15.20	21.70	19.70	20.80	18.75	19.50	19.80	20.10	16.80	21.00	20.50
Ge	0.13	0.16	0.16	0.14	0.11	0.12	0.10	0.10	0.14	0.14	0.19	0.10	0.13
Hf	1.70	0.30	0.50	4.20	2.30	2.00	1.70	2.00	4.90	2.80	7.80	2.60	4.10
In	0.08	0.30	0.04	0.06	0.06	0.05	0.04	0.04	0.07	0.06	0.06	0.05	0.05
Li	24.20	21.40	19.60	5.30	5.50	13.40	32.80	7.30	20.90	21.10	19.50	38.00	14.70
Mn	1340	1020	1030	942	1090	1060	811	835	930	802	470	785	922
Re	<0.002	<0.002	<0.002	<0.002	<0.002	<0.002	<0.002	<0.002	<0.002	<0.002	<0.002	<0.002	<0.002
S	0.30	0.02	0.15	<0.01	<0.01	<0.01	<0.01	<0.01	<0.01	<0.01	<0.01	<0.01	<0.01
Sb	1.72	13.50	0.96	0.47	0.25	0.55	1.25	0.24	0.55	0.47	0.90	0.80	0.73
Se	4.00	1.00	1.00	1.00	1.00	<1	1.00	1.00	1.00	1.00	1.00	<1	1.00
Sn	1.30	21.40	2.00	1.70	1.00	1.30	0.80	0.90	5.20	0.90	1.80	0.90	2.20
Ta	0.47	0.57	0.80	0.62	0.31	0.23	0.15	0.18	0.68	0.27	0.83	0.51	0.54
Te	0.86	<0.05	0.11	<0.05	<0.05	<0.05	<0.05	<0.05	<0.05	<0.05	<0.05	<0.05	<0.05
Th	2.80	8.40	2.10	5.20	1.10	0.90	0.40	0.70	2.60	3.30	5.50	1.10	4.40
Tl	0.57	0.99	0.82	0.10	0.14	0.06	0.04	0.05	0.26	0.08	0.32	0.07	0.26
U	0.80	0.90	0.70	1.90	0.50	3.60	0.70	1.00	9.10	0.80	2.00	0.50	1.30
W	0.60	4.00	0.40	0.70	0.30	0.20	0.10	0.10	0.50	16.80	45.10	19.40	59.40

Appendix Table 6 (continued). Whole Rock Four-Acid ICP-MS from ALS

Sample ID:	A1501	1245	WA-1	WA-4	WA-5	WA-7	WA-10	WA-11	WA-6	WA-20	WA-19	NS-2	NS-4
Rock Name	Andesite	Andesite	Quartz diorite	Quartz diorite	Quartz diorite	Aplite	Diorite	Granodiorite	Granodiorite	Aplite	Diorite	Granodiorite	Granodiorite
Longitude	-122.30	-122.32	-122.15	-122.17	-122.20	-122.20	-122.16	-122.04	-122.21	-122.22	-122.19	-122.25	-122.21
Latitude	44.60	44.57	45.85	45.80	45.79	45.79	45.79	45.78	45.79	45.716	45.723	44.873	44.851
(wt.% oxides)													
SiO_2	57.25	65.10	59.64	56.27	58.62	76.32	53.31	65.31	67.73	68.84	60.17	66.06	64.40
TiO_2	1.00	0.92	0.87	0.92	0.80	0.24	1.33	0.63	0.47	0.51	1.09	0.58	0.58
Al_2O_3	15.63	13.94	15.78	18.82	16.44	12.09	16.99	14.38	13.34	14.42	16.08	14.23	14.70
FeO*	5.84	5.44	7.18	6.72	6.43	2.01	8.54	5.66	4.14	4.09	6.87	4.40	4.66
MnO	0.10	0.12	0.11	0.11	0.14	0.08	0.17	0.18	0.18	0.04	0.11	0.08	0.26
MgO	2.94	2.11	3.22	2.75	3.76	0.48	5.44	2.54	1.97	1.77	3.66	1.94	2.26
CaO	7.44	1.05	5.71	8.45	6.69	1.61	8.79	4.73	3.79	4.17	7.35	4.04	5.02
Na_2O	3.30	5.85	3.68	4.02	3.92	3.32	3.50	3.95	3.55	3.73	3.22	3.88	3.26
K_2O	0.35	0.37	1.01	0.63	1.06	4.34	0.58	2.36	3.02	2.48	1.34	2.31	1.08
P_2O5	0.21	0.29	0.17	0.14	0.13	0.03	0.16	0.19	0.15	0.09	0.22	0.11	0.12
total_I	94.06	95.19	97.36	98.82	98.00	100.51	98.81	99.94	98.35	100.15	100.10	97.64	96.34
(ppm)													
Ba	230	130	200	270	420	580	200	480	530	460	380	480	350
La	10.00	11.80	13.70	6.20	9.60	26.60	10.10	19.20	17.20	21.90	17.90	20.30	13.30
Ce	24.80	30.80	36.20	16.55	25.20	55.80	26.10	46.90	38.60	46.70	43.90	46.80	32.30
Rb	2.40	4.30	22.50	5.30	10.20	99.40	7.90	56.70	60.10	51.50	14.00	50.90	22.50
Sr	639	366	369	556	493	155	506	341	327	367	495	363	538
Y	15.30	16.80	17.20	12.00	13.10	12.50	17.80	22.60	14.20	13.70	21.90	16.60	11.50
Zr	92.80	80.90	6.60	11.60	5.70	5.90	115.50	4.10	4.70	3.90	148.50	23.80	16.90
Nb	6.20	7.80	8.00	4.30	5.40	7.40	7.40	8.40	7.60	8.20	9.00	7.90	5.90
Co	25.70	15.20	23.30	22.20	22.70	4.10	33.50	14.20	10.60	13.90	25.90	12.30	14.20
Cr	25.00	19.00	45.00	29.00	73.00	17.00	94.00	57.00	48.00	27.00	65.00	37.00	29.00
Ni	44.70	9.20	32.30	27.70	42.30	7.30	63.60	30.40	25.20	23.10	42.70	26.20	20.50
Sc	16.50	17.30	16.60	18.80	17.00	4.00	27.60	13.50	9.40	9.50	19.70	11.20	12.00
V	154	98	129	170	142	20	218	99	62	73	157	77	87
Ag	0.06	0.04	0.02	0.05	0.05	0.06	0.07	0.10	0.10	0.04	0.07	0.05	0.48
Cu	17.70	33.20	50.10	91.10	71.30	37.80	55.00	220.00	133.50	83.80	94.90	37.50	50.00
Mo	0.42	0.85	2.53	2.04	1.22	2.10	1.52	3.24	2.70	1.66	2.55	2.52	2.54
Pb	7.80	16.40	3.80	5.00	6.20	11.60	3.80	10.00	8.80	6.00	9.80	5.70	30.80
Zn	83.00	83.00	30.00	85.00	60.00	18.00	96.00	47.00	28.00	21.00	88.00	62.00	820.00
As	4.10	2.10	15.70	15.70	9.10	6.20	4.80	19.40	9.20	7.20	12.50	4.00	15.30
Be	0.89	1.29	1.28	0.91	1.07	1.20	0.91	1.29	1.22	1.54	1.17	1.20	0.99
Bi	0.05	0.05	0.14	0.08	0.11	0.15	0.04	0.12	0.05	0.05	0.07	0.05	0.79
Cd	0.17	0.40	0.03	0.12	0.09	0.04	0.09	0.04	0.07	0.03	0.14	0.13	3.52
Cs	2.49	0.62	1.12	0.65	0.59	1.65	1.89	2.44	1.03	1.00	0.42	0.66	1.36
Ga	22.60	16.75	20.50	22.90	19.65	14.75	21.60	19.50	18.05	18.65	20.90	18.85	19.10
Ge	0.09	0.10	0.11	0.10	0.10	0.14	0.10	0.13	0.13	0.13	0.12	0.12	0.12
Hf	2.80	2.50	0.30	0.50	0.30	0.30	3.10	0.20	0.20	0.20	4.10	1.00	0.70
In	0.04	0.06	0.09	0.05	0.09	0.03	0.06	0.04	0.04	0.04	0.06	0.04	0.05
Li	39.90	20.70	3.60	15.20	9.10	6.70	8.00	12.20	14.00	12.00	8.10	10.10	18.30
Mn	804	947	842	881	1080	639	1340	1420	1360	316	815	609	2020
Re	<0.002	<0.002	<0.002	<0.002	<0.002	<0.002	<0.002	<0.002	<0.002	<0.002	<0.002	<0.002	<0.002
S	<0.01	<0.01	0.03	0.04	<0.01	<0.01	0.04	0.01	0.02	0.02	<0.01	<0.01	0.72
Sb	1.10	1.40	1.05	0.76	1.37	0.59	0.23	0.96	0.53	0.51	0.88	0.68	4.37
Se	1.00	1.00	1.00	1.00	1.00	<1	1.00	1.00	1.00	1.00	1.00	1.00	1.00
Sn	0.80	1.80	1.80	1.70	1.40	1.30	1.00	3.30	2.50	1.30	1.20	1.30	0.90
Ta	0.48	0.51	0.51	0.28	0.38	0.69	0.48	0.57	0.62	0.70	0.58	0.59	0.46
Te	<0.05	<0.05	<0.05	<0.05	<0.05	<0.05	<0.05	<0.05	<0.05	<0.05	<0.05	<0.05	0.17
Th	1.20	1.40	3.90	0.90	2.50	13.10	1.40	7.70	10.00	7.90	5.30	4.40	3.30
Tl	0.07	0.11	0.39	0.06	0.35	0.38	0.09	0.33	0.27	0.25	0.44	0.30	0.34
U	0.40	0.60	0.60	0.50	0.80	1.80	0.50	2.50	2.80	2.90	3.10	1.10	1.10
W	26.90	16.00	0.40	0.70	0.30	0.50	0.20	1.00	0.90	0.40	0.70	0.40	0.40

Appendix Table 6 (continued). Whole Rock Four-Acid ICP-MS from ALS

Sample ID:	NS-5	NS-6	NS-7	NS-10	BO-1	QV-3	QV-6	QV-7	QV-8	BR-1	BR-2	BR-4	BO-3
Rock Name	Granodiorite	Diorite	Diorite	Diorite	Quartz monzonite	Diorite	Diorite	Granodiorite	Granite	Diorite	Granodiorite	Granodiorite	Quartz diorite
Longitude	-122.19	-122.17	-122.18	-122.22	-122.63	-122.29	-122.3	-122.28	-122.31	-122.32	-122.32	-122.32	-122.63
Latitude	44.85	44.858	44.854	44.844	43.597	44.601	44.594	44.562	44.519	44.246	44.235	44.23	43.609
(wt.% oxides)													
SiO_2	65.04	54.93	55.11	54.83	66.81	53.30	61.26	63.16	70.09	62.05	69.48	65.98	56.08
TiO_2	0.59	0.91	1.13	1.02	0.67	0.85	0.88	0.74	0.54	0.74	0.44	0.74	0.79
Al_2O_3	14.04	15.51	15.64	16.61	13.55	15.76	15.59	14.44	12.60	14.87	13.77	14.23	15.23
FeO*	4.79	7.85	7.41	7.46	4.40	6.75	5.44	5.42	3.05	5.06	3.11	4.25	7.04
MnO	0.08	0.12	0.13	0.17	0.10	0.14	0.09	0.09	0.06	0.10	0.07	0.07	0.16
MgO	1.46	3.37	3.33	4.18	1.64	5.32	2.17	3.23	0.90	3.05	1.29	1.86	4.26
CaO	5.82	6.07	6.17	7.81	4.28	7.58	4.65	4.83	2.28	5.25	3.60	3.72	7.22
Na_2O	3.36	3.69	3.91	3.40	3.67	3.24	4.15	3.41	3.83	3.69	2.94	3.50	3.30
K_2O	1.63	0.16	0.67	0.36	2.20	1.52	1.84	2.18	3.29	1.60	2.37	2.77	1.17
P_2O5	0.11	0.16	0.17	0.16	0.14	0.14	0.18	0.19	0.10	0.16	0.10	0.15	0.14
total_l	96.90	92.78	93.68	96.00	97.46	94.59	96.26	97.68	96.73	96.58	97.18	97.27	95.39
(ppm)													
Ba	550	100	320	220	600	120	370	400	710	360	540	590	340
La	20.10	9.20	6.20	9.20	18.70	5.60	13.30	14.50	26.30	10.20	13.90	14.00	8.50
Ce	40.60	23.00	17.40	24.60	43.80	14.55	32.30	36.70	61.30	27.40	33.90	36.80	23.20
Rb	31.00	0.80	3.60	1.60	56.40	18.50	32.40	42.50	79.90	23.20	57.60	52.20	16.60
Sr	386	618	474	704	314	615	510	412	222	555	440	494	426
Y	15.20	8.70	13.40	13.60	25.20	10.90	22.30	16.40	27.10	14.20	12.70	17.10	18.10
Zr	25.10	44.30	16.20	13.30	22.00	65.20	158.00	103.00	7.80	94.10	98.70	25.30	7.20
Nb	7.50	5.70	5.70	5.40	8.40	3.30	6.20	9.10	11.30	5.40	6.80	7.60	5.30
Co	10.30	24.30	22.00	24.40	11.30	33.10	19.20	33.90	23.90	16.70	8.00	15.10	24.10
Cr	19.00	50.00	41.00	40.00	131.00	85.00	15.00	57.00	10.00	69.00	30.00	86.00	86.00
Ni	12.70	36.60	16.60	22.80	10.20	61.50	6.70	37.20	7.40	28.20	8.60	28.90	37.30
Sc	13.50	16.40	18.80	22.20	14.20	22.50	18.70	16.30	8.50	16.00	7.50	13.60	24.70
V	102	135	138	187	91	189	124	106	45	121	54	106	173
Ag	0.05	0.22	0.21	0.20	0.11	0.97	0.07	0.17	0.04	0.05	0.03	0.06	0.11
Cu	22.40	591.00	147.50	110.50	68.00	96.90	35.80	71.20	20.30	44.90	13.20	88.30	46.40
Mo	3.78	2.37	3.10	1.82	5.25	0.53	0.75	0.83	1.16	0.71	0.39	1.46	0.51
Pb	9.90	6.70	5.30	14.80	20.30	13.40	7.10	10.10	10.30	6.40	7.40	4.90	21.30
Zn	62.00	145.00	96.00	370.00	81.00	149.00	68.00	91.00	31.00	68.00	46.00	41.00	111.00
As	7.30	9.60	9.90	4.80	7.80	40.20	12.10	7.80	2.50	4.90	4.40	7.20	18.70
Be	0.97	0.84	0.84	0.76	1.13	0.69	1.22	1.27	1.59	1.00	1.19	1.03	0.80
Bi	0.03	0.06	0.04	0.15	0.19	0.03	0.03	0.02	0.07	0.01	0.04	0.09	0.04
Cd	0.26	0.08	0.09	0.60	0.06	0.56	0.37	1.12	0.70	0.12	0.04	0.09	0.13
Cs	0.36	0.12	0.34	0.29	2.79	2.26	1.79	1.69	1.80	3.10	1.10	0.80	0.78
Ga	18.80	20.00	21.50	22.00	17.50	19.15	21.60	20.30	17.00	19.80	17.10	17.35	18.60
Ge	0.11	0.09	0.09	0.09	0.12	0.08	0.10	0.12	0.14	0.12	0.13	0.13	0.11
Hf	0.80	1.30	0.70	0.60	0.90	1.90	4.40	3.10	0.50	2.80	3.00	1.00	0.40
In	0.03	0.12	0.06	0.16	0.04	0.04	0.05	0.05	0.04	0.04	0.02	0.07	0.06
Li	11.90	19.90	16.50	8.90	7.90	32.30	34.20	30.50	11.70	18.00	30.80	20.70	10.40
Mn	593	953	972	1320	797	1070	659	723	447	796	521	518	1270
Re	<0.002	<0.002	0.00	<0.002	<0.002	<0.002	<0.002	<0.002	<0.002	<0.002	<0.002	0.00	<0.002
S	0.01	<0.01	0.07	0.01	0.01	0.02	0.03	0.21	0.04	<0.01	<0.01	<0.01	<0.01
Sb	1.68	0.84	0.57	1.69	0.97	5.61	0.87	1.57	0.22	1.17	1.55	1.14	1.12
Se	1.00	1.00	1.00	1.00	<1	1.00	1.00	1.00	1.00	1.00	<1	1.00	<1
Sn	1.60	1.10	1.10	0.80	3.50	2.50	1.30	2.90	1.50	1.00	1.00	1.70	1.40
Ta	0.61	0.36	0.35	0.35	0.61	0.35	0.60	1.06	1.26	0.36	0.55	0.52	0.36
Te	<0.05	<0.05	<0.05	<0.05	<0.05	<0.05	<0.05	<0.05	<0.05	<0.05	<0.05	<0.05	<0.05
Th	7.40	0.80	0.50	1.20	6.70	0.60	4.10	3.10	8.60	1.50	4.60	2.20	2.10
Tl	0.28	0.03	0.13	0.09	0.29	0.61	0.26	0.43	0.34	0.40	0.55	0.45	0.29
U	1.80	1.30	0.60	0.60	1.60	0.30	1.50	0.90	1.80	1.30	1.70	1.20	0.60
W	0.40	0.20	0.20	0.30	1.30	41.90	42.20	129.00	115.50	0.60	0.40	0.40	0.40

Appendix Table 6 (continued). Whole Rock Four-Acid ICP-MS from ALS

Sample ID:	BO-4	BO-5	BO-6	BO-8	BO-9	BO-10	BO-11	BO-12	BO-13	BO-14	BO-15	BO-16	BO-17
Rock Name	Granodiorite	Quartz diorite	Quartz diorite	Quartz diorite	Quartz diorite	Quartz diorite	Quartz diorite	Quartz diorite	Quartz diorite	Quartz diorite	Quartz diorite	Quartz diorite	Quartz diorite
Longitude	-122.63	-122.64	-122.63	-122.64	-122.63	-122.63	-122.63	-122.64	-122.64	-122.64	-122.65	-122.65	-122.64
Latitude	43.604	43.593	43.588	43.584	43.581	43.58	43.58	43.579	43.58	43.577	43.576	43.574	43.573
(wt.% oxides)													
SiO_2	71.33	61.92	64.21	61.51	63.98	64.85	63.69	60.91	65.17	61.35	61.51	66.57	60.35
TiO_2	0.50	0.70	0.71	0.83	0.74	0.76	0.80	0.87	0.63	0.78	0.74	0.64	0.81
Al_2O_3	13.34	13.72	13.81	14.28	14.49	14.66	14.96	14.36	13.15	13.68	14.19	13.38	14.21
FeO*	3.62	5.87	5.16	6.24	5.62	5.25	5.76	6.46	4.80	5.93	5.54	4.84	6.20
MnO	0.02	0.11	0.11	0.25	0.10	0.09	0.12	0.11	0.13	0.23	0.11	0.08	0.06
MgO	0.96	3.76	2.42	2.97	2.65	2.24	2.57	3.40	2.17	3.28	2.98	1.96	3.88
CaO	4.09	5.41	4.81	4.72	4.18	4.62	5.19	5.53	3.61	5.12	4.70	3.67	4.41
Na_2O	3.17	2.80	2.94	3.11	3.02	3.81	3.76	3.34	3.29	2.49	3.13	3.26	2.93
K_2O	1.04	1.59	1.65	2.76	1.99	2.24	1.95	1.66	2.40	2.47	2.13	2.61	1.70
P_2O5	0.19	0.15	0.14	0.17	0.15	0.17	0.17	0.20	0.14	0.16	0.14	0.13	0.14
total_l	98.25	96.03	95.96	96.85	96.93	98.70	98.98	96.84	95.48	95.50	95.19	97.12	94.69
(ppm)													
Ba	200	540	590	680	600	590	520	470	550	630	490	540	210
La	13.30	12.00	15.00	12.40	14.90	17.10	13.60	12.70	16.30	13.30	12.50	17.50	10.30
Ce	41.50	32.00	38.00	31.80	35.30	41.00	35.00	33.40	35.40	30.00	29.20	38.10	24.70
Rb	29.40	21.90	25.60	57.90	35.70	52.10	37.20	23.70	54.20	40.60	43.20	60.40	29.50
Sr	337	439	358	401	356	366	391	483	307	343	400	313	371
Y	26.40	17.90	20.00	18.10	20.30	21.30	19.60	17.10	19.30	17.60	16.80	20.30	15.50
Zr	3.10	16.60	10.70	44.20	40.90	27.60	24.70	48.20	40.10	36.30	36.90	45.90	39.70
Nb	5.80	5.90	7.40	6.30	6.90	7.70	7.10	6.60	6.70	6.00	5.80	7.10	5.20
Co	5.70	18.50	15.40	19.60	16.70	15.90	16.30	18.30	14.80	18.90	18.20	10.30	20.60
Cr	79.00	186.00	82.00	61.00	71.00	71.00	87.00	80.00	66.00	78.00	58.00	79.00	68.00
Ni	4.30	54.00	15.30	15.00	18.10	13.50	15.70	12.40	17.30	17.00	23.30	14.70	32.10
Sc	12.10	19.10	17.00	19.30	18.40	15.70	16.90	23.00	13.80	20.70	16.30	13.20	18.50
V	60	136	120	153	127	111	135	171	101	157	129	97	157
Ag	0.06	0.04	0.02	0.32	0.06	0.03	0.13	0.10	0.05	0.10	0.07	0.06	0.03
Cu	139.00	20.60	21.50	36.50	29.00	27.60	32.10	25.90	12.90	22.30	32.60	23.00	33.60
Mo	37.30	1.23	1.14	1.14	0.61	1.19	1.11	0.95	0.88	0.52	0.59	0.74	0.65
Pb	15.30	21.80	7.00	45.50	7.20	6.40	22.20	7.90	10.50	91.40	6.30	8.20	4.20
Zn	67.00	79.00	73.00	189.00	143.00	45.00	97.00	71.00	92.00	343.00	62.00	41.00	24.00
As	4.20	19.20	13.20	30.00	16.10	21.10	15.90	8.30	12.30	52.00	43.60	29.00	40.50
Be	1.20	0.78	0.98	0.96	1.00	0.97	1.03	0.99	1.00	0.88	0.92	1.02	0.90
Bi	0.29	0.42	0.13	0.13	0.05	0.11	0.03	0.02	0.10	0.05	0.35	0.34	0.02
Cd	0.29	0.29	0.16	0.38	0.59	0.15	0.18	0.07	0.19	1.19	0.03	0.08	0.04
Cs	1.30	0.59	0.43	2.42	1.72	1.81	0.96	1.48	1.08	0.73	1.18	1.10	6.84
Ga	14.10	17.30	18.20	18.55	18.50	17.40	17.90	19.00	16.35	18.10	16.40	16.25	17.05
Ge	0.13	0.11	0.09	0.12	0.12	0.12	0.11	0.11	0.12	0.13	0.12	0.13	0.11
Hf	0.10	0.60	0.40	1.60	1.40	1.00	1.10	1.60	1.50	1.60	1.30	1.70	1.40
In	0.09	0.12	0.09	0.05	0.08	0.06	0.05	0.05	0.07	0.05	0.08	0.09	0.15
Li	15.30	33.00	11.80	26.90	29.90	16.80	20.90	26.70	24.80	31.10	18.10	21.50	40.30
Mn	142	862	832	1930	769	718	903	867	971	1780	887	587	474
Re	0.11	<0.002	<0.002	<0.002	<0.002	0.00	<0.002	<0.002	<0.002	<0.002	<0.002	<0.002	<0.002
S	0.90	<0.01	0.01	<0.01	<0.01	0.01	<0.01	<0.01	0.01	<0.01	<0.01	<0.01	<0.01
Sb	1.41	12.05	1.82	3.44	2.02	2.32	0.49	0.95	4.93	9.78	2.53	4.56	7.30
Se	1.00	1.00	1.00	<1	1.00	1.00	1.00	1.00	1.00	1.00	1.00	1.00	1.00
Sn	3.00	1.80	1.60	1.40	1.20	1.20	1.60	1.40	1.50	1.20	1.20	1.80	1.60
Ta	0.42	0.42	0.53	0.43	0.50	0.55	0.51	0.44	0.51	0.42	0.43	0.54	0.37
Te	<0.05	<0.05	<0.05	0.09	<0.05	<0.05	<0.05	<0.05	<0.05	<0.05	<0.05	<0.05	<0.05
Th	6.90	3.80	4.20	3.40	4.10	4.80	4.80	3.20	5.10	3.80	3.50	5.80	2.50
Tl	0.48	0.54	0.56	0.96	0.44	0.43	0.32	0.38	0.63	0.80	0.35	0.55	0.35
U	1.40	0.90	1.00	1.20	1.30	1.30	1.30	1.00	1.40	1.20	1.00	1.70	0.80
W	1.20	1.00	0.70	0.70	0.70	0.80	0.70	0.50	0.70	0.90	0.60	0.80	0.50

Appendix Table 6 (continued). Whole Rock Four-Acid ICP-MS from ALS

Sample ID:	BO-18	BO-20	BO-21
Rock Name	Quartz diorite	Quartz diorite	Quartz diorite
Longitude	-122.65	-122.63	-122.62
Latitude	43.572	43.586	43.586
(wt.% oxides)			
SiO_2	52.04	63.93	58.13
TiO_2	1.12	0.75	0.82
Al_2O_3	16.27	13.59	14.81
FeO*	8.36	5.20	6.68
MnO	0.15	0.10	0.12
MgO	4.58	2.01	3.98
CaO	8.76	4.60	6.30
Na_2O	2.95	3.65	3.32
K_2O	0.90	1.64	1.14
P_2O5	0.22	0.17	0.14
total_l	95.35	95.63	95.45
(ppm)			
Ba	340	430	330
La	11.50	17.50	8.40
Ce	27.20	36.50	20.20
Rb	5.30	35.40	16.40
Sr	814	335	505
Y	14.70	21.40	13.50
Zr	65.20	49.60	42.20
Nb	3.70	7.40	4.40
Co	26.20	13.70	23.10
Cr	52.00	62.00	80.00
Ni	5.60	11.20	23.90
Sc	28.60	15.60	23.00
V	261	123	175
Ag	0.05	0.09	0.05
Cu	21.40	27.00	63.40
Mo	0.47	0.65	0.53
Pb	7.10	9.10	8.20
Zn	97.00	78.00	78.00
As	7.90	16.60	8.70
Be	0.86	0.98	0.69
Bi	0.02	0.02	0.02
Cd	0.13	0.09	0.12
Cs	0.70	0.63	2.18
Ga	20.30	17.45	16.20
Ge	0.11	0.12	0.09
Hf	2.00	1.80	1.70
In	0.06	0.05	0.04
Li	29.10	20.80	13.00
Mn	1180	771	950
Re	<0.002	<0.002	<0.002
S	<0.01	<0.01	<0.01
Sb	0.96	3.46	0.77
Se	1.00	1.00	1.00
Sn	1.00	1.40	1.20
Ta	0.22	0.53	0.33
Te	<0.05	<0.05	<0.05
Th	2.70	3.80	1.70
Tl	0.16	0.43	0.22
U	0.90	1.30	0.70
W	0.20	0.80	0.40

Appendix 7. Zircon Geochemistry

7.1 Ti-in-zircon Thermometry (for all analyses) Related to Petrogenesis

Variations in Ti-in-zircon temperatures also help us distinguish unique characteristics of the Western Cascade magmas. Temperatures range from 675 to 950 °C. There are no obvious trends in temperature with respect to Hf. We would expect to see temperatures decrease with increasing Hf, which is a proxy for magma differentiation (Claiborne et al., 2010; Lee 2008). The lack of trends is likely due to the lack of precision and accuracy in measuring Ti by laser ablation, but could also be related to magma chamber processes.

Within each sample, the range of temperatures calculated by Ti concentrations tend to be approximately 100° C with the exception of the Spirit Lake Pluton sample analyzed by LA-ICP-MS, the Washougal district samples, and the Nimrod Stock, suggesting that generally zircon crystallization is restricted to small temperature ranges within a given magma chamber. It is possible that zircon crystallization is short-lived, or controversially, these magmas cool slowly and linger at temperatures ideal for zircon crystallization for longer periods of time. Possibly the Nimrod Stock and the Spirit Lake Pluton have longer-lived zircon crystallization histories or have inherited zircons with Ti concentrations distinct from the rest of their zircon populations. Zircons from samples with the samples with porphyry textures as demonstrated by phenocrysts set in a fine-grained (<0.2 mm) aplitic to micrograniticgroundmass (the North Fork mafic latite porphyry, the North Santiam dikes and the Boulder Creek dike from Quartzville) are restricted to the lowest Ti-in-zircon temperatures (< 800° C), which suggest that these porphyries are the lowest temperature magmas in the Western Cascades.

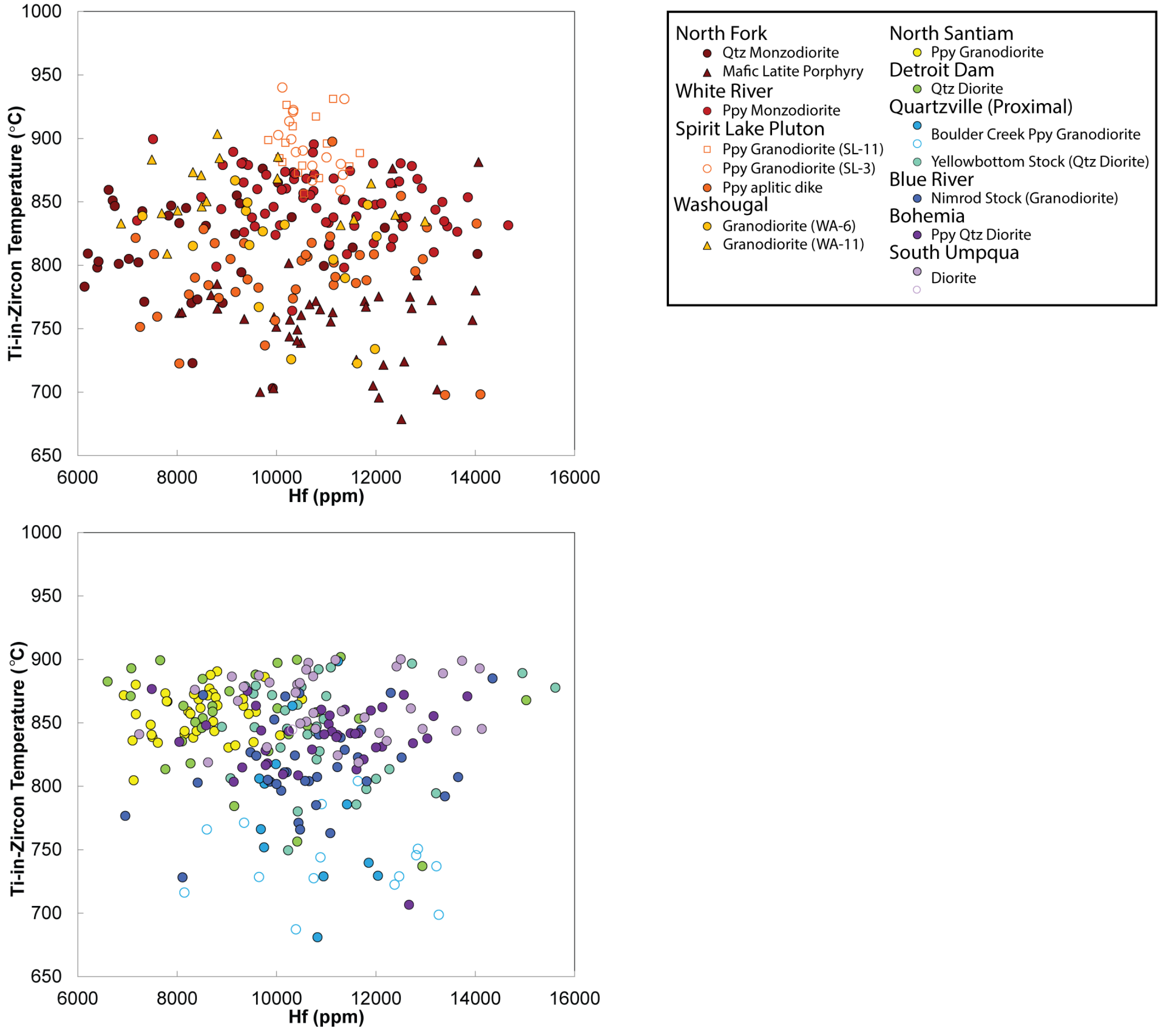

Appendix Figure 6: All Ti-in-zircon temperatures displayed for Washington (top) and Oregon (bottom) districts.

Appendix Table 7. Zircon Trace Element Spot Analyses from SUMAC SHRIMP-RG

Spot ID	Note	Ti (48) ppm	Ti (49) ppm	Fe (56) ppm	Y (89) ppm	La (139) ppm	Ce (140) ppm	Nd (146) ppm	Sm (147) ppm	Eu (153) ppm	Gd (155) ppm	Dy (179) ppm	Er (182) ppm	Yb (188) ppm	Hf (194) ppm	U (254) ppm	Th (248) ppm
WCOS-SL11-6.1		37.15	36.84	0.18	1683	0.047	11.64	2.88	5.67	1.28	48.5	181	288	446	11,138	164	122
WCOS-SL11-1.1		31.43	31.69	0.13	1836	0.105	12.35	3.22	5.97	1.24	51.2	190	307	476	10,326	198	149
WCOS-SL11-3.1		28.79	29.37	0.36	1792	0.090	13.37	3.51	6.21	1.31	48.7	185	308	472	9,830	220	158
WCOS-SL11-2.1		24.42	24.81	32.56	837	0.062	9.29	0.86	2.55	0.57	23.0	88	146	239	10,517	97	57
WCOS-SL11-4.2		23.29	23.54	0.20	1837	0.045	13.21	3.25	6.29	1.37	55.5	198	314	483	10,431	213	153
WCOS-SL11-4.1		22.48	23.14	0.56	2,058	0.060	15.24	3.30	6.41	1.22	55.1	212	349	541	10,855	283	207
WCOS-SL11-10.1		28.18	28.37	0.29	1,524	0.078	12.95	3.42	6.05	1.23	44.6	158	262	410	11,013	188	122
WCOS-SL11-11.1		24.30	24.20	0.11	1,183	0.014	12.39	1.35	3.26	0.76	32.0	126	199	304	11,465	141	96
WCOS-SL11-12.1		26.51	25.97	8.07	570	0.018	9.83	0.34	1.22	0.26	12.3	55	99	182	11,676	98	46
WCOS-SL11-14.1		24.98	25.32	0.15	616	0.004	8.59	0.48	1.37	0.35	13.5	59	107	191	10,117	104	47
WCOS-SL11-8.1		28.32	28.76	0.12	691	0.020	8.48	0.77	1.84	0.41	16.8	68	120	209	10,177	95	49
WCOS-SL11-15.1		20.23	20.37	0.13	1,126	0.011	9.31	1.05	3.42	0.87	33.2	120	189	286	10,552	139	80
WCOS-SL11-9.1		33.34	33.43	0.12	1,584	0.052	11.58	3.52	6.37	1.22	46.4	166	268	421	10,793	177	124
WCOS-SL11-7.1		35.83	36.57	0.34	3,164	0.109	16.99	4.06	7.41	1.68	78.5	317	531	788	10,202	432	383
WCOS-SL11-13.1		25.64	26.15	0.14	2,521	0.074	15.95	3.63	6.96	1.49	67.7	257	433	643	10,057	365	285
WCOS-SL3-3.1		25.76	26.10	0.31	449	0.009	6.65	0.29	0.83	0.27	9.1	42	80	143	11,005	73	30
WCOS-SL3-4.1		26.66	27.36	0.36	930	0.014	7.33	0.78	2.40	0.65	24.4	98	157	247	10,390	103	60
WCOS-SL3-1.1		24.37	24.80	2.84	675	0.072	6.47	0.67	2.07	0.48	17.7	69	116	192	10,721	87	43
WCOS-SL3-5.1		24.69	24.59	0.34	730	0.012	6.95	0.41	1.53	0.38	17.1	71	129	216	11,294	95	49
WCOS-SL3-12.1		32.37	32.53	1.54	490	0.018	8.09	0.56	1.27	0.28	11.5	47	86	144	10,257	85	41
WCOS-SL3-13.1		29.72	29.84	0.42	978	0.020	7.45	1.72	4.01	0.96	32.8	106	166	256	10,034	101	62
WCOS-SL3-9.1		34.72	35.16	0.57	3,951	0.125	22.52	4.31	11.08	2.96	116.5	422	661	996	10,337	638	627
WCOS-SL3-2.1		28.93	29.32	0.28	1,603	0.080	11.01	2.62	5.14	1.24	46.8	168	273	409	10,298	256	179
WCOS-SL3-10.1		22.97	23.20	2.11	2,030	0.045	18.90	3.22	6.69	1.21	54.2	208	337	512	11,337	306	237
WCOS-SL3-11.1		20.69	20.93	0.26	1,901	0.066	20.26	3.49	6.75	1.04	51.6	189	309	469	11,283	320	229
WCOS-SL3-14.1		37.09	37.04	1.14	2,861	0.119	14.90	4.82	8.64	2.28	84.6	315	491	746	11,365	374	290
WCOS-SL3-7.1		26.91	27.32	1.92	1,736	0.047	15.65	3.50	6.85	1.20	52.0	187	289	430	10,531	232	180
WCOS-SL3-8.1		22.10	22.38	0.88	788	0.016	6.55	0.61	1.89	0.53	20.0	79	135	222	10,721	97	50
WCOS-SL3-15.1		34.35	34.35	1.28	1,724	0.129	10.82	3.87	6.85	1.38	52.6	191	297	451	10,333	207	141
WCOS-SL3-6.1		39.72	40.00	0.86	3,326	0.105	15.98	4.08	7.41	1.66	82.3	332	549	801	10,117	459	432
WCOS-2-2.1	Inclusion	5.06	4.78	14.24	1,966	11.412	56.79	9.27	9.13	1.96	61.4	202	333	568	8,146	417	364
WCOS-2-9.1		5.74	5.76	4.33	1,030	0.070	19.21	0.48	1.44	0.29	16.2	85	192	411	10,748	333	132
WCOS-2-11.1	Inclusion	9.10	9.13	11.98	2,386	4.133	55.16	4.31	6.83	1.27	57.8	229	414	717	9,348	708	654
WCOS-2-15.1	Inclusion	8.63	8.66	6.65	659	3.476	12.58	1.70	1.36	0.39	12.8	60	120	232	8,598	105	42
WCOS-2-13.1		3.61	3.55	3.51	1,145	0.073	25.47	0.54	1.58	0.27	16.4	93	216	456	10,391	531	210
WCOS-2-3.1		5.80	5.84	0.93	1,653	0.238	21.40	1.85	4.53	1.08	39.7	161	296	525	9,647	323	197
WCOS-2-5.1		4.14	4.18	5.98	1,252	0.021	34.11	0.57	1.80	0.33	19.1	107	237	491	13,265	588	268
WCOS-2-4.1		6.98	6.99	0.39	1,529	0.024	32.58	0.83	2.11	0.52	25.6	134	287	587	12,810	488	255
WCOS-2-6.1		6.36	6.31	12.68	1,317	0.304	31.30	0.62	1.80	0.35	20.6	113	252	517	13,217	546	256
WCOS-2-1.1		5.42	5.52	0.80	2,846	0.048	79.51	1.50	4.79	0.40	49.8	254	513	1,007	12,375	1,707	1,010
WCOS-2-10.1		10.54	10.77	8.01	791	0.592	11.73	0.82	1.23	0.40	14.1	71	148	301	10,908	130	47
WCOS-2-12.1	Inherited	5.83	5.84	2.43	993	0.039	17.48	0.51	1.49	0.35	16.7	85	184	369	12,467	258	114
WCOS-2-8.1	Inherited	6.86	6.78	0.92	918	0.102	16.70	0.53	1.48	0.39	16.1	80	170	346	10,884	248	106
WCOS-2-14.1	Inherited	12.58	12.46	25.02	4,767	0.803	100.87	3.46	7.67	0.43	83.9	423	845	1,640	11,636	2,448	1,675
WCOS-2-7.1	Inherited	7.36	7.30	0.33	3,169	0.021	103.11	1.94	6.45	1.11	65.9	302	567	1,070	12,845	2,003	1,877
WCOSNU-11-1		18.24	18.53	0.19	3,335	0.108	17.94	4.29	9.68	1.92	94.4	347	568	861	10,316	530	382

Appendix Table 8. Zircon Trace Element Spot Analyses from OSU - LA-ICP-MS

Spot ID	Note	P (31) ppm	Y (89) ppm	Nb (93) ppm	La (139) ppm	Ce (140) ppm	Pr (141) ppm	Nd (146) ppm	Sm (147) ppm	Eu (153) ppm	Gd (157) ppm	Tb (159) ppm	Dy (163) ppm	Ho (165) ppm	Er (166) ppm	Tm (169) ppm	Yb (172) ppm	Lu (175) ppm	Hf (179) ppm	Th (232) ppm	U (238) ppm
WCOS-2-1		248	2571	4.0	0.40	17.2	0.23	0.97	3.08	0.59	30	11.2	151	65	361	71	549	135	12,962	246	325
WCOS-2-2	Inclusion	700	802.2	3.1	9.00	26.5	2.54	7.03	2.74	0.37	15	4.1	55	24	110	27	248	43	7,581	50	163
WCOS-2-3	Inclusion	1238	1550	5.9	14.42	46.9	4.54	7.35	4.47	0.58	24	7.9	112	43	212	51	504	74	9,430	230	457
WCOS-2-4	Inherited	491	1151	2.8	0.76	12.8	0.19	1.74	1.58	0.42	16	6.9	72	31	163	37	356	54	8,284	75	247
WCOS-2-5	Inclusion	4366	1421	8.2	60.43	136.7	17.19	36.29	10.92	0.90	34	8.7	103	42	206	47	400	74	10,279	308	540
WCOS-2-6		273	1,329	4.4	0.17	17.0	0.06	0.39	1.61	0.35	16	6.5	90	35	178	43	388	76	10,685	153	363
WCOS-2-7	Inclusion	981	1,607	6.1	9.23	37.9	2.14	5.67	2.64	0.45	24	9.7	113	46	250	59	490	87	10,284	239	484
WCOS-2-8	Inherited	429	4,074	7.5	No_Data	44.1	0.20	2.58	6.93	0.82	64	22.8	268	102	534	112	886	165	12,969	561	795
WCOS-2-9	Inherited	308	2,056	5.0	0.43	22.2	0.24	1.15	3.13	0.42	29	10.8	144	51	293	61	500	88	10,908	290	427
WCOS-2-10	Inclusion	758	3,230	5.2	7.12	36.6	1.44	4.41	4.53	0.84	46	14.6	216	90	486	96	769	203	19,858	427	521
WCOS-2-11	Inclusion	1375	1,698	8.2	14.73	54.5	5.32	11.17	5.57	0.47	29	7.5	97	41	236	50	436	76	11,545	358	691
WCOS-2-12		566	1,921	19.0	2.45	33.7	0.65	2.59	4.05	0.49	28	10.7	130	52	251	54	491	87	8,885	455	554
WCOS-2-13	Inclusion	2221	1,188	3.1	34.92	117.2	8.42	20.79	6.80	1.21	28	9.8	88	34	163	34	304	56	8,187	79	150
WCOS-2-14		453	1,648	7.2	2.58	28.6	0.80	1.76	2.93	0.43	29	8.2	128	45	279	54	511	87	11,436	347	516
WCOS-2-15		205	1,273	2.8	No_Data	12.0	No_Data	0.09	1.49	0.49	18	7.4	97	34	176	40	371	67	10,947	152	232
WCOS-2-16		548	1,941	3.3	3.69	33.7	1.33	6.20	7.90	1.80	51	15.1	178	60	259	53	448	63	9,432	139	172
WCOS-2-17		264	1,259	2.4	No_Data	10.2	0.02	0.48	1.80	0.63	20	7.3	85	37	174	45	400	69	9,758	87	198
WCOS-2-18		310	4,017	4.7	No_Data	25.4	No_Data	2.90	10.06	3.30	87	27.9	305	110	530	108	840	146	8,287	326	291
WCOS-2-19	Inclusion	5242	1,570	2.7	92.43	180.4	26.41	58.52	15.21	1.50	43	12.0	114	45	219	45	349	72	10,821	102	144
WCOS-2-20		515	2,327	7.7	5.24	26.9	1.41	3.42	5.47	1.28	40	12.7	164	66	308	68	552	97	9,260	202	260
WCOS-2-21	Inherited	352	1,816	2.4	0.90	13.6	0.48	1.80	4.35	1.07	37	13.0	141	54	257	55	405	80	11,417	117	167
WCOS-2-22		842	1,769	3.8	10.27	38.0	1.92	5.44	3.98	0.72	28	10.3	119	47	239	54	426	87	11,817	183	280
WCOS-2-23		309	2,221	6.6	No_Data	30.1	0.07	1.57	4.67	1.30	39	14.9	165	61	289	66	536	95	9,653	566	364
WCOS-2-24		193	1,102	2.1	No_Data	8.0	No_Data	0.36	1.51	0.52	16	5.6	72	29	153	36	293	59	9,685	50	101
WCOS-2-25	Inclusion	182	1,353	1.8	0.63	8.6	0.14	1.24	2.28	1.09	30	9.9	114	41	196	41	354	60	9,749	60	117
WCOS-2-26	Inclusion	4893	1,698	3.3	57.82	143.8	17.43	43.45	13.19	1.49	44	14.2	135	51	239	50	443	83	10,285	141	291
WCOS-2-27	Inclusion	5442	2,057	7.3	120.18	279.1	31.53	77.71	21.30	2.05	56	14.7	150	60	275	52	542	82	10,695	1079	822
WCOS-2-28		351	2,058	7.6	3.23	29.2	0.90	3.10	2.74	0.51	29	11.6	139	57	289	60	536	105	11,237	242	380
WCOS-2-29		253	1,285	3.4	No_Data	14.0	0.04	0.53	1.92	0.38	19	7.3	82	37	190	39	368	66	11,799	149	237
WCOS-2-30		294	968	2.9	0.98	15.3	0.18	0.75	1.34	0.22	13	5.3	74	29	141	32	255	52	11,854	115	234
WCOS-2-31	Inclusion	1775	7,897	7.7	19.11	82.5	5.41	17.55	24.44	6.47	171	53.7	592	229	1075	227	1681	335	9,350	1466	1633
WCOS-2-32		341	3,159	16.7	No_Data	37.8	No_Data	BDL	6.50	1.81	57	19.4	252	104	454	101	919	140	9,581	466	936
WCOS-2-33		287	3,619	8.2	No_Data	27.5	No_Data	BDL	6.71	3.18	70	24.0	276	109	494	102	853	160	9,987	384	616

Appendix Table 8 (continued). Zircon Trace Element Spot Analyses from OSU - LA-ICP-MS

Spot ID	Note	P (31) ppm	Y (89) ppm	Nb (93) ppm	La (139) ppm	Ce (140) ppm	Pr (141) ppm	Nd (146) ppm	Sm (147) ppm	Eu (153) ppm	Gd (157) ppm	Tb (159) ppm	Dy (163) ppm	Ho (165) ppm	Er (166) ppm	Tm (169) ppm	Yb (172) ppm	Lu (175) ppm	Hf (179) ppm	Th (232) ppm	U (238) ppm
WCOS-2-34	Inclusion	2039	5,192	18.9	21.61	124.4	6.66	19.15	15.31	1.83	113	34.3	395	148	679	134	1029	184	10,314	1138	991
WCOS-2-35		525	1,225	2.2	5.77	17.3	1.22	3.31	3.08	0.71	23	7.4	93	32	160	38	284	55	9,732	70	144
WCOS-2-36		97	1,974	4.1	No_Data	8.2	No_Data	BDL	4.75	1.42	42	13.6	170	64	314	73	685	112	10,320	259	443
WCOS-2-37		326	2,376	5.1	No_Data	15.0	No_Data	1.14	3.73	1.05	40	13.0	162	72	307	73	608	101	8,894	220	292
WCOS-2-38		302	1,573	2.1	No_Data	11.3	0.06	0.73	2.42	0.57	26	9.5	122	49	221	54	403	75	12,040	115	220
WCOS-2-39	Inclusion	858	1,746	6.8	14.47	53.2	3.66	8.15	5.16	0.68	33	12.2	143	56	280	56	575	82	10,881	223	422
WCOS-2-40		246	1,295	4.9	No_Data	14.4	0.05	0.48	1.67	0.38	18	7.1	95	37	199	45	404	75	10,825	108	244
WCOS-12-1		416	5,603	4.0	No_Data	25.0	0.55	5.47	12.82	2.79	148	40.6	476	169	703	140	939	187	11,233	436	247
WCOS-12-2		309	6,032	2.5	No_Data	18.3	0.46	4.13	10.45	3.02	133	39.0	481	176	850	138	955	197	9,052	416	234
WCOS-12-3	Inherited	350	4,709	3.3	No_Data	17.1	0.29	4.05	9.73	2.57	112	36.2	407	150	601	120	855	148	9,579	365	254
WCOS-12-5		149	1,590	1.4	No_Data	10.6	0.06	0.77	3.04	0.75	25	11.1	147	52	216	52	333	69	15,026	87	83
WCOS-12-6		230	1,596	1.1	No_Data	11.1	0.36	2.85	5.19	1.50	44	14.4	163	56	216	45	359	59	9,914	67	104
WCOS-12-7		314	4,326	2.4	0.31	21.8	0.31	4.64	11.76	2.05	104	30.3	370	132	529	110	653	151	8,941	227	165
WCOS-12-8		250	2,834	1.6	No_Data	13.7	0.18	2.36	7.43	1.38	65	21.5	244	85	370	68	437	95	10,796	138	114
WCOS-12-9		202	1,949	1.1	No_Data	10.9	0.20	2.25	5.97	1.26	50	15.9	164	60	241	48	356	66	8,495	111	99
WCOS-12-4		286	3,611	2.0	No_Data	19.1	0.45	3.43	8.18	2.30	86	26.2	304	109	455	86	587	124	12,935	194	128
WCOS-12-10		406	5,798	3.9	No_Data	19.1	0.44	3.81	11.76	2.71	140	45.2	486	174	745	131	929	186	10,348	396	237
WCOS-12-11		332	3,851	3.4	0.02	21.7	0.44	3.71	12.94	3.26	112	40.3	412	128	596	114	856	134	7,207	328	349
WCOS-12-12		362	5,676	2.9	0.07	20.0	0.54	4.11	10.07	2.81	132	37.6	466	159	660	123	844	179	10,017	380	244
WCOS-12-13		383	6,003	2.4	No_Data	19.8	0.39	4.87	12.73	2.85	131	41.2	478	168	790	140	939	203	10,418	384	247
WCOS-12-14		317	3,999	2.9	No_Data	14.7	0.42	3.96	9.31	1.74	90	28.4	352	128	525	96	678	136	7,762	304	254
WCOS-12-15		329	3,770	2.6	No_Data	17.0	0.30	4.09	9.22	2.25	95	27.9	321	114	538	97	730	121	8,708	230	207
WCOS-12-16		380	4,628	3.1	No_Data	17.2	0.45	3.90	11.03	2.17	112	35.3	348	127	566	112	732	130	8,977	290	269
WCOS-12-17		272	2,223	2.0	No_Data	12.2	0.14	2.30	4.98	1.14	53	17.4	205	74	321	62	440	86	9,495	165	139
WCOS-12-18		329	3,841	2.0	No_Data	15.0	0.49	3.68	9.74	2.22	94	31.0	343	125	540	102	658	125	8,513	252	196
WCOS-12-19		180	1,990	1.4	No_Data	10.4	0.14	2.18	6.16	1.31	48	16.3	180	63	276	51	395	74	10,622	79	92
WCOS-12-20		435	6,317	3.6	0.07	24.8	0.49	4.92	13.06	2.68	137	44.0	512	181	779	151	949	193	11,291	440	258
WCOS-12-21		171	1,802	0.9	No_Data	9.3	0.14	2.17	5.10	1.13	47	14.5	167	59	244	50	362	69	9,837	81	81
WCOS-12-22	Inherited	293	2,741	1.4	No_Data	11.3	0.20	2.56	7.64	1.58	65	22.2	260	84	328	68	518	82	7,066	146	155
WCOS-12-23	Inherited	246	2,373	1.0	No_Data	11.4	0.32	3.17	8.42	1.68	61	21.7	222	76	334	64	504	78	8,098	124	134
WCOS-12-24		292	2,194	2.2	No_Data	18.2	0.32	2.40	7.55	1.26	55	20.0	206	79	292	59	527	74	7,658	175	155
WCOS-12-25		149	1,146	0.5	No_Data	6.6	0.16	2.17	4.11	0.82	28	9.2	107	37	160	32	253	42	9,149	50	61

Appendix Table 8 (continued). Zircon Trace Element Spot Analyses from OSU - LA-ICP-MS

Spot ID	Note	P (31) ppm	Y (89) ppm	Nb (93) ppm	La (139) ppm	Ce (140) ppm	Pr (141) ppm	Nd (146) ppm	Sm (147) ppm	Eu (153) ppm	Gd (157) ppm	Tb (159) ppm	Dy (163) ppm	Ho (165) ppm	Er (166) ppm	Tm (169) ppm	Yb (172) ppm	Lu (175) ppm	Hf (179) ppm	Th (232) ppm	U (238) ppm
WCOS-12-26		235	2,354	2.2	No_Data	15.2	0.39	3.27	7.67	1.73	59	23.7	233	94	363	67	565	84	10,412	135	152
WCOS-12-27		298	3,586	0.9	No_Data	12.0	0.25	3.38	8.43	1.48	67	23.8	294	104	435	80	514	118	6,600	153	113
WCOS-12-28		425	5,336	3.6	No_Data	21.0	0.54	4.88	12.78	3.12	140	46.0	485	166	671	133	944	166	8,268	388	274
WCOS-12-29		318	1,382	0.9	No_Data	13.3	0.20	1.82	4.89	1.20	39	11.8	135	49	196	40	358	48	5,697	70	151
WCOS-12-30		381	5,386	3.9	0.08	17.7	0.37	4.09	10.88	2.78	132	42.5	498	178	722	131	914	174	8,125	411	268
WCOS-12-31		161	2,172	1.2	No_Data	11.5	0.25	2.99	7.11	1.24	55	18.2	218	72	272	58	409	73	8,516	121	103
WCOS-12-32		496	5,994	4.2	0.12	28.9	0.61	5.58	16.85	4.05	160	50.7	563	186	789	148	1122	189	8,713	436	330
WCOS-12-33		314	3,192	2.2	No_Data	16.0	0.33	3.24	8.65	1.82	78	26.3	289	103	417	85	642	112	8,238	214	189
WCOS-12-34		284	3,307	1.9	No_Data	14.7	0.21	2.48	7.73	1.65	70	24.1	285	101	452	87	599	127	11,661	197	132
WCOS-12-35		427	5,081	3.1	0.09	20.3	0.61	5.19	13.41	2.87	127	40.8	457	165	684	133	940	159	8,679	320	287
WCOS-12-36		378	3,555	1.9	No_Data	19.4	0.41	5.07	13.05	2.71	106	34.2	354	116	456	106	780	111	7,077	224	300
WCOS-12-37		172	1,734	0.6	No_Data	12.1	0.18	2.17	5.75	1.27	45	14.0	174	61	249	51	398	57	9,035	90	131
WCOS-12-38		302	2,627	1.9	No_Data	16.5	0.27	3.36	9.22	1.74	75	21.4	245	85	365	73	574	93	8,364	158	199
WCOS-12-39	Inherited	212	2,710	1.0	No_Data	16.0	0.42	3.53	9.38	1.72	66	21.8	267	89	386	72	530	105	10,244	135	116
WCOS-12-40	Inherited	222	2,984	1.1	No_Data	11.8	0.35	2.45	7.63	1.35	66	23.6	248	101	426	80	521	106	10,020	141	112
WCOS-7-1		279	2,175	5.1	0.46	27.0	0.50	2.04	2.80	0.54	36	12.8	169	74	380	70	533	150	20,907	340	326
WCOS-7-2		244	2,069	1.4	No_Data	10.6	0.33	3.05	5.47	1.38	47	18.3	184	70	322	58	361	89	9,911	122	115
WCOS-7-3		237	1,849	1.3	No_Data	11.3	0.15	2.46	3.63	0.91	37	13.4	149	62	289	53	377	88	10,212	121	131
WCOS-7-4		215	897	1.1	0.15	7.9	0.16	1.27	2.13	0.70	19	6.2	75	30	141	28	227	49	9,075	45	85
WCOS-7-5	Inherited	223	1,324	1.6	0.06	15.4	0.05	0.53	1.70	0.50	24	8.0	107	45	211	45	323	88	21,705	128	150
WCOS-7-6	Inherited	195	1,901	1.2	No_Data	10.6	0.27	3.17	5.19	1.37	39	15.2	161	63	292	55	414	81	9,558	116	135
WCOS-7-7		178	1,928	1.0	No_Data	13.7	No_Data	1.55	4.51	1.21	43	15.5	155	67	295	53	404	91	14,949	112	104
WCOS-7-8		272	1,216	0.7	0.51	10.8	0.18	1.57	4.42	1.07	29	9.8	115	40	180	36	261	57	12,004	66	104
WCOS-7-9		148	1,110	0.7	No_Data	7.9	0.01	1.40	3.32	0.86	21	7.6	100	36	162	34	252	51	10,427	53	64
WCOS-7-10	Inherited	154	1,311	0.5	No_Data	8.6	0.05	1.38	3.50	0.99	30	9.9	120	37	200	37	273	58	10,806	61	71
WCOS-7-11		203	1,408	0.6	No_Data	9.9	0.12	1.65	4.59	1.15	35	11.5	120	48	221	42	306	65	12,271	67	73
WCOS-7-12		172	1,633	0.7	No_Data	8.3	0.26	2.87	4.85	1.23	37	13.3	134	52	240	48	342	77	10,623	92	125
WCOS-7-13		177	1,121	0.7	No_Data	8.9	0.12	0.55	2.87	0.81	27	8.6	102	39	172	34	242	44	8,901	61	74
WCOS-7-14	Inherited	148	870	0.8	No_Data	8.4	0.01	0.48	2.24	0.48	18	5.4	80	35	131	31	248	44	11,809	38	77
WCOS-7-15		180	783	1.1	No_Data	6.2	0.08	0.16	1.67	0.40	14	4.8	56	23	112	26	207	41	9,853	34	74
WCOS-7-16		223	1,494	1.5	No_Data	9.5	0.29	2.17	4.22	0.99	29	11.8	122	47	206	43	311	69	10,790	78	117
WCOS-7-17		235	1,501	1.0	0.05	15.2	0.05	1.38	3.40	1.25	33	12.5	138	61	235	53	393	73	13,211	94	138

Appendix Table 8 (continued). Zircon Trace Element Spot Analyses from OSU - LA-ICP-MS

Spot ID	Note	P (31) ppm	Y (89) ppm	Nb (93) ppm	La (139) ppm	Ce (140) ppm	Pr (141) ppm	Nd (146) ppm	Sm (147) ppm	Eu (153) ppm	Gd (157) ppm	Tb (159) ppm	Dy (163) ppm	Ho (165) ppm	Er (166) ppm	Tm (169) ppm	Yb (172) ppm	Lu (175) ppm	Hf (179) ppm	Th (232) ppm	U (238) ppm
WCOS-7-18		189	1,489	1.1	No_Data	9.5	0.43	3.25	5.49	1.20	37	12.4	137	47	235	46	333	70	10,807	85	105
WCOS-7-19	Inherited	343	2,602	1.4	No_Data	13.1	0.42	3.92	7.96	1.87	56	21.1	230	89	395	71	527	107	10,421	165	147
WCOS-7-20	Inherited	110	346	0.4	0.07	6.3	No_Data	0.08	0.55	0.23	4	2.7	30	10	54	13	105	20	10,234	18	40
WCOS-7-21	Inherited	152	985	0.6	No_Data	7.1	0.02	0.87	2.26	0.59	20	7.3	77	32	132	28	218	46	11,608	44	59
WCOS-7-22		161	1,077	0.9	No_Data	9.2	0.13	1.11	2.90	0.76	22	8.0	92	34	156	32	240	48	10,847	57	82
WCOS-7-23	Inherited	315	1,554	2.2	1.83	14.1	0.47	3.07	3.85	0.82	26	13.1	102	45	261	48	362	64	14,180	88	109
WCOS-7-24	Inherited	227	955	1.1	1.15	9.7	0.43	1.52	2.28	0.53	20	7.5	72	30	146	30	241	50	10,866	48	77
WCOS-7-25		226	2,118	1.3	No_Data	11.6	0.36	3.00	6.09	1.48	49	18.5	203	75	299	60	457	94	9,368	123	136
WCOS-7-26	Inherited	457	3,058	4.2	No_Data	25.7	0.12	2.20	6.26	1.64	58	23.8	253	106	502	90	644	151	15,612	364	273
WCOS-7-27	Inherited	287	3,300	2.3	0.04	13.6	0.43	3.71	6.57	1.78	65	25.1	294	116	508	98	701	151	9,535	289	250
WCOS-7-28		301	3,124	1.6	No_Data	13.4	0.38	3.44	8.08	1.91	65	21.8	267	105	456	83	597	124	10,171	235	203
WCOS-7-29		296	3,082	2.1	No_Data	14.4	0.42	4.17	9.46	2.64	86	27.2	303	108	492	90	687	137	11,000	208	211
WCOS-7-30	Inherited	363	2,456	1.6	1.37	16.9	0.52	3.18	5.79	1.39	42	18.2	197	79	381	71	463	129	12,726	166	145
WCOS-7-31	Inherited	340	3,745	3.5	0.16	18.3	0.44	4.47	8.32	2.20	71	26.6	323	114	584	97	824	170	10,948	353	294
WCOS-7-32	Inherited	243	1,915	1.6	0.00	12.6	0.35	2.23	4.10	1.18	46	13.9	169	63	296	55	428	85	10,503	158	140
WCOS-7-33	Inclusion	937	1,280	1.8	9.80	26.9	3.82	12.60	4.27	1.14	26	10.0	96	42	184	39	344	63	9,465	78	124
WCOS-7-34		395	1,689	4.3	4.52	26.9	1.39	4.41	2.89	0.66	24	10.8	103	50	270	60	530	106	13,675	276	373
WCOS-7-35		452	1,025	2.7	5.47	24.1	1.93	4.50	2.18	0.31	17	6.7	69	34	160	33	259	67	11,093	134	182
WCOS-7-36		223	1,160	2.3	No_Data	14.1	0.19	0.72	2.13	0.56	23	7.7	106	42	202	46	408	75	9,331	145	358
WCOS-7-37		259	1,934	1.7	No_Data	11.7	0.47	3.14	6.31	1.53	52	17.6	193	71	308	61	491	88	9,583	136	154
WCOS-7-38	Inherited	219	2,177	1.4	No_Data	10.9	0.33	3.33	5.98	1.53	51	17.6	200	75	318	69	525	92	11,071	132	127
WCOS-7-39		220	1,459	1.1	No_Data	11.2	0.25	2.46	5.47	1.28	38	15.7	156	52	241	48	363	63	9,031	86	118
WCOS-7-40		270	2,370	2.0	No_Data	12.9	0.42	3.16	6.06	1.71	58	20.3	227	97	366	70	589	102	10,080	162	182
WA-6-1	Inherited	205	1,384	0.8	0.67	11.9	0.35	1.14	2.54	0.93	26	9.2	102	36	164	33	258	51	11,834	71	100
WA-6-2		143	1,274	0.6	No_Data	11.0	0.08	1.05	3.09	0.95	27	9.3	97	38	170	34	315	49	11,624	65	117
WA-6-3	Inherited	122	1,394	0.7	No_Data	11.0	0.12	1.49	3.27	1.17	38	10.4	109	39	182	36	274	51	11,143	86	112
WA-6-4		191	1,359	1.0	No_Data	14.8	0.13	1.41	2.84	0.88	26	10.1	99	32	168	36	275	51	10,165	99	171
WA-6-5		191	1,566	1.3	No_Data	11.7	0.23	2.21	4.03	1.41	36	11.5	130	49	218	44	341	58	8,316	103	181
WA-6-6		192	1,606	1.1	No_Data	10.8	0.10	1.86	3.76	1.02	32	10.7	113	44	205	39	292	61	10,297	97	127
WA-6-7		131	546	0.7	No_Data	6.6	0.03	0.19	0.75	0.28	10	3.7	42	15	74	15	128	24	11,381	24	58
WA-6-8		142	863	1.7	No_Data	10.5	0.04	0.49	1.22	0.47	14	5.1	61	23	119	25	192	41	12,014	69	112
WA-6-9		163	1,033	1.1	No_Data	8.5	0.05	0.93	1.66	0.60	20	6.5	65	27	133	26	235	51	9,725	56	109

Appendix Table 8 (continued). Zircon Trace Element Spot Analyses from OSU - LA-ICP-MS

Spot ID	Note	P (31) ppm	Y (89) ppm	Nb (93) ppm	La (139) ppm	Ce (140) ppm	Pr (141) ppm	Nd (146) ppm	Sm (147) ppm	Eu (153) ppm	Gd (157) ppm	Tb (159) ppm	Dy (163) ppm	Ho (165) ppm	Er (166) ppm	Tm (169) ppm	Yb (172) ppm	Lu (175) ppm	Hf (179) ppm	Th (232) ppm	U (238) ppm
WA-6-10		227	1,202	3.2	No_Data	10.7	0.06	0.44	1.51	0.70	18	5.8	72	32	153	36	318	68	9,165	55	161
WA-6-11	Inherited	160	1,945	1.7	No_Data	14.0	0.39	3.49	6.25	1.93	52	17.5	184	59	242	46	387	70	7,302	144	217
WA-6-12		183	2,108	1.5	No_Data	11.9	0.19	3.80	5.31	1.80	51	16.4	174	62	271	48	395	77	9,385	133	169
WA-6-13		193	3,274	4.9	No_Data	26.4	0.56	7.24	9.00	4.19	84	28.3	285	87	420	92	669	126	9,414	304	757
WA-6-14	Inherited	523	2,416	1.6	4.98	22.5	1.98	6.42	5.56	1.67	55	16.0	191	72	391	61	432	118	17,121	164	199
WA-6-15	Inclusion	667	1,044	1.3	4.75	20.1	1.80	5.44	2.53	0.58	20	6.1	68	31	141	27	230	44	12,157	62	93
WA-6-16	Inherited	64	709	0.8	No_Data	4.8	No_Data	BDL	0.97	0.42	13	5.4	54	20	101	20	160	34	9,643	41	87
WA-6-17		150	1,163	1.7	0.42	9.7	0.22	1.07	2.11	0.58	24	7.2	87	35	156	26	245	50	12,093	67	117
WA-6-18		143	1,039	0.9	No_Data	9.3	0.14	1.37	2.24	0.75	26	7.9	71	30	140	27	244	42	7,305	76	121
WA-6-19		119	867	1.5	0.08	10.1	No_Data	0.68	1.12	0.34	13	4.4	58	23	114	23	192	39	11,982	57	97
WA-6-20		155	1,057	1.1	No_Data	10.4	0.07	1.10	1.86	0.74	16	8.4	72	29	139	26	216	37	9,455	53	121
WA-11-21		227	1,981	2.6	No_Data	20.6	0.20	2.15	4.20	1.69	37	13.9	146	55	256	56	470	88	11,288	125	238
WA-11-22		273	1,654	2.9	No_Data	10.1	0.13	1.32	2.64	0.86	26	8.7	113	45	233	48	441	82	10,027	75	176
WA-11-23		140	573	0.7	No_Data	5.4	0.02	0.49	1.03	0.43	14	4.3	43	16	77	15	157	25	8,492	22	69
WA-11-24	Inherited	155	696	1.0	0.20	7.6	0.05	0.47	1.06	0.23	11	3.9	49	20	94	19	155	34	11,902	43	119
WA-11-25		445	2,931	2.0	3.23	19.1	1.34	5.64	6.75	1.82	57	21.2	207	80	375	66	576	113	12,391	167	173
WA-11-26	Inherited	181	438	1.2	No_Data	8.4	No_Data	0.26	0.64	0.43	7	3.1	37	11	64	13	124	23	8,589	31	59
WA-11-27		152	590	0.6	0.06	7.2	No_Data	0.28	1.60	0.34	11	3.6	45	15	87	17	156	26	7,797	38	88
WA-11-28		209	532	1.3	1.36	10.1	0.16	1.54	1.08	0.33	12	3.5	46	16	81	18	159	25	8,807	29	80
WA-11-29		221	1,492	1.0	0.01	10.2	0.11	1.35	3.30	1.01	32	10.3	120	44	203	42	312	60	12,987	71	138
WA-11-30		498	1,744	1.2	1.93	21.1	0.75	2.47	3.57	1.38	48	15.5	142	51	239	44	403	64	10,018	118	199
WA-11-31		207	963	1.0	No_Data	6.7	0.06	1.51	2.20	0.72	21	6.3	76	29	128	26	231	43	8,482	42	83
WA-11-32	Inclusion	3141	1,823	0.9	35.97	136.3	21.54	59.39	12.45	1.21	50	13.2	130	49	223	44	312	73	14,332	97	155
WA-11-33		188	1,122	1.1	No_Data	10.1	0.07	0.82	1.87	0.60	18	7.2	66	33	140	30	265	60	11,555	65	278
WA-11-34		317	1,621	1.8	0.53	12.1	0.21	2.59	4.08	1.44	37	12.7	127	50	231	50	378	65	8,317	102	172
WA-11-35		215	1,502	1.5	No_Data	8.4	0.17	1.58	2.87	1.03	30	12.0	116	43	211	42	376	61	7,491	80	144
WA-11-36		183	1,683	0.9	No_Data	11.5	0.40	3.58	5.35	1.85	43	14.6	150	53	244	48	421	62	6,869	108	146
WA-11-37		228	909	1.0	No_Data	7.0	0.09	1.24	2.84	0.68	17	6.5	80	33	122	22	209	35	7,688	40	105
WA-11-38		171	1,065	0.7	No_Data	8.0	0.12	1.87	3.26	1.12	25	9.2	96	30	139	30	254	39	8,008	50	95
WA-11-39		245	1,083	1.3	No_Data	6.5	0.17	1.90	2.85	1.03	26	8.3	94	32	153	32	286	38	8,854	47	96
WA-11-40		212	1,433	1.0	No_Data	11.5	0.20	2.91	4.72	1.49	37	13.3	127	49	192	36	353	59	12,019	87	157

Appendix Table 8 (continued). Zircon Trace Element Spot Analyses from OSU - LA-ICP-MS

Spot ID	Note	P (31) ppm	Y (89) ppm	Nb (93) ppm	La (139) ppm	Ce (140) ppm	Pr (141) ppm	Nd (146) ppm	Sm (147) ppm	Eu (153) ppm	Gd (157) ppm	Tb (159) ppm	Dy (163) ppm	Ho (165) ppm	Er (166) ppm	Tm (169) ppm	Yb (172) ppm	Lu (175) ppm	Hf (179) ppm	Th (232) ppm	U (238) ppm
WCOSNU-33-01		319	1,269		0.21	23.2	0.18	1.00	2.19	0.55	17	8.9	105		231		535	94	11,291	157	240
WCOSNU-33-02		384	1,841		0.74	22.2	0.38	1.80	3.99	0.93	36	12.5	157		320		627	118	10,797	178	188
WCOSNU-33-03		343	1,292		0.27	21.6	0.12	0.79	2.66	0.54	22	9.7	116		215		404	74	9,553	137	193
WCOSNU-33-04		756	1,723		3.61	32.2	1.14	3.66	4.27	1.09	33	13.3	161		296		595	107	9,660	223	310
WCOSNU-33-05		305	1,631		0.51	31.9	0.28	1.44	2.59	0.60	26	11.4	137		292		509	114	13,372	359	494
WCOSNU-33-06		374	2,168		0.49	25.1	0.25	1.39	3.54	0.96	38	13.2	180		369		648	143	11,418	233	254
WCOSNU-33-07		231	745		0.72	21.0	0.30	0.78	1.49	0.21	11	4.3	55		136		264	60	9,935	177	258
WCOSNU-33-08		362	1,710		0.22	27.4	0.20	1.38	3.86	0.96	36	13.8	176		309		582	124	10,442	304	257
WCOSNU-33-09		387	1,007		1.72	23.3	0.46	1.36	2.09	0.57	19	7.3	93		198		377	73	11,703	151	183
WCOSNU-33-10		649	1,572		6.24	36.1	1.59	4.60	4.02	0.80	26	11.5	123		242		494	83	10,203	190	203
WCOSNU-33-11		600	1,379		3.21	28.3	0.76	2.54	3.73	0.89	33	12.9	137		278		536	92	7,298	237	345
WCOSNU-33-12	Inclusion	616	1,743		12.08	50.7	3.28	8.79	5.78	0.77	40	13.7	178		333		585	115	10,066	340	370
WCOSNU-33-13	Inclusion	2039	1,561		25.82	87.4	6.69	16.29	6.20	1.30	32	11.3	146		268		528	103	8,256	273	263
WCOSNU-33-14		344	1,435		4.46	34.2	0.85	2.87	3.22	0.82	28	10.9	129		249		430	93	10,094	326	259
WCOSNU-33-15		682	1,982		5.67	47.2	1.57	4.58	3.90	0.72	35	13.5	161		343		589	117	10,872	357	317
WCOSNU-33-16		348	1,163		0.31	24.4	0.24	1.13	2.56	0.61	23	7.5	115		234		492	83	8,108	158	328
WCOSNU-33-17		266	1,040		No_Data	26.2	0.06	0.83	2.54	0.43	21	8.0	96		198		323	72	10,205	273	226
WCOSNU-33-18	Inclusion	2649	1,847		33.24	90.6	9.40	21.99	9.83	1.81	49	15.0	174		319		570	114	9,828	196	194
WCOSNU-33-19		504	1,496		0.57	28.4	0.26	1.48	2.83	0.71	25	10.7	133		266		530	100	10,256	331	423
WCOSNU-33-20		485	1,193		2.34	25.4	1.08	3.95	4.09	0.72	22	8.8	104		206		406	84	9,585	147	197
WCOSNU-33-21	Inclusion	1295	1,598		24.51	70.4	5.04	12.23	5.48	0.96	29	10.7	129		259		453	104	11,768	238	270
WCOSNU-33-22		656	2,078		3.17	35.9	1.13	4.55	5.57	1.18	43	17.7	214		371		625	133	11,085	257	296
WCOSNU-33-23		479	1,888		1.03	28.9	0.50	1.83	3.13	0.73	31	13.0	157		357		623	127	10,370	211	294
WCOSNU-33-24		325	1,496		0.13	24.2	0.11	1.07	2.46	0.63	23	9.8	129		261		484	105	11,225	182	227
WCOSNU-33-25	Inclusion	1778	1,604		30.52	93.1	8.11	20.31	7.07	1.24	35	12.5	140		288		489	106	11,204	180	209
WCOSNU-33-26		423	1,162		0.36	24.4	0.17	1.26	2.42	0.74	20	7.4	100		203		476	77	9,987	188	352
WCOSNU-33-27	Inclusion	6731	1,726		15.36	83.9	7.62	18.91	11.69	1.83	46	14.3	163		308		503	101	9,579	257	264
WCOSNU-33-28	Inclusion	833	1,571		6.00	37.7	1.81	4.89	4.99	1.08	32	12.0	135		255		498	88	10,710	189	251
WCOSNU-33-29	Inclusion	3316	1,588		21.54	85.3	6.25	14.29	6.19	0.94	36	10.3	151		277		523	104	10,479	214	349
WCOSNU-33-30		315	932		0.08	21.1	0.11	0.66	2.12	0.58	20	7.8	110		226		457	89	9,956	148	330
WCOSNU-33-31		448	3,541		0.14	54.0	1.27	10.20	18.98	6.54	120	39.6	426		635		1005	169	8,963	316	225
WCOSNU-33-32		547	2,062		3.35	34.2	1.01	3.91	4.91	0.93	40	15.6	185		344		636	130	12,237	278	274
WCOSNU-33-33		301	1,729		0.39	22.7	0.26	1.39	3.73	0.82	28	12.5	143		272		580	101	12,299	193	237

Appendix Table 8 (continued). Zircon Trace Element Spot Analyses from OSU - LA-ICP-MS

Spot ID	Note	P (31) ppm	Y (89) ppm	Nb (93) ppm	La (139) ppm	Ce (140) ppm	Pr (141) ppm	Nd (146) ppm	Sm (147) ppm	Eu (153) ppm	Gd (157) ppm	Tb (159) ppm	Dy (163) ppm	Ho (165) ppm	Er (166) ppm	Tm (169) ppm	Yb (172) ppm	Lu (175) ppm	Hf (179) ppm	Th (232) ppm	U (238) ppm
WCOSNU-33-34	Inherited	326	1,204		0.34	22.3	0.12	0.76	2.00	0.63	20	8.4	107		202		373	77	10,156	180	227
WCOSNU-33-35		274	1,352		0.79	18.2	0.37	1.69	3.09	0.73	33	11.2	138		268		429	95	10,474	144	129
WCOSNU-33-36		393	1,264		1.88	28.5	0.52	1.70	2.24	0.54	19	8.5	103		195		415	83	9,871	176	226
WCOSNU-33-37	Inherited	567	1,881		1.66	32.1	0.86	2.78	4.09	0.95	31	13.6	154		318		572	116	12,312	303	257
WCOSNU-33-38		636	1,087		2.60	26.5	0.95	2.26	2.50	0.55	20	7.6	99		202		364	72	10,918	167	173
WCOSNU-33-39		475	1,964		1.39	26.0	0.51	2.59	4.63	1.18	43	15.2	197		365		681	118	10,816	223	259
WCOSNU-33-40	Inclusion	####	1,430		307.79	584.4	55.63	####	34.91	2.13	80	17.8	156		249		392	82	11,416	260	207
WCOSNU-33-41		382	1,349		No_Data	22.1	No_Data	lo_Dat	1.91	0.07	26	10.5	132		254		560	84	9,825	241	487
WCOSNU-33-42		371	1,765		No_Data	20.3	0.31	1.93	4.15	1.06	39	14.1	152		327		588	115	10,825	178	254
WCOSNU-33-43		343	1,422		No_Data	25.2	0.07	0.70	2.30	0.60	23	10.4	136		311		523	100	11,374	206	214
WCOSNU-33-44		753	1,503		1.51	34.8	0.52	2.48	3.46	1.05	35	14.6	139		328		657	129	9,297	265	389
WCOSNU-33-45		378	1,539		0.11	23.2	0.22	1.72	4.42	0.80	31	13.3	160		277		629	105	10,848	185	364
WCOSNU-33-46		435	2,388		1.62	31.9	0.49	2.04	4.16	0.88	37	13.2	205		440		680	180	11,323	206	181
WCOSNU-33-47		287	2,510		No_Data	22.1	0.19	1.43	4.70	1.00	41	16.2	200		438		583	169	9,321	185	146
WCOSNU-33-48	Inclusion	3658	1,713		51.42	127.8	12.48	25.90	9.22	1.33	36	12.8	152		295		547	112	10,513	227	183
WCOSNU-33-49		498	1,899		6.69	47.1	1.46	3.50	3.34	0.59	28	11.9	165		366		632	143	13,655	253	274
WCOSNU-33-50		402	1,902		3.76	37.3	1.06	3.37	4.08	1.01	39	13.7	200		357		686	132	11,800	323	258
WCOSNU-33-51	Inclusion	993	1,310		20.01	48.1	5.69	11.34	6.25	4.22	28	9.2	113		231		362	84	11,681	695	133
WCOSNU-33-52	Inherited	341	1,079		1.23	23.0	0.37	1.42	1.97	0.48	19	7.5	91		224		403	73	10,177	133	215
WCOSNU-33-53	Inherited	309	2,109		0.37	23.5	0.16	1.17	3.30	0.81	31	12.4	180		380		565	149	14,348	208	203
WCOSNU-33-54	Inherited	287	2,191		No_Data	30.3	No_Data	0.76	3.65	0.67	34	13.1	171		382		633	154	12,287	289	243
WCOSNU-33-55	Inclusion	2988	1,027		32.91	85.7	8.99	18.70	6.49	0.89	24	8.0	92		173		319	71	9,589	86	116
WCOSNU-33-56		399	2,312		1.58	31.1	0.53	2.89	8.22	1.60	50	18.5	230		401		783	130	11,638	255	294
WCOSNU-33-57		349	1,524		2.55	31.1	0.79	2.18	3.06	0.59	26	10.0	118		261		495	99	11,815	201	215
WCOSNU-33-58		520	1,468		2.61	33.9	0.92	2.60	3.46	0.87	25	10.4	122		264		516	102	11,090	238	320
WCOSNU-33-59		448	1,722		2.33	47.7	0.58	2.26	3.43	0.58	32	11.2	145		282		497	108	11,618	597	400
WCOSNU-33-60		1010	1,018		0.20	17.7	0.23	0.51	1.50	0.31	15	5.6	76		184		346	75	10,971	224	559
WCOSNU-33-61		358	2,395		2.46	30.2	0.76	2.95	4.45	0.89	38	13.7	180		399		578	157	9,436	203	160
WCOSNU-33-62		684	1,875		3.56	35.4	1.20	3.12	3.95	1.16	34	13.6	182		374		688	141	11,608	233	272
WCOSNU-33-63		345	1,488		0.32	26.0	0.16	0.99	3.23	0.78	25	10.0	107		254		464	96	11,086	222	290
WCOSNU-33-64		505	1,378		3.31	30.2	0.90	2.88	3.37	0.76	26	9.7	119		255		443	86	8,437	191	298
WCOSNU-33-65		273	1,910		0.06	27.1	0.19	1.39	4.32	1.14	41	15.8	190		366		651	122	10,652	259	293
WCOSNU-33-66		498	1,932		1.50	29.3	0.50	1.90	3.57	0.90	32	11.3	148		326		595	119	11,216	297	322

Appendix Table 8 (continued). Zircon Trace Element Spot Analyses from OSU - LA-ICP-MS

Spot ID	Note	P (31) ppm	Y (89) ppm	Nb (93) ppm	La (139) ppm	Ce (140) ppm	Pr (141) ppm	Nd (146) ppm	Sm (147) ppm	Eu (153) ppm	Gd (157) ppm	Tb (159) ppm	Dy (163) ppm	Ho (165) ppm	Er (166) ppm	Tm (169) ppm	Yb (172) ppm	Lu (175) ppm	Hf (179) ppm	Th (232) ppm	U (238) ppm
WCOSNU-33-67		632	1,347		7.84	35.1	2.10	4.68	2.70	0.56	20	7.4	99		238		382	102	12,787	137	132
WCOSNU-33-68		326	921		0.24	26.2	0.15	0.72	1.86	0.41	16	5.8	75		165		391	58	6,957	146	243
WCOSNU-33-69		561	2,652		0.68	57.5	0.49	2.95	6.40	0.92	58	23.3	278		534		994	191	9,957	503	578
WCOSNU-33-70		798	991		4.03	26.6	1.49	3.33	2.70	0.52	18	6.0	86		177		353	70	8,373	85	150
WCOSNU-33-71	Inherited	369	1,381		2.94	26.8	0.75	1.99	2.82	0.62	25	9.2	117		272		395	103	13,388	211	147
WCOSNU-33-72	Inclusion	766	2,259		13.99	56.0	3.58	8.38	4.74	0.86	35	12.9	179		425		595	168	13,419	281	204
WCOSNU-33-73		393	1,132		0.57	24.1	0.25	1.26	2.58	0.66	21	7.7	91		216		498	83	9,477	168	423
WCOSNU-33-74		342	1,560		1.38	32.4	0.49	1.86	3.37	0.83	27	9.7	133		271		547	114	8,522	212	299
WCOSNU-33-75	Inherited	267	2,318		0.12	36.0	0.17	1.85	4.87	1.05	39	13.7	208		438		673	171	9,905	318	192
WCOSNU-33-76		375	1,891		2.86	41.1	0.91	2.23	4.38	0.75	35	12.8	162		366		736	138	13,638	315	524
WCOSNU-33-77		366	2,838		0.61	34.4	0.47	1.36	3.30	0.54	32	14.1	173		499		755	208	13,474	569	790
WCOSNU-33-78		461	1,425		0.48	29.6	0.41	1.40	2.68	0.74	28	11.0	147		269		566	102	9,592	231	321
WCOSNU-33-79		324	2,183		0.04	36.7	0.22	1.65	4.68	1.00	35	14.0	185		389		712	146	12,044	331	356
WCOSNU-33-80		518	3,195		0.59	97.0	0.56	2.99	8.90	0.78	70	22.7	296		580		854	189	12,425	1200	579
WCOSNU-33-81	Inclusion	1269	1,329		24.07	93.1	7.61	12.07	5.80	0.60	26	9.9	122		241		441	91	11,511	290	262
WCOSNU-33-82	Inclusion	1457	1,214		35.17	96.9	8.10	19.02	6.82	0.62	26	8.8	101		197		370	78	11,455	219	299
WCOSNU-33-83	Inclusion	1801	1,435		22.67	71.7	5.53	10.73	5.79	0.91	30	10.6	121		251		458	95	10,525	181	278
WCOSNU-33-84		445	1,182		0.06	26.7	0.13	0.74	2.40	0.31	19	7.4	89		182		392	74	8,413	183	364
WCOSNU-33-85	Inclusion	412	1,351		48.02	107.8	10.86	22.87	8.89	3.07	27	9.9	116		197		417	77	10,703	350	150
WCOSNU-33-86		392	1,423		1.57	37.1	0.42	1.74	2.54	0.40	23	9.0	119		246		464	96	12,519	278	334
WCOSNU-33-87		301	2,096		0.27	24.3	0.27	1.65	4.38	1.05	43	16.3	187		387		594	145	12,019	224	163
WCOSNU-33-88	Inclusion	2453	1,361		40.41	112.3	10.52	22.42	8.02	1.04	31	8.9	109		219		382	80	12,283	321	306
WCOSNU-33-89		309	1,089		2.08	21.1	0.39	1.52	2.11	0.52	19	7.2	87		204		395	80	9,857	156	329
WCOSNU-33-90		475	4,613		0.89	90.9	0.89	5.33	14.45	2.25	96	35.0	453		807		1302	266	8,940	1458	1195
WCOSNU-33-91		418	998		0.06	21.1	0.13	0.70	2.29	0.47	21	7.1	97		174		395	74	9,999	173	456
WCOSNU-33-92		292	800		0.05	16.3	0.07	0.52	1.45	0.35	14	5.9	69		152		297	58	11,083	96	167
WCOSNU-33-93	Inclusion	1337	1,347		13.42	56.6	3.39	8.85	4.24	0.77	27	10.1	122		234		469	91	11,926	216	272
WCOSNU-33-94		394	879		1.69	22.2	0.63	1.69	2.49	0.42	16	6.3	80		168		345	66	10,576	137	228
WCOSNU-33-95	Inclusion	4735	1,862		60.77	170.3	16.68	39.46	13.50	1.93	53	15.6	195		337		630	121	11,363	258	307
WCOSNU-33-96		427	1,122		0.59	21.7	0.25	1.15	2.92	0.58	25	9.0	100		205		396	80	11,608	120	169
WCOSNU-33-97		509	2,384		0.02	29.6	0.23	2.32	6.12	1.70	55	20.5	238		406		772	152	8,554	250	309
WCOSNU-33-98		455	5,303		0.13	60.1	0.50	5.69	17.92	4.42	137	42.1	520		868		1573	314	10,459	657	395
WCOSNU-33-99		303	1,352		0.11	18.4	0.15	1.61	3.55	0.96	29	11.4	123		229		399	83	11,338	119	143

Appendix Table 8 (continued). Zircon Trace Element Spot Analyses from OSU - LA-ICP-MS

Spot ID	Note	P (31) ppm	Y (89) ppm	Nb (93) ppm	La (139) ppm	Ce (140) ppm	Pr (141) ppm	Nd (146) ppm	Sm (147) ppm	Eu (153) ppm	Gd (157) ppm	Tb (159) ppm	Dy (163) ppm	Ho (165) ppm	Er (166) ppm	Tm (169) ppm	Yb (172) ppm	Lu (175) ppm	Hf (179) ppm	Th (232) ppm	U (238) ppm
WCOSNU-33-100		674	1,323		4.76	27.3	1.31	3.93	2.93	0.65	25	9.9	122		233		431	82	10,358	119	191
WCOSWR-01-01	Inherited	342	1,223		1.66	18.8	0.54	2.54	4.25	1.23	34	10.6	131		200		352	59	9,310	130	165
WCOSWR-01-02	Inherited	246	415		0.08	10.6	0.13	0.38	1.10	0.26	9	3.3	38		68		140	22	9,128	39	72
WCOSWR-01-03	Inherited	271	1,011		0.29	13.1	0.20	1.65	3.39	0.96	29	9.3	107		171		291	48	9,335	92	129
WCOSWR-01-04		160	822		No_Data	11.8	0.07	0.92	2.68	0.69	21	7.1	75		124		249	40	8,485	62	109
WCOSWR-01-05		186	651		No_Data	14.7	0.06	0.48	1.47	0.39	15	4.6	64		116		205	37	12,346	122	106
WCOSWR-01-06	Inherited	213	805		No_Data	9.8	0.16	1.24	2.81	0.79	24	7.4	86		141		242	41	8,916	59	109
WCOSWR-01-07		214	784		No_Data	9.9	0.13	1.23	3.12	0.83	22	7.2	71		124		214	32	7,515	54	106
WCOSWR-01-08		215	523		No_Data	7.8	0.08	0.40	1.47	0.43	15	4.3	66		109		194	32	10,336	43	98
WCOSWR-01-09	Inherited	174	475		No_Data	10.4	0.04	0.26	0.90	0.25	9	3.7	42		77		142	26	10,351	41	77
WCOSWR-01-10		133	702		0.12	10.5	0.06	0.50	1.93	0.48	16	5.8	70		115		218	35	10,742	46	70
WCOSWR-01-11		189	455		No_Data	10.3	0.04	0.36	1.11	0.30	10	3.5	45		87		149	29	10,601	48	82
WCOSWR-01-12	Inherited	201	610		0.05	11.3	0.06	0.45	1.56	0.42	14	4.9	58		101		177	32	9,428	59	100
WCOSWR-01-13	Inherited	260	612		0.05	10.6	0.07	0.48	1.61	0.39	13	5.2	61		105		223	37	10,374	47	109
WCOSWR-01-14	Inherited	182	440		No_Data	9.7	0.03	0.26	0.93	0.24	9	3.2	40		74		128	25	10,193	39	71
WCOSWR-01-15		188	1,083		No_Data	12.4	0.14	1.51	4.19	0.97	32	10.8	116		187		276	48	10,104	84	109
WCOSWR-01-16		230	1,807		No_Data	15.6	0.29	2.57	6.34	1.57	46	15.6	152		298		523	69	9,126	161	203
WCOSWR-01-17		126	524		0.06	9.0	0.06	0.45	1.64	0.45	14	5.0	54		91		176	26	9,563	40	64
WCOSWR-01-18		153	444		0.11	10.0	0.04	0.24	0.89	0.21	7	3.2	41		70		146	24	9,941	34	84
WCOSWR-01-19		578	740		0.84	13.4	0.31	1.32	2.16	0.52	17	5.5	63		111		229	44	9,020	69	112
WCOSWR-01-20	Inclusion	1689	800		9.33	35.7	2.73	5.93	3.20	0.57	17	5.6	71		137		230	46	11,138	74	120
WCOSWR-01-21	Inherited	255	983		0.07	12.5	0.15	1.37	3.28	0.75	22	7.6	89		156		285	51	9,347	71	135
WCOSWR-01-22		189	1,049		No_Data	13.1	0.18	1.54	3.61	1.03	27	9.8	108		176		283	51	9,793	88	122
WCOSWR-01-23		193	918		No_Data	11.2	0.15	1.10	2.65	0.62	21	7.4	89		161		245	53	11,049	86	115
WCOSWR-01-24	Inherited	170	600		0.07	14.7	0.06	0.44	1.29	0.30	13	4.7	55		102		178	33	10,996	80	109
WCOSWR-01-25	Inherited	513	911		2.66	15.2	0.65	2.62	2.96	0.83	22	7.3	86		153		257	46	8,766	71	106
WCOSWR-01-26	Inherited	193	1,192		No_Data	13.3	0.23	1.87	4.59	1.05	34	12.1	134		219		353	64	9,768	123	141
WCOSWR-01-27	Inherited	362	985		0.55	17.6	0.27	1.34	2.53	0.58	27	9.0	98		171		296	53	12,611	102	154
WCOSWR-01-28		186	485		0.03	10.3	0.06	0.59	1.52	0.33	12	4.6	51		90		173	26	7,194	47	101
WCOSWR-01-29		216	716		0.07	12.0	0.07	0.77	2.09	0.60	15	6.0	61		114		190	38	10,174	72	100
WCOSWR-01-30	Inherited	196	829		0.07	10.8	0.12	0.87	2.61	0.58	23	7.9	84		152		236	40	10,681	64	95
WCOSWR-01-31	Inherited	279	612		0.53	12.0	0.15	0.73	1.26	0.31	13	5.1	57		109		191	39	10,538	54	95

Appendix Table 8 (continued). Zircon Trace Element Spot Analyses from OSU - LA-ICP-MS

Spot ID	Note	P (31) ppm	Y (89) ppm	Nb (93) ppm	La (139) ppm	Ce (140) ppm	Pr (141) ppm	Nd (146) ppm	Sm (147) ppm	Eu (153) ppm	Gd (157) ppm	Tb (159) ppm	Dy (163) ppm	Ho (165) ppm	Er (166) ppm	Tm (169) ppm	Yb (172) ppm	Lu (175) ppm	Hf (179) ppm	Th (232) ppm	U (238) ppm
WCOSWR-01-32	Inherited	193	1,130		0.15	70.2	0.10	0.72	1.68	0.31	16	7.1	93		216		545	115	13,852	1341	2443
WCOSWR-01-33	Inclusion	1516	1,462		18.26	51.3	4.72	12.58	7.92	1.95	49	13.6	152		239		371	66	10,098	149	152
WCOSWR-01-34	Inherited	244	1,156		0.01	12.7	0.18	1.47	3.39	0.83	28	9.7	113		188		316	60	9,336	89	124
WCOSWR-01-35	Inherited	133	781		0.05	12.4	0.03	0.64	1.64	0.42	20	7.2	74		142		197	48	12,305	53	74
WCOSWR-01-36	Inherited	174	536		No_Data	10.6	0.04	0.48	1.16	0.29	11	3.9	51		99		176	34	11,606	44	79
WCOSWR-01-37	Inclusion	618	641		4.51	18.2	1.45	2.70	2.17	0.52	16	4.7	66		109		176	34	10,473	47	70
WCOSWR-01-38	Inherited	232	910		No_Data	9.0	0.14	1.04	2.95	0.68	23	7.8	94		151		231	43	9,612	66	91
WCOSWR-01-39	Inherited	365	1,154		1.44	18.1	0.52	1.99	3.10	0.61	29	9.0	110		195		311	55	10,799	111	111
WCOSWR-01-40		194	747		No_Data	10.1	0.11	0.76	2.19	0.54	18	6.7	73		127		206	39	10,069	60	84
WCOSWR-01-41	Inherited	188	650		0.07	11.6	0.08	0.43	1.72	0.44	12	5.3	64		108		197	31	8,891	50	129
WCOSWR-01-42		233	430		No_Data	8.8	0.02	0.34	1.07	0.36	10	3.8	50		97		196	36	8,887	44	98
WCOSWR-01-43		249	1,638		0.07	13.9	0.32	2.67	5.73	1.57	50	15.2	188		297		440	74	9,295	169	176
WCOSWR-01-44	Inherited	180	404		No_Data	10.7	0.01	0.17	0.84	0.21	8	3.2	41		71		139	25	9,980	43	82
WCOSWR-01-45	Inherited	263	892		No_Data	10.1	0.12	0.92	2.20	0.59	22	7.2	93		153		283	54	12,497	60	96
WCOSWR-01-46		170	545		No_Data	10.1	0.04	0.43	1.27	0.31	12	4.5	56		92		143	32	11,304	45	65
WCOSWR-01-47		137	499		No_Data	12.0	0.04	0.27	0.82	0.21	10	4.2	48		91		161	31	13,638	54	94
WCOSWR-01-48	Inherited	258	1,430		0.05	13.5	0.19	2.15	4.19	0.92	43	12.4	151		237		344	73	11,989	117	117
WCOSWR-01-49		193	826		0.17	10.9	0.11	0.92	2.01	0.50	19	6.1	75		138		243	48	11,481	72	94
WCOSWR-01-50		296	1,162		No_Data	12.6	0.13	0.83	2.18	0.55	23	8.0	101		204		324	67	11,945	83	147
WCOSWR-01-51		183	962		0.04	11.7	0.11	0.90	3.09	0.62	29	9.0	111		187		277	58	13,199	86	99
WCOSWR-01-52		288	1,111		No_Data	15.2	0.10	1.20	3.02	0.71	27	9.6	113		205		311	71	11,337	130	156
WCOSWR-01-53		185	1,100		0.06	14.0	0.10	1.09	2.75	0.62	27	9.0	107		195		290	60	11,957	90	119
WCOSWR-01-54		213	760		No_Data	13.1	0.08	0.54	1.63	0.50	17	5.7	71		128		236	50	12,724	67	106
WCOSWR-01-55	Inherited	133	870		No_Data	10.7	0.07	0.90	2.30	0.58	24	7.6	83		144		220	45	13,337	50	69
WCOSWR-01-56		126	455		No_Data	8.8	0.05	0.33	0.92	0.23	10	3.6	43		79		155	29	12,429	31	61
WCOSWR-01-57	Inherited	247	1,377		No_Data	14.3	0.18	1.62	4.45	1.19	40	13.1	144		240		388	64	12,300	129	147
WCOSWR-01-58	Inherited	214	1,527		0.13	13.0	0.19	2.19	4.29	0.90	36	13.0	144		256		384	79	9,505	124	128
WCOSWR-01-59		226	1,017		0.71	11.9	0.28	1.37	3.01	0.89	31	10.2	106		175		279	50	9,043	112	111
WCOSWR-01-60	Inherited	171	556		No_Data	9.0	0.06	0.55	1.53	0.31	13	4.1	51		90		169	33	10,315	40	65
WCOSWR-01-61	Inherited	193	1,049		0.13	11.6	0.17	1.29	2.99	0.80	28	10.1	98		172		267	61	12,836	70	67
WCOSWR-01-62	Inherited	116	781		No_Data	10.1	0.10	0.68	2.12	0.44	21	6.9	78		138		218	44	11,361	72	85
WCOSWR-01-63	Inherited	156	359		No_Data	8.4	0.02	0.21	0.64	0.19	7	2.7	32		67		115	23	12,924	29	51
WCOSWR-01-64	Inherited	229	1,968		No_Data	13.6	0.29	2.47	5.41	1.35	48	17.1	186		306		477	97	10,757	180	175

Appendix Table 8 (continued). Zircon Trace Element Spot Analyses from OSU - LA-ICP-MS

Spot ID	Note	P (31) ppm	Y (89) ppm	Nb (93) ppm	La (139) ppm	Ce (140) ppm	Pr (141) ppm	Nd (146) ppm	Sm (147) ppm	Eu (153) ppm	Gd (157) ppm	Tb (159) ppm	Dy (163) ppm	Ho (165) ppm	Er (166) ppm	Tm (169) ppm	Yb (172) ppm	Lu (175) ppm	Hf (179) ppm	Th (232) ppm	U (238) ppm
WCOSWR-01-65		297	1,774		0.32	15.4	0.51	3.41	6.18	1.45	52	18.6	191		322		487	91	11,380	185	170
WCOSWR-01-66	Inherited	289	1,110		No_Data	12.0	0.16	1.37	3.08	0.79	28	9.5	114		181		292	61	11,150	93	124
WCOSWR-01-67		257	929		0.20	12.4	0.19	1.03	2.38	0.48	22	7.5	88		168		297	60	12,467	64	110
WCOSWR-01-68		104	562		No_Data	8.5	0.03	0.38	1.32	0.31	12	5.2	56		97		160	30	11,418	38	58
WCOSWR-01-69		383	611		2.32	20.0	0.75	2.04	1.61	0.34	13	4.8	55		108		188	38	13,435	74	106
WCOSWR-01-70	Inherited	340	1,115		0.05	11.4	0.11	1.49	3.32	0.70	32	9.1	106		191		296	61	10,542	91	113
WCOSWR-01-71		187	956		0.04	12.4	0.13	1.22	2.97	0.78	26	8.8	102		171		295	55	11,065	96	111
WCOSWR-01-72	Inherited	229	573		No_Data	9.3	0.05	0.47	1.55	0.37	15	4.1	56		106		185	39	11,737	41	75
WCOSWR-01-73		176	352		No_Data	9.5	0.03	0.28	0.87	0.23	8	3.4	42		67		149	21	8,788	37	109
WCOSWR-01-74	Inclusion	750	893		5.94	26.0	1.50	3.93	2.29	0.39	17	6.1	69		154		189	62	11,834	54	115
WCOSWR-01-75		143	454		No_Data	6.9	0.01	0.28	0.82	0.21	9	3.8	47		99		144	31	14,662	29	47
WCOSWR-01-76	Inherited	218	989		0.01	11.1	0.09	1.46	3.45	0.95	28	10.4	120		163		302	48	10,749	69	105
WCOSWR-01-77	Inherited	279	2,354		0.03	25.8	0.41	3.52	8.03	1.90	73	23.3	253		382		611	99	12,446	308	289
WCOSWR-01-78		256	1,827		0.12	15.2	0.30	2.62	5.87	1.51	52	17.7	196		305		474	88	10,733	178	186
WCOSWR-01-79		176	1,098		No_Data	13.4	0.11	1.27	3.66	0.84	32	10.1	120		178		297	62	13,167	92	104
WCOSWR-01-80		377	1,086		1.01	18.8	0.53	1.45	2.77	0.57	25	7.7	94		169		275	58	12,110	104	148
WCOSWR-01-81		197	588		No_Data	10.9	0.01	0.38	1.30	0.32	12	4.2	57		103		178	39	13,375	56	92
WCOSWR-01-82	Inherited	390	1,200		1.98	16.4	0.80	3.15	4.11	0.80	32	11.2	127		199		340	60	11,566	104	121
WCOSWR-01-83	Inherited	495	5,945		0.27	58.1	0.69	7.22	20.81	3.70	170	56.2	608		965		1144	292	12,543	794	414
WCOSWR-01-84		174	1,056		No_Data	11.5	0.20	1.19	2.85	0.84	25	8.0	102		181		290	57	11,145	82	114
WCOSWR-01-85		27	163		No_Data	1.8	0.00	0.18	0.44	0.13	4	1.2	16		28		45	9	1,721	13	18
WCOSNU-11-01	Inherited	224	1,705		No_Data	11.9	0.23	2.50	5.39	1.20	51	16.1	179		299		486	88	9,338	103	127
WCOSNU-11-02		253	2,108		0.04	13.4	0.35	3.14	6.66	1.55	59	18.3	235		313		620	108	9,644	109	161
WCOSNU-11-03	Inherited	321	4,244		0.01	21.4	0.58	4.65	11.16	1.86	92	33.7	440		800		1115	220	14,090	319	265
WCOSNU-11-04		153	508		No_Data	7.3	0.02	0.33	1.20	0.24	12	4.0	48		84		161	27	8,622	25	71
WCOSNU-11-05	Inherited	207	1,237		0.03	13.2	0.10	1.32	4.03	0.64	32	10.5	124		197		346	58	10,601	75	134
WCOSNU-11-06	Inherited	257	1,845		0.02	12.4	0.22	2.63	5.78	1.14	51	16.6	218		342		512	90	10,417	137	174
WCOSNU-11-07	Inherited	174	902		1.64	11.8	0.28	1.20	1.52	0.31	18	5.2	73		149		211	53	12,885	56	58
WCOSNU-11-08	Inherited	231	1,046		No_Data	10.5	0.23	1.88	3.54	0.78	31	9.7	110		183		318	52	11,093	67	83
WCOSNU-11-09	Inherited	201	1,013		0.02	9.2	0.06	1.03	2.31	0.47	25	8.2	103		193		252	67	13,735	63	58
WCOSNU-11-10	Inherited	441	3,779		0.14	25.1	0.67	5.47	11.31	2.10	110	35.3	417		688		944	180	12,713	430	295
WCOSNU-11-11	Inclusion	334	3,344		0.07	19.6	0.38	3.27	9.56	1.77	89	32.0	373		572		818	155	10,384	266	348

Appendix Table 8 (continued). Zircon Trace Element Spot Analyses from OSU - LA-ICP-MS

Spot ID	Note	P (31) ppm	Y (89) ppm	Nb (93) ppm	La (139) ppm	Ce (140) ppm	Pr (141) ppm	Nd (146) ppm	Sm (147) ppm	Eu (153) ppm	Gd (157) ppm	Tb (159) ppm	Dy (163) ppm	Ho (165) ppm	Er (166) ppm	Tm (169) ppm	Yb (172) ppm	Lu (175) ppm	Hf (179) ppm	Th (232) ppm	U (238) ppm
WCOSNU-11-12	Inherited	189	1,672		0.07	13.2	0.19	1.44	3.36	0.97	34	10.9	136		298		453	112	13,349	87	81
WCOSNU-11-13		215	1,859		0.10	11.1	0.26	2.70	5.93	1.35	50	15.6	205		376		516	105	12,415	105	115
WCOSNU-11-14	Inherited	282	3,925		0.13	15.1	0.50	4.06	8.93	1.72	99	31.9	383		684		751	196	10,311	261	149
WCOSNU-11-15	Inherited	168	1,997		0.02	9.8	0.15	1.78	4.86	0.85	46	15.5	193		329		391	108	10,783	77	59
WCOSNU-11-16		284	1,816		0.06	13.8	0.35	2.52	6.02	1.06	49	16.5	191		342		516	100	11,313	125	219
WCOSNU-11-17		228	2,293		No_Data	14.3	0.26	2.62	5.87	1.09	53	18.4	243		427		653	119	10,741	200	258
WCOSNU-11-18		135	731		No_Data	8.8	0.04	0.61	1.93	0.33	19	6.8	71		130		238	38	11,772	41	76
WCOSNU-11-19	Inherited	153	1,016		No_Data	9.1	0.12	1.25	3.17	0.89	30	9.2	99		159		279	45	7,237	53	84
WCOSNU-11-20		228	2,020		No_Data	13.6	0.29	2.90	7.58	1.82	62	20.3	224		387		526	108	11,187	127	153
WCOSNU-11-21	Inherited	188	1,296		0.12	10.4	0.34	2.52	5.37	1.23	42	12.2	144		210		368	63	12,501	80	98
WCOSNU-11-22	Inherited	262	1,539		No_Data	14.9	0.20	1.45	3.89	0.74	39	13.4	148		242		356	73	13,617	93	138
WCOSNU-11-23		188	1,394		No_Data	10.8	0.17	1.51	4.12	0.72	39	12.0	145		217		332	63	8,357	79	124
WCOSNU-11-24	Inherited	229	1,138		No_Data	8.6	0.13	1.49	3.86	0.75	36	11.8	121		174		298	54	10,470	65	96
WCOSNU-11-25	Inherited	205	1,186		0.02	9.8	0.14	1.34	3.83	0.78	34	12.1	137		216		390	71	9,805	71	103
WCOSNU-11-26	Inherited	182	2,256		0.04	12.1	0.18	1.99	6.44	1.13	59	18.4	237		408		544	122	14,132	101	115
WCOSNU-11-27		197	657		No_Data	9.1	0.02	0.35	1.20	0.24	12	4.8	62		113		197	38	12,704	41	76
WCOSNU-11-28	Inherited	187	1,114		0.02	8.8	0.11	1.23	2.76	0.54	28	9.3	111		190		304	59	12,939	63	89
WCOSNU-11-29		351	3,126		0.04	17.9	0.42	3.57	8.96	1.95	83	27.4	345		518		885	154	9,222	308	335
WCOSNU-11-30	Inherited	258	1,601		0.35	12.6	0.33	2.36	5.76	1.13	46	13.8	178		283		475	88	9,057	121	148
WCOSNU-11-31		261	1,365		0.02	10.6	0.29	2.16	4.32	0.89	40	12.7	147		234		342	65	9,102	119	140
WCOSNU-11-32		376	2,645		0.01	13.9	0.38	3.03	7.60	1.35	68	22.5	299		440		722	127	10,641	232	288
WCOSNU-11-33		275	1,518		No_Data	10.7	0.23	2.83	5.17	0.98	44	15.4	177		258		419	75	10,598	127	177
WCOSNU-11-34		369	2,342		0.02	14.1	0.30	2.86	6.31	1.22	61	19.6	250		426		648	117	9,858	192	306
WCOSNU-11-35		137	1,088		No_Data	6.7	0.05	0.65	1.67	0.37	16	6.9	89		172		209	59	11,232	39	43
WCOSNU-11-36	Inherited	489	6,310		0.69	27.7	0.99	6.66	17.68	2.76	184	58.4	662		1119		1254	324	12,218	571	353
WCOSNU-11-37		270	2,617		0.02	15.9	0.38	3.39	7.57	1.11	60	21.5	244		455		650	135	12,072	180	207
WCOSNU-11-38	Inherited	282	2,193		0.02	12.1	0.42	3.12	7.44	1.45	63	21.4	234		373		559	104	10,738	179	166
WCOSNU-11-39	Inherited	190	812		No_Data	7.4	0.05	0.72	2.38	0.36	21	7.1	82		136		204	41	11,651	38	64
WCOSNU-11-40	Inherited	225	550		No_Data	7.7	0.04	0.37	1.55	0.30	14	4.4	56		102		171	31	10,480	39	75
SRM01-108-01	Inherited	171	6,900		0.09	22.6	0.34	4.83	14.65	4.99	131	47.7	531		842		1014	273	10,305	215	171
SRM01-108-02	Inherited	184	9,204		0.22	30.0	0.83	7.69	20.28	6.49	198	70.0	704		1120		1363	337	9,171	294	261
SRM01-108-03	Inherited	98	2,691		0.06	16.7	0.30	2.33	5.84	1.79	46	15.9	179		328		621	118	8,309	141	225

Appendix Table 8 (continued). Zircon Trace Element Spot Analyses from OSU - LA-ICP-MS

Spot ID	Note	P (31) ppm	Y (89) ppm	Nb (93) ppm	La (139) ppm	Ce (140) ppm	Pr (141) ppm	Nd (146) ppm	Sm (147) ppm	Eu (153) ppm	Gd (157) ppm	Tb (159) ppm	Dy (163) ppm	Ho (165) ppm	Er (166) ppm	Tm (169) ppm	Yb (172) ppm	Lu (175) ppm	Hf (179) ppm	Th (232) ppm	U (238) ppm
SRM01-108-04		164	4,289		0.11	21.7	0.59	4.76	13.62	5.72	92	36.4	363		574		1053	149	10,029	159	212
SRM01-108-05		149	5,355		0.86	22.5	0.59	4.22	11.07	4.15	111	39.0	396		670		939	202	12,507	260	543
SRM01-108-06		90	2,140		0.01	8.1	0.15	1.52	5.09	1.68	40	12.1	159		243		393	72	7,219	49	96
SRM01-108-07		157	2,926		No_Data	17.2	0.32	3.93	10.35	3.75	73	25.2	249		346		562	91	5,297	102	203
SRM01-108-08		210	3,726		No_Data	28.5	0.09	1.66	5.69	2.20	52	20.4	273		431		773	110	5,145	194	348
SRM01-108-09		115	1,523		No_Data	8.7	0.19	1.65	3.55	1.34	29	10.2	116		187		350	47	5,341	42	119
SRM01-108-10		171	5,005		0.04	28.2	0.52	5.72	21.36	7.36	124	44.7	468		650		1252	165	9,200	175	233
SRM01-108-11	Inherited	120	3,867		No_Data	16.4	0.34	3.27	10.16	3.71	86	33.1	345		541		838	149	11,532	144	148
SRM01-108-12	Inherited	134	3,950		0.06	12.7	0.23	2.78	7.90	2.49	75	29.3	289		491		609	168	12,180	101	88
SRM01-108-13		208	9,256		0.18	39.3	1.07	9.28	27.04	8.75	224	83.0	810		1143		1546	331	9,264	317	241
SRM01-108-14		133	3,052		No_Data	16.2	0.14	1.44	4.39	1.50	39	15.0	192		373		681	132	8,577	105	136
SRM01-108-15	Inherited	107	3,907		0.58	12.4	0.30	2.82	6.42	2.15	62	22.6	233		461		573	154	9,722	108	86
SRM01-108-16	Inherited	146	4,840		No_Data	17.7	0.50	4.51	12.00	4.20	108	36.5	423		632		950	198	8,916	138	135
SRM01-108-17	Inherited	193	7,010		0.14	32.5	0.71	6.86	20.92	7.46	181	60.2	694		957		1329	230	6,703	252	222
SRM01-108-18		125	3,078		0.10	15.5	0.43	3.65	9.21	3.37	70	24.1	261		376		675	104	6,620	105	172
SRM01-108-19	Inherited	91	2,575		No_Data	15.8	0.34	2.47	6.96	2.46	47	16.6	179		331		710	100	9,922	92	168
SRM01-108-20	Inherited	148	3,481		No_Data	17.8	0.37	3.03	10.73	3.58	70	27.8	295		438		801	127	7,298	135	220
SRM01-108-21	Inherited	126	3,162		0.09	12.2	0.25	2.40	7.53	2.42	59	19.5	222		405		660	101	8,286	69	119
SRM01-108-22	Inherited	80	1,184		No_Data	6.6	0.16	0.98	2.69	0.88	20	8.0	81		123		269	34	7,028	30	126
SRM01-108-23		207	5,827		0.25	31.7	0.66	7.00	19.28	6.52	136	45.4	531		787		1184	188	7,687	250	303
SRM01-108-24		181	4,587		0.06	25.4	0.68	5.64	15.30	5.43	117	36.3	397		540		1050	138	7,827	187	250
SRM01-108-25		110	1,929		No_Data	11.2	0.29	2.07	6.05	2.08	44	15.3	158		229		498	65	6,137	79	172
SRM01-108-26		119	3,873		0.04	15.4	0.52	2.99	8.56	2.97	82	29.6	324		414		724	129	11,056	116	134
SRM01-108-27	Inclusion	124	2,168		0.07	14.2	0.26	2.18	4.84	2.04	44	14.5	144		251		563	78	6,393	104	527
SRM01-108-28	Inherited	109	3,435		No_Data	14.3	0.34	3.19	7.62	2.63	62	23.8	235		406		649	116	9,293	126	181
SRM01-108-29		126	3,899		0.09	15.0	0.45	3.58	9.90	3.19	79	27.9	321		510		745	169	10,954	152	194
SRM01-108-30		83	1,502		0.28	8.8	0.19	1.59	4.12	1.60	32	11.3	123		188		359	52	6,117	55	340
SRM01-108-31	Inherited	113	1,187		No_Data	14.0	0.10	0.66	2.06	0.82	17	6.9	79		152		352	51	5,898	106	265
SRM01-108-32		194	5,997		0.11	33.4	0.86	6.77	19.93	6.62	160	49.4	549		787		1339	220	7,879	262	310
SRM01-108-33		111	2,156		0.06	12.6	0.25	2.20	4.83	1.92	36	13.1	145		269		602	88	8,410	98	224
SRM01-108-34		118	2,499		0.14	12.1	0.24	2.06	6.29	2.70	54	18.8	189		283		542	81	6,416	82	156
SRM01-108-35		168	4,442		0.08	21.9	0.51	4.46	13.38	4.74	112	35.9	378		553		966	159	9,049	172	219
SRM01-108-36	Inherited	158	7,069		0.07	30.4	0.75	7.04	21.65	7.00	157	49.6	578		829		1197	218	7,337	207	206

Appendix Table 8 (continued). Zircon Trace Element Spot Analyses from OSU - LA-ICP-MS

Spot ID	Note	P (31) ppm	Y (89) ppm	Nb (93) ppm	La (139) ppm	Ce (140) ppm	Pr (141) ppm	Nd (146) ppm	Sm (147) ppm	Eu (153) ppm	Gd (157) ppm	Tb (159) ppm	Dy (163) ppm	Ho (165) ppm	Er (166) ppm	Tm (169) ppm	Yb (172) ppm	Lu (175) ppm	Hf (179) ppm	Th (232) ppm	U (238) ppm
SRM01-108-37	Inherited	200	6,497		0.18	26.9	0.66	6.06	19.32	6.42	151	55.8	593		917		1388	236	8,180	218	237
SRM01-108-38		159	3,182		0.62	19.4	0.44	3.36	10.13	3.71	82	29.1	296		377		644	98	5,467	139	171
SRM01-108-39		159	3,046		0.08	19.0	0.38	4.23	13.95	4.66	86	26.0	313		429		741	94	6,744	122	202
SRM01-108-40	Inherited	169	5,463		No_Data	20.8	0.33	3.50	10.97	4.54	106	34.1	426		596		859	183	10,742	155	149
SRM01-108-41		103	1,157		0.03	9.5	0.05	0.51	1.55	0.73	17	6.2	81		144		322	48	4,624	33	107
SRM01-108-42	Inherited	138	6,189		No_Data	20.9	0.41	4.49	10.68	2.99	101	37.2	435		728		885	236	14,045	206	218
SRM01-108-43		177	4,402		0.08	23.4	0.52	5.61	15.34	5.46	101	39.3	392		575		991	141	8,042	161	201
SRM01-108-44	Inherited	124	3,065		0.18	16.8	0.37	3.76	9.01	3.37	76	26.9	228		380		652	103	6,204	127	152
SRM01-108-45		178	3,996		No_Data	24.2	0.54	5.48	15.14	5.56	91	39.3	346		499		929	134	6,825	141	229
SRM01-113-01	Inherited	132	2,828		0.07	28.8	0.11	1.16	3.55	0.70	34	13.7	166		370		720	159	10,789	315	451
SRM01-113-02		103	2,022		0.08	20.5	0.14	0.87	2.50	0.80	29	11.6	119		247		517	90	8,044	117	290
SRM01-113-03	Inherited	114	1,806		0.02	12.4	0.07	0.54	1.87	0.32	17	8.2	97		226		467	98	9,935	80	246
SRM01-113-04		120	1,996		No_Data	19.5	0.05	0.84	2.57	0.64	27	10.5	118		245		495	94	8,802	244	404
SRM01-113-05		116	1,778		0.09	13.8	0.10	0.65	2.13	0.51	24	9.5	101		217		478	90	9,948	127	284
SRM01-113-06	Inclusion	332	2,340		15.90	58.7	3.91	6.84	5.20	1.22	32	12.7	149		288		619	117	10,815	424	511
SRM01-113-07		93	2,879		No_Data	15.8	0.21	1.58	3.98	1.11	37	13.9	159		346		639	140	10,494	166	283
SRM01-113-08	Inherited	96	2,159		0.15	13.6	0.18	0.65	1.93	0.47	22	10.0	113		265		501	152	12,334	126	177
SRM01-113-09	Inherited	105	2,146		0.10	17.6	0.17	1.10	3.08	0.79	33	11.6	138		281		565	110	11,129	131	256
SRM01-113-10		102	2,228		0.02	9.9	0.16	1.15	3.43	1.18	32	12.4	131		259		516	102	11,769	91	189
SRM01-113-11	Inherited	90	1,545		0.06	11.3	0.08	0.74	2.28	0.51	18	8.6	93		184		376	75	9,668	85	214
SRM01-113-12		110	1,857		No_Data	16.4	0.07	0.54	1.94	0.35	22	10.3	107		217		428	88	12,151	178	357
SRM01-113-13	Inclusion	172	2,381		7.28	35.5	1.40	3.20	3.50	0.48	27	11.8	134		277		548	113	13,333	283	431
SRM01-113-14		126	2,800		1.52	26.3	0.41	1.23	3.31	0.68	29	14.5	170		344		653	135	11,608	413	540
SRM01-113-15		123	2,137		No_Data	12.1	0.19	1.17	3.60	0.83	32	12.5	135		257		498	95	12,058	125	295
SRM01-113-16	Inclusion	898	3,038		79.25	122.9	16.59	31.73	11.23	1.22	49	16.7	194		424		730	156	14,496	440	525
SRM01-113-17		153	2,388		3.18	23.4	0.61	2.08	4.39	0.73	33	13.3	173		298		703	103	9,350	385	645
SRM01-113-18		136	2,283		4.04	22.8	0.90	2.31	3.16	0.61	25	11.7	139		284		607	117	11,089	201	376
SRM01-113-19	Inherited	118	2,449		0.02	16.3	0.07	0.82	2.73	0.62	27	10.9	133		307		700	128	14,004	135	296
SRM01-113-20		101	2,049		No_Data	10.5	0.06	0.98	3.17	0.70	28	10.8	122		249		452	95	11,941	90	193
SRM01-113-21	Inherited	90	1,358		No_Data	12.4	0.03	0.37	1.56	0.20	14	5.8	80		180		362	75	12,571	92	238
SRM01-113-22	Inherited	86	1,886		No_Data	14.1	0.12	0.69	2.56	0.53	22	10.4	124		253		504	100	12,718	124	215
SRM01-113-23		179	2,451		5.39	22.8	1.28	3.19	4.11	0.77	30	11.1	143		300		596	118	11,798	134	351

Appendix Table 8 (continued). Zircon Trace Element Spot Analyses from OSU - LA-ICP-MS

Spot ID	Note	P (31) ppm	Y (89) ppm	Nb (93) ppm	La (139) ppm	Ce (140) ppm	Pr (141) ppm	Nd (146) ppm	Sm (147) ppm	Eu (153) ppm	Gd (157) ppm	Tb (159) ppm	Dy (163) ppm	Ho (165) ppm	Er (166) ppm	Tm (169) ppm	Yb (172) ppm	Lu (175) ppm	Hf (179) ppm	Th (232) ppm	U (238) ppm
SRM01-113-24	Inclusion	1149	2,295		87.90	141.2	19.45	32.46	10.52	1.62	34	11.0	126		265		511	108	11,730	173	357
SRM01-113-25	Inherited	117	2,145		0.02	10.0	0.16	1.00	3.71	0.78	28	12.4	131		251		498	98	12,514	114	280
SRM01-113-26	Inherited	74	1,270		No_Data	10.7	0.07	0.46	1.25	0.24	13	5.8	68		158		367	69	12,328	65	188
SRM01-113-27	Inherited	110	3,056		0.06	24.9	0.27	2.10	5.63	2.26	44	16.7	167		324		724	132	8,092	231	329
SRM01-113-28	Inherited	83	1,690		0.10	16.0	0.06	0.56	2.01	0.48	16	7.1	93		199		441	91	12,829	151	285
SRM01-113-29	Inherited	90	2,873		0.05	15.7	0.17	0.96	3.28	0.60	32	14.0	162		357		649	139	13,232	142	273
SRM01-113-30		91	1,717		No_Data	15.5	0.12	0.73	2.41	0.62	23	10.1	112		209		459	83	10,259	90	191
SRM01-113-31	Inherited	93	3,644		No_Data	20.8	0.08	0.74	3.19	0.63	33	13.3	167		392		617	193	10,421	188	256
SRM01-113-32	Inherited	123	4,325		No_Data	38.7	0.12	1.74	5.61	1.81	49	25.3	288		626		962	229	12,055	364	380
SRM01-113-33		94	1,823		No_Data	15.1	0.10	0.66	1.99	0.50	20	8.4	99		227		479	102	10,247	103	251
SRM01-113-34	Inherited	87	2,208		0.10	15.7	0.03	0.45	1.89	0.68	24	10.4	100		261		513	126	14,065	211	249
SRM01-113-35		231	2,491		8.21	23.3	1.86	3.48	3.62	0.40	29	11.9	151		319		579	110	10,490	160	441
SRM01-113-36		105	2,664		No_Data	27.6	0.11	1.02	4.10	0.71	34	14.6	162		326		642	119	9,996	304	484
SRM01-113-37		82	1,697		No_Data	10.0	0.03	0.65	2.57	0.47	22	7.6	103		218		431	84	10,413	75	197
SRM01-113-38		89	1,555		No_Data	16.5	0.10	0.48	2.76	0.46	19	9.2	107		209		476	80	10,272	83	331
SRM01-113-39		87	1,667		No_Data	16.3	0.09	0.60	1.71	0.45	16	8.2	95		209		416	83	12,686	226	330
SRM01-113-40		81	1,502		No_Data	10.2	0.07	0.98	2.83	0.58	24	10.2	98		186		433	74	8,809	74	234
SRM01-113-41		80	2,117		No_Data	16.8	0.08	0.64	2.42	0.69	24	9.9	119		256		530	106	10,664	112	286
SRM01-113-42		134	2,064		4.63	27.6	1.38	2.21	2.69	0.74	20	10.5	117		246		560	105	13,127	240	318
SRM01-113-43	Inherited	106	2,923		0.14	24.9	0.08	0.65	2.79	0.49	29	13.2	147		356		656	161	13,943	407	409
SRM01-113-44		93	2,356		0.08	27.7	0.06	0.94	2.94	0.87	28	11.8	144		310		649	121	10,876	360	517
SRM01-113-45		80	1,418		No_Data	8.8	0.03	0.67	1.82	0.48	15	6.6	78		179		378	66	8,681	63	212
WCOS14-03-01		177	3,001		0.21	20.8	0.46	3.17	9.60	1.77	75	23.5	269		352		590	95	7,164	573	1012
WCOS14-03-02	Inherited	147	1,912		0.89	29.5	0.26	2.80	5.02	0.87	37	14.4	162		246		426	64	8,237	562	803
WCOS14-03-03		205	1,998		4.58	24.4	1.43	5.26	5.39	0.83	39	12.6	142		242		412	64	9,766	344	685
WCOS14-03-04	Inherited	157	1,907		No_Data	23.1	0.19	2.06	5.85	0.74	35	13.1	156		251		508	71	10,623	477	748
WCOS14-03-05		132	1,793		No_Data	25.0	0.12	1.24	3.30	0.67	31	10.7	135		225		426	69	8,756	460	779
WCOS14-03-06		230	4,489		0.09	66.2	0.60	4.28	13.42	2.09	112	39.3	437		632		893	152	9,348	1895	1913
WCOS14-03-07	Inclusion	523	1,443		22.80	65.9	6.48	16.63	6.99	0.80	31	10.2	125		177		378	51	7,372	268	649
WCOS14-03-08	Inherited	178	1,549		4.18	30.9	1.61	5.93	4.51	0.56	30	10.3	127		204		409	62	10,505	319	604
WCOS14-03-09		176	3,227		0.04	32.0	0.31	2.43	7.29	1.00	56	20.1	243		402		655	110	13,392	915	1204
WCOS14-03-10		125	1,738		No_Data	14.2	0.21	1.62	4.47	0.80	32	10.2	121		201		376	53	7,254	265	594

Appendix Table 8 (continued). Zircon Trace Element Spot Analyses from OSU - LA-ICP-MS

Spot ID	Note	P (31) ppm	Y (89) ppm	Nb (93) ppm	La (139) ppm	Ce (140) ppm	Pr (141) ppm	Nd (146) ppm	Sm (147) ppm	Eu (153) ppm	Gd (157) ppm	Tb (159) ppm	Dy (163) ppm	Ho (165) ppm	Er (166) ppm	Tm (169) ppm	Yb (172) ppm	Lu (175) ppm	Hf (179) ppm	Th (232) ppm	U (238) ppm
WCOS14-03-11	Inherited	144	3,117		No_Data	25.5	0.24	2.16	6.46	0.95	53	18.7	262		398		582	126	12,946	785	719
WCOS14-03-12		220	2,889		3.19	47.0	1.41	5.80	8.68	1.43	64	20.3	235		377		659	90	9,075	1057	1184
WCOS14-03-13	Inherited	108	3,214		No_Data	29.1	0.19	2.35	6.43	1.09	60	18.8	229		382		571	130	11,150	533	538
WCOS14-03-14		150	4,740		0.22	36.8	0.56	3.97	11.37	2.08	100	31.1	417		616		834	190	12,504	820	831
WCOS14-03-15		199	2,172		2.02	26.4	0.42	2.58	4.53	0.82	44	15.4	174		263		523	76	11,152	529	821
WCOS14-03-16	Inherited	137	3,334		No_Data	20.3	No_Data	2.38	7.82	1.30	65	23.0	253		392		608	104	9,635	608	794
WCOS14-03-17	Inclusion	282	1,791		9.50	33.1	1.96	6.24	4.90	0.54	36	12.1	141		208		398	67	11,183	414	599
WCOS14-03-18		228	1,356		1.59	16.7	0.70	2.16	3.04	0.63	25	7.5	115		167		359	57	8,358	465	594
WCOS14-03-19		114	2,020		0.11	19.0	0.20	1.97	5.17	0.85	40	14.5	171		268		455	70	11,122	352	584
WCOS14-03-20		199	4,520		1.05	33.4	0.64	6.37	12.13	2.13	95	29.7	376		560		821	142	11,080	1224	1110
WCOS14-03-21	Inclusion	475	2,449		19.28	62.2	6.40	17.00	9.90	1.13	56	16.6	202		292		473	81	9,775	626	785
WCOS14-03-22	Inherited	119	2,305		0.05	20.1	0.14	1.25	3.89	0.47	31	12.1	147		279		348	108	13,027	502	506
WCOS14-03-23		131	1,732		No_Data	12.9	0.13	1.58	4.07	0.71	36	10.9	144		218		367	55	8,630	237	531
WCOS14-03-24		200	3,253		3.16	37.1	1.49	6.20	9.55	1.48	64	19.5	282		411		685	105	8,837	640	1336
WCOS14-03-25		134	1,595		No_Data	21.1	0.11	0.84	3.22	0.53	28	9.9	125		196		340	54	8,532	555	1004
WCOS14-03-26		123	1,442		No_Data	16.4	0.10	0.91	2.93	0.48	26	8.8	106		177		329	59	7,598	327	752
WCOS14-03-27		209	2,793		1.85	36.1	0.88	3.34	6.68	0.82	51	19.9	224		333		586	99	11,677	780	959
WCOS14-03-28		178	3,249		No_Data	33.2	0.37	2.24	8.50	1.35	60	20.9	243		382		583	105	11,810	847	1025
WCOS14-03-29		133	1,741		0.10	22.6	0.15	0.92	3.46	0.56	33	11.3	132		222		356	66	10,707	463	627
WCOS14-03-30		130	2,404		No_Data	28.6	0.22	2.01	4.83	0.90	50	16.5	206		291		480	87	11,600	581	670
WCOS14-03-31	Inherited	140	1,988		2.31	26.6	0.70	3.11	4.83	0.75	36	12.7	157		237		417	70	9,969	447	657
WCOS14-03-32	Inherited	215	4,658		3.63	56.1	1.55	6.52	9.94	1.54	96	28.2	411		613		820	160	14,027	1620	1109
WCOS14-03-33	Inherited	116	2,171		No_Data	26.7	0.20	2.01	5.59	0.63	49	14.9	178		269		469	62	5,454	539	1026
WCOS14-03-34		173	3,448		0.31	37.6	0.32	2.96	7.52	1.15	70	22.1	281		413		644	114	10,331	1278	1167
WCOS14-03-35	Inherited	142	2,261		1.70	30.1	0.56	2.39	5.05	0.58	38	14.0	192		316		464	96	14,104	687	638
WCOS14-03-36	Inclusion	1657	#####		10.92	49.8	11.42	68.75	#####	48.50	912	272.4	2275		1397		1249	142	9,174	1465	814
WCOS14-03-37		143	1,392		No_Data	13.7	0.08	1.20	3.37	0.79	29	9.5	114		192		389	52	7,535	242	562
WCOS14-03-38	Inherited	153	4,295		0.66	58.4	0.72	4.73	10.58	1.37	96	29.3	397		516		765	133	9,417	1750	1336
WCOS14-03-39		154	2,125		0.07	22.3	0.18	1.99	4.75	0.96	36	13.5	172		252		452	75	8,044	541	905
WCOS14-03-40		209	1,744		0.85	21.4	0.56	2.25	3.77	0.53	31	11.3	134		240		360	64	11,961	395	502
WCOS14-03-41	Inherited	151	2,232		0.41	25.4	0.24	1.37	3.88	0.67	35	13.2	163		269		441	79	10,587	491	715
WCOS14-03-42	Inherited	166	3,280		0.71	32.7	0.51	3.14	6.03	0.89	53	20.8	248		439		582	146	12,794	904	829
WCOS14-03-43	Inherited	124	1,810		No_Data	18.7	0.04	1.75	4.16	0.66	32	10.4	139		218		442	71	8,690	360	646

Appendix Table 8 (continued). Zircon Trace Element Spot Analyses from OSU - LA-ICP-MS

Spot ID	Note	P (31) ppm	Y (89) ppm	Nb (93) ppm	La (139) ppm	Ce (140) ppm	Pr (141) ppm	Nd (146) ppm	Sm (147) ppm	Eu (153) ppm	Gd (157) ppm	Tb (159) ppm	Dy (163) ppm	Ho (165) ppm	Er (166) ppm	Tm (169) ppm	Yb (172) ppm	Lu (175) ppm	Hf (179) ppm	Th (232) ppm	U (238) ppm
WCOS14-03-44	Inherited	137	2,510		0.24	25.2	0.28	2.18	6.00	0.97	52	16.7	198		291		478	79	10,388	721	840
WCOS14-03-45		108	1,373		0.14	17.1	0.05	0.92	2.73	0.46	24	8.2	97		178		307	51	9,175	362	539
WCOSJD-152-01		107	1,129		No_Data	10.5	0.06	0.49	1.74	0.60	15	5.5	73		138		316	59	7,125	69	159
WCOSJD-152-02	Inherited	84	621		No_Data	5.4	0.01	0.30	1.17	0.30	10	3.9	44		75		142	25	8,431	26	65
WCOSJD-152-03		115	905		No_Data	8.4	0.03	0.66	1.92	0.46	14	5.0	65		109		214	40	9,586	39	111
WCOSJD-152-04		103	842		0.11	4.8	0.14	0.78	2.09	0.57	15	6.5	63		106		195	33	6,927	33	59
WCOSJD-152-05		112	1,959		No_Data	9.4	0.30	2.31	5.52	1.25	35	15.2	171		226		415	80	10,073	121	138
WCOSJD-152-06		94	1,333		0.15	7.9	0.11	1.52	3.33	0.75	28	9.6	100		158		272	45	8,748	57	98
WCOSJD-152-07	Inherited	91	611		No_Data	5.3	0.03	0.32	1.04	0.34	10	3.9	46		77		149	26	8,148	25	55
WCOSJD-152-08		95	674		No_Data	5.6	0.03	0.47	0.99	0.34	11	3.1	47		76		151	27	8,150	28	73
WCOSJD-152-09		113	773		0.81	9.4	0.27	1.10	1.66	0.45	12	4.4	55		93		195	33	9,032	38	92
WCOSJD-152-10		95	1,471		0.04	8.1	0.18	1.09	3.43	1.08	30	10.5	108		190		331	55	7,102	110	188
WCOSJD-152-11		101	1,314		No_Data	6.2	0.14	1.14	3.22	0.87	22	9.3	93		168		276	57	8,806	48	74
WCOSJD-152-12		112	1,414		0.41	9.2	0.26	1.59	4.45	0.82	25	11.2	101		184		379	56	7,467	79	167
WCOSJD-152-13		96	887		No_Data	6.0	0.08	0.59	1.78	0.49	15	6.1	60		107		198	36	7,805	38	94
WCOSJD-152-14		87	843		No_Data	6.5	0.08	0.60	1.83	0.45	16	5.9	68		124		219	40	8,672	54	101
WCOSJD-152-15		129	2,347		0.29	9.2	0.43	2.44	5.98	1.50	46	14.6	169		270		442	76	8,648	100	166
WCOSJD-152-16		94	1,155		No_Data	7.1	0.02	0.92	2.45	0.81	21	7.1	81		144		290	46	8,724	56	144
WCOSJD-152-17		73	641		No_Data	5.7	0.04	0.42	0.90	0.30	11	3.5	47		75		150	27	9,538	27	59
WCOSJD-152-18		91	1,104		No_Data	5.7	0.05	0.99	2.46	0.69	20	7.3	84		128		250	42	8,338	41	81
WCOSJD-152-19	Inherited	86	1,060		No_Data	5.4	0.12	0.77	2.11	0.60	19	7.1	71		127		219	36	8,471	35	64
WCOSJD-152-20		92	1,963		No_Data	8.0	0.23	2.28	4.25	1.04	34	13.6	137		224		358	68	8,649	105	129
WCOSJD-152-21		83	1,419		0.18	10.2	0.25	1.82	4.06	0.94	32	10.0	125		190		282	53	9,335	103	111
WCOSJD-152-22		80	636		0.27	6.6	0.21	0.65	1.13	0.32	10	4.1	45		81		140	28	8,720	26	46
WCOSJD-152-23		77	639		0.11	5.7	0.03	0.34	0.93	0.29	9	3.5	42		75		133	25	8,324	28	51
WCOSJD-152-24		109	1,179		0.21	7.7	0.25	1.59	4.22	0.81	23	8.7	103		153		297	48	7,503	54	138
WCOSJD-152-25	Inherited	81	960		No_Data	6.0	0.06	0.69	1.99	0.57	16	6.3	68		117		206	33	8,480	41	66
WCOSJD-152-26		105	843		0.85	9.5	0.40	1.29	1.83	0.47	14	4.8	57		100		200	34	9,328	36	69
WCOSJD-152-27		67	643		No_Data	5.4	No_Data	0.38	1.19	0.39	9	3.9	47		79		160	28	7,611	27	91
WCOSJD-152-28		98	1,293		0.06	8.6	0.17	1.17	3.59	0.83	27	9.4	97		153		287	48	5,530	83	168
WCOSJD-152-29		192	1,314		4.01	14.2	1.15	3.85	2.58	0.62	19	7.4	91		164		223	61	12,670	57	79
WCOSJD-152-30		76	1,060		No_Data	5.7	0.10	0.98	2.22	0.51	18	6.9	79		127		211	38	8,617	45	83

Appendix Table 8 (continued). Zircon Trace Element Spot Analyses from OSU - LA-ICP-MS

Spot ID	Note	P (31) ppm	Y (89) ppm	Nb (93) ppm	La (139) ppm	Ce (140) ppm	Pr (141) ppm	Nd (146) ppm	Sm (147) ppm	Eu (153) ppm	Gd (157) ppm	Tb (159) ppm	Dy (163) ppm	Ho (165) ppm	Er (166) ppm	Tm (169) ppm	Yb (172) ppm	Lu (175) ppm	Hf (179) ppm	Th (232) ppm	U (238) ppm
WCOSJD-152-31		83	1,114		No_Data	6.4	0.13	0.91	2.81	0.80	24	8.1	83		144		216	42	9,439	47	82
WCOSJD-152-32		80	1,301		No_Data	6.3	0.13	1.54	3.89	0.95	25	9.6	97		163		282	48	8,223	52	83
WCOSJD-152-33	Inherited	76	670		0.10	5.7	0.04	0.43	1.38	0.27	11	4.1	49		93		165	26	7,166	31	66
WCOSJD-152-34	Inherited	76	912		No_Data	5.1	0.07	1.02	2.08	0.67	18	6.6	69		110		209	33	7,170	34	61
WCOSJD-152-35		80	707		No_Data	6.8	0.07	0.56	2.14	0.52	14	5.3	55		85		214	27	5,789	38	122
WCOSJD-152-36		80	1,530		No_Data	7.6	0.16	1.51	3.90	0.87	28	8.6	110		165		308	58	10,515	60	89
WCOSJD-152-37	Pb Loss	70	964		No_Data	5.2	0.10	0.76	2.01	0.55	17	6.0	68		117		185	38	8,267	37	60
WCOSJD-152-38		75	786		No_Data	5.2	0.04	0.67	1.58	0.48	13	4.8	62		92		178	35	7,763	28	60
WCOSJD-152-39		106	866		No_Data	8.0	0.04	0.77	1.85	0.52	14	6.0	63		105		213	34	9,762	41	92
WCOSJD-152-40		80	652		No_Data	4.8	0.01	0.42	1.28	0.36	12	3.5	44		80		164	28	7,790	24	54
WCOSJD-152-41		67	633		No_Data	6.0	0.03	0.34	1.19	0.37	11	3.7	43		79		158	25	7,486	34	75
WCOSJD-152-42		85	1,374		No_Data	6.8	0.16	1.15	3.59	0.76	31	9.9	101		166		268	45	9,171	65	102
WCOSJD-152-43		59	737		No_Data	4.8	0.04	0.47	1.29	0.42	14	4.4	52		92		171	27	8,776	25	45
WCOSJD-152-44		71	670		No_Data	5.5	0.04	0.37	1.04	0.36	12	4.0	47		83		170	36	8,391	29	66
WCOSJD-152-45		84	707		No_Data	5.0	0.02	0.38	1.28	0.35	13	4.7	59		88		179	28	8,811	28	60
WCOSNU-25-01		373	2,765		12.93	51.7	4.19	11.35	7.15	0.85	52	17.1	213		394		674	116	11,555	455	531
WCOSNU-25-02		214	1,795		3.35	15.9	0.96	3.56	3.62	0.80	33	10.6	131		210		372	75	10,902	124	171
WCOSNU-25-03	Inclusion	296	1,023		9.05	21.7	2.60	7.09	3.19	0.48	18	6.1	72		133		250	51	11,898	61	117
WCOSNU-25-04		82	1,470		No_Data	7.5	0.29	1.64	4.01	1.03	28	11.3	113		190		328	59	7,489	75	126
WCOSNU-25-05	Inherited	87	1,203		No_Data	7.5	0.08	1.04	2.18	0.56	22	6.2	83		143		275	49	9,691	67	155
WCOSNU-25-06	Inherited	86	2,906		No_Data	10.7	0.30	2.67	6.99	2.27	58	21.0	226		345		530	103	9,139	84	116
WCOSNU-25-07		103	1,109		No_Data	6.9	0.06	1.06	2.52	0.53	19	5.7	84		158		280	51	10,130	46	139
WCOSNU-25-08		84	1,525		No_Data	9.1	0.12	1.10	3.62	0.64	32	10.2	113		202		349	65	12,124	86	200
WCOSNU-25-09		187	1,191		3.98	13.3	1.14	3.57	2.52	0.52	21	6.8	90		154		293	53	11,489	52	101
WCOSNU-25-10	Inherited	154	787		5.03	15.4	1.40	3.39	2.18	0.30	12	4.9	55		99		181	41	11,051	64	120
WCOSNU-25-11		101	1,461		No_Data	16.0	0.07	0.57	2.25	0.36	24	7.9	107		196		311	64	12,747	302	294
WCOSNU-25-12	Inclusion	1192	1,004		63.53	113.9	17.97	45.35	14.47	1.39	35	7.3	71		131		232	42	13,346	55	123
WCOSNU-25-13	Inherited	68	798		0.05	6.8	0.05	0.38	0.99	0.22	11	4.1	50		107		195	38	11,223	41	88
WCOSNU-25-14		60	867		0.07	7.8	0.03	0.61	1.13	0.33	12	4.7	73		124		234	43	12,561	49	102
WCOSNU-25-15		166	3,700		No_Data	33.7	0.15	1.48	4.27	0.99	46	17.1	239		509		949	177	9,586	346	747
WCOSNU-25-16	Inherited	75	673		0.12	5.6	0.05	0.25	0.91	0.22	11	3.2	46		93		158	34	11,114	39	70
WCOSNU-25-17		86	999		No_Data	6.6	0.01	0.46	1.23	0.29	14	5.0	60		114		222	44	11,647	47	89

Appendix Table 8 (continued). Zircon Trace Element Spot Analyses from OSU - LA-ICP-MS

Spot ID	Note	P (31) ppm	Y (89) ppm	Nb (93) ppm	La (139) ppm	Ce (140) ppm	Pr (141) ppm	Nd (146) ppm	Sm (147) ppm	Eu (153) ppm	Gd (157) ppm	Tb (159) ppm	Dy (163) ppm	Ho (165) ppm	Er (166) ppm	Tm (169) ppm	Yb (172) ppm	Lu (175) ppm	Hf (179) ppm	Th (232) ppm	U (238) ppm
WCOSNU-25-18	Inherited	85	1,277		No_Data	7.5	No_Data	0.74	2.07	0.55	19	7.7	84		169		281	59	11,584	85	132
WCOSNU-25-19	Inherited	200	1,237		6.02	17.9	1.83	4.76	2.85	0.42	20	7.1	82		158		247	52	12,001	69	112
WCOSNU-25-20		77	1,510		No_Data	7.1	0.13	1.13	2.51	0.57	25	8.0	107		181		313	61	11,609	65	98
WCOSNU-25-21	Inherited	74	799		No_Data	7.4	0.03	0.52	1.28	0.35	12	4.6	61		116		198	36	11,069	38	87
WCOSNU-25-22		78	902		No_Data	7.6	0.03	0.43	1.08	0.30	14	5.3	59		128		231	49	13,161	59	99
WCOSNU-25-23		101	1,212		No_Data	7.8	0.15	0.83	2.74	0.53	21	6.5	90		150		328	51	8,044	74	192
WCOSNU-25-24		86	963		0.13	8.9	0.20	0.50	1.49	0.40	15	5.6	71		131		263	46	9,819	62	156
WCOSNU-25-25		74	529		0.02	5.9	0.01	0.24	0.96	0.18	8	3.0	36		71		141	30	9,780	30	73
WCOSNU-25-26	Inclusion	278	2,092		7.46	30.0	2.63	7.13	5.59	0.71	39	13.4	145		267		422	77	10,917	250	311
WCOSNU-25-27		92	999		No_Data	7.7	0.07	0.36	1.46	0.33	15	5.8	72		130		219	48	11,375	57	107
WCOSNU-25-28		70	872		No_Data	6.8	0.01	0.46	1.09	0.33	14	4.5	59		129		225	39	12,666	45	71
WCOSNU-25-29	Inclusion	525	1,265		23.35	46.9	6.95	18.43	6.86	1.11	27	8.2	101		167		300	57	10,806	61	112
WCOSNU-25-30		67	720		No_Data	7.2	No_Data	0.39	1.07	0.28	11	4.4	53		94		188	34	9,780	43	109
WCOSNU-25-31	Inherited	80	668		0.47	7.2	0.10	0.49	1.33	0.29	10	4.3	44		91		218	35	8,583	49	131
WCOSNU-25-32		79	1,205		No_Data	6.6	0.04	0.78	2.43	0.51	20	7.6	84		146		295	46	9,414	52	118
WCOSNU-25-33		69	548		No_Data	7.5	No_Data	0.25	0.79	0.17	10	2.8	41		77		166	29	10,435	33	120
WCOSNU-25-34	Inherited	79	874		0.04	8.1	0.02	0.36	1.66	0.36	13	5.1	67		138		252	41	10,248	61	118
WCOSNU-25-35		124	993		2.55	11.1	0.65	1.55	1.75	0.38	13	5.5	66		133		235	50	11,049	48	94
WCOSNU-25-36		149	1,216		3.42	14.2	0.89	2.32	2.44	0.47	23	8.1	93		170		286	59	12,131	69	97
WCOSNU-25-37		85	621		No_Data	6.6	No_Data	0.32	0.69	0.26	8	3.8	41		89		170	33	11,754	46	114
WCOSNU-25-38		192	1,433		4.87	16.4	1.68	4.88	4.31	0.90	27	10.3	111		186		299	59	9,310	62	113
WCOSNU-25-39		118	1,189		0.39	6.9	0.24	1.05	2.16	0.48	20	7.1	76		150		263	54	10,716	57	115
WCOSNU-25-40		87	1,472		No_Data	8.1	0.09	0.79	2.06	0.50	22	7.0	92		196		267	66	13,840	84	94
WCOSNU-25-41		166	874		3.33	12.3	0.85	2.11	2.26	0.41	13	5.3	60		126		263	42	8,885	49	135
WCOSNU-25-42		66	976		No_Data	7.2	0.06	0.68	2.16	0.52	20	7.1	73		122		259	45	11,204	46	93
WCOSNU-25-43	Inclusion	1654	1,184		49.90	98.9	15.00	34.53	11.46	1.33	32	8.5	89		145		244	52	8,894	69	130
WCOSNU-25-44		136	954		2.49	10.7	0.78	1.73	2.00	0.38	16	5.8	62		130		229	45	10,960	48	89
WCOSNU-25-45	Inherited	95	1,180		No_Data	9.4	0.05	0.52	1.75	0.37	17	5.4	85		152		301	55	13,034	73	150

Inherited	Grain whose age has not been included in mean weighted age calculation because age is older than main population; antecrystic or xenocrystic
Pb Loss	Grain whose age has not been included in mean weighted age calculation because age was inaccurately younger than main population due to Pb loss
Inclusion	Interpreted as a fluid, melt, apatite, or other phase inclusion, based off anomalously high concentrations of P, La, Pr, and Nd